SCHOOL OF ELECTRICAL AND ELECTRONIC ENGINEERING

ELECTRIC POWER SYSTEMS RESEARCH GROUP

COORDINATED AND NON-COORDINATED CONTROL OF ENERGY STORAGE FOR VOLTAGE SUPPORT IN LOW VOLTAGE DISTRIBUTION NETWORKS

A THESIS PRESENTED FOR THE DEGREE OF DOCTOR OF PHILOSOPHY

LEI WANG

APRIL 2016

Abstract

Energy storage is seen as one of a number of crucial technologies if the integration of renewables in distribution networks increases. The work in this thesis considers how to operate energy storage to overcome issues presented by solar photovoltaic (PV) in low voltage (LV) distribution networks. Two control strategies have been developed and applied in a smart grid laboratory to mitigate voltage rise and reverse power flows caused by PV. The first strategy examines the performance of non-coordinated control of energy storage for voltage support. The second strategy involves coordinating the on-load tap changer (OLTC) and energy storage for voltage support and reducing reverse power flows, and it illustrates that coordinated storage unit is a more effective and viable alternative to upgrading network infrastructure. After considering a single storage unit in the network, strategies for controlling multiple storage units are investigated. The main objective of this method is to solve overvoltage with multiple energy storage in LV networks with a proliferation of PV systems. The scheme is based on voltage sensitivity analysis and a battery aging model which influences which storage units are operated to maintain the network voltage within limits. The battery aging model is included to improve to reduce degradation when operated to resolve voltage excursions thus reducing the maintenance and battery replacement costs.

To get a better performance of the storage unit for voltage support, a systematic model that includes the PV generator and the energy storage based on linearized differential equations is constructed. The model was used to examine: the dynamic performance of battery storage systems and their active and reactive power voltage regulation feedback controller; small disturbance of active and reactive power exchange with the power system; a methodology to utilise active and reactive power of the energy storage for voltage support.

In summary, the study presented by this thesis shows energy storage can be operated in the LV distribution network where significant amounts of PV generators are installed. It allows distribution network operators to have a deeper understanding of how to operate single and multiple energy storage units in future LV distribution networks.

Declaration

I hereby declare that no part of this dissertation has been subject of any other degree or qualification, and that all sources of information have been referenced.

Chapter 3 and Chapter 4 of this thesis have been published by the author.

Chapter 3

L. Wang, A. Crossland, D. Liang, N. Wade, and D. Jones, "Using a smart grid laboratory to investigate battery energy storage to mitigate the effects of PV in distribution networks," in *22nd International Conference and Exhibition on Electricity Distribution (CIRED 2013),* 2013, pp. 0504–0504. DOI: 10.1049/cp.2013.0769

D. Liang, P. Taylor, **L. Wang**, D. Miller, and V. Thornley, "Coordinated voltage and power flow control in distribution network," in *22nd International Conference and Exhibition on Electricity Distribution (CIRED 2013),* 2013, pp. 0711–0711. DOI: 10.1049/cp.2013.0887

Chapter 4

L. Wang, D. H. Liang, A. F. Crossland, P. C. Taylor, D. Jones, and N. S. Wade, "Coordination of Multiple Energy Storage Units in a Low-Voltage Distribution Network," IEEE Trans. Smart Grid, vol. PP, no. 99, pp. 1–1, 2015 DOI: 10.1109/TSG.2015.2452579

Acknowledgements

I would like to express my sincere gratitude and appreciation to **Prof. Phil Taylor** and **Dr. Neal Wade** for their invaluable guidance and encouragement throughout the course of this work. I never forget their advice and suggestions from which benefited me significantly. Not only did they educate me with the technical knowledge but assisted with my development of my critical, innovative thoughts. The encouragement from them was my main weapon when I confronted the challenges and difficulties. Without their help, this work would not be possible and I am grateful to them for their supportive and friendly attitude.

I am eternally indebted to my both parents and parents in law for their everlasting support and unconditional love. My special appreciation goes to my life partner and lovely wife, **Mrs Jing Chen**, for bringing joy to my life in so many different ways, and for all the sacrifices she has had to make over the course of my studies. Her patience and understanding has been an inspiration, and it is with pride and gratification that I delicate this dissertation to her.

My special appreciation goes to **Dr Andrew Crossland,** and **Dr Oghenetejiri Anuta** for provision of their expertise, and technical support for publishing papers. Without their superior support, collaborations and great friendship, the research work would not be possible.

I am grateful to obtain advice, knowledge and insightful discussion with my dearest friend, **Dr Song Guo and Dr Daniel Liang**. Because of them, I formed the steps for achieving my research target. They also have significantly broadened my knowledge, and encouraged me to take an alternative route; moving back to down under and walking out of the academic world into the industry.

Appreciation to my dear friends from down under, **Miss Christina Xie, Mr Ryne Li**, **Mr Cheng Gu and his wife**, and **Dr Yao Wang** who always encouraged me and support me to go back to the beautiful Australia. I will see you guys at the beginning of the next year. Although I have been in the UK for more than four years, every night I close my eyes a voice always around my head, says there is always a great journey waiting on me; just drive the car to the Cottesloe beach, get stripped to the waist and fall into the beautiful great Indian Ocean.

List of Publications

L. Wang, D. H. Liang, A. F. Crossland, P. C. Taylor, D. Jones, and N. S. Wade, “Coordination of Multiple Energy Storage Units in a Low-Voltage Distribution Network,” IEEE Trans. Smart Grid, vol. PP, no. 99, pp. 1–1, 2015 DOI: 10.1109/TSG.2015.2452579

L. Wang, A. Crossland, D. Liang, N. Wade, and D. Jones, “Using a smart grid laboratory to investigate battery energy storage to mitigate the effects of PV in distribution networks,” in *22nd International Conference and Exhibition on Electricity Distribution (CIRED 2013),* 2013, pp. 0504–0504. DOI: 10.1049/cp.2013.0769

D. Liang, P. Taylor, **L. Wang**, D. Miller, and V. Thornley, “Coordinated voltage and power flow control in distribution network,” in *22nd International Conference and Exhibition on Electricity Distribution (CIRED 2013),* 2013, pp. 0711–0711. DOI: 10.1049/cp.2013.0887

List of Abbreviations

NGET	National Grid Electricity Transmission plc
TSO	Transmission System Operator
SONI	System Operator for Northern Ireland
TO	Transmission Owner
DNO	Distribution Network Operator
Ofgem	The Office of Gas and Electricity Market
HVDC	High Voltage Direct Current
HVAC	High Voltage Alternating Current
DG	Distributed Generation
CHP	Combined heat and power
FiT	Feed in Tariffs
DECC	Department of Climate Change
LV	Low Voltage
PV	Photovoltaic
MV	Medium Voltage
FACTS	Flexible Alternating Current Transmission System
SVC	Static VAR Compensator
DSTATCOM	distribution STATCOM
DSR	Demand side response
ESS	Energy Storage Systems
BESS	Battery Energy Storage Systems
RTDS	Real Time Digital Simulator
PHIL	Power Hardware in the Loop
ENWL	Electricity North West Limited
SoC	State of Charge
VSC	Voltage Source Converter
VSF	Voltage Sensitivity Factor
PI	Proportional Integral
PLL	Phase Locked Loop
dq	Direct Quadrature
OLTC	On Line Tap Changer

Nomenclature

I_d	Direct axis current
I_q	Quadrature axis current
R	Resistance
L	Inductance
ΔV	Voltage difference
V_{s}	Substation secondary bus voltage
V_{PV}	The PV generator voltage
P_{L}	Active power consumed by the load
Q_{L}	Reactive power consumed by the load
P_{PV}	Active power of the PV generator
Q_{PV}	Reactive power of the PV generator
VUF	Voltage unbalanced factor
VSF	Voltage sensitivity factor
V_{uptld}	Voltage upper threshold
V_{midtld}	Voltage middle threshold
V_{lwtld}	Voltage lower threshold
Q_{req}	Required reactive power for voltage support
P_{req}	Required active power for voltage support
P_{max}	Rated maximum active power
Q_{max}	Rated maximum reactive power
V_{ave}	Three phase average voltage
M	Operational matrix
A	Availability matrix
F	Nomination matrix
L	Remaining cycle life
$\Delta\dot{\mathbf{x}}$	Linearized state vector
$\Delta\mathbf{y}$	Linearized output vector
A	State matrix
B	Input matrix
C	Output matrix

$\mathbf{D}$	Forward matrix
Λ	Eigenvalues
Z	Damping ratio
f	Frequency
δ_n	Angle between the D axis of the global reference and d axis of the nth subsystem reference frame
o	Steady state operating points
Δf_q^g	linearized voltage or current components in global reference rotating frame
Δf_d^g	linearized voltage or current components in global reference rotating frame
ω_{SBS}	Local energy storage frequency
i_{dq}^{GBS}	dq axis components of the converter current
v_{dqBS}^{S}	dq axis components of the converter voltage
v_{dq}^{GBS}	dq axis components of bus voltage
KpdBS	Proportional gain of energy storage voltage regulator in d axis
KpqBS	Proportional gain of energy storage voltage regulator in q axis
KpidBS	Integral gain of energy storage voltage regulator in d axis
KpiqBS	Integral gain of energy storage voltage regulator in q axis
β	Percentage of the reactive power capability increased in respect to the rated active power
α	Percentage of the rated active power reduction
$P_{\text{rated}}^{\text{BS}}$	Energy storage rated active power
$P_{\text{req}}^{\text{BS}}$	Energy storage required active power for voltage support
$Q_{\text{insd}}^{\text{BS}}$	Energy storage increased reactive power
$v_{\text{thred}}^{\text{PCC}}$	PCC voltage threshold
$P_{\text{thred}}^{\text{BS}}$	Active power threshold
$Q_{\text{thred}}^{\text{BS}}$	Reactive power threshold
$v_{\text{mead}}^{\text{PCC}}$	Measured PCC voltage

Table of Contents

Abstract ii

Declaration iii

Acknowledgements iv

List of Publications v

List of Figures xiv

List of Tables xix

Chapter 1 : Introduction 1

1 Distributed Generation 4

1.1 Distributed generation international review and UK relevance 4

1.2 Impacts of distributed generation 6

1.3 Major positive impact of distributed generation 6

1.4 Major negative impact of distributed generation 7

1.5 Summary 9

2 Mitigating issues associated with DG in the distribution network 10

2.1 Distribution flexible alternating current transmission system devices 10

2.2 Active power curtailment 11

2.3 Demand side response 12

2.4 Energy storage system 12

2.5 Summary 14

3 Approach and Objectives 14

4 Network description and source data 15

5 Contributions 17

6 Thesis Layout 18

Chapter 2 : Potential roles and operational control strategies for energy storage in LV distribution networks 20

1. Potential role for energy storage in the low voltage distribution network 21
1.1 Introduction of energy storage system and its relevance technologies 22
2 Operational control strategies of energy storage systems for voltage support 30
2.1 Decentralised, centralised, and coordinated control of storage units 30
2.2 Energy storage power circuit 35
2.3 Energy storage low level control and measurement 36
3 Summary and conclusion 40
Chapter 3 : Functional strategies for use of energy storage system for voltage support 42
1 Introduction 42
2 Theory 42
2.1 Experimental technique 42
2.2 Real time digital simulator 44
2.3 Voltage sensitivity factor 45
3 Case Study 1: Using a smart grid laboratory to investigate battery energy storage to mitigate the effect of PV in LV distribution network 46
3.1 Introduction 46
3.2 Energy storage implementation 48
3.3 Simulation results 49
4 Case Study 2: Coordinated voltage and power flow control in LV distribution Network 53
4.1 Introduction 53
4.2 Coordinated control of the storage unit and the OLTC 54
4.3 Source data and network description 56
4.4 Simulation results 57
5 Summary and Conclusion 61

Chapter 4 : Coordination of multiple battery energy storage units in a low voltage distribution network 62
1 Introduction 62
2 Proposed coordinated control method for multiple storage units 63
2.1 Design of decentralised controller 64
2.2 Design of centralised controller 66
2.3 Implementation of coordinated control scheme 70
3 Description of case study 72
3.1 Network Description and Source Data 72
3.2 Simulation Techniques 73
4 Application of coordinated control to case study network 75
4.1 Real Time Steady State Implementation 75
4.2 Asset Management 79
5 Discussion 82
6 Summary and Conclusion 84
Chapter 5 : Small signal stability analysis of energy storage for voltage support based the LV distribution network 86
1 Introduction 86
2 Small signal stability of the dynamic system 87
3 Description of Case Study Network 89
4 Formulation of state space model 90
4.1 Small signal model of the energy storage converter model and its control systems 94
4.2 State space model of the PV generator 101
4.3 Small Signal Dynamic Model of Case Study Network 103
4.4 Steady space model of the overall system 105

to determine the system is asymptotically stable or marginally stable..... 107
5 Eigenvalue analysis of the overall system 107
5.1 Eigenvalue analysis 108
5.2 Simulation studies..... 112
6 Discussion 115
7 Summary and conclusion 117
Chapter 6 : Active and reactive power control strategy of the energy storage for voltage support in LV distribution network in respect to small signal stability..... 118
1.1 Introduction 118
2 Theory of active and reactive power operation of the energy storage 119
3 Method to implement active/reactive power control of the energy storage for voltage support in the LV distribution network in respect to small signal stability 121
3.1 Preliminary evaluation of active and reactive power setting of the energy storage for voltage support in the case study network 124
3.2 Small signal stability analysis of energy storage active/reactive power at different operating conditions 127
3.3 Proposed active/reactive power operation control strategy of the energy storage for voltage support..... 129
4 Description of case study and simulation results..... 131
4.1 Case study 1: Step changed solar irradiation 133
4.2 Case study 2: Real solar irradiations 135
4.3 Energy storage state of charge..... 138
5 Discussion of Results 139
6 Summary and Conclusion 140
Chapter 7 : Discussion, Conclusions and Further Research..... 141
1 Discussion..... 141
1.1 Control 141

1.2 Low level control 145
1.3 Modelling and Analysis 146
1.4 Steady state modelling and analysis 146
1.5 Dynamic modelling and analysis 147
1.6 Tools 149
1.7 Summary of discussion 150
2 Conclusion 151
3 Further research 152
Appendix I

List of Figures

Figure 1-1: Transmission electricity operating regions in the UK 1

Figure 1-2: Distribution electricity operating regions in the UK 2

Figure 1-3: Cumulative solar generators monthly deployment 5

Figure 1-4: Benchmark residential urban radial distribution network, and there are 106 residential loads with 42 PV generators in feeder 4 16

Figure 1-5: (a) Load profiles (b) three irradiance profiles 17

Figure 2-1: UK energy storage projects deployment between 2013 and 2020..... 21

Figure 2-2: Comparison of storage technologies 22

Figure 2-3 Cost for energy storage systems 23

Figure 2-4: The concept of decentralised control of storage units..... 31

Figure 2-5: The concept of centralised control for storage units..... 32

Figure 2-6: Coordinated control of storage units 33

Figure 2-7: Overview of developed coordinated controller containing a centralised controller interacting with several decentralised BESS controllers..... 35

Figure 2-8: Schematic diagram of energy storage 35

Figure 2-9: Energy storage unit hierarchical control interface based on voltage controller (a) block diagram of power circuit and control structure (b) block diagram of voltage control scheme 37

Figure 2-10: External voltage regulators for terminal voltage regulation 38

Figure 2-11 External active/reactive power controller for power regulation..... 38

Figure 2-12 External frequency droop controller for power sharing..... 40

Figure 3-1 Layout of PHIL Emulation 43

Figure 3-2: Two bus distribution system with embedded PV generation..... 47

Figure 3-3: Voltage variation with solar irradiance at the end of the feeder, 10:40-11:00, 6th June 49

Figure 3-4 Cumulative distribution function of voltage at the end of feeder at 6th June 50

Figure 3-5 Total probability of overvoltage (greater than 1.1p.u.) for the different simulations 51

Figure 3-6 Voltage rise reduction by energy storage at time 10:40-11:00, 6th June 52

Figure 3-7 VUF before and after integration of storage, 10:40-11:00, 6th June 52

Figure 3-8 RTDS (Emulated) storage charging power, 10:40-11:00, 6th June..... 53

Figure 3-9 Coordinated control of voltage and power flow 55

Figure 3-10 the case study network with high penetration of HP, EV and solar PV . 56

Figure 3-11 Average domestic daily load profile and typical consumption profile of HP and EV 57

Figure 3-12 Average PV profile from 20 British Gas domestic customers in 2011 ... 57

Figure 3-13 Projected daily power flow profile of LV distribution transformer 58

Figure 3-14 Feeder end voltage in baseline study and with coordinated control 58

Figure 3-15 Transformer reverse power flow absorbed by battery 59

Figure 3-16 Charging power of the storage 59

Figure 3-17 Voltage at the end of the feeder in baseline study and with coordinated control 60

Figure 3-18 Transformer power flow mitigated by storage 60

Figure 4-1: Coordinated control of multiple energy storage units 63

Figure 4-2: Decentralised controller of BESS; (a) Q-operation (b) P-operation 65

Figure 4-3: Battery cycle to failure trend based on both original and curve fitting data 70

Figure 4-4: the main flowchart of proposed coordinated control scheme 71

Figure 4-5: Benchmark residential urban radial distribution network 73

Figure 4-6: Comparison between results from MATLAB and RTDS simulations 74

Figure 4-7: (a) Average voltage profiles at branch 4 with non-coordinated and coordinated control (b) BESS4 SoC with coordinated control at time between 9:00 and 15:00 76

Figure 4-8: Performance between 11:30 and 14:00, detailing (a) average voltages at branch 4 under coordinated and non-coordinated control, (b) active power imported to BESSs under non-coordinated control, (c) active power imported to BESSs under coordinated control, (d) coordinated control signal to BESS3 from branch 4 and (e) coordinated control signal to BESS1 from branch 4. 78

Figure 4-9: Active power charged and discharged from BESS4 with its SoC during one whole day 79

Figure 4-10: Remaining cycle life of each BESS without the aging model being implemented in the coordinated controller 80

Figure 4-11: Remaining cycle life of each BESS with the aging model implemented in the coordinated controller 80

Figure 5-1: Single line diagram of the case study LV distribution network under consideration 89

Figure 5-2: The process of small signal analysis based on object oriented approach 91

Figure 5-3: Global and local rotating reference frames of the case study network ... 91

Figure 5-4: Block diagram of small signal model of the case study network 93

Figure 5-5: Three phase equivalent circuit of VSC AC side 94

Figure 5-6: Voltage regulation control loop for d axis 97

Figure 5-7: d axis Inner current control loop 98

Figure 5-8: Equivalent case study network 103

Figure 5-9: Dominant cluster of eigenvalues under designated operating condition 109

Figure 5-10: Eigenvalue locus with energy storage voltage controller gain KpdBS change 110

Figure 5-11: Eigenvalue locus with energy storage voltage controller gain KqdBS change 111

Figure 5-12: Eigenvalue locus with PV generator controller gain KpdPV change .. 111

Figure 5-13: Energy storage voltage controller response to step changes in the PV generator (a) Solar PV outputs (b) Energy storage active/reactive power corresponding with changes in PV generator (c) Close look of dynamic response of energy storage at 2 seconds (d) Current IdBS and IqBS (e) PCC voltage after controlled by energy storage 113

Figure 5-14: Energy storage voltage controller response to the change of the real solar irradiance..... 116

Figure 6-1: Rated active power reduction corresponding to the capability of reactive power increasing 120

Figure 6-2: Percentage of increased reactive power related to percentage of rated active power reduction 121

Figure 6-3: Flow chart illustrating procedures used in this thesis investigating the active/reactive power control of energy storage for voltage support in the LV distribution network 122

Figure 6-4: Storage rated active power reduction corresponding to the increased reactive power capability for voltage support (a) active/reactive charging from the storage at PV output 150kW (b) active/reactive charging from the storage at PV output 200kW (c) active/reactive charging from the storage at PV output 250kW (d) active/reactive charging from the storage at PV output 300kW 125

Figure 6-5: Active power redundancy with different reduction percentage of the rated active power of the storage corresponding to different PV output 126

Figure 6-6: Locus of eigenvalues variation with exchanging power of the energy storage for voltage support at different PV outputs (red cross represented for 30% reduction of the rated active power, incorporated with the increased reactive power, blue cross represented for using active power only 128

Figure 6-7: Flowchart of the energy storage active/reactive power control strategy for voltage regulation 130

Figure 6-8: Step changed PV profile applied for first case study [note that the time axis has been compressed to the time represented in the simulation] 132

Figure 6-9: Real solar irradiance PV profile applied for second case study [note that the time axis has been compressed to the time represented in the simulation 133

Figure 6-10: Simulation results of proposed voltage regulation controller for voltage support under step changed solar irradiance (a) Voltage controlled by voltage regulation controller compared with baseline voltage (b) Voltage regulation by using active power solely imported to the energy storage (c) Proposed active/reactive power control strategy for voltage regulation..... 134

Figure 6-11: Simulation results of proposed voltage regulation controller for voltage support under real solar irradiance (a) Baseline voltage (b) PCC voltage profiles with active power control only and with proposed active/reactive power control strategy (c) Voltage regulation by using active power solely (d) Proposed active/reactive power control strategy for voltage regulation (e) Close look of reactive power performance at time period T2 (f) Close look of reactive power performance at time period T4 (g) Close look of reactive power performance at time period T5 137

Figure 6-12: Comparison with SoC under active power control only and proposed active/reactive power control..... 138

List of Tables

Table 2-1 Energy storage technologies cost and characteristics 24

Table 2-2 List of battery energy storage projects in LV and MV networks in the UK 26

Table 2-3 Benefits of energy storage to LV distribution networks 28

Table 3-1 Load and solar irradiance profiles used 47

Table 4-1: Threshold values for determine control action for overvoltage condition. 65

Table 4-2 Selected threshold and time constant for case study 75

Table 4-3: Cost of ownership with and without aging model 81

Table 4-4: Summary of losses with and without aging model with 75% efficient BESSs and a loss incentive of £60/MWh 81

Table 5-1: System operating parameters 107

Table 5-2: Eigenvalues of the case study system 109

Table 6-1: System operating points corresponding to sensitivity analysis of the system eigenvalues 127

Chapter 1: Introduction

The Great Britain (GB) transmission electricity network carries the bulk movement of power at extra its high voltage 400kV, 275kV, and 132kV assets that connect separately owned generation and distribution systems through approximately 23,000 km of lines [1]. It is owned and maintained by three regional transmission companies as seen by Figure 1-1. National Grid Electricity Transmission plc (NGET) operates electric power transmission network in England and Wales [2]. In Scotland, the operation and ownership of Scottish Power Transmission Limited is in Northern Scotland, and a tie line is interconnected from Northern Scotland to southern and central Scotland which is operated and owned by Scottish Power Transmission Limited [3] [4]. The GB transmission power system as a whole is operated by a single Transmission System Operator (TSO). This role is performed by NGET that mange the security of the GB power network to maintain and balance the supply with demand on real time basis [5].

Figure 1-1: Transmission electricity operating regions in the UK [6]

In GB, Distribution Network Operators (DNOs) operate the distribution network that transport the electricity from the transmission level to residential homes and

businesses [7]. Currently, six different groups own fourteen licensed DNOs as shown in the GB (Figure 1-2) [7][8].

Since TOs and DNOs are natural monopolies, the amount charged by these companies is regulated by The Office of Gas and Electricity Market (Ofgem) [5][8]. As the regulator, Ofgem has a major role in protecting customers' interests by regulating activities of these electricity groups [9]. This is done through ensuring competition, the delivery of Government schemes, investment and the development of a more environmentally sustainable system for present and future generation [9].

Figure 1-2: Distribution electricity operating regions in the UK [7]

The existing UK electrical power system is currently experiencing a period of fundamental change in the energy landscape [1]. At the end of 2015, intermittent renewable electricity capacity in the UK reached 29.7 GW [10]. This increased by 26% compared to the year before [10]. According to [11], the installed capacity of solar power has increased to 8.8 GW in the year of 2015. This is 29% of all renewable capacity. In addition, electricity produced by wind power delivers a rising percentage of the energy with approximately 13.6 GW of installed capacity [12]. This consists of 8.5 GW onshore capacity and 5.1GW offshore capacity [12]. Presently, solar and wind power has the largest share of

renewable capacity around 75% in the UK [11]. Bioenergy is subsequently shared the renewable capacity of 18% [12]. In 2020, renewable electricity contributions in the UK will ensure that 15% of energy needs will be met from these green resources. This helps meeting objective in the 2009 EU Renewable Directive [13].

According to Climate Change Act, the UK government has set a legally binding target to reduce greenhouse gas emissions by 80% by 2050 [14] [15]. The act introduced a system that restricts the total amount of carbon emission in a given time period [14]. For the electricity sector, this act is able to force an increasing amount of energy used in the UK to come from low carbon technologies, such as renewables and nuclear. It can help the UK electricity to continue to be a secure supply of energy, and cut the greenhouse gas emission and stimulate investment in new businesses and jobs [16]. In order to decarbonise, the generation mix in the UK will have to change. This is shaped by displacing the traditional generation technology with increased capacity of renewable generation [17]. Accordingly, future electricity networks will face significant challenges, and the UK energy industry has to provide low carbon energy in an affordable, secure and sustainable way [18]. If large intermittent renewable energy generating plants connect to the high voltage transmission network, more flexible and secure system operation is firstly required with more widespread deployment of balancing technologies, such as demand side response (DSR), energy storage, and interconnection to balance supply and demand [17][19]. Secondly, the electricity market and network will require a significant change to deliver the scale of the long term investment needed [20]. Thirdly, it is likely to look towards “smarter” ways of operating the electricity network to cope with the large integration of renewable energy and the advert of varying load profiles [20]. “Smart” comprises a series of technologies, such as the use of dynamic ratings to enhance lines thermal rating, and coordinated High Voltage Direct Current (HVDC) control systems which work in parallel with the High Voltage Alternating Current (HVAC) systems [20].

At distribution level, renewable energy sources connecting to the networks are called Distributed Generation (DG). If a large number of small renewable sources are connected throughout distribution networks, this is likely to pose a

threat to distribution networks secure operation, such as reverse power flow, power quality issues, oscillatory stability and fault level contributions [21]. A number of pathways to achieve carbon reductions up to 2050 are proposed in [15] and [22]. Under all future scenarios, there is expected to be large increase in renewables embedded in distribution power systems. Therefore, the effects of DGs on the power system and its advantages and disadvantages are now presented.

1 Distributed Generation

DG is also known as distributed energy resources (DER) or embedded generation (EG) [23] . It is often defined as small scale power generators that are typically in the range of 1kW to 10MW [24][25]. These small/medium scale generating systems often use the renewable energy technologies, such as wind, photovoltaic (PV) and combined heat and power (CHP), to connect to power distribution networks rather than at transmission level [23][25]. DG systems are different from traditional centralised power generators, such as coal fired or nuclear powered plants. In contrast, DG systems are decentralised and simpler to deploy that allow homes or businesses to be driven by their own electric renewable energy systems [25].

1.1 Distributed generation international review and UK relevance

Due to concerns of climate change, the recent legislative trends launched around the globe are likely to increase the utilisation of DG units in distribution power systems. Feed in Tariffs (FiT) have encouraged, the use of small/medium scale DG units with the capacity dramatically increased to 87.3 GW worldwide in the year 2014 [26]. This capacity will be doubled to 165 GW by 2023 [26]. The aim of FiT is to encourage the development of small/medium scale renewable and low-carbon electricity generation technologies in distribution networks [27]. This scheme is intended to overcome barriers that confront market entry for DGs [28]. It is used to provide cost based compensation to renewable energy DG units' users, and offer price certainty and long term contracts that help finance renewable energy investment [28] [29].

In the UK, FiT scheme was introduced on 1st April 2010 by the Department of Climate Change (DECC) [30] [27]. This scheme enables domestic

customers/businesses to get payments from their energy supplier [31]. Most renewable energy techniques qualify for the scheme, including solar generators, wind turbines, hydroelectricity, and CHP [31].

Since the FiT scheme launched, a large number of DG units have been installed in the UK. Many residential customers have purchased small scale rooftop PV systems. In 2013, the UK was ranked in sixth position globally for the most solar PV capacity installed in the small scale segment [32]. These small scale PV generators are less than or equal to 100 kW, and are comprised of residential and non-residential rooftops [32]. For homeowners, the residential PV generators are less than 4 kW in the UK [32]. These residential solar generators are able to reduce homeowners' consumption of grid electricity and gas during the daytime, and this also reduces these customer's energy bills in addition to gaining revenue from the FiT. At the beginning of 2015, the overall capacity of solar PV has reached 5.143 GW as shown in Figure 1-3[33][34], which is produced from around 659,000 installations. Most of these PV systems have been installed in low voltage (LV) distribution networks.

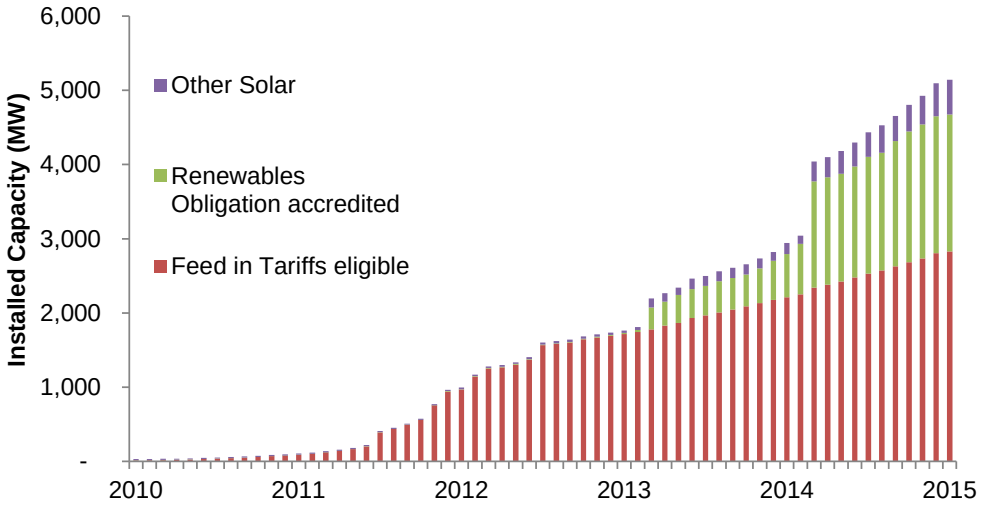

Figure 1-3: Cumulative solar generators monthly deployment [33]

In the UK, the installed capacity of wind power has reached 12 GW with 7,950 MW of onshore capacity and 4,050 MW offshore capacity in 2015 [35]. Apart from large scale onshore/offshore wind turbines installed that are connected to the transmission level or sub transmission level, a large number of small and medium scale wind turbine (with installed capacity approximately 70 MW) have

powered many homes and businesses in the UK distribution network. Small wind turbines are designated as up to 50 kW, and these are suitable for homes or small farms [10][36]. Medium wind turbines are designed between the range 50 kW and 500 kW, and are best for large farms, communities and businesses [10][36]. These small/medium wind turbines installed enable customers to gain the benefit from the FiT as well [37].

In addition to these forms of generation, there are few examples of small scale hydro installed in the UK. This is limited uptake due to the fact that there are few locations where this type of generator can be installed.

1.2 Impacts of distributed generation

DG systems serve as a supplement to the power system. Although these small/medium scale generating systems are attractive to limit greenhouse gas emission and reduce power transfer through high loss transmission lines, these DGs also may pose a threat to distribution systems secure operation [38]. This is mainly because the existing passive distribution networks have not been designed to include these new forms of generators.

1.3 Major positive impact of distributed generation

Undoubtedly, DGs, such as solar PV or wind power, are considered to be those that are clean, reliable, low cost and inexhaustible [39]. Large increase in renewables embedded in distribution network is an effective and attractive way to reduce carbon footprint. With integration of DGs can also offer many potential benefits to distribution systems planning and operations [38]. On a local basis, there are opportunities for DNOs to employ these DGs to reduce peak loads and to provide ancillary services to improve power quality [38]. These DG units, including solar, micro turbines, and wind systems require power electronics converter systems for grid connection. This means that DGs can provide fast and flexible control of voltage and real/reactive power of the unit. This can be done by DNOs to provide financial incentives to customer owners of DG units to dispatch them for peak demand period and at other times of system need. However, according to IEEE 1547, DGs currently are not allowed to provide power or ancillary services, and they must operate with fixed power factor with respect to the local system [40] [41].

In addition to the potential benefits for distribution system planning and operations, these small/medium scale generators can also be used to provide customers' requirements for most of the time. The customer can be able to export excess generation to the grid or purchase some generation from the grid if their owned generation cannot meet their demand [42].

Introducing these low cost, small/medium size generator units can provide customer's demand requirement locally so that this can reduce the power transfer of electrical energy from high loss transmission lines [42].

1.4 Major negative impact of distributed generation

Although increasing numbers of DGs, such as wind or PV, have had positive effects in helping countries achieve their climate targets, large quantities of DGs connections can raise several technical concerns in the operation of distribution systems. For example, these will turn distribution networks from being conventional passive to active. Some of problems are reported in [43][44], and it is summarised as follows:

Steady state voltage

Steady state voltage problems involve over and/or under voltage situations for the durations longer than 1 minute [45]. Steady state overvoltage is described as voltage magnitude is above its nominal value. On the other hand, steady state undervoltage is under its nominal value. Static voltages can affect the performance of appliances and electrical equipment connected to the network and will change with different loading conditions [46]. In the UK, the steady state voltage variation must not be exceeded 10% above or 6% below the nominal value in LV distribution networks [47]. In medium voltage (MV) distribution networks, steady state overvoltage must not be exceeded 6% above or 6% below [47]. Large amounts of DG, such as solar generator/wind power, introduced at a distribution network may result in loss of steady state voltage regulation if the existing voltage control cannot respond to excessive in PV/wind power output for long duration [48][49].

Losses and reverse power flow

DG units can affect power losses as they change the magnitude and direction of the power flow [50]. Excessive amounts of DGs connection can cause reverse power flow and losses increased [50][51]. Many research works have considered the optimal size and location of DG units installed in distribution networks to minimise losses [52].

Power quality and reliability

Power quality of the system may be adversely affected by introducing a large number of DGs in distribution networks. For example, DGs employ power electronics converter systems for grid connection. This can lead to increased emission of harmonics and mutual disturbances. Harmonics have a wide range of impacts on the network components and customer side of the system [53][54]. This would result in variation in root mean square (rms) voltage and flicker, thermal effects on transformers, rotating generators and motors, disturbances of electronics equipment and system resonance [53]. Therefore, different filtering techniques to reduce harmonics caused by DGs have applied in [55][56].

Additionally, fast fluctuation of PV or wind power output can result in voltage fluctuation. Voltage fluctuations are general variations of the voltage envelope or random voltage changes [57]. It can result in degradation of equipment service life and their performance, and cause instability of the internal voltages and currents of electronic equipment [58][59]. This is also disturbance for customers because it may cause fluctuating brightness of lights for instance [60][61].

Reliability issue is also a major concern in distribution networks. Intermittency power out of DG units always challenges the power management system and system reliability [62].

Transient voltage will happen at the point of common coupling of a DG as a result of sudden connection/disconnection of these DGs [44].

Voltage unbalance is a power quality issue within the low voltage distribution network, exacerbated by large presence of the random location and rating of PV

generators. This must not exceed 1.3% for the systems with a nominal voltage below 33kV [63]. Unbalanced voltages can lead to power loss in LVDNs and it can severely affect the power system equipment as a small unbalance in the phase voltages can lead to an excessively larger unbalance in the phase currents [64].

System stability

Market deregulation and environmental concerns have encouraged renewable energy to be installed largely in distribution networks. As such, distribution networks are facing different types of stability issues. In [65], different oscillatory modes and their dominant generators have been identified in a distribution network under large integration of solar PV generators and wind power generations. Low damped oscillatory modes with frequencies 1.5-4Hz were observed in the network [65]. This is harmful to the stability of a system.

The transient stability of a distribution system with high commitment of DGs and synchronous generators is reported in [66]. The finding shows that large number of DG connection can result in greater maximum rotor speed deviation [66]. This can cause system instability.

Other issues

In addition to the issues discussed above, DGs can contribute increasing short circuit level [44]. Re-coordination of the protection system may be required due to the DG contribution to the fault level [44] [62] .

1.5 Summary

Although such distributed renewable energy units have many benefits to their owners, they are challenging for network operators. Main Issues introduced by presence of DG units in distribution networks are summarised and presented as

- Steady state overvoltage can occur if the existing voltage control in a distribution network cannot respond to excessive in DGs power output for long duration.
- If DG units' outputs are greater than local demand, this can cause reverse power flow and increased losses.

- Power quality issues can be presented as voltage fluctuation, harmonics distortion, voltage imbalance.
- Different types of system stability issues, such as small signal stability and transient stability, can occur if renewable energy units are installed largely in distribution networks.
- DGs can increase short circuit level, and re-coordination of the protection system is therefore required.

Challenges mentioned above are widely seen to be the major impact of DG units on distribution networks in respect with safety and secure operation of a network. As such, these issues presented need to be mitigated to allow wide spread integration of DG units in the distribution network.

2 Mitigating issues associated with DG in the distribution network

To overcome challenges that are caused by presence of DG units in distribution networks, several technologies are introduced in this section.

Currently, there are a number of different technologies that can be able to overcome challenges introduced by utilisation of renewable energy in distribution networks. The characteristics of these technologies are discussed as following.

2.1 Distribution flexible alternating current transmission system devices

The concept of flexible alternating current transmission system (FACTS) is a family of power electronics based devices, such as static synchronous compensator (STATCOM) and static VAR compensator (SVC), that can be used to enhance AC system controllability, stability and power transfer capability as well [67]. Similarly, on the distribution side, these power electronics based devices are commonly called distribution FACTS (DFACTS). These compensators can address power quality problems, such as voltage harmonics, source current harmonics and voltage imbalance, and can be used for voltage support as well [68].

In [69], the application of distribution STATCOM (DSTATCOM) for improving power quality issues that introduced to the grid by DGs was investigated. The

DSTATCOM is a shunt device and apply its reactive power function that can operate in current control model for compensation overvoltage/undervoltage, voltage imbalance [69]. The series connected DFACTS device, which is commonly called dynamic voltage restorer (DVR), was used to compensation of grid harmonics and voltage sag [70] [71]. Furthermore, an application of DSTATCOM based on genetic algorithm (GA) was proposed for harmonics reduction and mitigation of voltage fluctuation [72].

In addition to improve power quality, these DFACTS devices can also be used for enhancement of PV installation capacity in distribution systems [73][74]. In [68], the use of DSTATCOM in reactive power compensation for grid voltage control during fast fluctuation of solar irradiance to increase the PV installation capacity without voltage violation was investigated.

Power flow control methods based on DFACTS devices with DGs are reported in [75][76]. In addition, transient stability issues of a distribution network with DGs and DFACTS was investigated [77]. The results showed that using DFACTS devices can effectively improve transient stability of a distribution network [77].

DFACTS devices use their reactive power function that is suitable for overcoming the challenges introduced by DGs. However, due to the low X/R ratio in LVDN, these devices are not very effective for LV voltage support [78].

2.2 Active power curtailment

Active power curtailment (APC) is a droop based technique that can be used to reduce the amount of active power injected by DGs in terms of PV inverters, in order to avoid overvoltage [79]. This technique can meet the requirement of voltage support in the LV distribution network. In the UK, the APC is likely to be required as the LV distribution network has high R/X ratio for example [80]. In [81], droop coefficients of APC for each PV generator are different so that the proposed APC scheme not only can prevent overvoltage, but also affect feeder end PV owner's revenues. In [82], overvoltage prevention based on APC is introduced by reducing PV generators output according to the same droop coefficients. Therefore, the capacity of reactive power outputs of solar generators' inverter is increased. This can help prevent overvoltage. However,

the strategy introduced in [82] is undesirable in the LV distribution network because of high R/X ratio. In addition, although the APC prevents overvoltage, this reduces PV system owners' profits and the amount of renewably generated energy. As such, the APC method is not suitable for meeting the low carbon footprint.

2.3 Demand side response

Demand side response (DSR) means changing the time that equipment is used or adjusting the power consumption of devices [83]. This can be achieved through changing the behaviour of customer premises and/or automated control of loads [83] . DSR can also provide voltage control but requires demand with suitable characteristic [84]. As reported in [85], voltage violation caused by large number of installation of DGs can be solved through demand shifting to increase the load on the network and therefore alleviate the overvoltage. The major benefits and challenges of electricity DSR are presented in [86]. DSR can be used to increase the installation of DG units and relieve voltage constrained power transfer problems [86].

According to sensitivity analysis in [85], customers at the end of feeders are most effective to shift load as they have a larger impact on network voltages. However, this is not appropriate under the current UK regulation policy because the energy market needs to treat all customers equally. In addition, according to [86] and [87], there are many exiting barriers to apply DSR in distribution networks. For example, it is difficult to convince customers to change their energy usage behaviour as this technique may pose a threat to customers' privacy [87]. In addition, although the benefits and value of DSR are flexible for providing both system operation and development, there has not been enough clarity due to lack of methodologies for the quantification of costs and benefits [86].

2.4 Energy storage system

Compared with technologies discussed above, a storage device, whether installed at the secondary substation or distributed along the feeders, can be used for mitigating all challenges that caused by large number of DGS units connection in the distribution network. Benefits of energy storage in distribution

networks contain: voltage regulation, power flow management, peak shaving, power factor correction, mitigation of power quality issues, such as voltage swell/sag, voltage imbalance, voltage fluctuation and harmonic reduction [88].

In [89], a strategy based on battery energy storage system (BESS) for voltage support is proposed. The proposed strategy controls the BESS to export active and reactive power, with reactive power priority. The export of active and reactive power from the energy storage system is optimized for voltage control by using the ratio of voltage sensitivities of active and reactive power export, to minimize the BESS size.

A coordinated voltage control scheme integrating the energy storage is proposed under unbalanced conditions [90]. The energy storage is operated cooperatively with an on-load tap changer (OLTC) to mitigate overvoltage and voltage unbalance problems. In [91], the energy storage in a low voltage microgrid is used to charge/discharge its active/reactive power functions according to assumed schedule and to compensate for current harmonics, unbalance and voltage fluctuation. Therefore, the proposed control strategy of the energy storage can be able to overcome various technical issues generated by DGs integration.

A systematic small signal model that covers energy storage and DGs in a micro-grid is presented [92]. The model is analysed based on eigenvalues and sensitivity to different operating points and control strategies of DG or energy storage device. It is observed that the storage unit can significantly improve the system dynamic stability and mitigate the instantaneous active/reactive power unbalance that caused by utilisation of renewable energy [92]. The similar approach is developed in [93], the storage is concluded to improve system stability in micro-grid by injecting active/reactive power during power shortage, DG trip, islanding, and load dynamics.

In addition, a power flow management and voltage control strategy based on the energy storage in a 11kV UK distribution network is evaluated [94]. It is reported that the energy storage is desirable to reduce the steady state voltage fluctuation and reduce reverse power flow if DG units' outputs are greater than local demand.

2.5 Summary

DFACTS devices can mitigate challenges that caused by DGs in distribution networks. However, these devices can only able to provide reactive power function which is not desirable for the LV distribution network in the UK due to the low X/R ratio. In networks with a low X/R ratio, such as in the residential LV networks in the UK, active power is much more effective for voltage control.

Although DSR and APC are effective for curtailment, there are many existing barriers to apply both technologies in distribution networks. In addition, these two technologies are not able to provide ancillary services, such as improving power quality and system stability, for secure operation of a distribution network.

The energy storage system is a controllable device which allows power to be imported or exported as needed by the network. It is seen as one form of mitigation method to reduce impacts of DGs on distribution networks in terms of high R/X ratio LV networks. However, although many studies quantify benefits of energy storage to distribution networks at planning stage, there is little research study which looks at how to operate one or multiple energy storage to overcome issues caused by DGs in LV distribution networks.

3 Approach and Objectives

The work in this thesis primarily deals with operational control strategies for energy storage systems for voltage support in LV distribution networks. The following methodology is employed:

- **Real time simulation**: The real time simulation of energy storage average model based on classical the dq decoupling control method is first developed in a Real Time Digital Simulator (RTDS) to analyse and propose operation control strategies for energy storage for voltage support and reverse power flow. The RTDS model can provide detailed information of real-time performance of these models. The proposed coordinated multiple energy storage control scheme in a LV distribution network is also developed in RTDS, in order to assess the dynamic performance of the proposed coordinated controller.

- **Hardware implementation**: The experiment implementation in this work is achieved using the real time power hardware in the loop (PHIL) in a Smart Grid Laboratory. The experimental network is connected to the RTDS system through 3-phase power amplifier. This contains a PV emulator, an energy storage unit and RTDS/amplifier network emulation system.
- **Linear model development**: Small signal dynamic results are presented from eigenvalue analysis of the system linearized model and a further application is proposed. The small signal linearized system model is numerically analysed in the MATLAB environment. The Simpower based average model is also used to simulate time domain simulation to verify the accuracy of the linearized model and control strategies for energy storage for voltage support.

4 Network description and source data

The work from this thesis has particular focus on the UK power system especially that in the North West of the UK where the project sponsor, Electricity North West Limited (ENWL), operates a LV distribution network.

- **Network structure**: Using maps of the distribution network and technical data provided by ENWL, a 4 wire LV model has been developed. One feeder is modelled in detail; it contains 106 domestic loads of which 42 have PV systems as shown in Figure 1-4. The network has a relatively high R/X ratio value (3.75—6.25). This means that active power is much more effective in voltage support. A 3 kW rated PV system is placed on every domestic property with a roof facing ±30° of due south. The position of the secondary transformer LV fixed tap position (1.03p.u.) is chosen to prevent voltage drop, while maximising the voltage rise headroom in the LV network. The UK regulation on the steady state voltage is applied, in which the customer voltage must be in the range 230 V +10%/−6% [95]. A 2.5 km feeder from the primary substation is included in the model.
- **Load profile**: the load data has been collected from LV monitoring equipment connected to secondary transformers in the ENWL network

as shown in Figure 1-5(a). Each load has an after diversity maximum demand (ADMD) of 1.2 kW, and ADMD represents the maximum demand which the electrical distribution network (local transformer) is required to supply, expressed as an average per property.

- **Solar irradiance profile**: Since a PV generator has no inertia in the form of rotating mass, the rate of change of solar power output can change rapidly [96]. To reflect the effectiveness of operational control strategies for energy storage systems for voltage support in LV distribution networks, three realistic solar irradiance data with a 6 second resolution (see Figure 1-5 (b)) are selected and collected from a domestic property in Retford, Nottinghamshire, U.K. (at latitude northern 53.3169°N and 0.9408°W Western longitude). As depicted in Figure 1-5 (b), these three different solar irradiances contain different amounts of fluctuation in output that may have different effects on the use of energy storage for voltage support.

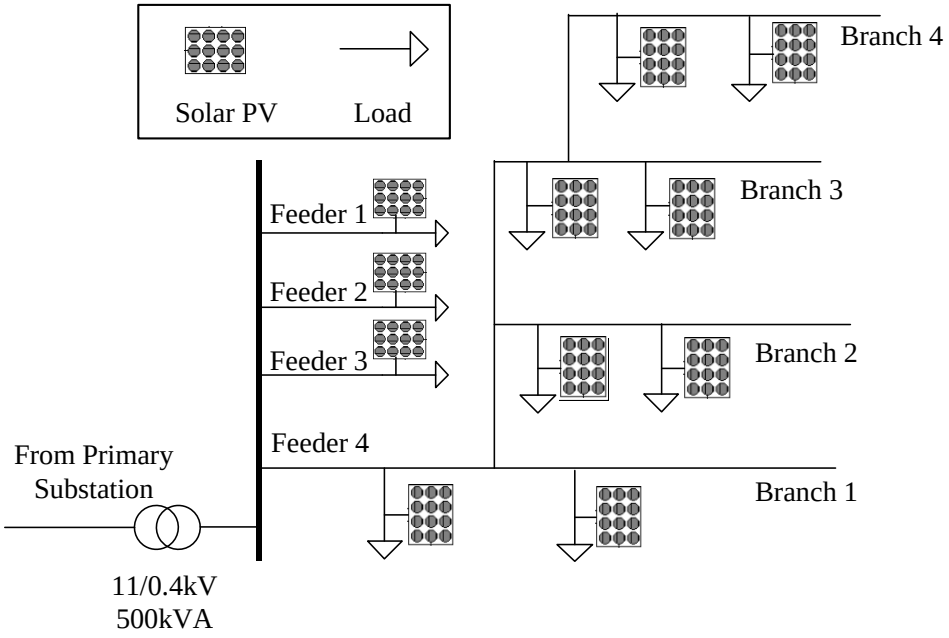

Figure 1-4: Benchmark residential urban radial distribution network, and there are 106 residential loads with 42 PV generators in feeder 4

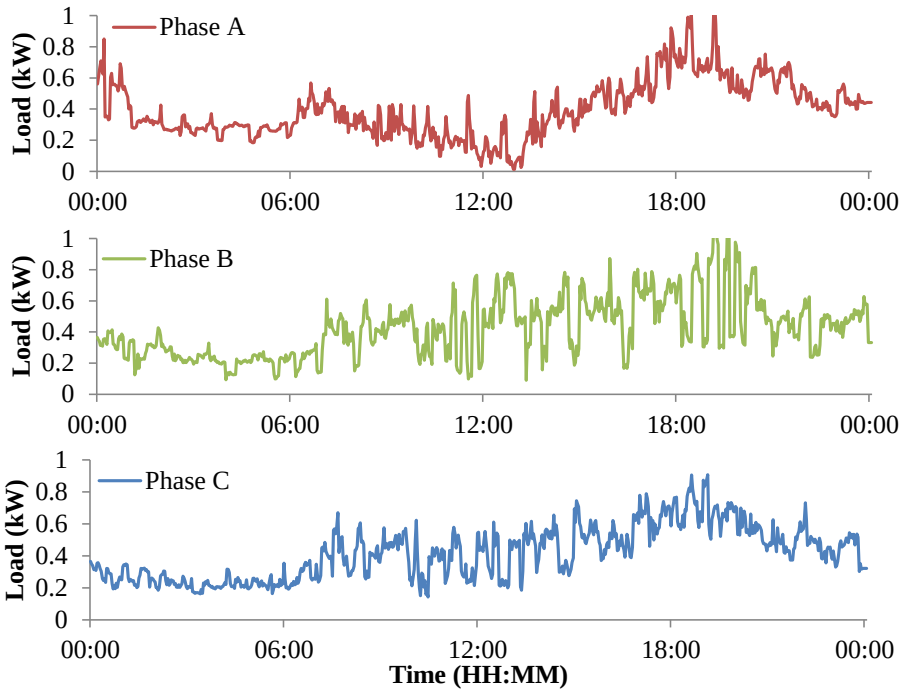

(a)

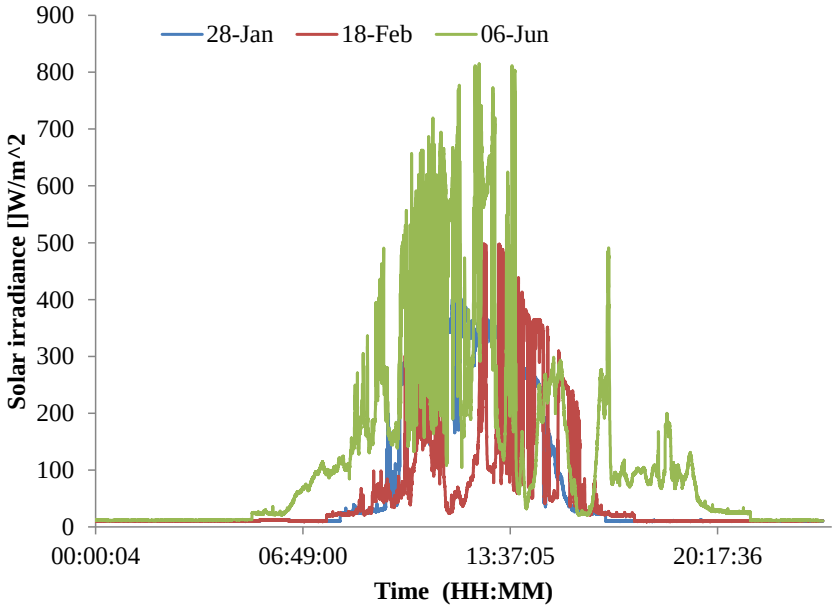

(b)

Figure 1-5: (a) Load profiles (b) three irradiance profiles

5 Contributions

Contributions of the thesis are presented as following:

- Two functional control strategies for the use of the single storage unit for voltage support are introduced. The first strategy investigates voltage problems under different solar irradiance profiles at different seasons and the integration of energy storage unit into LV distribution networks to solve the associated voltage problems. It is shown that using active

power from single phase energy storage can effectively bring the voltage within regulatory limits, and enable voltage unbalance to be reduced within statutory limits. The second strategy proposes a coordinated control method for solving voltage excursions and reducing reverse power flow to help the existing distribution network adapt to future scenarios with high numbers of connected LCT loads and PV generators. This relieves transformer overloaded and mitigates voltage excursions by coordinating storage charging/discharging functions with an OLTC.

- The largest single contribution is a new method for coordination of multiple energy storage units for voltage support in the LV distribution network is proposed. The method is modelled using multiple suitably sized storage units to manage the overvoltage problem by considering voltage sensitivity analysis and a battery aging model. This influences which energy units are selected to provide strict maintenance of voltage limits. The proposed method uses storage units more evenly and so reduces the costs of battery replacements to the energy storage operator in terms of both number batteries and maintenance visits.
- A systematic approach is constructed including the PV generator and the energy storage based on linearized differential equations. This is used to perform eigenvalue sensitivity analysis to define the range of energy storage voltage regulation controllers' parameters, and to investigate whether energy storage exchanging active and reactive power with the grid for voltage support can reach the system stability margin. In addition, a methodology to utilise active and reactive power of the energy storage for voltage support is presented.

6 Thesis Layout

The power distribution network in the future will be fundamentally different to the one presently operated in the UK. In order to decarbonise, a large number of renewable energy systems will be embedded in distribution networks to reduce carbon footprint. This may pose many challenges to secure operation of distribution networks. Energy storage is seen as one way to reduce the impact of DGs on distribution networks in terms of high R/X ratio LV networks. Therefore, there is interest in the use of energy storage in the distribution

system. Although there are many studies looking at the benefits of energy storage to customers and to businesses, there is little understanding of how to operate energy storage to overcome issues presented by PV generators in LV distribution networks. There is also a question how to utilise energy storage active/reactive power to provide services to LV distribution networks where the R/X ratio is large. To fill the gap mentioned above, the work in this thesis mainly focuses on operational control strategies for energy storage systems for voltage support in LV distribution networks. The next six chapters of the thesis are presented as follow:

Chapter 2 presents a background literature review into benefits of energy storage systems to distribution networks, and introduces operational control strategies of energy storage systems for voltage support in low voltage distribution networks.

Chapter 3 presents two case studies that illustrate the expected impacts of PV generation on overvoltage and reverse power flow and two functional strategies of energy storage from smart grid laboratory with RTDS are presented.

Chapter 4 introduces the coordinated control of multiple energy storage systems in a low voltage distribution network. A methodology of coordination of multiple energy storage for voltage support is discussed and the detailed procedures and mathematical formulations are presented.

Chapter 5 introduces a low voltage distribution network dynamic model that includes one PV generator and one energy storage device. Detailed operational modes and control strategies for the study system are described. The detailed procedures and mathematical formulations to develop a small signal model of the system are provided. The application of the proposed model is validated through a series of case studies.

Chapter 6 discusses an active and reactive power control strategy of the energy storage for voltage support in the LV distribution network in respect to small signal stability.

Chapter 7 presents the discussion, conclusion and further research.

Chapter 2: Potential roles and operational control strategies for energy storage in LV distribution networks

There are expected to be a number of challenges in future LV distribution networks caused by intermittent power production from renewable sources and particularly for DNOs. To overcome these issues, there is interest in the use of energy storage in the LV distribution network. Energy storage will become extremely important in the move towards a low carbon economy, and it has the potential to save the energy system over £4bn by 2050 [97]. Energy storage was recognised by chancellor George Osborne as a leading technology for large integration of renewable energy in 2012 [98]. As such, the UK government pledged to support the development of the energy storage across the country [97]. In the past two years up to 2015, more than £80m has been invested to support energy storage projects across all regions of the UK [99]. The UK government has set a target to achieve 2000 MW energy storage installation by 2020 [100]. This can provide annual saving of £120 million/year. If total installed energy storage capacity reaches up to 10,000 MW by 2050, this can produce the annual savings of £10 billion/year [101]. Energy storage projects developed between the years 2013 to 2020 are shown in Figure 2-1 [100]. However, the UK presently is at risk of falling behind in developing energy storage due to lack of commercial framework [100]. The market of energy storage in the UK needs a strategy to set out the market and realise the potential of this technology. Ofgem also realises this and supports a number of storage projects in distribution networks [102]. Apart from installed large capacity pumped hydro storage, there is limited uptake as there are few locations where this type of storage can be installed. There is wide interest in the use of energy storage in the distribution network in terms of LV networks. However, according to the [103], there are several commercial and regulatory elements, such as classification of storage unit and capacity market, which have effects on deployment of the energy storage for the GB power grid. As such, constructing an appropriate regulatory framework and commercial arrangements plays an important role for future storage deployment. If there is a market established for network operators to install storage widely, there will need to be significant technical innovation in storage technology.

To explain the use of energy storage in future LV distribution networks, storage technologies and applications are firstly presented as follows.

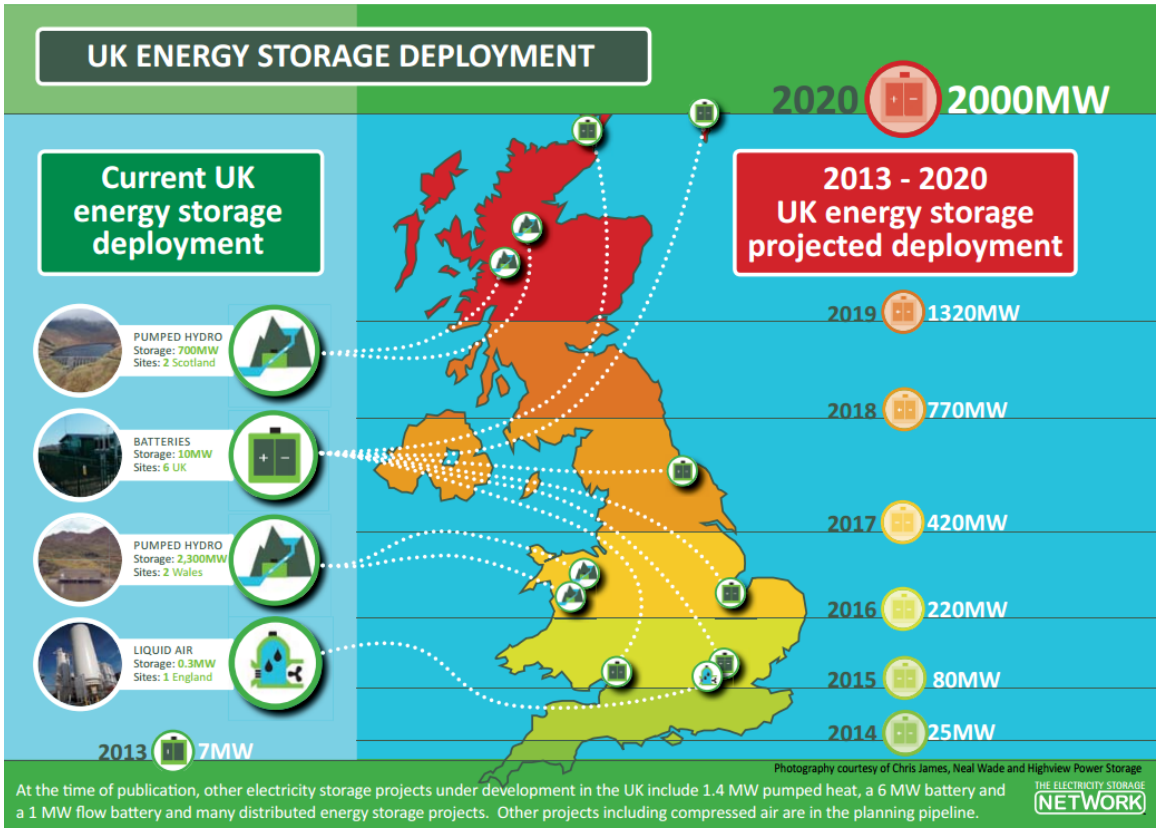

Figure 2-1: UK energy storage projects deployment between 2013 and 2020 [100]

1. Potential role for energy storage in the low voltage distribution network

There will be many benefits for applying energy storage in LV distribution networks. For example, in a LV distribution network, storage installed in customer side can help residential customers to become active member of the power system [104], and overcome challenges, such as voltage fluctuation and voltage unbalance, caused by PV generators. This also enables customers to reduce their utility bills by absorbing excess PV output, and providing power backup and purchasing off peak electricity to support loads during peak times [105]. Energy storage is a general term for a range of technologies that take energy from the power grid onto store and release when needed. Energy storage based on different technologies has different applications [106][107].

1.1 Introduction of energy storage system and its relevance technologies

Energy storage can be broadly classified as three main technology groups according to its discharge time, power rating and service types as shown in Figure 2-2 [108].

The first is large scale energy storage projects include pumped hydroelectric storage (PHS) and compressed air energy storage (CAES). These can provide a bulk storage capability with several hours of charge/discharge capability [109][110]. CAES stores energy by absorbing surplus power from grid to compress air that is stored in a cavern as potential energy [111][112][113]. The compressed air is heated and expanded through a gas turbo-generator to generate electricity when the energy demand increases [112][113]. PHS is a type of hydroelectric energy storage that can store energy in form of water [113]. Both types of energy storage can provide the power capacity between the range of 100 and 1000 MW with efficiency at 65-85% [106] [107] [110]. The capital cost of CAES is much lower than PHS, but requires more site specific data to evaluate its suitability [106][107] and [114]. However, these large scale energy storage schemes require installation in a feasible location [106]. This would be a problematic in the UK as a limited number of favourable locations are available.

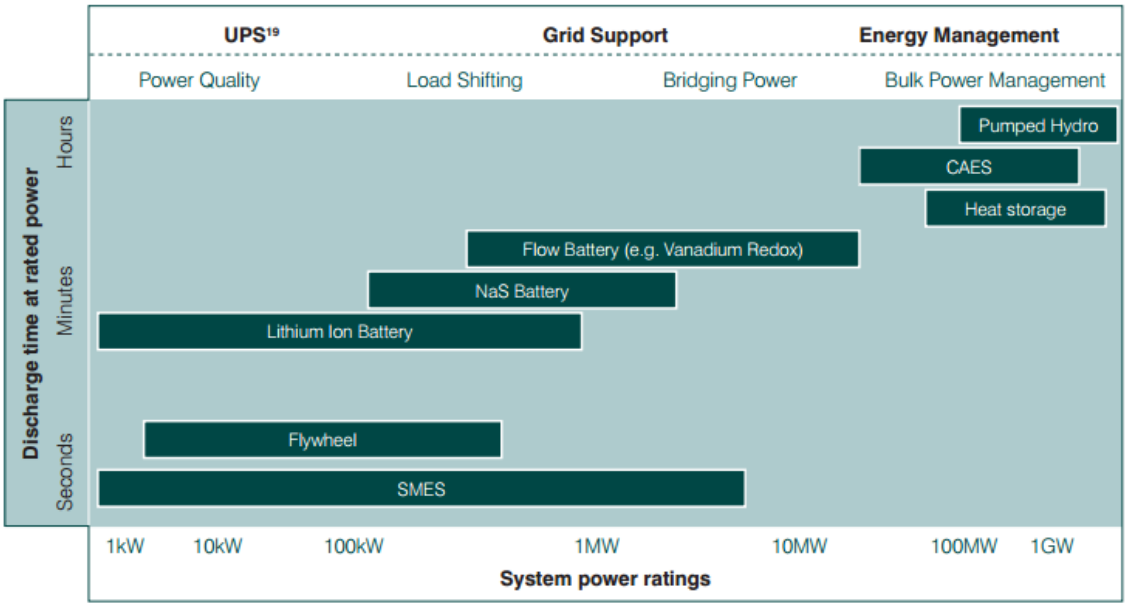

Figure 2-2: Comparison of storage technologies [108]

The second is medium term discharge energy storage devices that include a group of batteries that store energy using chemical reaction [106][107]. Presently, there exist various technologies for batteries, such as lead-acid batteries, valve regulated lead acid batteries, nickel-cadmium batteries, sodium-sulphur batteries, lithium-ion batteries, zinc-bromine batteries and vanadium-redox batteries [115]. Battery storage with high energy efficiency at 60%-95% can provide a number of important benefits to the utility grid [107]. However, these batteries have low energy densities, high maintenance costs, short cycle life and a limited discharge capacity [106][107]. In addition, according to [116], vanadium-redox batteries provides many benefits over other battery storage technologies. Presently, the vanadium-redox battery has been commercialised for several megawatt scale energy storage projects due to its long cycle life (>11,000 & 20 years), instant recharge by electrolyte swap, low maintenance, fully dischargeable, and economics improve with scale [116][117]. As depicted in Figure 2-3, vanadium-redox batteries have lower whole life costs than all the other conventional battery technologies [116][117]. This is due to their longer cycle lives and consequently lower replacement costs [116]. This battery technology has been concluded to be technically and economically feasible for offering grid ancillary services, such as frequency response and voltage support [116].

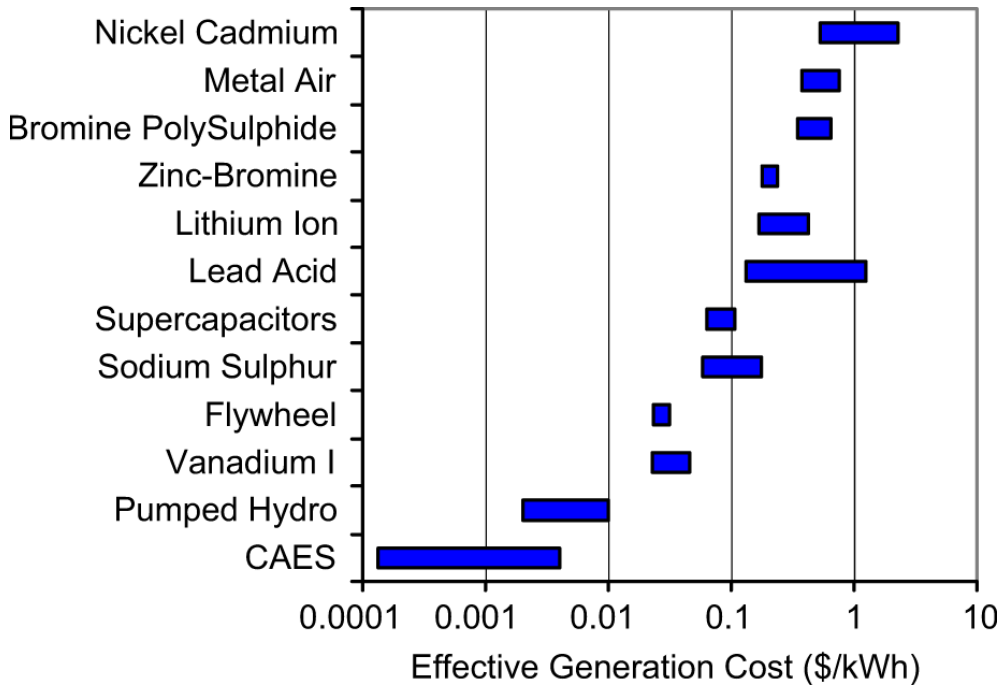

Figure 2-3 Cost for energy storage systems [116][117]

The third is short term discharge energy storage devices that contain superconducting magnetic energy storage, flywheels and capacitors. This type of energy storage can provide large power in a very short time with efficiency 90%-95% and have long cycles lives [107]. Accordingly, these technologies are desirable for short power quality applications by improving transient voltage disturbance and ride through of interruptions for example [107][118]. These devices are not widely being used in utility application [119][120], since the cost of the short term discharge energy storage devices is high as seen by Table 2-1.

Table 2-1 summarises the cost and technical characteristics of different energy storage technologies [119][120][121]. Here, the cost of the storage is the sum of the cost of power conversion and the cost of energy storage itself. The cost of power conversion is priced in $/kW, and it is the rate at which energy can be

Table 2-1 Energy storage technologies cost and characteristics [119][120][121]

Duration Category	Technology	Power Cost (US $/kW)	Energy Cost (US $/kWh)	Efficiency	Cycles
Hours to days (Long)	Pumped hydro	1200	75	85	25000
	CAES	700	5	70	25000
Minutes to hours (Medium)	Advanced lead acid batteries (2000 cycle life)	400	330	80	2000
	Lead acid with carbon-enhanced electrodes	400	330	75	20000
	Vanadium redox batteries	400	600	65	5000
	Lithium-ion batteries	400	600	85	4000
	Zinc-bromine batteries	400	400	70	3000
	Sodium-sulphur batteries	350	350	75	3000
	Nickel-cadmium batteries	1200+	1500+	75	1500
Up to a minute (Short)	Flywheels	600	2000+	95	25000
	Superconducting Magnetic	500	10000	95	25000

used [117][118]. The cost of energy storage itself is the amount of energy stored that can be used to delivery to the electricity grid, and it is priced in $/kWh [117] [118].

1.1.1 Energy storage technologies for LV distribution network and trial installations

Considering that LV distribution networks commonly contain many DGs, such as PV generators that are often small scale. This requires energy storage for only a few kW to be installed in LV distribution networks [105][122]. As such, batteries are one of the desirable solutions to effectively reduce challenges that caused by PV generators [105]. A comparison of the technology options for LV distribution networks are also conducted in [123], and it stated that batteries are desirable for installation at residential LV networks. This is because these batteries are a financially viable by providing several hours of services in LV networks. Batteries store electric energy in dc form and use a power electronics converter to exchange energy with the utility grid [124]. This provides the capabilities for batteries to reduce the voltage excursion, PV output fluctuation and unbalanced grid as stated in [125][126] and [127].

Presently, there are a number of battery energy storage projects that have been installed in LV and MV distribution networks in the UK as shown in Table 2-2 through the low carbon networks fund (LCNF) [102]. The aim of the LCNF is to support projects sponsored by the DNOs with £500m to encourage new technology and commercial arrangements [102].

Battery storage installed by UK power networks (UKPN) is a LCNF first tier project. A 200kWh Lithium-ion battery storage is installed at a site at Hemsby Norfolk. The objective of this project is to understand the impact and potential benefits of storage on a LV distribution network [128]. Using the storage has investigated if it can effectively overcome the challenge of intermittent power production from wind sources, and it has the potential to reduce voltage fluctuation and manage demand on the LV distribution network [128].

Table 2-2 List of battery energy storage projects in LV and MV networks in the UK

Names	DNOs	Starts-Ends	Types	Numbers	Power /Capacity
Demonstrating the benefits of short-term discharge energy storage on an 11kV distribution network	UK Power Networks	09/2010-01/2014	Lithium-ion	1	600kW/200 kWh
Low voltage connected energy storage SSET1008	Scottish and Southern Energy	01/2012 - 03/2014	Lithium-ion	3	25kVA/25 kWh
Customer-led network revolution	Northern Power Grid	09/2010-12/2015	Lithium-ion	6	2500kVA/5000kWh 100kVA/200kWh 50kVA/100kWh
Buildings, renewables and integrated storage, with tariffs to overcome network limitations	Western Power Distribution	12/2011-12/2015	Lead acid	31	2kW/4.8kWh 8kW/20kWh

As part of a wider project to illustrate zero carbon homes in Slough, Scottish and Southern Energy (SSE) has installed three 25kWh energy storage connected through a four quadrant operation power converter on the LV network [129]. These batteries are used to mitigate the effects of PV generators and prevent network reinforcement [129].

The customer-led network revolution (CLNR) project is operated by Northern Power Grid (NPG). Six battery storage systems have been installed at various network locations and voltage levels to provide thermal, voltage and reactive

power support to the NPG distribution network [130][131]. The CLNR project aims to evaluate a range of applications of battery storage systems in the distribution network, and it has demonstrated that utilising the fleet of batteries installed can defer network reinforcement, and asset replacement [130]. In addition, power quality problems and reverse power flow have been mitigated as well[130].

In addition to projects described above, buildings, renewables and integrated storage, with tariffs to overcome network limitations (BRISTOL) is a second tier LCNF project operated by Western Power Distribution (WPD). Thirty single phase battery storage with capacity 4.8kWh have been installed in domestic lofts to prevent network upgrades that could be caused by PV installation [132]. Apart from installing single phase home energy storage, larger storage units with capacity 8kW/20kWh have been installed in schools. These batteries are linked to the local network to export the batteries' power at peak times [132].

1.1.2 Benefits of energy storage to low voltage distribution networks

Energy storage installed in LV networks can offer many benefits to both customers and DNOs. Customers can become active members of the utility grid by releasing stored energy when needed. This can defer asset replacement and network upgrades [104]. For the literature, the benefits from energy storage to LV and MV distribution networks are summarised in Table 2-3 [133] [134].

Using energy storage for voltage profile improvement with a large number of PV generators integrated in LV networks has been investigated as stated in [133][135]. The literature shows that battery energy storage with the proposed operation strategies is an effective way of preventing overvoltage and therefore increasing PV generators network penetration. Smoothing out voltage fluctuation by using energy storage is proposed in [126] [136] and [137]. In [126], a state of charge (SoC) based control strategy is developed in which that the proposed control strategy can manage energy storage power and SoC within a specific target while smoothing PV outputs by considering the effect of extending the cycle life of battery storage. In [136], mitigation of PV fluctuation is achieved by a ramp rate control strategy based on operation of battery storage. Energy storage for mitigating voltage unbalance on LV distribution

networks is examined in [138]. The results demonstrate that the energy storage device can effectively reduce the voltage imbalance as well as the network

Table 2-3 Benefits of energy storage to LV distribution networks

Benefits	• Description
Power quality	• Smoothing out voltage fluctuation, and voltage swell/sag • Compensation for voltage harmonics distortion • Mitigating voltage unbalance
Demand side management	• Reducing peak load to avoid peak load charges.
Reliability	• Increasing reliability through its island operation capabilities, suitable for sustaining power supply in the LV-grid if the MV-grid fails
Voltage regulation	• Maintaining voltage within legal limits
Reverse power flow	• Absorbing excessive PV outputs to reduce reverse power flow
Stability issues	• Improving the system dynamic stability by mitigating oscillatory modes of the system
Deferral of assets replacement, and network upgrades	• Deferring upgrades of the distribution network where changing generation/demands cause problems with peak loading or voltage

losses in the network where PV generators are connected. A control method based on model predictive control (MPC) is proposed to utilise energy storage in a LV micro-grid for reduction of harmonics and providing energy management [139]. The MPC is an advanced method for process control, and is a multivariable control algorithm [140]. The advantage of MPC is the fact that it uses a dynamic model of the process to predict the future response for a plant [141]. However, the limitation of the MPC is that it is not able to deal with plant model uncertainties [142]. The MPC developed in [139] is used to optimise the steady state and the transient control problems separately to reduce the overall computational overhead.

To mitigate voltage excursions caused by the large connection of low carbon technologies (LCT) loads, such as air source heat pumps (ASHPs) and electric vehicles (EVs), a coordinated control strategy of battery storage with DSR for demand side management is proposed in [143]. The coordinated control scheme firstly instructs the energy storage to export active power into the LV network if the voltage excursion happens at the remote end. However, a possible scenario happens such that if the power rating and the capacity of the

battery storage is insufficient to bring the voltage within the legal limit. In this case, the DSR will be implemented and called by coordinated control scheme to solve the voltage excursion. By using the battery storage with DSR in LV networks, this paper shows effective prevention of undervoltage problem, and a reduction in the capacity of battery energy storage as DSR can remove the need for the storage intervention.

LV microgrid system dynamic stability is improved by mitigating oscillatory modes of the system to improve system damping using energy storage device [92]. Transient stability improvement is achieved by using storage in a microgrid [144]. Here, the storage is used to solve fast transient problems.

By offering a number of technical benefits to LV networks regulation using energy storage, there are many examples of how storage in LV networks can ensure financial benefits to DNOs. In the LV network, there are two main financial benefits, cable re-conducting and replacing the secondary transformer, which can be achieved. In [145], a financial model is developed to compare the cost of replacing the LV network assets with the cost of installation of energy storage. It concludes that energy storage is one of the desirable solutions to allow deferral of asset replacement and network upgrades. In this example, the storage allows the existing low voltage network assets to remain in operation, being supported by energy storage for voltage regulation.

Although much literature quantifies the benefits of energy storage to LV distribution networks, operational control strategies of energy storage, such as coordination control of multiple energy storage, are needed to address the steady increase in connection of PV generators to residential LV networks. The coordination of multiple energy storage in LV distribution networks would provide visibility for DNOs to learn how to control, manage and deploy energy storage units in their networks. In addition, presently, there is little study which examines energy storage active and reactive power exchanging with the LV utility grid under small disturbance. Because of a significant presence of PV generators and energy storage near future, the LV distribution network cannot be considered as passive. The large connection of PV generators or energy storage may have large influence on power system dynamics. Therefore, system stability issues in the future may be an important concern for DNOs.

There is a need for the development of the linearized state space model for PV generator and energy storage. This will explore whether an energy storage system exchanging active and reactive power with the grid for voltage support can reach the system stability margin.

2 Operational control strategies of energy storage systems for voltage support

Energy storage units can be envisioned in many future distribution networks to address the challenges brought by introducing DG units. There are three types of high level operational control strategies for storage units in LV distribution networks; these are decentralised control, centralised control and coordinated control [146][147]. Applying different operational control strategies in LV distribution network may have different impacts on energy storage itself aging degradation condition, and performance of addressing overvoltage as well. Advantages and disadvantages of decentralised, centralised, coordinated control for energy storage units are described in following section.

2.1 Decentralised, centralised, and coordinated control of storage units

2.1.1 Decentralised control

In decentralised control, the energy storage uses local measurements to control its charging/discharging function as seen in Figure 2-4. This type of control strategy does not require a wider communication scheme and so is in some respects robust, reliable and cost effective compared to centralised control [79]. The storage voltage or power set point is determined based on local measurements. Decentralised control of the energy storage for voltage support with a large number of PV connections is explored in [96]. Here, the storage unit is used to provide voltage support and frequency regulation by droop control response under a MV distribution network.

A decentralised control strategy for parallel operation of multiple DG inverters is developed in [148]. This control scheme is based on droop control technique to realise power sharing without communication control wire interconnections for the parallel operation of DGs. Decentralised control based on the droop technique can be also used in operation of multiple energy storage units.

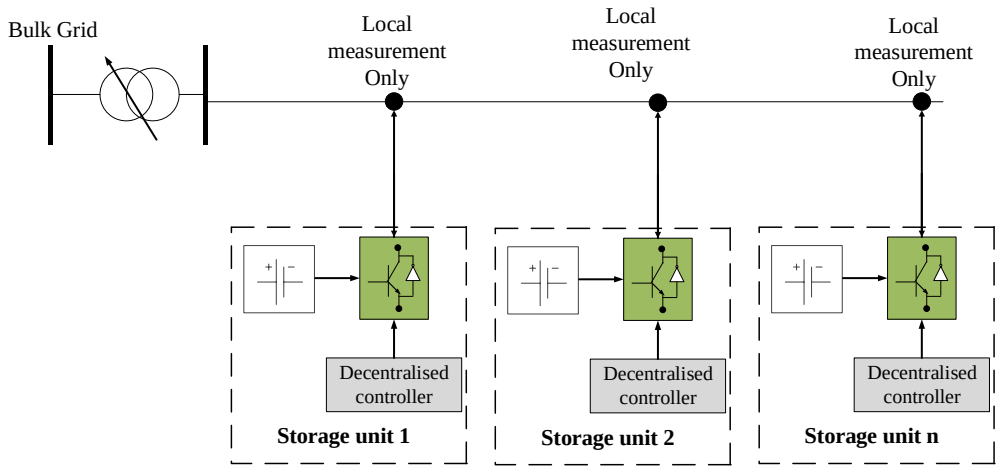

Figure 2-4: The concept of decentralised control of storage units

However, when multiple energy storage units are installed in a LV network, due to no communication between energy storage units, support cannot be received from other storage devices if a unit has reached either an extreme state-of-charge (SoC), a power limit or in the event of complete unit failure. Although the droop based technique has been applied for decentralised control strategy for power sharing [148], equally sharing the power among storage units may accelerate the usage of storage units. This is because the voltage sensitivity factor (VSF) of each unit is different in response to voltage problems at different locations. In addition, because the LV distribution network contains high R/X ratio, the change of the voltage angle or magnitude will introduce coupling between active and reactive power flow by using conventional droop control method [149]. This makes traditional droop control method is impractical. As a result, droop based decentralised control may not be suitable for operation of multiple storage devices in the LV network.

2.1.2 Centralised control

In centralised control, the power or voltage set point and charging/discharging control actions of each storage unit are determined in a centralised controller as illustrated in Figure 2-5. This method is desirable for systems where multiple storage units are connected to a common bus or located in close proximity [150]. The centralised control concept has been applied in large utility power systems for many years to realise the frequency regulation in a large network and has been applied to micro-grids recently for voltage and frequency regulation [151] [152]. This approach requires online information of the network

state and high computation speed [146]. The centralised control scheme has been applied to coordinate multiple DGs in a distribution network for proving power support, compensation for power quality issues, and ancillary services [153].

This control scheme may also be used for operation of multiple storage units in a LV distribution network. However, a significant drawback of this control approach is cost, since it requires a fast, high reliability communications network [146]. Accordingly, in the event of communication failure, each storage unit would not be able to respond to a voltage excursion, or would need to fail safe to a decentralised control mode.

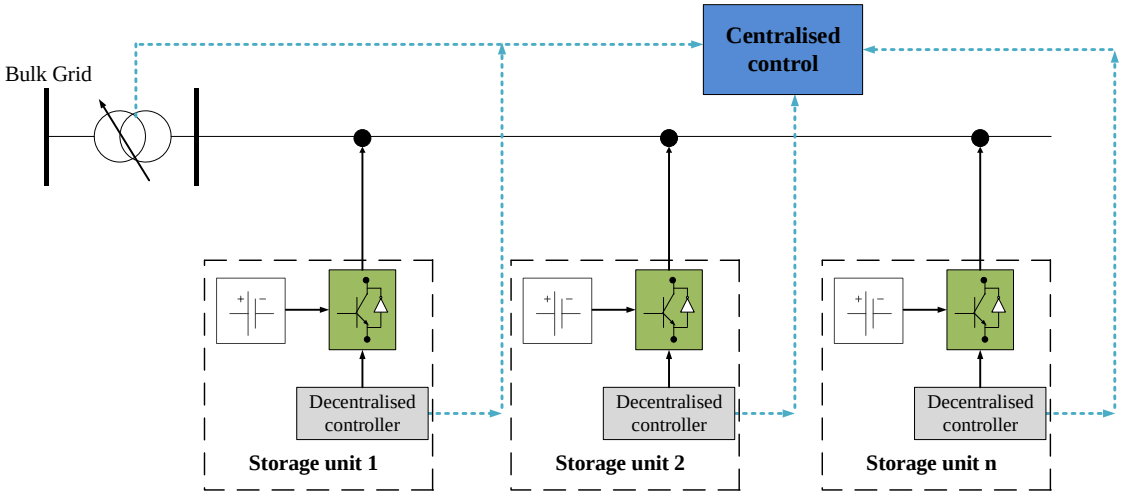

Figure 2-5: The concept of centralised control for storage units

2.1.3 Coordinated control

In coordinated control, the control strategy combines the positive features of both centralised and decentralised control [139] [154]. The distinctive features of this control are robustness with respect to intermittency and latency of feedback and tolerance to connection and disconnection of network components. Coordinated schemes for DGs have been studied widely in distribution networks. There are two types of coordinated control for the application of storage units as seen in Figure 2-6; coordinated control of storage units with other technologies, and coordinated control of multiple energy storage. In Figure 2-6, the red dash line indicates that storage units coordinated with an on load tap changer (OLTC) to address problem such as overvoltage. Whereas, the blue dash line indicates coordinated control of multiple energy

storage. Such control strategy can be desirable for LV distribution networks as the secondary transformer tap is fixed and is not able to change automatically in response to network conditions.

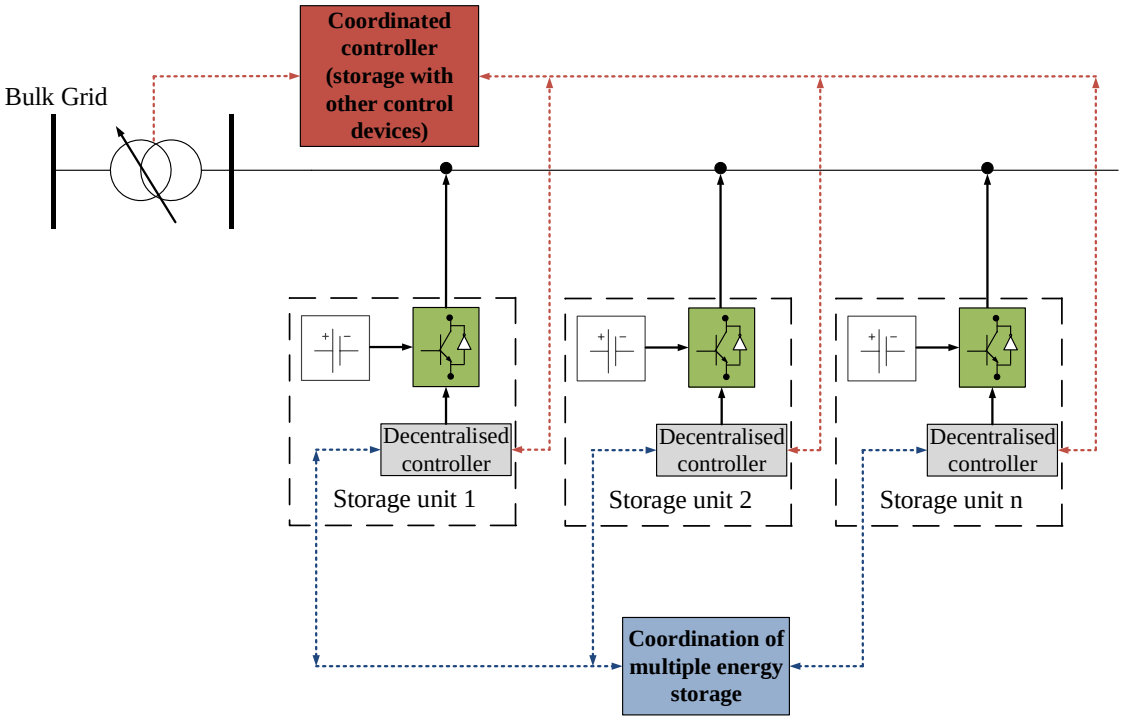

Figure 2-6: Coordinated control of storage units

Coordinated control of storage units with other technologies has recently been applied in distribution network for voltage regulation, managing reverse power flow, reducing voltage unbalance and improvement of stability issues. Coordinated control of the storage with the OLTC of the primary transformer is considered in [154]. This reduces the number of tap changes and to enables the tap changer to work when there is reverse power flow. This method can limit the storage depth of discharge, and therefore the storage cycle life is extended. In [90], a coordinated voltage regulation scheme integrating energy storage is proposed under unbalanced conditions. The storage is operated cooperatively with an OLTC to mitigate voltage rise and voltage unbalance problems. A fuzzy logic based coordinated control of storage units with DGs is developed for the micro-grid [155]. The work particularly focuses on mitigating active power fluctuation at the point of common coupling (PCC) under grid-connected operation, and frequency control under islanding operation. The designed method enables the system stability to be improved under both small and large disturbances. In addition to above literature, coordinated control strategy of

battery storage with DSR for demand side management is proposed for voltage regulation in [143].

Although these coordinated control methods can provide benefits to system operation, they may not be suitable for LV distribution networks. This is due to the fact that firstly the LV distribution network in the UK starts at the secondary transformer that has a fixed tap that does not change automatically in response to network conditions. Secondly, at present DG units, such as PV generators, in the distribution network are not required to dispatch due to the regulation policy. Thirdly, DSR has many existing barriers to apply in distribution network as it is hard to persuade customers to change their energy usage behaviour for example. Accordingly, coordinated control strategies for multiple energy storage units will play an essential role for future LV distribution networks. Based on the discussion above, if this becomes a reality multiple energy storage units installed in the LV network, there will be a trend for coping with challenges due to the presence of PV generators.

However, one challenge to applying multiple energy storage systems in future distribution networks is the creation of a coordinated control strategy. In [146], coordination of multiple energy storage units based on a consensus algorithm for avoiding violation of voltage and thermal constraints is proposed. The consensus algorithm aims to collect energy storage units to work as a coherent group and share the required active power equally among the units. This allows the whole system to survive the failures of some of units. While using this algorithm for network loading management in a centralised controller, a decentralised controller in individual units uses reactive power for voltage support, without considering other units or the wider network. However, since the VSF of each energy storage system is different, this can lead to uneven utilization of energy storage in the network in response to voltage problems. In addition, some LV distribution networks have large amounts of underground LV cables where the R/X ratio is large. In such networks, the effect of reactive power compared with active power is less pronounced when addressing overvoltage.

In this thesis, a new coordinated control of multiple energy storage systems based on voltage sensitivity analysis and a battery aging model is developed as

shown in Figure 2-7. The coordination scheme employs a centralised controller that determines which energy storage units are used to address any voltage excursion, whilst the decentralised controller of each storage unit uses local measurements to determine specific set points for active and reactive power. The status of each storage unit, such as the active and reactive power limit, SoC, and energy storage lifetime, is communicated to the centralised controller to update each storage status within a series of control matrices. The proposed coordinated control method for doing this is discussed in Chapter 4.

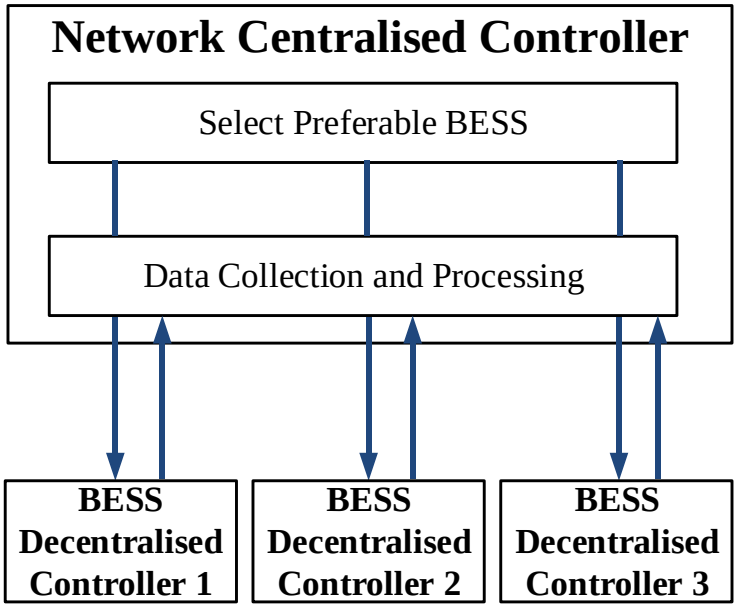

Figure 2-7: Overview of developed coordinated controller containing a centralised controller interacting with several decentralised BESS controllers

2.2 Energy storage power circuit

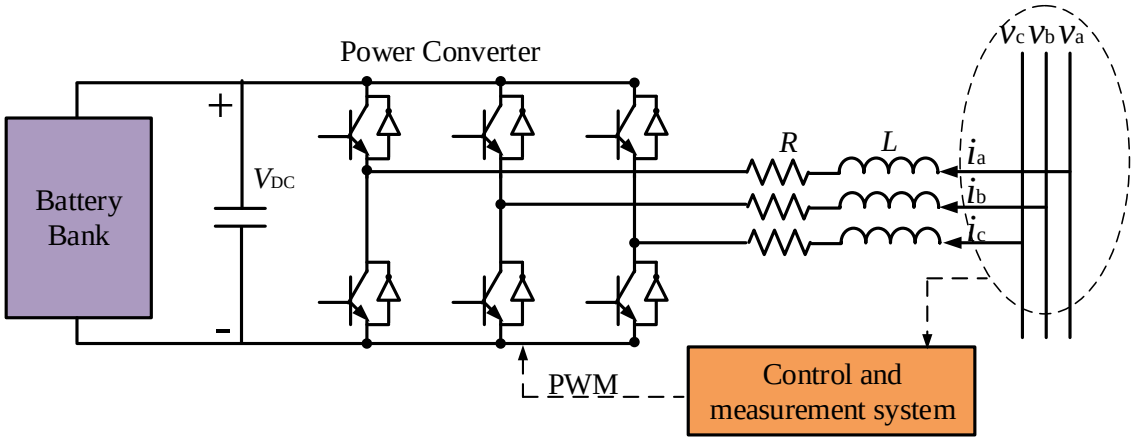

Figure 2-8: Schematic diagram of energy storage

Storage employs power electronics converter systems for grid connection. The schematic diagram of a storage system including battery bank and power electronics converter with its corresponding control and measurement system is shown in Figure 2-8. The filter is equivalent to the series connection of a resistor R and an inductance L for each phase [92].

V_{dc} is the DC bus voltage and can be considered constant usually for dynamic analysis. In this thesis, the DC side is represented as an ideal source by a fixed voltage, and a three phase average VSC model is used while disregarding switching harmonics. Therefore, it introduces no dynamic behaviours in the converter model.

2.3 Energy storage low level control and measurement

The storage unit hierarchical control and measurement system based on voltage regulators is shown in Figure 2-9. The Figure 2-9 (a) illustrates the block diagram of the power circuit and control structure. There are two control loops from its control structure. The Figure 2-9 (b) shows the block diagram of voltage control scheme. According to Figure 2-9 (b), it is composed of two controllers containing external voltage controller and inner current decoupling controller. External voltage controllers generate the reference current for the inner current controller based on voltage requirements locally or remotely. The inner current controllers then produce reference voltages for the power converter. A phase locked loop (PLL) is used to recognise the frequency of the utility system to ensure energy storage synchronisation. The PLL is a control system that enables the phase from the output signal to be related to the phase from the input signal. The dq transformation is applied to enable both active and reactive components of AC output power to be independently controlled this is described in Appendix A2. According to various system requirements, such as maintaining voltage within the specified range, and balancing supply and demands, there are three types of control modes for storage in decentralised controllers defined [156]. These include voltage control mode, active/reactive power control mode, and droop control mode.

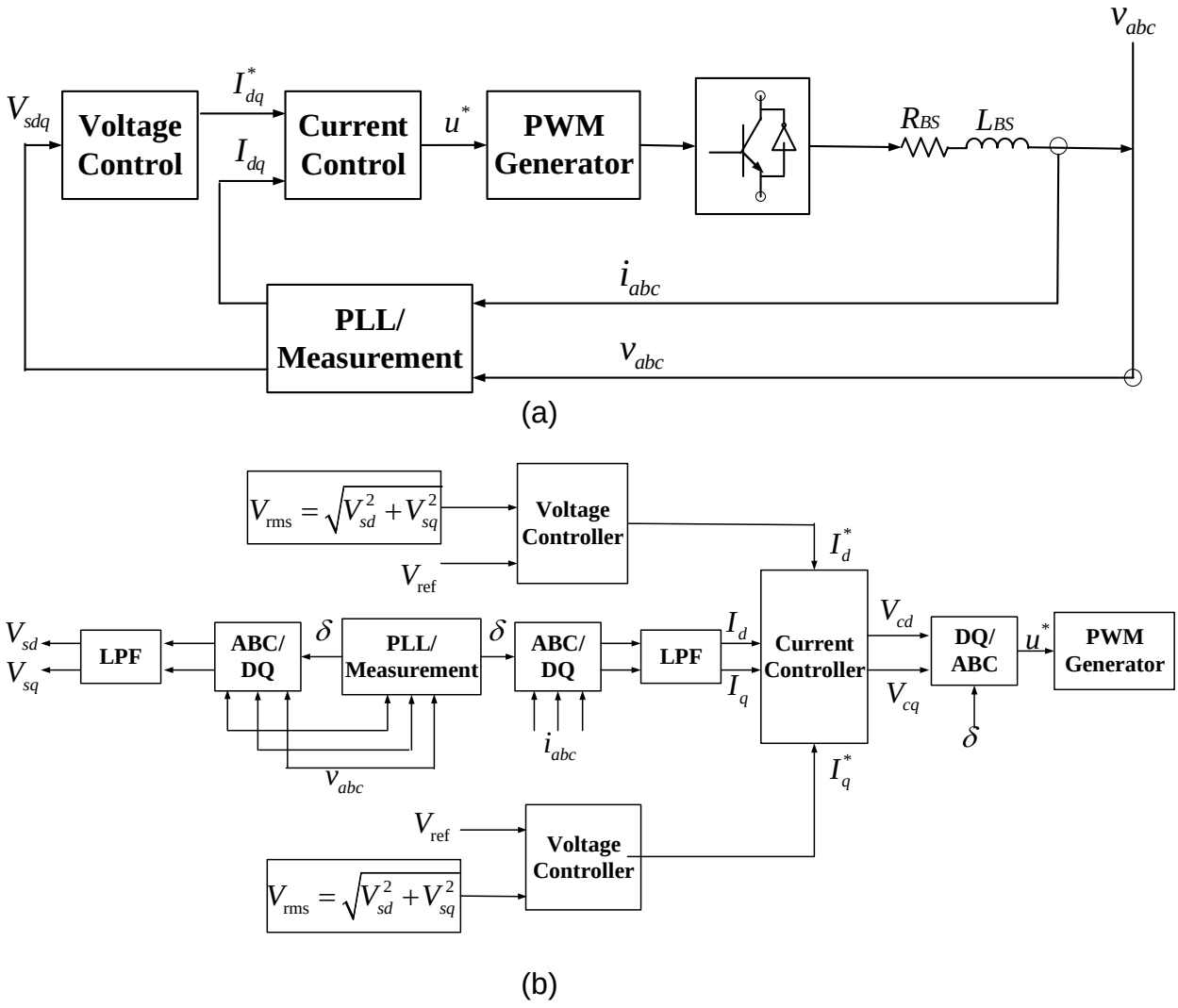

Figure 2-9: Energy storage unit hierarchical control interface based on voltage controller (a) block diagram of power circuit and control structure (b) block diagram of voltage control scheme

2.3.1 Voltage control mode

Voltage control mode purely focuses on voltage regulation. Figure 2-10 shows the external voltage controllers for terminal voltage regulation. In this mode, both active and reactive power of the storage unit is controlled to regulate the PCC or a remote voltage at a pre-specified level. Both *d and q* axis voltage controllers employ proportional integral (PI) regulator based on voltage errors to generate current references I_d^* and I_q^*. These two quantities then feed into current controllers that produce voltage references by using errors between *dq* current references and measured *dq* current I_d and I_q. The generated *dq* reference voltage is then transformed into the *abc* axis based on the phase angle provided by PLL. The reactive voltage regulator (*q*-axis) is widely employed in micro-grids (grid-connected mode) and MV networks for

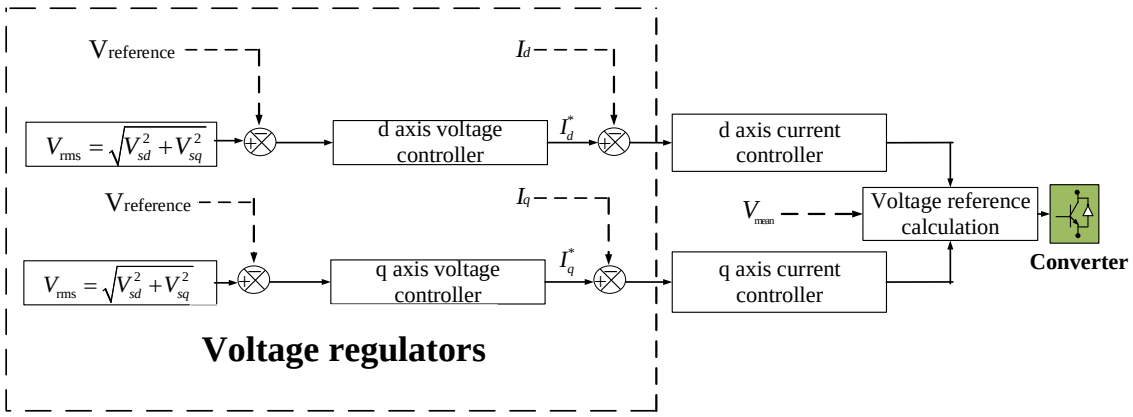

Figure 2-10: External voltage regulators for terminal voltage regulation

maintaining voltage at legal limit as indicated in [157] [158]. However, the effect of reactive power compared with active power is less sufficient when solving voltage excursions in LV distribution networks where the R/X ratio is large. Therefore, reactive power solely controlled voltage regulator may not able to meet the voltage regulation requirement. The active power controlled voltage regulator also needs to be employed for such purpose.

2.3.2 Power control mode

Power control mode is used for energy management [159]. The external active/reactive power controller for power regulation is shown in Figure 2-11 [159]. Actual active/reactive power inputs are calculated and compared with reference active and reactive power set points. For the power control mode, these set points can be provided by an energy management system from a centralised or a coordinated controller. The calculated active/reactive power errors will be fed into power control loop to generate reference current I_d^* and I_q^*.

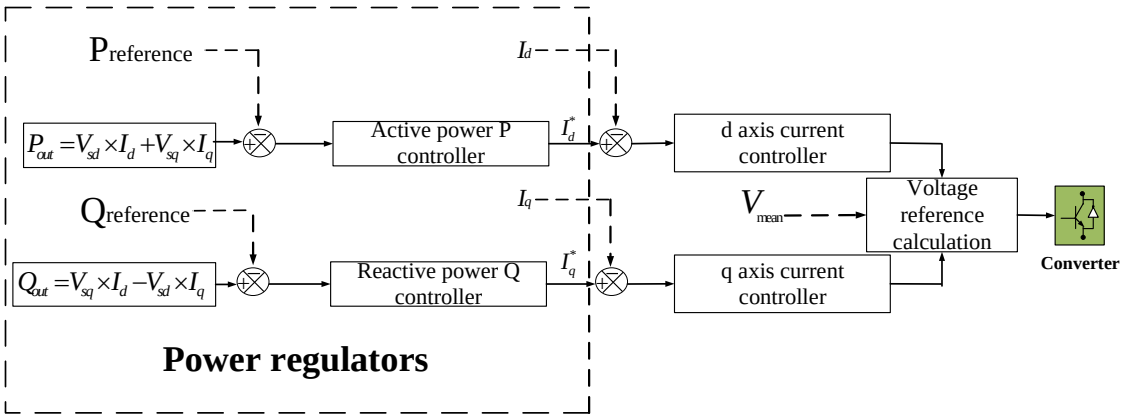

Figure 2-11 External active/reactive power controller for power regulation

These two reference currents are used to produce voltage correction factors to compensate for the power errors. Using a voltage feed-forward controller, new voltage references are generated that will be translated into switching signals and fed to the converter PWM control. Such a mode is used to smooth the power flow at the PCC or remote branch. This enables generation and consumption to be balanced.

2.3.3 Droop control mode

The droop control is a control method for primary frequency control, and it allows synchronous generators to operate in parallel for load sharing purpose [160]. In power system, synchronous generators will share any increase in the load by decreasing the frequency according to their governor droop characteristic [160]. Figure 2-12 illustrates an external frequency droop controller for power sharing. Droop control mode is largely used in micro-grids to decrease the reference frequency if the load increases by power sharing among generators in a grid. Similarly, reactive power is also shared by introducing the droop setting in the voltage magnitude. Such a control mode is widely chosen in micro-grid because the frequency of the micro-grid system in autonomous operation mode freely changes if generator units are not able to enforce the base frequency of the system. The frequency deviation can be mitigated by introducing the frequency droop characteristic to dynamically share the power among generator units in the islanded system.

In LV distribution networks, since the VSF of each unit is different in response to voltage problems at different locations, droop control mode equally sharing the power among storage units may increase the usage of storage units. This is not desirable for the use of energy storage units. Furthermore, the change of the voltage angle or magnitude will introduce coupling between active and reactive power flow by using such droop control model in the LV distribution network where contains high R/X ratio [149]. Therefore, this thesis will not consider the use of the droop control mode for voltage regulation purpose.

All these control modes can be varied to meet different requirements. As stated in [158] [161], the active and reactive power control mode is operated if the

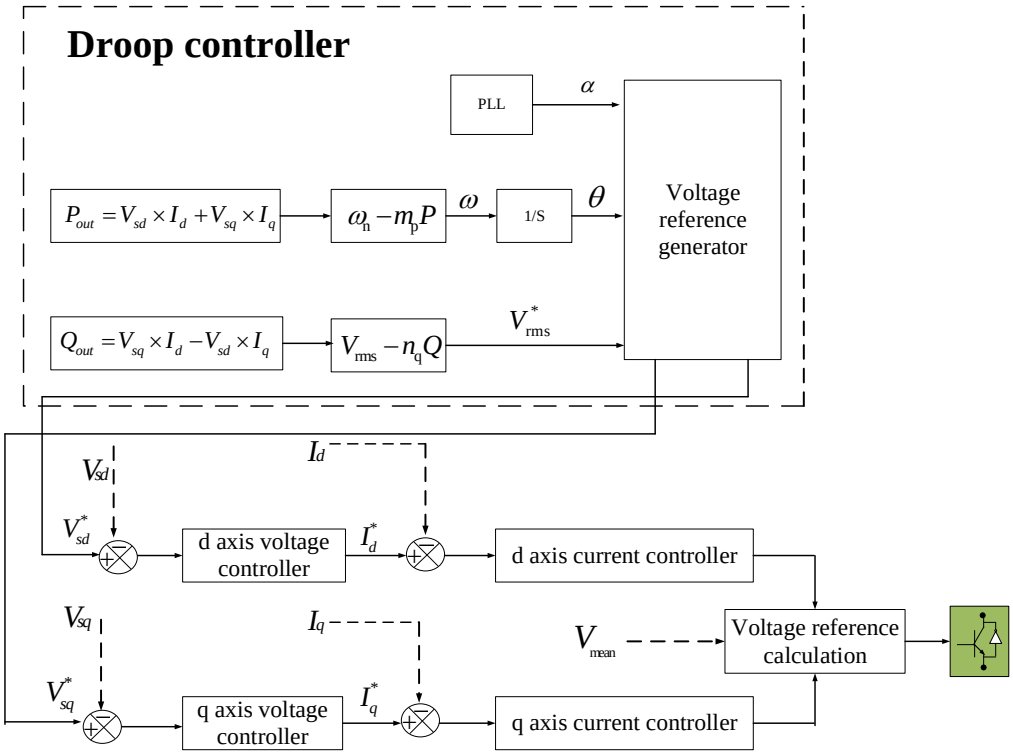

Figure 2-12 External frequency droop controller for power sharing

micro-grid is in grid-connected mode. If the micro-grid is in islanded mode, power control model will be shifted into droop control mode that is used to regulate the frequency variation by sharing powers among the storage units based on their rating.

3 Summary and conclusion

Storage units are one form of mitigation for addressing problems caused by PV generators in LV distribution network. Within the reviewed literature there are many studies looking at storage technologies for various applications. Considering LV networks that contain small scale PV generators, the storage device is one feasible solution to cope with large connection of these solar generators. However, there is also a research question of how to operate these storage units in LV distribution networks.

To determine this, three types of high level operational control strategies for energy storage in LV networks are introduced. In comparing these high level control strategies, the distinctive feature of coordinated control strategy that combines the positive features of both centralised and decentralised control is

robustness with respect to intermittency and latency of feedback and tolerance to connection and disconnection of network components [139] [147] [156].

In addition, low level control strategies for energy storage in the LV distribution network are presented. Voltage control mode mainly focuses on voltage regulation, power control mode can be used for energy management, and the conventional droop control mode can share the power among the storage units. However, conventional droop control is not desirable for the application of multiple energy storage units in the LV distribution network where the line impedance is inductive and line resistance cannot be neglected.

Chapter 3: Functional strategies for use of energy storage system for voltage support

1 Introduction

Two case studies based on the smart grid laboratory described in section 2.1 have been investigated to overcome voltage rise and reverse power flow issues caused by significant PV generator connections. The first case study examines characteristics of decentralised control based battery storage unit for voltage support. In this study, analysis is carried out to compare overvoltage on days with different load and generation patterns. The second case study illustrates that by coordinating storage unit with OLTC, it can effectively solve over/under voltage and reverse power flow problem without upgrading network infrastructure. The coordinated control method in the second case study is evaluated by Real Time Digital Simulator (RTDS) simulation in the smart grid laboratory. Voltage sensitivity factor is used in this chapter for designing active and reactive power voltage regulation controller rather than employing PI controller, because voltage sensitivity factors are simple to use and are positive for steady state analysis based real time simulation [162].

2 Theory

2.1 Experimental technique

The experiment application in the first case study is achieved using the real time power hardware in the loop (PHIL) system which was developed in a smart grid laboratory. The experimental physical LV network is connected to a RTDS system through a 3-phase power amplifier. The experimental physical LV network is connected to a RTDS system through a 3-phase 4-quadrant power amplifier (PAS 2000) that is designed by Spitzenberger. The frequency range of the power amplifier is specified with 5kHz signal bandwidth and the reverse power flow capability is 21kVA [163]. The power amplifier enables the experimental low voltage network in the laboratory to cooperate with distribution network models which were built in RTDS software. The laboratory setup contains a PV emulator, battery energy storage system, three phase four wire network and the RTDS/amplifier network emulation system as shown in Figure

3-1. The RTDS transmits ±10V signals that reflect the parameters of the real-time model that are sent to the three-phase power amplifier to set the system voltages on the experimental LV network. Simultaneously, current monitoring signals from the power amplifier are received by the RTDS. These current signals reflect power flow between the experimental network and the network model built in the RTDS software, and are treated as input of the controllable current source in the RSCAD which is graphical user interface for RTDS simulator hardware.

The PV emulator from the smart grid laboratory is used to emulate a PV generator at the end of the feeder for the distribution network that is modelled in the RSCAD. The PV emulator is a 1.7 kW programmable DC power source with a SMA sunny-boy inverter. It is interfaced with the LabVIEW which is used to model the PV profile. The PV profile modelled from the LabVIEW is then used to control the programmable DC power source to simulate the PV output.

The laboratory battery is used to emulate the storage that is located at the end of the feeder for the first case study. It includes a capacity of 13kWh lead-acid battery bank and a 5 kW SMA Sunny-Island 4500 bidirectional inverter. The lead-acid battery bank was installed in the laboratory to reduce the capital costs, and this allows the interaction of the storage unit with LV networks to be investigated. However, the other chemistries could be operated in the laboratory with additional expense. This storage unit is controllable especially in active and reactive power import/export through LabVIEW.

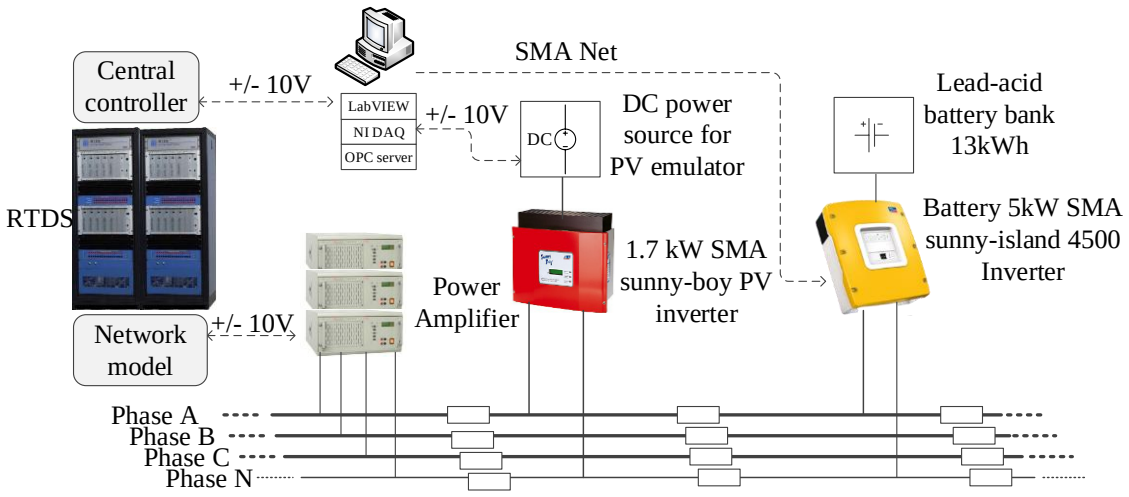

Figure 3-1 Layout of PHIL Emulation

The first case study contains the radial LV residential distribution network in Northern England as described earlier that is constructed in RSCAD. The simplified LV distribution network model still consists of large number of power components. As such, it is not possible to implement the whole network in one rack of RTDS. As such, the network model is divided into 2 subsystems; each subsystem is allocated to a rack. A power electronics average model of a PV generator and a storage unit based on the dq decoupling control method are needed, and are built in RSCAD. The PV emulator from the smart grid laboratory is also used in the network. Additionally, the laboratory battery unit has been used.

2.2 Real time digital simulator

There are several applications that the RTDS has been used extensively, such as investigation of power system equipment interaction, power hardware in the loop testing, and closed loop testing of control and protective relay [164][165]. The RTDS is a digital power system simulator for operating power system networks in continuous real-time simulation [164]. Utilising modular custom software and hardware, the RTDS can perform electromagnetic transient (EMT) power system simulations by using Dommel algorithm with a time step $50\mu s$ [164][165][166][167]. The Dommel algorithm applies the trapezoidal rule of integration to solve differential equations of the power system [167]. The trapezoidal rule is not able to provide continuous solutions, and it calculates the solution at discrete instants in time [165][167]. This takes many seconds to perform a single time step for large complex power network models by off-line software, such as Power System Computer Aided Design (PSCAD) and MATLAB/Simpower [164][165]. However, the RTDS has the capability to continuously perform the calculation for a single time step in a measured time that is exactly equal to the time step [165]. Hence, it is named as Real Time Digital Simulator.

To achieve real time simulation, the RTDS takes advantage of two levels of inherent parallelism in the Dommel algorithm [165]. The first level is to solve equations representing the power system by using the processor which is called rack [165][168]. Power system equations and control components solved by each rack are said to be within the same mathematical subsystem [165]. The

second level is to solve such power system that is not possible to implement the whole network in one rack [165][168]. The power system is divided into several subsystems, and each subsystem is solved in parallel using individual rack from the RTDS [165][168].

The latest processor introduced by RTDS Company is the PB5. The PB5 processor based RACK includes two Freescale MC7448 RISC processors operating at 1.7GHz for each one [169]. Two PB5 processors are in each RACK. One PB5 processor can be used to provide network solution, and the other PB5 processor can be used to solve the power system equations and control components.

The RTDS software is called RSCAD that is the link to RTDS hardware. The RSCAD is similar to PSCAD, and it is installed in a computer [170]. The RSCAD provides users with a number of predefined power and control system component models to simulate the large complex power system and analyse simulation results [170].

The RTDS software (RSCAD) is communicated with RTDS hardware through a Giga-Transceiver Workstation InterFace Card (GTWIF) [168]. The GTWIF is the communication interface between the RTDS hardware simulator and Local Area Network (LAN) [168]. Each GTWIF is used to assign a unique IP address, and this can provide a communication for computers accessible on the LAN [168]. Furthermore, the RTDS hardware also contains a Giga-Transceiver Network Interface card (GTNET) that is used to interface Ethernet based communication protocols with the RTDS simulator [168][171]. It communicates with the PB5 processor card by a GT optical port [168].

2.3 Voltage sensitivity factor

The voltage sensitivity factor represents how the variations in nodal active or reactive power leads to a change in voltage at a specified network location [162][172]. It means that a relatively large voltage sensitivity factor indicates that a change in power leads to a relatively large change in voltage at a given network location. The sensitivities of voltages to the active and reactive power injections can be determined through the use of a Jacobian matrix [162][172]. For radial distribution networks, only the voltage magnitude is of interest [172]

so the voltage variation with its sensitivity factor matrix can be simplified to a compact form [162][172],

$$[\Delta \mathbf{V}] = \begin{bmatrix} \frac{\partial \mathbf{V}}{\partial \mathbf{P}} & \frac{\partial \mathbf{V}}{\partial \mathbf{Q}} \end{bmatrix} \begin{bmatrix} \Delta \mathbf{P} \\ \Delta \mathbf{Q} \end{bmatrix} \quad (3.1)$$

The sensitivity matrix in equation (3.1) is reliant on the network operation and configuration. The VSF can vary with the change of PV output in a network. This implies that the VSF matrix will need to be constantly recalculated. However, online recalculation of the VSF matrix is difficult in distribution networks. This is because the level of real time information available in distribution level is much less than that at the transmission level [162]. Such real time information is necessary to know the full load flows through the distribution network to permit VSF calculation. In reality, the voltage sensitivity matrix does not change largely with the network operating conditions [172][173], and sensitivity analysis completed by the authors on this network used to this thesis confirms this.

3 Case Study 1: Using a smart grid laboratory to investigate battery energy storage to mitigate the effect of PV in LV distribution network

3.1 Introduction

High level connection of PV generators in LV distribution networks may pose several technical challenges as discussed in section 1.2.2, Chapter one. The objective of this case study is to investigate the characteristic of the storage unit from both smart grid laboratory and simulation model for voltage support. In this study, a large concentration of PV generators has been applied to an LV network as shown in Figure 1-4. The high resolution (6 second) solar irradiance data that measured at a domestic property in the UK are used in the work as specified in Figure 1-5 (b). These solar irradiance profiles represent different seasons. The load data was as described in Figure 1-5 (a). In order to present and compare the worst overvoltage and voltage imbalance scenario, the solar irradiances under different days have been selected as illustrated in Table 3-1.

It was found that lab storage capacity/rating are insufficient to solve the problem. Accordingly, both a single-phase RTDS simulation model and lab based storage are used in conjunction with each other, and are sited at the end

of the longest feeder in the network to show how to reduce voltage problems caused by the PV.

The voltage rise and voltage unbalance tracked in this study are explained next.

Table 3-1 Load and solar irradiance profiles used

Scenario	Time
Winter Sunny Day 28-Jan 2011	9:30-10:30, 11:30-12:30
Cloudy Day 18-Feb 2011	10:30-11:30, 13:30-14:30
Summer Day 06-Jun 2011	10:15-11:15, 12:30-13:30

- Overvoltage in the LV network

Figure 3-2 is a single line diagram of a simplified distribution network with a PV generator connected alongside a load. The voltage across this network is expressed as

$$\Delta V = V_{\mathrm{PV}} - V_{\mathrm{s}} = \frac{R(P_{\mathrm{PV}} - P_{\mathrm{L}}) + X(Q_{\mathrm{PV}} - Q_{\mathrm{L}})}{V_{\mathrm{PV}}} \tag{3.2}$$

Where V_{s} is the substation secondary bus source voltage, V_{PV} is the PV generator voltage, *R* and *X* are the feeder line resistance and reactance. P_{PV} and Q_{PV} are the active and reactive power of the PV generation. P_{L} and Q_{L} are the active and reactive power consumed by the load.

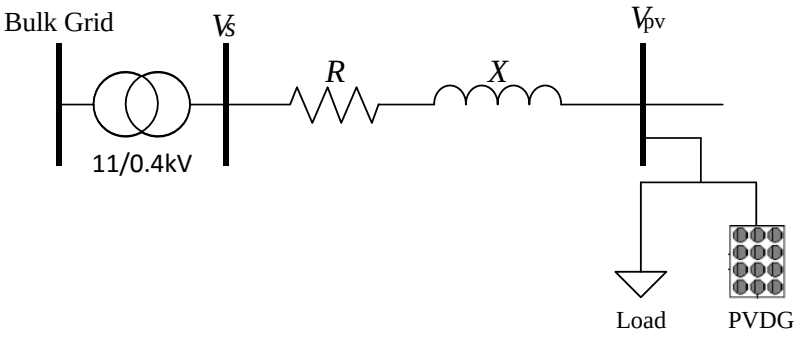

Figure 3-2: Two bus distribution system with embedded PV generation

Networks with no distributed generation have unidirectional power flow and voltages decrease along the line. If $P_{\mathrm{PV}} > P_{\mathrm{L}}$, this may cause voltage rise along the feeder. Consequently the network operator needs to consider that the upper voltage limits may be exceeded in networks with PV installed.

- Voltage unbalance

Voltage unbalance is a power quality issue, which can be made worse by the random location and rating of PV generators in LV distribution networks [174]. Electric motors and their controllers operate inefficiently under voltage unbalanced condition. In extreme cases, voltage unbalance can cause overheating electric motors and causes intermittent shutdown of motor controllers [175]. Voltage unbalance is limited to less than 1.0% at 33kV and 132kV, and nominal voltage below 33kV must not exceed 1.3% [63]. The voltage unbalance factor is defined below:

$$\%VUF = \frac{\text{Negative Sequence Voltage}}{\text{Positive Sequence Voltage}} \times 100\% \tag{3.3}$$

3.2 Energy storage implementation

The storage is sited at the end of the longest feeder in the network where the voltage rise is more severely. It operates in such way that it solely uses local measurement according to the decentralised control concept. The import or export power required of energy storage is determined with VSF by equation (3.4) and (3.5).

$$\Delta P_{\text{req}} = \frac{\Delta V_{i,\,\text{req}}}{VSF_{\text{iP}}} \tag{3.4}$$

$$\Delta Q_{\text{req}} = \frac{\Delta V_{i,\,\text{req}}}{VSF_{\text{iQ}}} \tag{3.5}$$

Where, ΔP_{req} is the storage unit required active power and ΔQ_{req} is the energy storage device required reactive power, $\Delta V_{i,\,\text{req}}$ is the required voltage change at node i, and both VSF_{iP} and VSF_{iQ} are the voltage sensitivity factors for active power (p.u./kW) and reactive power (p.u./kVAr) at node i. The voltage required $\Delta V_{i,\,\text{req}}$ is determined by the error of measured voltage, $V_{i,\,\text{measured}}$ and $V_{i,\,\text{threshold}}$. The $V_{i,\,\text{threshold}}$ is the voltage rise limit which set up by UK regulation policy in the range 1.0p.u. +10%/-6% for LV distribution networks [95]. It is worth mentioning that the reactive power of the energy storage is not used for voltage support in this study for this chapter. This is because the case study network considered has a relatively high R/X ratio (3.75-6.75) so that active power is much more effective in managing voltage support. Doing so can avoid significantly increasing the reactive power being drawn by the secondary transformer which may have a great impact on losses and thermal limits in the MV network.

3.3 Simulation results

The analysis is firstly carried out to compare overvoltage on days with different load and PV generators, and the use of the storage unit to tackle the voltage excursion is then presented.

3.3.1 Effects of PV on LV distribution network

The results show that the voltage rise in the network is as expected strongly correlated to the solar irradiance as seen in Figure 3-3. Furthermore, the fluctuating nature of irradiance, due to passing clouds, means that there are corresponding amounts of voltage fluctuation in the LV distribution network.

Figure 3-4 shows the cumulative distribution function for the end of the feeder voltage with or without PV generation on 6th June at two different times of the day. The red line indicates cumulative voltage distribution between 10:15-11:15. This can be seen to have an overvoltage probability of 75%. The blue line indicates voltage cumulative distribution function at time period 12:30-13:30 which exhibits overvoltage probability 78%. The overvoltage proportion rate at 12:30-13:30 is higher than the overvoltage proportion rate at 10:15-11:15.

As stated in Figure 3-4, 16% overvoltage (blue line) is between 1.10p.u. and 1.14p.u. for 12:30-13:30. On the other hand, from 10:15-11:15, 36% overvoltage probability (red line) occurs in the voltage range between 1.10p.u. and 1.14p.u.

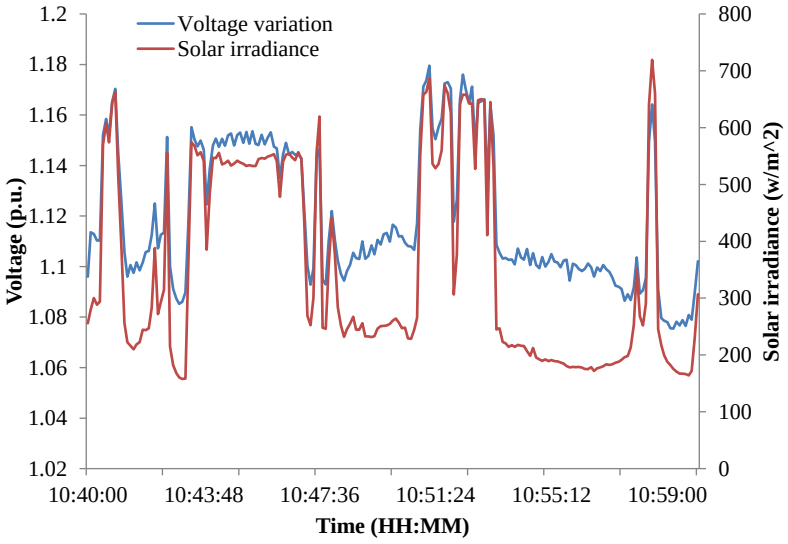

Figure 3-3: Voltage variation with solar irradiance at the end of the feeder, 10:40-11:00, 6th June

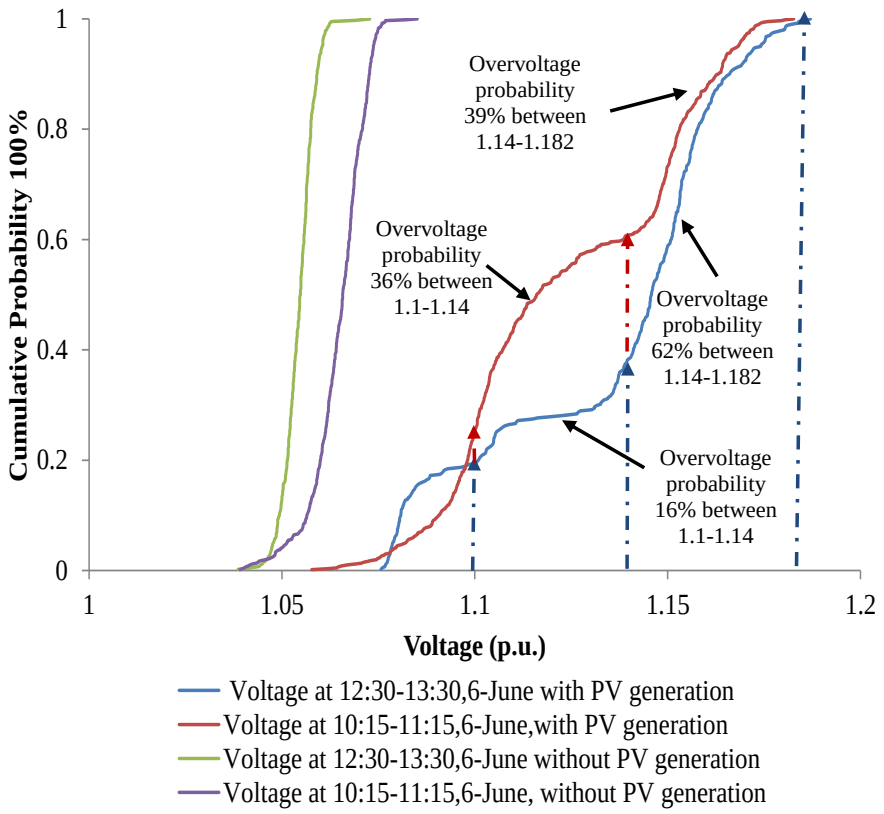

Figure 3-4 Cumulative distribution function of voltage at the end of feeder at 6th June

In addition, the overvoltage probability is more severe at voltages between 1.14p.u. and 1.182p.u. from 12:30-13:30 (i.e. 62%) as indicated by blue line in Figure 3-4. However, a 39% overvoltage probability (red line) is presented at the voltage range between 1.14p.u.and 1.182p.u.

These results show a direct correlation between the PV generated and the voltage level. In addition, the above discussion implies that more rapid charging of a storage unit will be required from 12:30-13:30 than 10:15-11:15.

A comparison analysis was carried out for overvoltage on different day (28-Jan, 18-Feb, and 06-Jan) as depicted in Figure 3-5. As expected, 28-Jan at both periods (9:30-10:30 and 11:30-12:30) has less overvoltage problems with overvoltage 31% in time period 9:30-10:30 and 49% for 11:30-12:30. This is because solar irradiance is comparably lower than the other two days. On the other hand, the overvoltage (75% of time 10:15-11:15 and 78% of time 12:30-13:30) is worse in summer/midday than in winter days as expected. Voltage unbalance increases with the amount of PV penetration as stated in Figure 3-7.

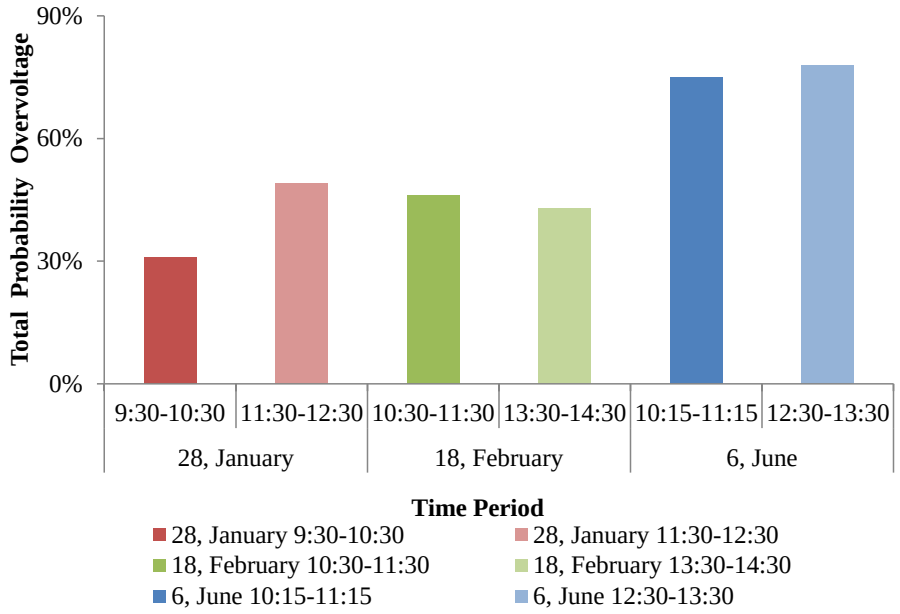

Figure 3-5 Total probability of overvoltage (greater than 1.1p.u.) for the different simulations

It shows voltage unbalance factor with PV penetration level for 10:15-11:15, 6-June. It indicates that voltage unbalance factor is linearly increased with the level of PV connection. The VUF is maintained the range of 1% to 4%. When the PV connection level reaches to 300%, the VUF is above 3%.

Understanding the fluctuation and severity of the voltage problem in this way is important because it has an effect on the control strategy of any energy storage to fix voltage problems in different seasons and at different times of day.

3.3.2 Use of energy storage unit to fix voltage problems

The effect of storage on fixing the voltage problem is investigated for the period 10:15 to 11:15 on 6th June. The energy storage unit is sited at the end of the feeder where overvoltage is more severely. The energy storage unit is controlled to enter charging mode if voltage is higher than a threshold value (1.1p.u.) and the import power is calculated based on VSF (as described above). As shown in Figure 3-6 and Figure 3-7, this improves the conditions in the network as follows:

- The magnitude of the voltage is brought within legal limits- fixing the voltage excursion;
- The voltage fluctuation is reduced leaving a smoother voltage profile (the voltage standard deviation is reduced by 84%);

- The voltage unbalance factor has been reduced to within legally acceptable levels (less than 1.3%).

By improving the conditions in the network, the use of a storage unit can therefore be said to increase the permissible the level connection of PV in LV distribution networks. In addition, the use of a variable power (calculated from voltage sensitivity factor) demand into the energy storage is effective because it allows a lower rise in the energy storage state of charge (SoC) than would happen if the energy storage is charged at a constant rate (see Figure 3-8). This enables lower capacity and so cheaper storage to be used.

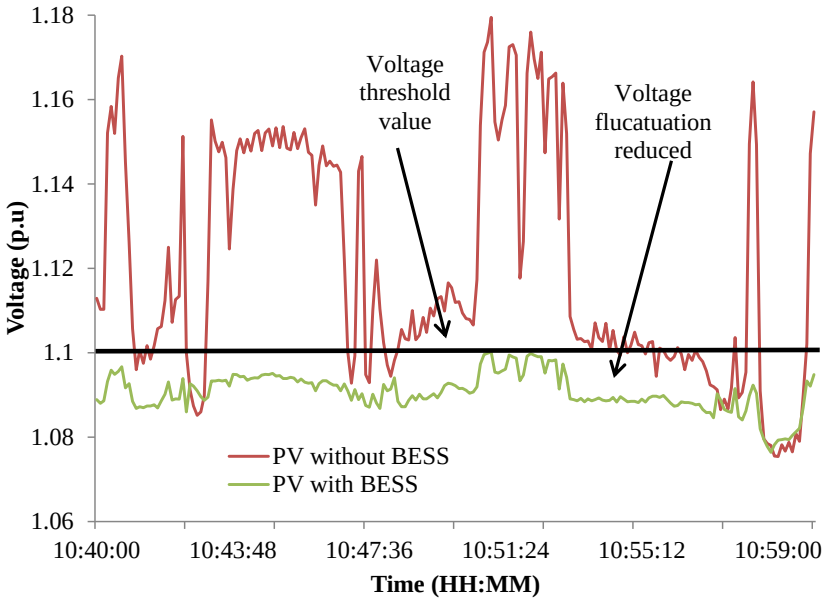

Figure 3-6 Voltage rise reduction by energy storage at time 10:40-11:00, 6th June

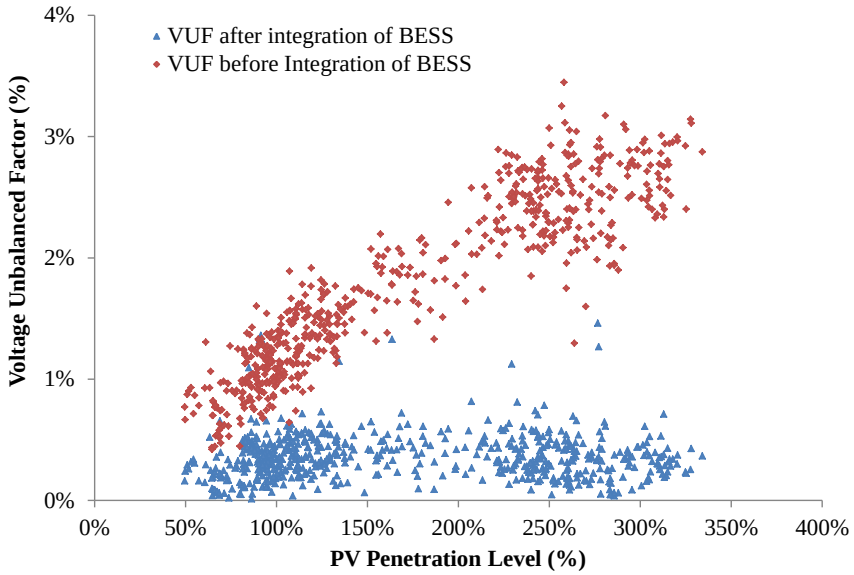

Figure 3-7 VUF before and after integration of storage, 10:40-11:00, 6th June

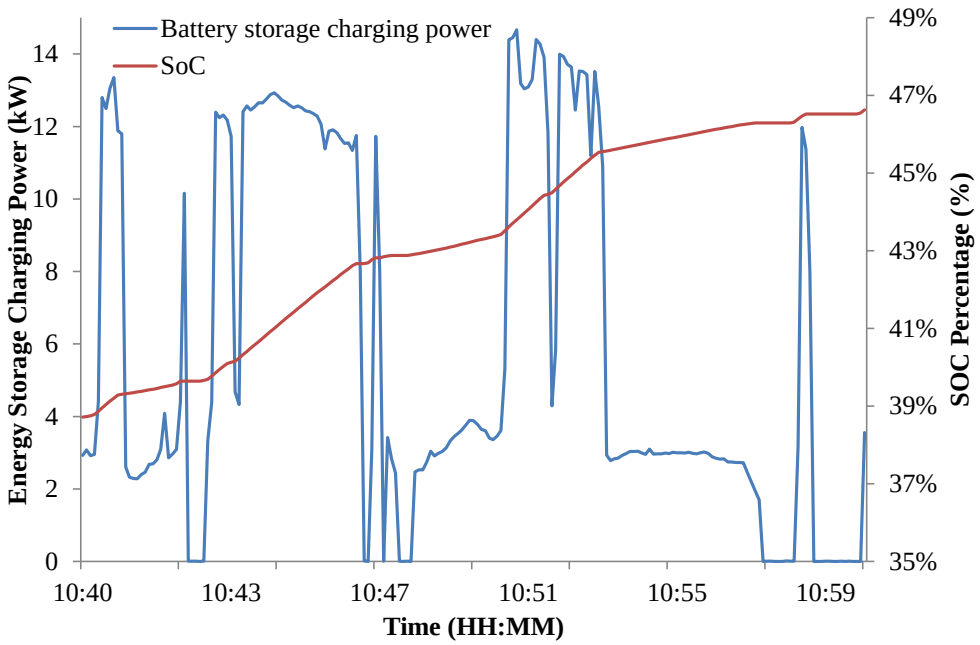

Figure 3-8 RTDS (Emulated) storage charging power, 10:40-11:00, 6th June

4 Case Study 2: Coordinated voltage and power flow control in LV distribution Network

4.1 Introduction

As already discussed, a large percentage of LCT loads, such as Heat Pumps (HPs) and EVs, will cause significant voltage drop along LV feeders. On the other hand, a large number of PV generators can cause overvoltage during summer sunny days. However this will not be the only problem confronted by LV networks in the future. In addition, the large connection of LCT loads and generations keep increasing, the devices on the networks such as MV/LV transformers will be overloaded by either LCT loads or reverse power from DGs. A collaborative work is implemented to develop a coordinated control method using the on load tap changer (OLTC) and the energy storage unit to solve both voltage excursion and reverse power flow problems. This collaborative work is according to customer led network revolution (CLNR) project sponsored by Northern Power Gird (NPG), and is partially contributed and supported by a senior research engineer from CLNR project. The load data and network for case study is provided by NPG.

4.2 Coordinated control of the storage unit and the OLTC

A coordinated control method based on the storage unit and OLTC from the secondary transformer for a LV distribution network is investigated in this case study. Figure 3-9 illustrates the proposed method that controls the voltage and power flow in the LV distribution network with coordination rather than individually. In this case study, the OLTC is assumed to be deployed in LV distribution network, and the reactive power functionality of energy storage unit is also banned to be applied.

At the beginning, the coordinated controller receives the required network measurements, such as voltage or power flow. This is used to check if there is a violation of voltage or power flow in the network. If the voltage excursion is happened, the OLCT equipped at the secondary transformer will be firstly operated. However, because the tap changing at the transformer will affect the voltage of other downstream loads, forecasting will be performed to ensure the tap operation does not cause voltage violation at the other location of the network. Such tap changing wears out the lifetime of the transformer, and this also requires more maintenance [176].

On the other hand, if the OLTC is not available to be used to tackle the voltage excursion, the coordinated controller will command a signal to energy storage unit to solve the voltage problem. In such case, the energy storage unit is controlled to import/export its active power that is calculated based on the VSF and the difference between the measured voltage and threshold voltage so that the voltage excursion can be solved.

Furthermore, if the coordinated controller receives the measurement of the power flow violation, the proposed coordinated controller will command a signal to the storage unit which is nearest of the location of violation to tackle the problem. Similarly, the coordinated controller will check and make sure the voltage from the network is not to be violated by power flow regulation using the battery unit. This can be done by employing the VSF at a given network location and required active power from the storage unit to determine whether the voltage at a given network location will be violated.

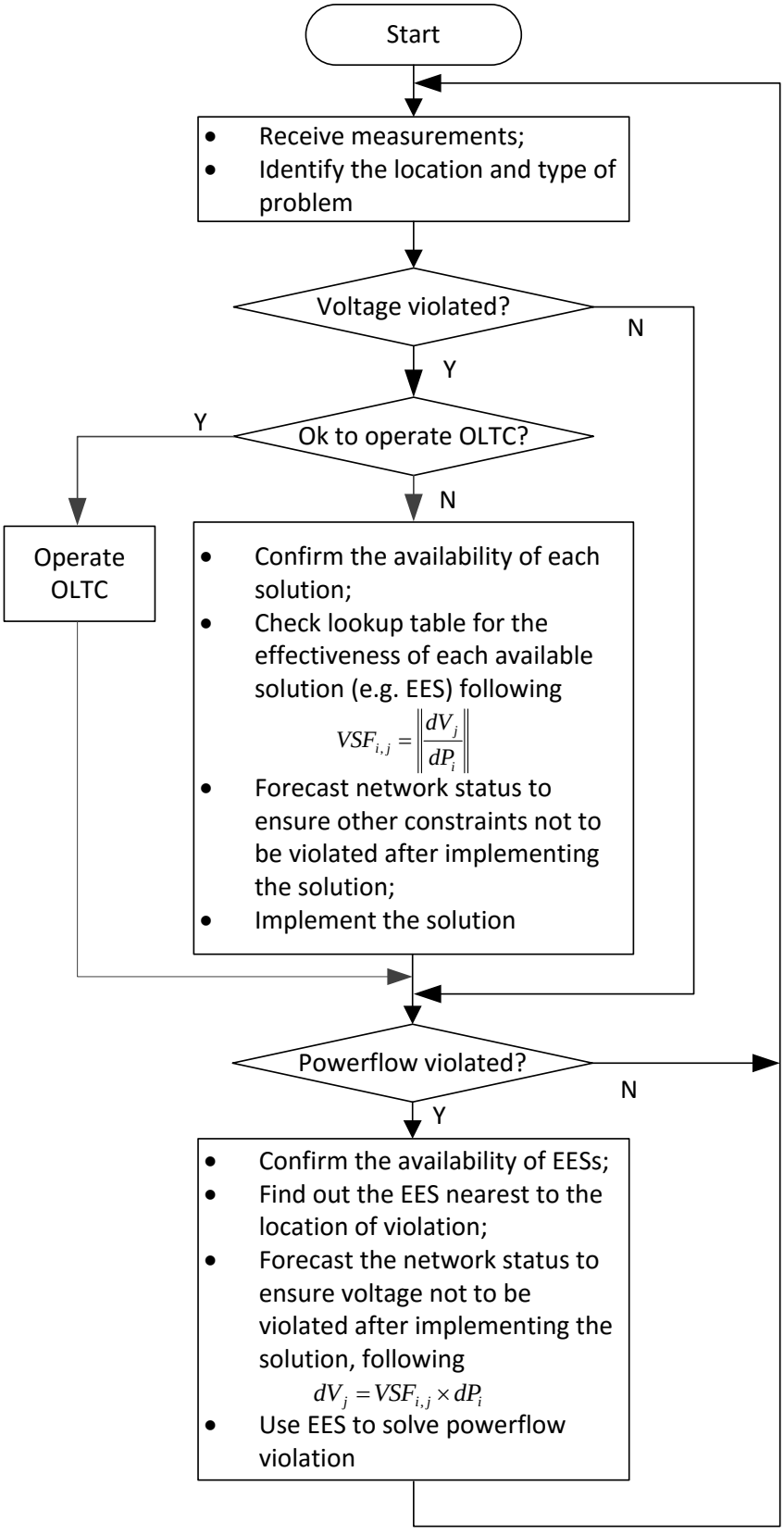

Figure 3-9 Coordinated control of voltage and power flow

4.3 Source data and network description

This case study is evaluated by RTDS from the smart grid laboratory. A distribution network provided by NPG from CLNR project is selected as shown in Figure 3-10 to evaluate the proposed coordinated control method. The network starts with a MV/LV 0.315 MVA OLTC transformer and supplies power to 196 residential customers. The connection of LCT loads and generation among these houses are: 60% EV, 60% HP and 90% solar PV. A 100kVA energy storage unit is located at the substation as shown in Figure 3-10. The OLTC and the storage unit are used for preventing voltage excursions and reducing reverse power flow to avoid transformer to be overloaded.

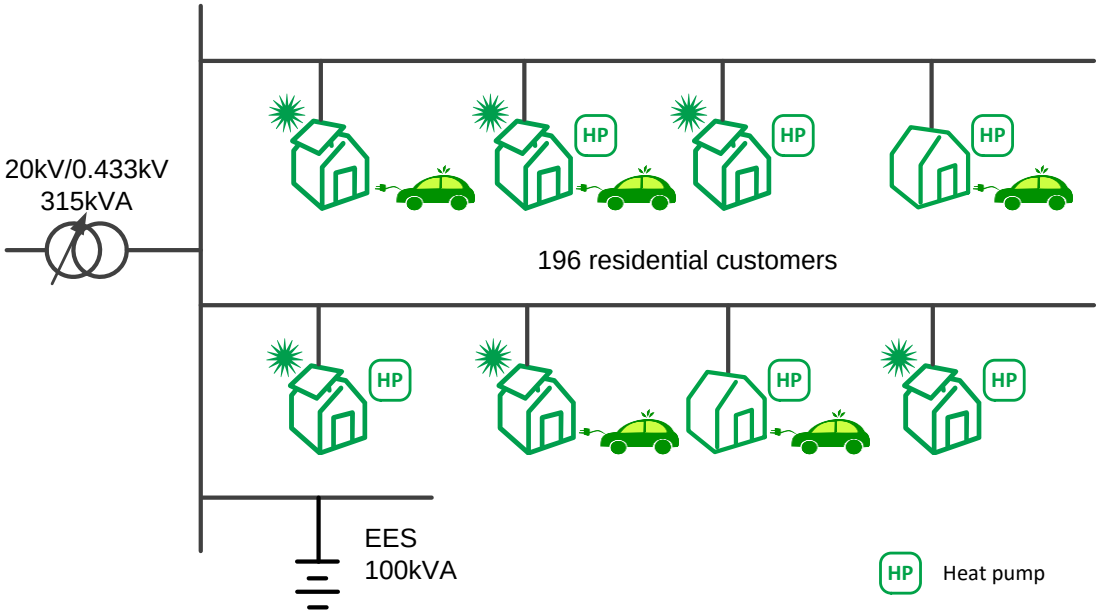

Figure 3-10 the case study network with high penetration of HP, EV and solar PV

An average domestic load profile from CLNR smart meter data of 5000+ customers in the period of May 2011 to May 2012 is used in this case study along with typical consumption profiles of EV and HP from the smart grid forum report [177] as shown in Figure 3-11. An average solar irradiance profile from 20 British Gas customers is used in the case study (see Figure 3-12).

According to above loads, generation profiles and their penetration levels, the power flow of the transformer can be calculated as equation (3.6):

$$P_{TX}=(P_{domestic}+P_{EV}\times 60\%+P_{HP}\times 60\% - P_{PV}\times 90\%)\times 196 \quad (3.6)$$

Where P_{TX} denotes the transformer power, and $P_{domestic}$, P_{EV}, P_{HP} and P_{PV} denote domestic load, EV consumption, HP consumption and PV generation.

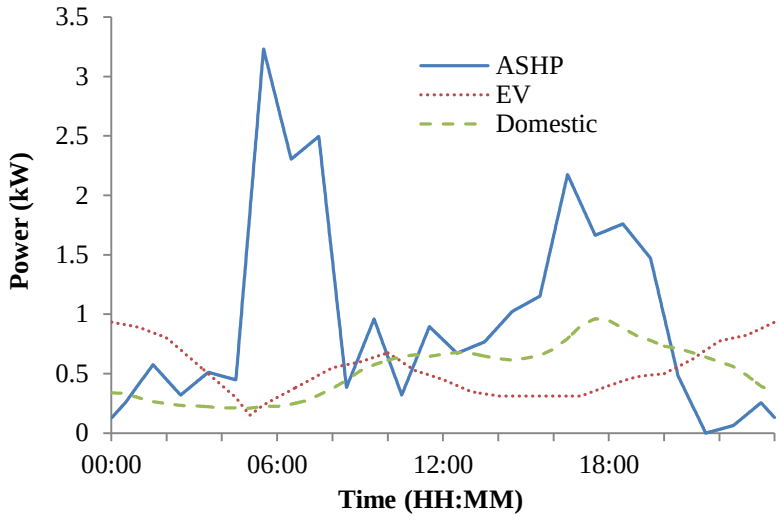

Figure 3-11 Average domestic daily load profile and typical consumption profile of HP and EV

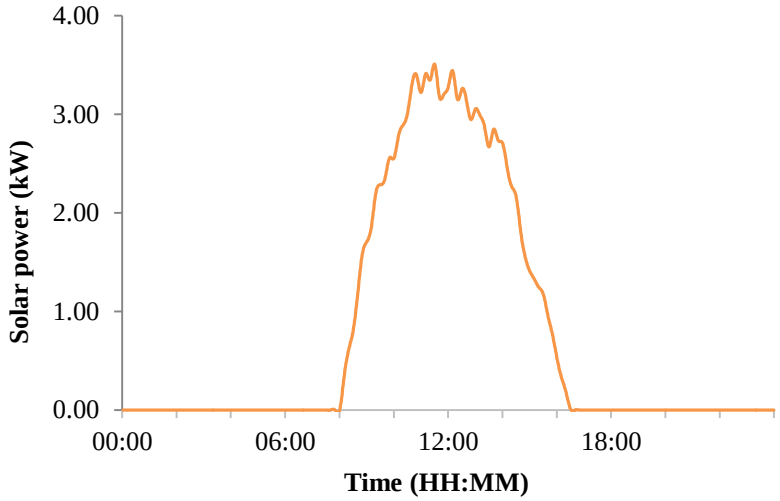

Figure 3-12 Average PV profile from 20 British Gas domestic customers in 2011

Figure 3-13 illustrates the 24 hours power flow of the transformer calculated with equation (3.6). The positive power peaks happens in early morning and late afternoon. The reverse power flow at mid-day (time periods 10:00 am and 14:00 pm) has potential to overload the transformer. As such, the energy storage unit has to absorb the power at these time periods, in order to prevent the transformer from being overloaded.

4.4 Simulation results

The proposed coordinated controller and a baseline study which occurs with no energy storage or curtailment of the PV generation or OLTC are implemented.

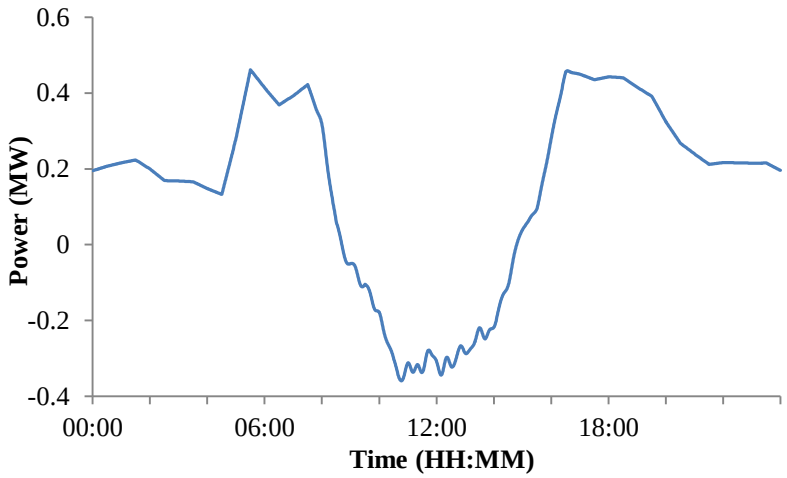

Figure 3-13 Projected daily power flow profile of LV distribution transformer

Figure 3-14 and Figure 3-15 show the voltage at the end of the feeder and the power flow of the transformer respectively in the baseline study (without OLTC or storage) and with coordinated control of OLTC and energy storage at day time. It illustrates that when the solar generators' output cause the transformer power flow reversed around 9 o'clock in the morning, and this also cause the overvoltage at the feeder end and overloading of the transformer at mid-day during the baseline study.

However, by coordinating the storage and OLTC, this issue can be mitigated. As shown in Figure 3-14, if the feeder end voltage reaches the legal limit (1.1p.u in the UK) at time around 10:00 o'clock, the coordinated controller first introduces the OLTC to reduce the voltage excursion between the time period 10:00 and 11:00 in the morning as indicated by the green line from Figure 3-14.

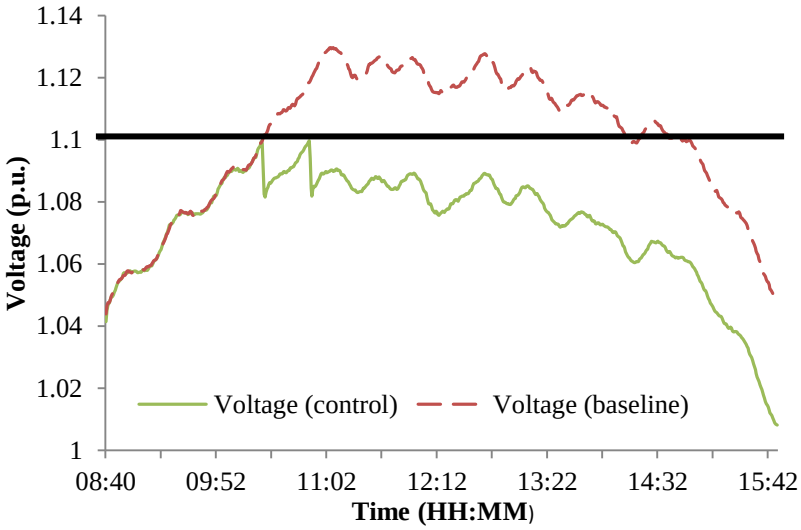

Figure 3-14 Feeder end voltage in baseline study and with coordinated control

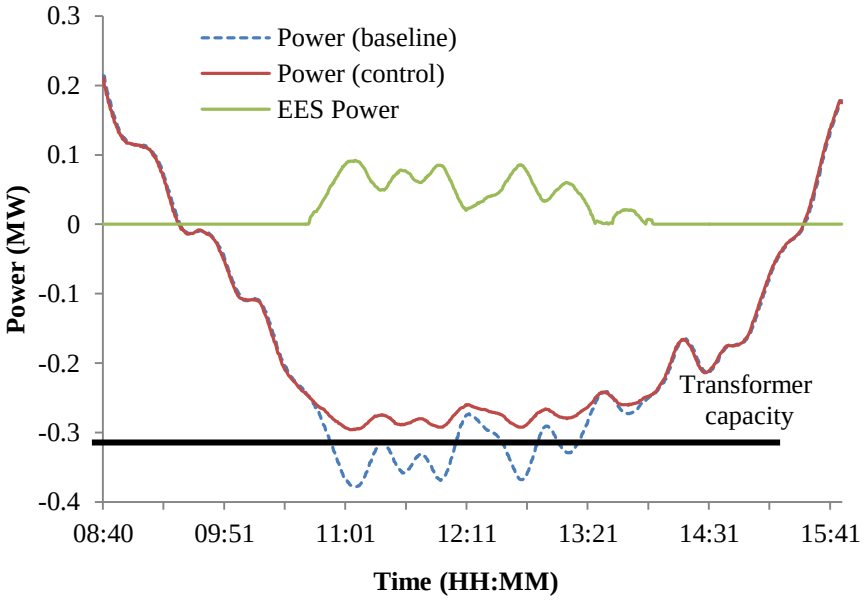

Figure 3-15 Transformer reverse power flow absorbed by battery

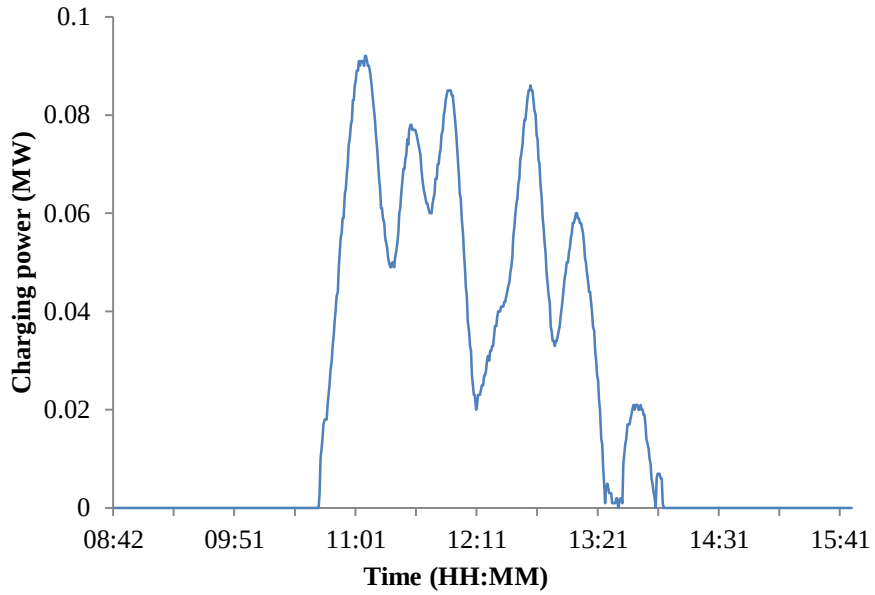

Figure 3-16 Charging power of the storage

However, if the transformer is overloaded, the controller commands the storage to absorb the excess active power. Thus, transformer overloading is mitigated as indicated by red line shown in Figure 3-15. The energy storage unit charging power is shown in Figure 3-16.

Figure 3-17 and Figure 3-18 illustrate the voltage at the end of the feeder and the transformer power flow for a baseline study (without operation of OLTC or storage) in comparison to proposed coordinated control method. This is shown for between the afternoon and midnight. Although PV power outputs are

reduced, residential and LCT loads are increased in the afternoon. Accordingly, the voltage at the end of the feeder drops significantly, and the transformer power flow changes direction again (i.e. there is no reverse power flow across the transformer).

Under the baseline study, the voltage reaches the regulatory limits between 16:00 and 20:00 as seen by Figure 3-17. Furthermore, the transformer starts to be overloaded at approximately 16:20 when the residential and LCT loads increase (see Figure 3-18).

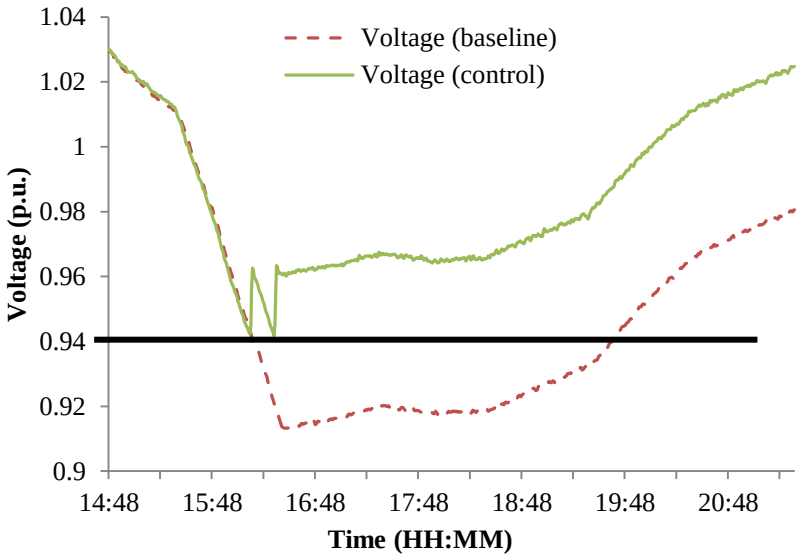

Figure 3-17 Voltage at the end of the feeder in baseline study and with coordinated control

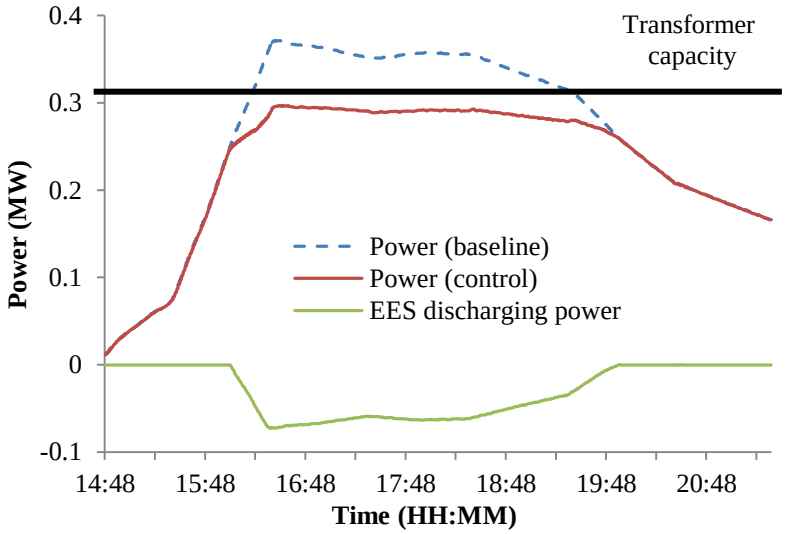

Figure 3-18 Transformer power flow mitigated by storage

On the other hand, in the case of coordinated control, undervoltage and transformer overloading do not occur. Between 16:00 and 17:00 the

coordinated controller detects a voltage excursion at the end of the feeder and firstly calls the OLTC to bring the voltage within the legal limit as indicated by green line in Figure 3-17. However, the transformer starts to become overloaded (beyond the value of 0.315 MVA) at 16:20. This is caused by the increasing load. The coordinated controller therefore commands the energy storage to discharge active power so that the overloading is mitigated as indicated by red line shown in Figure 3-18. The energy storage discharge power is shown in Figure 3-18 (green line).

5 Summary and Conclusion

This chapter has described the two functional strategies of energy storage for voltage support. This includes two case studies that are both developed in RTDS from a smart grid laboratory.

The first functional strategy investigates voltage problems under different solar irradiance profiles at different seasons and the integration of energy storage unit into LV distribution networks to solve the associated voltage problems. It is implemented based on the power hardware in the loop test bed. Real network, demand and generation data are used in a real time simulation and the storage is shown to provide a feasible solution to the problem.

The second functional strategy proposes a coordinated control method for solving voltage excursions and reducing reverse power flow to help the existing distribution network adapt to future scenarios with high numbers of connected LCT loads and PV generators. This relieves transformer overloaded and mitigates voltage excursions by coordinating storage charging/discharging functions with an OLTC.

As previously discussed, multiple energy storage units installed at LV networks will be a trend to address the voltage excursion by the presence of the PV generators. Therefore, coordinated control strategy for multiple energy storage units will play an essential part for future LV distribution networks. Accordingly, chapter 4 introduces a coordination strategy for multiple energy storage units in a LV distribution network. This strategy is developed based on the concept of voltage sensitivity analysis and a battery model is also included.

Chapter 4: Coordination of multiple battery energy storage units in a low voltage distribution network

1 Introduction

As stated previously in Chapter 2, multiple energy storage units installed in LV networks will be a trend for mitigating challenges caused by PV generators. However, there is a great challenge to apply multiple energy storage in future distribution networks. This is because it would be problematic to create an appropriate coordinated control strategy in which both the energy storage aging condition and voltage constraints need to be considered. Although some innovative research work focuses on how to coordinate multiple energy storage units in a distribution network, such as reference [146], these may not be efficient for voltage regulation in practical world. This is due to the fact that many systems do not consider about the battery aging condition while solving voltage problems.

In this chapter, a method for the coordination of multiple battery energy storage systems (BESS) is proposed for voltage regulation in a LV distribution network. This work has been published on IEEE transactions on smart grid (please see publications section and the primary author of the paper being the author of this thesis). The main objective of this method is to solve overvoltage problems with multiple suitably sized energy storage systems. The method is based on voltage sensitivity analysis and a battery aging model. These calculations give parameters that influence which battery storage units are selected to provide strict maintenance of voltage limits. So in this sense, battery aging analysis is included to modify the system's selection behaviour in response to battery degradation while consistently maintaining voltage limits.

The performance of coordinated control is compared with non-coordinated control using both a RTDS and a MATLAB/Open Distribution System Simulator (OpenDSS) model of a real UK LV distribution network with a high installed capacity of PV generators. The RTDS model is used to examine the effectiveness of the proposed controller under real time simulation. The work from MATLAB/OpenDSS is collaborative and contributed by a colleague from Durham University [147]. This is used to investigate the benefits of the

proposed method over a ten year period. According to simulation results from both RTDS and MATLAB/OpenDSS, a non-coordinated control design which uses multiple energy storage units in a single network might cause some storage units to operate more than others. This is shown to prematurely age some of the units in the network and increase costs to the system operator. Coordinated control can be used to utilise the multiple storage units more evenly and therefore reduces the costs of battery replacement to the storage operator in terms of both number of batteries and maintenance visits.

2 Proposed coordinated control method for multiple storage units

In this thesis, a new coordinated control of multiple BESSs based on voltage sensitivity analysis and a battery aging model is developed as shown in Figure 4-1. Both centralised and decentralised controllers are included in the proposed coordinated control scheme. The proposed coordinated method utilises the positive features of both centralised and decentralised control as discussed in Chapter 2. The functionality of centralised controller is to determine which energy storage units should be used to solve the voltage excursion by considering the remaining battery cycle life, energy storage availability and their VSF. As indicated in Figure 4-1, the selected storage then determines its individual power set points within its decentralised controller and communicates the results back to the centralised controller for subsequent

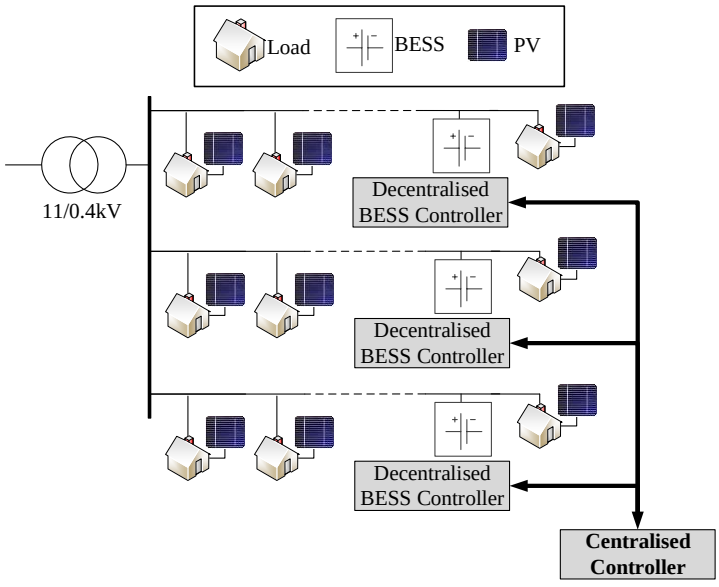

Figure 4-1: Coordinated control of multiple energy storage units

decision making. This is contract to decentralised control where each BESS only has access to local measurements of voltage, combined with a VSF, to determine active power P and reactive power Q set points. In coordinated control, several storage units are operated using both a centralised and a decentralised controller as shown in Figure 4-1.

2.1 Design of decentralised controller

Figure 4-2 shows the process in which the decentralised controller uses the average phase voltage, V_{ave} and its VSF to calculate active/reactive power to prevent overvoltage. Under decentralised control, each BESS has visibility only of local measurements. If a voltage excursion happens at this node, the storage determines its active and reactive power using local network voltage measurements and its VSF. In contrast to the work presented in Chapter 3, the coordinated control scheme proposed here considers the use of reactive power from storage, Q which is always prioritised above active power P to preserve battery SoC [178]. The battery SoC is conserved because Q does not use stored energy and is a function of the inverter.

While it is noted that changing the ratio of active power P and reactive power Q used by the controller will affect the voltage control performance, this work focuses on coordinated control and strategies to include battery aging models, so evaluation of enhanced P/Q ratios is not given here. This is presented based on small signal modelling in Chapter 6.

According to above discussion, the decentralised controller is divided into two parts: a reactive power controller and an active power controller. These two controllers take the actions shown in Table 4-1. These threshold values have been selected and tuned during experimentation, and will be individually set for different network configurations. Three thresholds are given: upper V_{uptld}, middle V_{midtld}, and lower V_{lwtld}. If V_{ave} is greater than the upper threshold V_{uptld}, a command will set the BESS to charge based on its VSF to solve the overvoltage. Between the middle threshold, and the lower threshold, the charging power is reduced. If the measured voltage drops below the lower threshold, for a pre-defined period of time, the BESS will stop charging as it is no longer needed.

Table 4-1: Threshold values for determine control action for overvoltage condition

Battery state and voltage thresholds	Controller action
Voltage at a measured node is greater than upper threshold V_{uptld}	Charge BESS at power based on VSF
BESS charging and voltage drops between middle threshold V_{midtld} and lower threshold V_{lwtld} for time constant	Reduce BESS charge power based on VSF
BESS charging and voltage drops below lower threshold, V_{lwtld} for time constant	Stop charging BESS

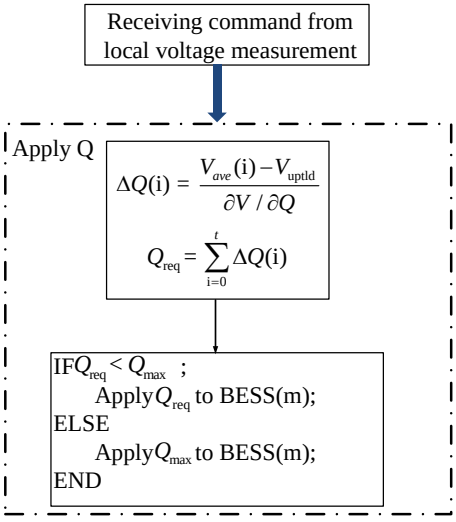

(a)

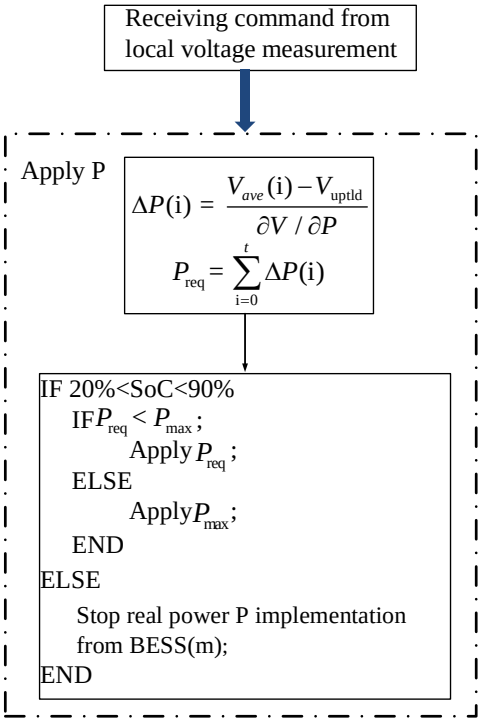

(b)

Figure 4-2: Decentralised controller of BESS; (a) Q-operation (b) P-operation

2.1.1 Decentralised reactive power controller

Each BESS identifies a local voltage excursion. Separate controllers are required to respond to over or undervoltage conditions, the descriptions that follow are for controlling overvoltage, but the same method is applied for undervoltage.

Q is initially applied to solve the voltage problem based on its local voltage sensitivity factor as shown in Figure 4-2 box (a) where t is the current time period. The difference between average phase voltage, V_{ave} and upper threshold voltage V_{uptld} are divided by the VSF, to calculate the required reactive power, Q_{req}. If the required reactive power, Q_{req} is less the maximum rated reactive power, Q_{max} the decentralised controller will apply required reactive power, Q_{req} to solve the voltage problem. Otherwise, the maximum rated reactive power, Q_{max} is applied.

2.1.2 Decentralised active power controller

If the required reactive power Q reaches its maximum power limit, the BESS active power P is applied, while Q continues at the rated maximum value. The required active power, P_{req} import from each energy storage unit is similarly calculated based upon a VSF and the difference between average phase voltage, V_{ave} and upper threshold voltage, V_{uptld} as shown in Figure 4-2 box (b). If the BESS is at its rated maximum power, P_{max} or if it's SoC is out of limit then the BESS has no further P capability, and this particular BESS is determined to not be able to solve the voltage problem. This can be addressed by increasing the BESS rating/capacity or by coordinating a fleet of BESSs through a coordinated controller as proposed by this thesis.

2.2 Design of centralised controller

The centralised controller maintains an operational matrix, $\mathbf{M}$ to select the preferred BESSs, which considers:

- The availability of each BESS to import/export active/reactive power is based upon its SoC, charge/discharge power and outage condition. This

information is contained in the availability matrix, **A**, which identifies if the preferable BESS is available to use.

- The preference for choosing each BESS in the network is based upon the remaining cycle life of each unit and the VSF relative to where the voltage problem occurs. This is contained in the nomination matrix, **F**, which determines if there is a preferable BESS based on the information provided.

The operational matrix **M** is used to select the preferable BESS to be used for voltage support. It is the product of the availability and nomination matrices and is split into active and reactive parts

$$\begin{bmatrix} \mathbf{M}_{\mathrm{P}} & 0 \\ 0 & \mathbf{M}_{\mathrm{Q}} \end{bmatrix} = \begin{bmatrix} \mathbf{F}_{\mathrm{P}} & 0 \\ 0 & \mathbf{F}_{\mathrm{Q}} \end{bmatrix} \begin{bmatrix} \mathbf{A}_{\mathrm{P}} & 0 \\ 0 & \mathbf{A}_{\mathrm{Q}} \end{bmatrix} \tag{4.1}$$

A detailed description of mathematical expressions and relationships between the availability and nomination matrices now follows.

2.2.1 Availability Matrix A

The diagonal energy storage availability matrix **A** indicates whether the active and reactive power functions of each BESS are available. The matrix is divided into two parts $\mathbf{A}_{\mathrm{P}}$ and $\mathbf{A}_{\mathrm{Q}}$

$$\mathbf{A}_{\mathrm{P}} = \begin{bmatrix} A_{P1} & & 0 \\ & \ddots & \\ 0 & & A_{Pm} \end{bmatrix} \tag{4.2}$$

and

$$\mathbf{A}_{\mathrm{Q}} = \begin{bmatrix} A_{Q1} & & 0 \\ & \ddots & \\ 0 & & A_{Qm} \end{bmatrix} \tag{4.3}$$

where the index m represents number of storage units in the network.

The active power availability matrix $\mathbf{A}_{\mathrm{P}}$ is an $m \times m$ diagonal matrix and is determined by the BESS SoC and its active power rating

$$A_{Pm} = \begin{cases} 1, & \mathrm{SoC} \leq 90\% \text{ and } P_{\mathrm{req}} < P_{\max} \\ 0, & \text{otherwise} \end{cases} \tag{4.4}$$

If $A_{Pm}= 1$, the BESS (m) can be used for charging or discharging active power. Otherwise, $A_{Pm}=0$; if the battery is at the SoC limit, maximum power limit or the BESS has a fault.

The reactive power availability $\mathbf{A}_{\mathrm{Q}}$ is also an $m \times m$ diagonal matrix similarly defined but without a SoC limit

$$A_{Qm} = \begin{cases} 1, & Q_{\mathrm{req}} < Q_{\max} \\ 0, & \text{otherwise} \end{cases} \tag{4.5}$$

The SoC is not included because the reactive power function is achieved using the BESS converter and does not rely on the finite energy store.

2.2.2 Nomination Matrix F

The nomination matrix, $\mathbf{F}$, is used to determine the preferred BESS to address a voltage excursion problem by considering the VSF and the aging condition

$$\begin{bmatrix} \mathbf{F}_{\mathrm{P}} & 0 \\ 0 & \mathbf{F}_{\mathrm{Q}} \end{bmatrix} = \begin{bmatrix} \mathbf{VSF}_{\mathrm{P}} & 0 \\ 0 & \mathbf{VSF}_{\mathrm{Q}} \end{bmatrix} \begin{bmatrix} \mathbf{L} & 0 \\ 0 & \mathbf{I} \end{bmatrix} \tag{4.6}$$

Where $\mathbf{F}_{\mathrm{P}}$ represents the active power nomination matrix and $\mathbf{F}_{\mathrm{Q}}$ denotes the reactive power nomination matrix. Both $\mathbf{VSF}_{\mathrm{P}}$ and $\mathbf{VSF}_{\mathrm{Q}}$ are the sensitivity factors in an $n \times m$ dimensional matrix for n voltage measurement locations in a distribution network and m storage units.

The second term in (4.6) represents the remaining cycle life, $\mathbf{L}$, of each BESS. The age matrix $\mathbf{L}$ is an $m \times m$ dimension matrix

$$\mathbf{L} = \begin{bmatrix} L_1 & & 0 \\ & \ddots & \\ 0 & & L_m \end{bmatrix} \tag{4.7}$$

Reactive power delivery is not affected by the battery aging condition, and so the reactive power nomination matrix $\mathbf{F}_{\mathrm{Q}}$ is only dependent on $\mathbf{VSF}_{\mathrm{Q}}$. As such, an $m \times m$ identity matrix $\mathbf{I}$ is used.

From the relationship discussed above, both the nomination matrix $\mathbf{F}$, and the operational matrix $\mathbf{M}$, are $2n \times 2m$ dimension matrices.

The remaining cycle life matrix, $\mathbf{L}$, of each BESS is introduced to stop the centralised controller from always nominating the BESS with the highest VSF over other units. Over a BESS project lifetime, total energy passing through the

BESSs in the network will increase as BESSs with a lower VSF are used more frequently. However, this shares out the aging of the BESS units so that when the maintenance regime is taken into account the overall project costs can be reduced. The benefit of using an aging model in this way is examined in a case study section.

Battery aging is affected by a number of factors such as depth of discharge; number of cycles, temperature etc. and it represents a major component of BESS costs. Decentralised control can focus on one BESS which can cause rapid aging. The coordinated controller offers an opportunity to manage aging rates by distributing usage of the BESSs within the LV network. In this work, the remaining cycle life of each BESS is determined using the depth of each daily cycle using a rainflow cycle counter model and a double exponential curve of the form

$$N_{m,\,t} = \alpha e^{aD_{m,\,t}} + \beta e^{bD_{m,\,t}} \tag{4.8}$$

This curve is derived for a lead acid battery [179], since this is a well understood technology for storage in LV network [180]. A number of more complex approaches for battery aging (e.g.[181]) are applicable in this coordinated controller if they provide a value of the deterioration, $\mathrm{L_m}$, of each BESS for the nomination matrix similar to that shown in [182]. However, it is felt that a simple aging model is appropriate for assessing the application of aging management within a coordinated controller.

For each day, this equation relates the number of cycles, $N_{m,\,t}$ that a battery unit can sustain, to a given depth of discharge, $D_{m,\,t}$ (expressed as a percentage) using fitting constants α, β, a and b. The MATLAB curve fitting tool is used to determine these fitting constants for a suitable valve–regulated lead–acid (VRLA) battery [183] as shown in (4.9).

$$N_{m,\,t} = 12500e^{-0.1158D_{m,\,t}} + 2070e^{-0.01537D_{m,\,t}} \tag{4.9}$$

This has been fitted against the five data points giving cycles to failure at different depths of discharge in the battery manufacturer's datasheet. As can be seen in the datasheet, the trend is distinct and equation (4.9) provides a fit to this with a 0.683% root-mean-square error. The battery cycle to failure trend according to both original data and curve fitting data as illustrated in Figure 4-3.

The remaining life of each unit is updated in the nomination matrix by the centralised controller at time step T using the expression

$$L_m = 1 - \sum_{t=1}^{T} \frac{1}{N_{m,t}} \tag{4.10}$$

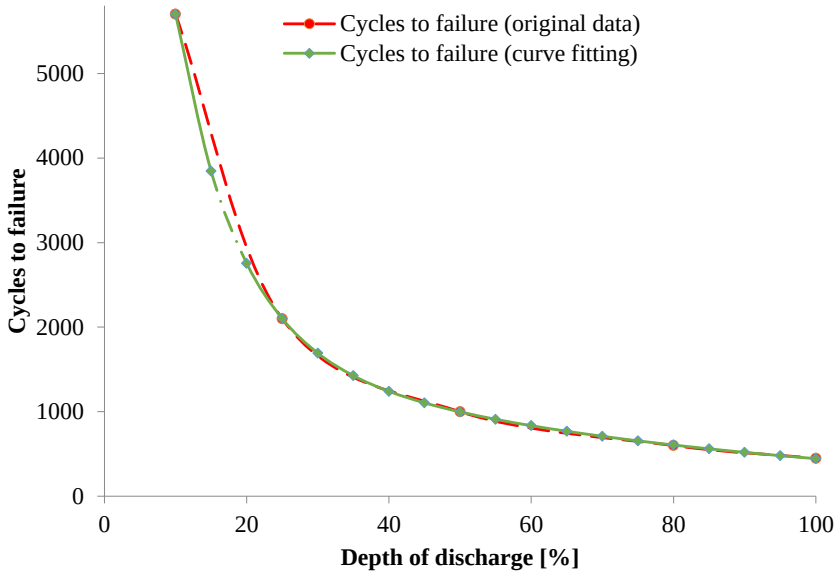

Figure 4-3: Battery cycle to failure trend based on both original and curve fitting data

In addition to the cycle life, batteries also have a calendar life which for VRLA batteries is typically around 5 years [180]. Extending a BESS's cycle life beyond the calendar life is not advantageous when considering the management of the asset.

2.3 Implementation of coordinated control scheme

Both centralised and decentralised controllers are included in the proposed coordinated control scheme. The centralised controller selects the preferred energy storage unit to be used, whereas the decentralised controller calculates and implements the required active/reactive power set-points. The flowchart in Figure 4-4 shows of the steps taken in the coordinated control scheme.

If there is a voltage excursion, voltage rise or drop, the availability matrix $\mathbf{A}_Q$ is first checked from the operational matrix $\mathbf{M}_Q$ (reactive power). If the availability matrix, $\mathbf{A}_Q = 1$ reactive power from the BESS can be applied to solve the voltage problem. The operational matrix $\mathbf{M}_Q$ (reactive power) uses equation (4.1) to select the most preferable BESS with the function

$$M_{\mathrm{Q}}^{*} = \arg\max(\mathbf{M}_{\mathrm{Q}}) \tag{4.11}$$

Once the most preferable BESS is selected, the decentralised controller calculates and implements the required reactive power Q_{req} to support voltage excursion. In addition, the availability matrix $\mathbf{A}_{\mathrm{Q}}$ is updated based on the reactive power output from the BESS converter. If the centralised controller's availability matrix, $\mathbf{A}_{\mathrm{Q}} = 0$ there is no remaining reactive power compensation available in the network, and the centralised controller enters $\mathbf{M}_{\mathrm{P}}$ mode. Q continues at the rated value.

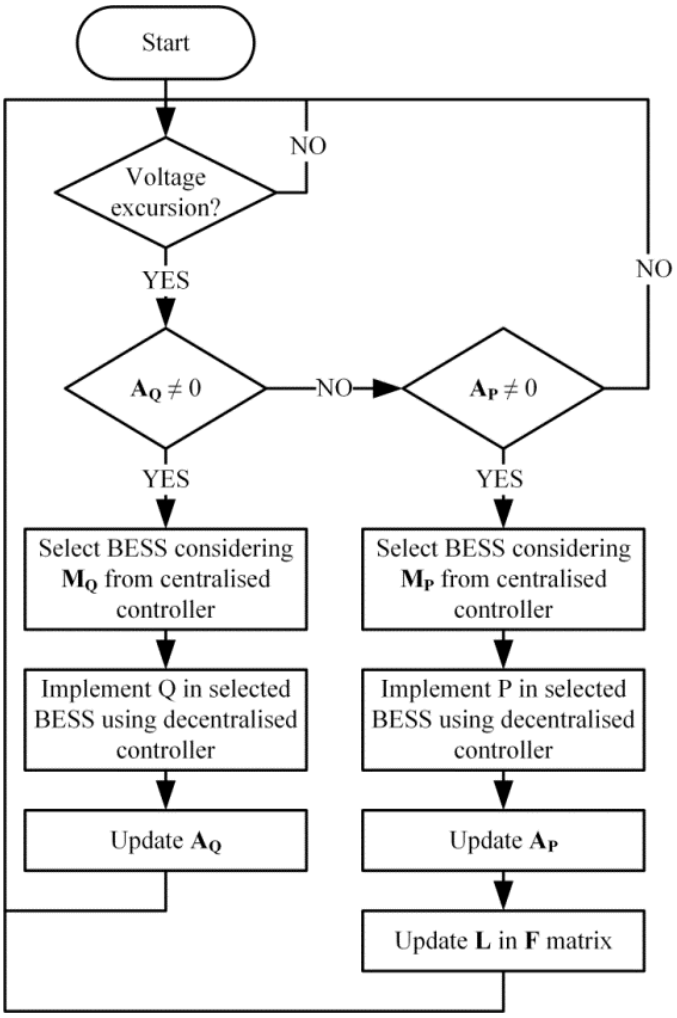

Figure 4-4: the main flowchart of proposed coordinated control scheme

Under $\mathbf{M}_{\mathrm{P}}$ operation mode, the active power operation matrix $\mathbf{M}_{\mathrm{P}}$ is checked in the centralised controller. The most preferable and available BESS unit is selected with and the decentralised controller will calculate and implement the required active power P_{req}.

$$M_{\mathrm{P}}^{*} = \arg\max(\mathbf{M}_{\mathrm{P}}) \tag{4.12}$$

The availability matrix, $\mathbf{A}_{\mathrm{P}}$ and life remaining $\mathbf{L}$ values for each unit are updated based on P and SoC. In addition, the difference between the required power and maximum rated power will be examined in the decentralised controller. If, for the selected energy storage unit BESS (m), $P_{\mathrm{req}} < P_{\mathrm{max}}$, and SoC is within limits then the decentralised controller communicates with the centralised controller to set the availability $A_p(m) = 1$, otherwise $A_p(m) = 0$ is set. In the case $A_p(m) = 0$, the rated power, P_{rated} from BESS (m) continues at the rated value until it reaches its SoC limit. The centralised controller $\mathbf{M}_{\mathrm{P}}$ will then continue to select the preferable BESS to solve the voltage problem.

3 Description of case study

3.1 Network Description and Source Data

The model of a real radial residential distribution network in Northern England as discussed previously (see Figure 1-4) is used in this work to evaluate the proposed coordinated control scheme. It contains 106 domestic loads of which 42 have PV generators. The solar irradiance from 6 June, a summer day, (see Figure 1-5 (a)) is selected to present the worst case of overvoltage across the network. As illustrated in Figure 1-5, the peak solar irradiance occurs between 9:00—15:00. Voltage rise is most likely to occur during this period. The 3 kW rated PV system is placed on every domestic property with a roof facing ±30° of due south as described in Chapter 1. The three single-phase load data is shown in Figure 1-5 (b) and each load has an after diversity of maximum demand (ADMD) of 1.2 kW.

A design decision has been taken to make all the storage units the same size. This standardizes the solution so as to benefit from economies of scale in manufacturing. Space is limited in residential LV networks, so this choice would allow standard installation and maintenance practices to be developed to suit the available space. A decision could be made to encourage installation of storage at customer premises, in which case the adoption of standard procedures would be important. To size and locate the storage units a method developed in previous work was used [184]. This method uses a genetic

algorithm to find the optimal locations for the fewest units of storage of a given size to remove all of the overvoltage in a LV network. Accordingly, locations of storage for the case study are presented as seen in Figure 4-5. This also concludes that, under the load and generation conditions investigated in this study, the network can be supported with four identical storage units, each rated at 25 kW/50 kWh.

Reactive power functionality is included to allow minor voltage deviation to be tackled without using the limited energy store. The case study network considered has a relatively high R/X ratio value (3.75—6.25). This means active power is much more effective in mitigating overvoltage. The maximum reactive power drawn from each BESS is therefore limited to 5 kVAr. Doing so also avoids substantially increasing the reactive power being drawn through the secondary transformer which could impact on losses and thermal limits in the MV network. Active power from the BESS is used to solve the voltage problem when the applied reactive power resource is insufficient.

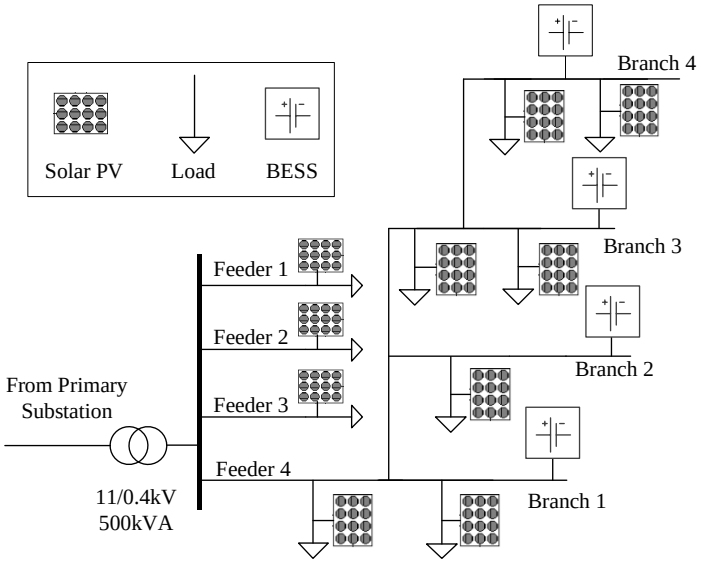

Figure 4-5: Benchmark residential urban radial distribution network

3.2 Simulation Techniques

Both RTDS models and Matlab/OpenDSS models of the controller have been used. In order to assess the dynamic performance of the proposed coordinated controller, a power electronics model of PV generators and energy storage, based on classical the dq decoupling control method are needed[185][186]. The RTDS model provides detailed information of real-time performance of these

models within one simulation environment. This approach also means that the RTDS model can be interfaced to real devices, allowing power hardware in-the-loop to be used in conjunction with the modelled network.

The MATLAB/OpenDSS model based on proposed method is constructed and contributed by a colleague from Durham University to evaluate the benefits of the ageing model in the proposed coordinated controller over a ten year period. To do this, standard, one hour resolution, annual irradiance [187] and load profiles [188] are used with a MATLAB model of the controller and network.

The MATLAB and RTDS models have been compared to ensure their consistency. To do so, the high resolution PV and load profiles shown in Figure 4-6 were implemented in both MATLAB and RTDS simulation and the results were compared. Figure 4-6 shows the comparison for voltages at Branch4; the root mean square error is of the order 0.00415 p.u. Although the MATLAB simulation does not run and prove the detailed controller, the overall simulation in terms of SoC and power exchanges that are the same. The two simulation techniques with their differing time steps and computational burden allow a thorough exploration of the control scheme at different time scales.

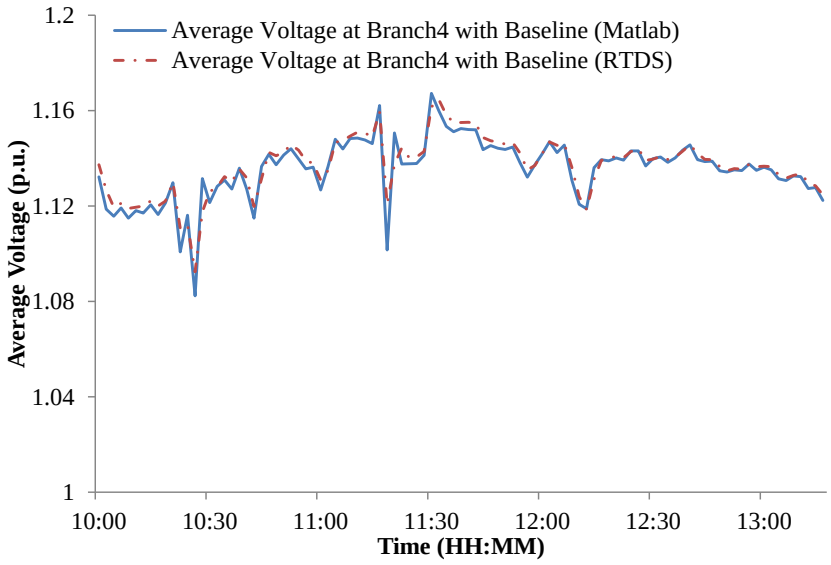

Figure 4-6: Comparison between results from MATLAB and RTDS simulations

Table 4-2 shows the thresholds and time constants selected for the decentralised controller of each BESS in the case study. These values have been selected and tuned during experimentation, and will change based on the network configuration.

Table 4-2 Selected threshold and time constant for case study

Parameter	Value
Upper Threshold	1.095
Middle Threshold	1.085
Lower Threshold	1.070
Middle Threshold Time Period	30 Seconds
Lower Threshold Time Period	2 minutes

4 Application of coordinated control to case study network

4.1 Real Time Steady State Implementation

The proposed coordinated and non-coordinated control methods are implemented and compared using the RTDS model. Both are compared to a baseline voltage which would occur with no energy storage or curtailment of the PV generation. Note that while the chosen modelling environment provides a 4-wire unbalanced model, the controller as currently conceived takes a single voltage measurement as input. It was chosen to take the average voltage, V_{ave} but it is recognised that other approaches could be taken such as using the most extreme phase voltage. The non-coordinated control method uses the decentralised controller only. Figure 4-7 (a) illustrates the average of the three phase voltages at branch 4 between 09:00 and 15:00. It can be seen that the baseline average voltage is raised above the limit of 1.10 between 09:40—13:30.

Under the non-coordinated control scenario (with only the decentralised controller), each BESS can only measure and solve its local voltage problem. Figure 4-7 (a) shows what happens when the charging capacity of BESS4 is reached at 12:30. The average voltage at branch 4 exceeds the limits between 12:30 and 13:20 because the storage cannot absorb any more active power beyond 90% SoC. The average voltage is lowered relative to the baseline by BESSs 1—3 although this is not enough to solve the problem as they are unaware of the excessive voltage at branch 4.

In the case of coordinated control, Figure 4-7 (a) shows that local overvoltage does not happen as the operational matrix $\mathbf{M}$ in the centralised controller selects a preferable BESS to solve the average voltage problems when BESS4 reaches its SoC limit. Figure 4-7 (b) illustrates that BESS4 with coordinated control reaches its SoC limit at 12:20, and the availability of BESS4, $A_P(4) = 0$.

The BESS4 is no longer available to support overvoltage at which point other units are used more aggressively.

The voltage profiles with coordinated and non-coordinated control between 11:30—14:00, when voltage rise is most extreme, are shown in Figure 4-8(a). Figure 4-8(b) and Figure 4-8(c) show the power exchange with the non-coordinated and the coordinated control methods. Under non-coordinated control the BESS has been allowed a higher power rating to demonstrate that if working alone this is required to bring the voltage within limits. With coordinated control, a power of 25 kW is needed from BESS4 to reduce the voltage rise at branch 4 compared to 30 kW with non-coordinated control.

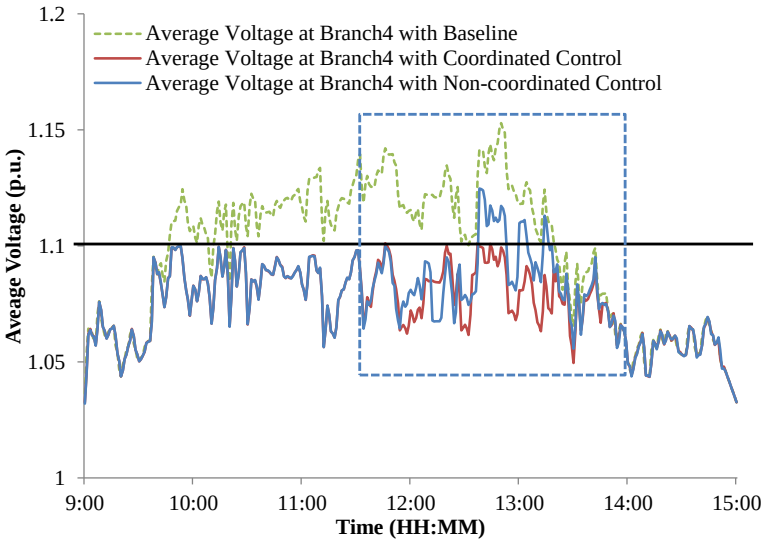

(a)

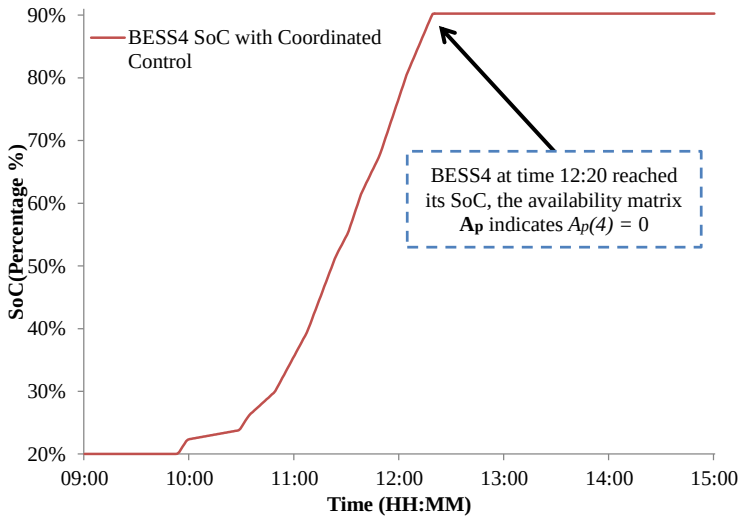

(b)

Figure 4-7: (a) Average voltage profiles at branch 4 with non-coordinated and coordinated control (b) BESS4 SoC with coordinated control at time between 9:00 and 15:00

The time sequence of active power exchange with coordinated control and non-coordinated control is summarised as follows:

- Between 11:30—12:20, under coordinated control, the centralised controller detects a voltage problem at branch 4 and calls the BESS4 decentralised controller to absorb active and reactive power. However, as the availability matrix $\mathbf{A}_P$ from the centralised controller indicates that the active power capability of BESS4 is insufficient, the operational matrix $\mathbf{M}_P$ in the centralised controller is used to decide the next preferable BESS to solve the voltage rise problem at branch 4. Based on the nomination matrix $\mathbf{F}_P$ and availability matrix $\mathbf{A}_P$, BESS3 is selected to provide additional active power. Figure 4-8(d) illustrates the resulting coordination command signal that is sent to BESS3. The effect of this can be seen in the difference between the charging power of BESS3 in Figure 4-8(b) and (c).
- Between 12:20—13:30, BESS4 reaches its SoC limit of 90%. As shown in Figure 4-8(a), the non-coordinated control is unable to solve the voltage problem after 12:20. BESS1-3 do not have visibility of the voltage at branch 4, and therefore do not provide sufficient power (see Figure 4-8(b)), to bring the branch 4 voltage within limits. Conversely, under coordinated control, BESS3 is selected to charge based on the updated operational matrix, $\mathbf{M}_P$ in response to BESS4 being unavailable. Since the required active power from BESS3 is beyond its rated power limits, BESS1 is also selected based upon, $\mathbf{M}_P$ to provide additional active power for branch 4 as shown in Figure 4-8(c). The coordination command signal from the operational matrix, $\mathbf{M}_P$ for BESS1 is shown in Figure 4-8(e).

Figure 4-9 illustrates the active power and SoC of BESS4 operating under coordinated control over a whole day. The energy storage reaches its SoC limit at 12:20. Due to the high charge rate, experiments have shown that to limit the voltage rise without coordinated support from the other units would require an energy capacity of 60 kWh in this case (compared to 50 kWh energy capacity in the case study).

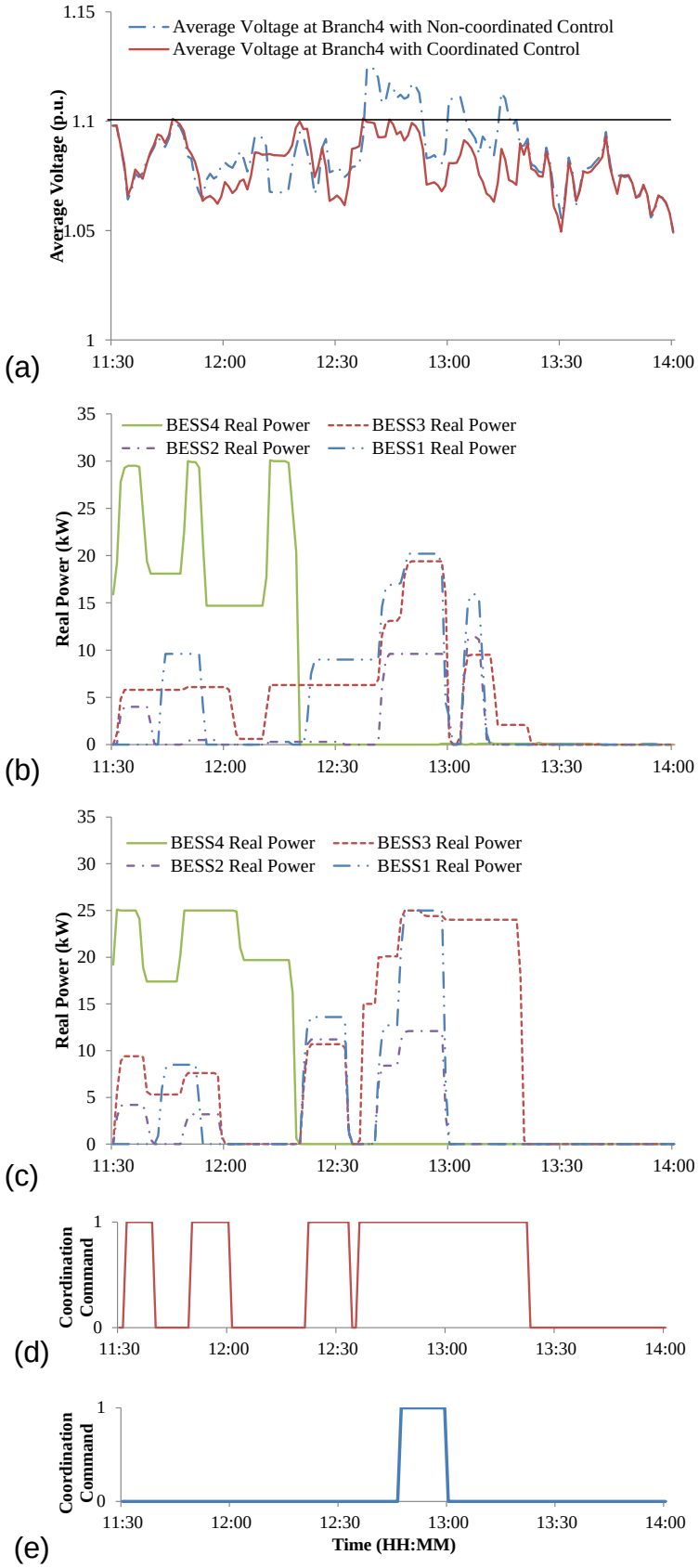

Figure 4-8: Performance between 11:30 and 14:00, detailing (a) average voltages at branch 4 under coordinated and non-coordinated control, (b) active power imported to BESSs under non-coordinated control, (c) active power imported to BESSs under coordinated control, (d) coordinated control signal to BESS3 from branch 4 and (e) coordinated control signal to BESS1 from branch 4.

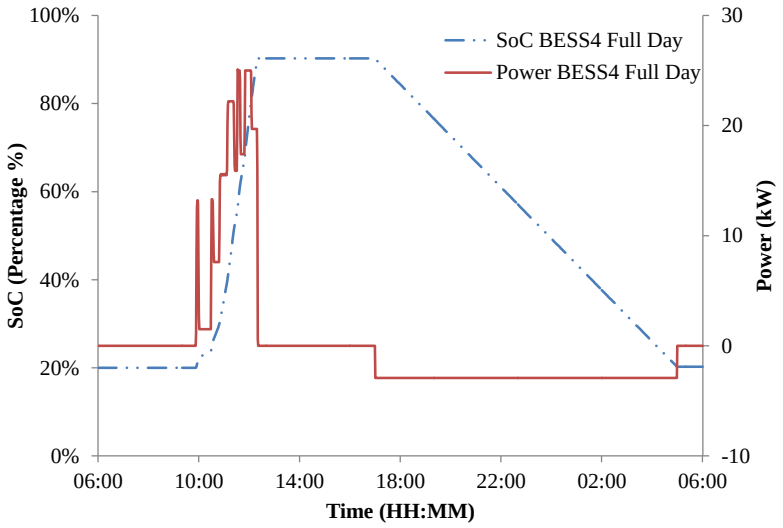

Figure 4-9: Active power charged and discharged from BESS4 with its SoC during one whole day

As shown in Figure 4-9 for BESS4, the unit is allowed to discharge overnight; this is true of all the BESSs. This increases the voltage within the network, and the power output is set to not cause voltage rise beyond the regulatory limits. It is noted that the BESS could be beneficial if the anticipated future increases in adoption of electric vehicles and heat pumps also cause voltage issues. After charging from PV the BESS can be used to prevent voltage drop by discharging during periods of higher loading.

4.2 Asset Management

Assessment of the asset management strategy has been performed by implementing the aging model described in section 2.2 Chapter 4 in a MATLAB/OpenDSS model. This is the collaborative and comparative work that was performed to investigate the benefits of the aging model over a ten year period. The performance of this model is compared to a baseline case with no aging model in the coordinated scheme. If successful, it should more evenly age the BESS units and preferably prevent all of the BESSs from exceeding their cycle life before their calendar life is reached.

Figure 4-10 shows the deterioration of the BESSs over a 10 year period under the coordinated control scheme without an aging model implemented (i.e. $\mathbf{L} = \mathbf{I}$). The BESSs reduce in cycle life over the study period as they are charged to manage voltage. The deterioration is much worse (the graph steeper) during the summer months when higher PV output leads to more severe overvoltage.

Without the aging model implemented, BESS3 and BESS4 reach the end of the cycle life before the 5 year calendar life is reached. This is because they have a higher VSF than BESS1 and BESS2 relative to where the voltage problem occurs, and are therefore always preferentially selected by the operational matrix **M**. As a result of this, BESS3 and BESS4 need replacing before their calendar life is reached, which increases the overall replacement costs to the storage operator (Table 4-3). The steepness of the curve of BESS1 contrasts with that of BESS4 which is much shallower due to it being used much less. BESS1 and BESS2 are replaced at the end of their calendar life, but still have cycle life remaining as they are selected less frequently by the operational matrix. In the base case simulations, six maintenance visits to the network are required, during which the batteries are replaced.

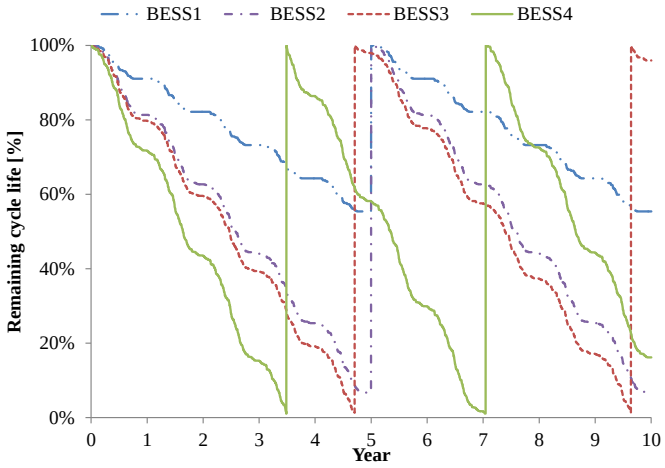

Figure 4-10: Remaining cycle life of each BESS without the aging model being implemented in the coordinated controller

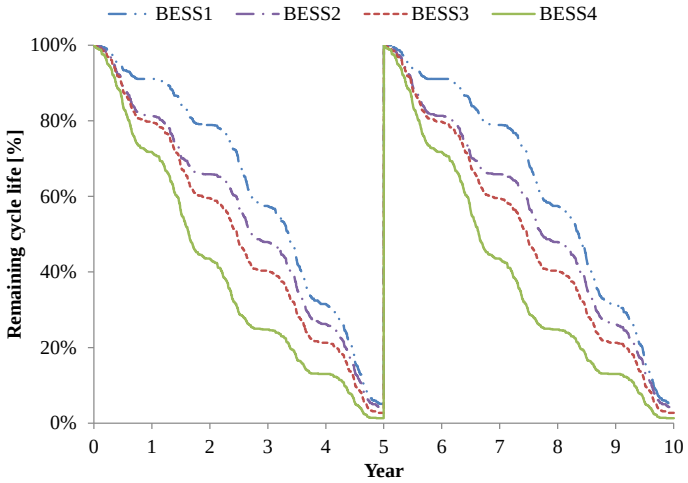

Figure 4-11: Remaining cycle life of each BESS with the aging model implemented in the coordinated controller

Figure 4-11 shows the deterioration of the battery with the aging model implemented. As stated previously, BESS4 is used more frequently in year one as overvoltage occurs most frequently at this location in the LV network due to the configuration of PV, loads and cables and due to the generation and demand profiles used in this modelling. However, as BESS4 ages, the coordinated controller with the aging model begins to use BESS3, BESS2 then BESS1 more frequently. Due to their lower VSF, BESS1-3 consume more power i.e. the average gradient of the aging graph in Figure 4-10 is steeper. There is more even use of the BESS assets and it can be seen that all of the BESSs are replaced only when the calendar life is reached. BESS4 is still needed towards the end of its calendar life, but to a smaller degree than previously as other units are now preferentially selected.

Table 4-3: Cost of ownership with and without aging model

Parameter	No aging model	Aging model	Benefit
BESS capacity cost [£/kWh]	£220		N/A
BESS power cost [£/kW]	£267		
Capital cost of each BESS	£17,675		
Discount rate	6%		
Replacement cost	£95,799	£92,310	£3,489
Maintenance visits per decade	6	2	4

Table 4-4: Summary of losses with and without aging model with 75% efficient BESSs [180]**and a loss incentive of £60/MWh**[189]

Scenario	No aging model	Aging model	Difference
BESS charging energy [kWh]	175,000	178,000	-3,000
Conversion losses for 75% round trip BESS efficiency [kWh]	43,750	44,500	-750
Cost of losses under UK regulation	£2,625	£2,670	-£45

The aging model has financial benefits by deferring the replacement of BESS3 and BESS4. It can be seen in Table 4-3 based on capacity cost of £220/kWh that deferring the replacement of BESS3 and BESS4 saves the network operator £3,489. Furthermore, two maintenance visits to the network to replace

batteries are required in comparison to the six visits needed without the aging model which represents further cost saving to the network operator.

Although the aging model reduces replacement costs, it does increase the overall charging energy because it more frequently nominates BESSs which have a lower VSF relative to the location of the voltage problem. This increases the total conversion losses in the BESSs. As shown in Table 4-4, the aging model causes an additional 750 kWh of loss over ten years which costs the network operator an extra £45 under the UK loss mechanism (£60/MWh [189]). This cost is small compared to the financial saving that the network operator gains from deferring the replacement of BESS3 and BESS4 which amounts to £3,489 under the model in this study.

5 Discussion

The method applied in this work has been shown to be effective in preventing overvoltage in a real LV network that is modelled with a large amount of PV. Non-coordinated and coordinated control methods have been implemented and tested for their ability to prevent overvoltage. The non-coordinated control method works in isolation, using a local voltage measurement and decentralised controller to determine BESS power set-points. By introducing a centralised control unit, the coordinated control also considers the additional factors of BESS aging and SoC to determine which BESS to use and the power set-points. The coordinated approach is shown to require smaller power and energy ratings for the BESS at the network location with the most severe voltage deviations. This results in a lower capital and operating cost in energy storage systems for the storage operator, as can be seen in Table 4-3 and Table 4-4. Additional costs from implementing a coordinated controller need to be considered to determine the feasibility of a coordinated control project.

The distance between each BESS has a strong influence on the ability of the units to support each other. The closer they are to each other, the greater the ability to support when one unit has failed or reached energy/power limits. However, it may not always be feasible to locate storage unit to close to each other for example due to space constraints or the need to provide support to different parts of an LV network.

The coordinated control strategy comprises both centralised and decentralised controllers and it is highly dependent on central communication and local measurement systems. In the event of communication failure each unit can operate independently by r**e**verting to non-coordinated control with local measurements. In this eventuality the decentralised controllers at each BESS are not aware of the wider network conditions and so may not be able to solve the most extreme voltage problems on the network.

Because the coordinated control approach allows for cooperative operation, if one of the BESS units fails, other BESS units will automatically be called to improve the voltage at the location of the failed unit. In the case of non-coordinated control, such mitigating measures are not possible.

The decentralised controllers are governed by voltage threshold values that, when combined with voltage sensitivity factors, cause power exchange to adjust up and down. The choice of voltage threshold values is influenced by the network operator's over- and under-voltage tolerance and the ramp rate of changes in solar irradiance. This analysis uses conservative parameters for voltage upper, middle and lower thresholds. However, these values could be tuned to reduce the BESS import and export of both active and reactive power. As the threshold values are narrowed there is a trade-off between the power and energy requirement and the risk of overvoltage.

As further PV systems are added to the network, the location and severity of the voltage excursions may change. By having several BESS operating with a coordinated control strategy, there is a greater potential for this method to adapt to the changing network conditions. In response to the measured voltages across the network, the controller will call on different combinations of BESS to support the voltage. Although the capacity of BESS4 could be increased to remove overvoltage, this investigation has considered a method that uses multiple units with a coordinated controller. By doing so, the proposed storage can adapt to changing generation/demand profile and has a level of robustness to failure of a single BESS i.e. if BESS4 were to fail, there is significant robustness to be able to solve most overvoltage using the other BESS units in this LV network. The tools provided by this work will enable a thorough investigation of the relationship between the number of units, their location in

the network and the resulting robustness as network conditions change with time. The decision to use identically sized BESS units is not necessarily the most effective choice, and this work could be extended by removing this constraint.

The LV secondary transformer fixed tap position was set to prevent under-voltage, in line with the usual practice of network operators. Since voltage deviations were a result of PV generation in these trials, only overvoltage was experienced. However, the coordinated control method can also be adapted to solve under-voltage, occurring under peak load conditions. This might be necessary if electric vehicles and heat pumps are installed, increasing the peak demands on the LV network.

Although the control method employed has been demonstrated using a UK LV network, it is inherently applicable to other LV networks.

6 Summary and Conclusion

In this chapter, a scheme for controlling multiple BESSs in an LV network is proposed and it has established in published work. This scheme coordinates the power and energy import and export of the BESSs to solve voltage rise caused by PV generation. A real LV network with measured load profiles and solar irradiance has been used as a case study.

The proposed coordinated control method has been verified using a 24 hour high-resolution implementation in RTDS and a 10 year low-resolution implementation in MATLAB. The main advantages of the coordinated control scheme for multiple BESS are as follows:

- By sharing power and energy between the BESSs, the scheme is able to solve real-time voltage problems that cannot be solved with independently controlled BESSs with the same power and energy capacity.
- The rated power and energy of BESS units at the locations with most severe requirements has been reduced, hence the largest unit is smaller when compared with a unit in the same location with non-coordinated control.

- The even sizing of the BESS units offers advantages in maintenance and economy of scale in manufacturing.
- There is greater potential for this proposed method to adapt to changes in location of extra PV generation, albeit to the limit where extra capacity would then be required. This is not the case with a non-coordinated control.
- The addition of an aging model more evenly utilises the BESSs and consequently reduces the cost of battery replacements for the storage operator, both in terms of battery replacement and maintenance requirements.

The proposed coordinated control can also be adapted for other operational aims, such as peak load shaving and undervoltage.

The storage decentralised controller in this work considers VSF to determine the energy storage import and export of both active and reactive power. Such decision is positive for steady state analysis based real time simulation. However, it may be negative for the network during small disturbance as the network operating condition changes [162]. Under such conditions, the Jacobian matrix has to be recalculated so that the new VSF can be obtained. However, online recalculation of the VSF matrix is problematic in distribution networks, where the level of on-line information available is much less than that at the transmission level [162], and this is why the decentralised controllers in this work are governed by voltage threshold values.

To get a better performance of energy storage for voltage support, a systematic approach for a small signal linearized model of the energy storage, the PV generator, and a LV network will be presented in Chapter 5. The overall system is represented in differential equation form. A detailed eigenvalue analysis will be carried out to investigate the network dynamic behaviour, select appropriate voltage feedback control parameters of the energy storage that can be able to cope with the PV fluctuation, and analyse system dynamics subsequent to internal and external disturbances.

Chapter 5: Small signal stability analysis of energy storage for voltage support based the LV distribution network

1 Introduction

Flexible and fast control of energy storage active and reactive power is an important requirement for voltage support in the distribution network. The storage employs a voltage source converter to connect with the utility grid. The voltage source converter, supported by a fast and proper selected control strategy, can enhance stability of the distribution network. This can be achieved by dynamically adjusting its instantaneous active and reactive power flows. Thus, it can enhance voltage quality that is reduced by fluctuating solar irradiance, and it can also minimize the risk of instability if appropriate control parameters are selected. However, if inappropriate control parameters from these installed energy storage systems are applied, the LV distribution network may experience oscillatory responses that can result in system instability. To get a better performance from energy storage for voltage support, small signal stability analysis is employed to linearize the nonlinear case study network at an equilibrium point under small disturbance.

In conventional power systems, the small signal stability often refers to small disturbance rotor angle stability, and it is an ability of the power system to maintain stability if it is subjected to small disturbances [190]. This means that a disturbance is considered to be sufficiently small when the linearized system around the operating point can characterise dynamics of the original system under such small disturbances [190][191] and [192]. In a conventional power system, the small signal instability can result from lack of synchronising torque [191]. This leads to increasing rotor angle through aperiodic mode. In addition, the small signal instability can also result from lack of damping torque [191]. Under such condition, the oscillatory instability modes is happened [191]. In addition, small signal instability can be classified as local or inter-area mode oscillations. The local oscillation mode is related to a single generator against the rest of power system, and it is affected by power plant and poorly tuned control parameters from excitation control systems [190]. For example, the high gain excitation control of a synchronous generator can improve transient

stability but result in small signal stability issues [192]. The inter-area oscillation means generators in the same area can oscillate against generators in the neighbouring area. It is caused by several complex reasons, such as large power transfers through weak ties between interconnected areas [190][191] [192]. In micro-grids, it has been reported that the majority of oscillatory small signal instability is related to DGs controllers and their associated control gains [93][150]. For instance, the high power controller droop gains can lead to an unstable system [93][150]. The small signal instability can be directly associated to system eigenvalues analysis [192]. If the eigenvalue is positive and real, there is an aperiodic instability. On the other hand, if the eigenvalue is complex and positive, there is an oscillatory instability. As energy storage will be important for solving several technical issues arising from large connected PV generators in future LV networks, the energy storage control system parameters should be properly designed by reducing overshoot with fast response time and without causing stability issues.

In this chapter, a detailed eigenvalue analysis is carried out to identify the trajectory of the eigenvalues in regard to the settings of voltage feedback controllers of energy storage. A sensitivity analysis is also performed. The eigenvalue analysis is examined by MATLAB and is varied through the time domain simulation using MATLAB/Simpower.

The objectives of this chapter are included by

- Introducing the detailed operation of the energy storage control techniques for voltage support under state space model
- Presenting a systematic approach to develop small signal model of a LV distribution network that includes an energy storage system and one PV generator. The objective of this model is used for eigenvalue analysis.
- Employing small signal model to select appropriate control parameters
- Demonstrating that the fast control action of electronically interfaced energy storage can be exploited to improve voltage profile.

2 Small signal stability of the dynamic system

The advantage of employing small signal analysis is that the system studies can be performed online closed to real time [193]. The behaviour of dynamic system

can be described as a set of *n* first order nonlinear ordinary differential equations (ODE). The linearized model is represented in state space form based on these set of first order nonlinear ODE as seen by equations 5.1 and 5.2 [194].

$$\Delta\dot{\mathbf{x}} = \mathbf{A}\Delta\mathbf{x} + \mathbf{B}\Delta\mathbf{u} \tag{5.1}$$

$$\Delta\mathbf{y} = \mathbf{C}\Delta\mathbf{x} + \mathbf{D}\Delta\mathbf{u} \tag{5.2}$$

Where $\Delta\mathbf{x}$ is the state vector, $\Delta\mathbf{y}$ is the output vector, and $\Delta\mathbf{u}$ is the input vector. The coefficient $\mathbf{A}$ is the state matrix and $\mathbf{B}$ is the input matrix, $\mathbf{C}$ is the output matrix and the forward matrix is $\mathbf{D}$ [194]. The matrix $\mathbf{A}$ is important for the small signal stability evaluation, since it reveals whether the system is stable. The analytical solution to equation (5.1) can be seen from equation (5.3) [192], if eigenvalues of matrix $\mathbf{A}$ is negative, the term e^{At} is exponential decay. This means the system is stable. However, if eigenvalues of $\mathbf{A}$ is positive, the term e^{At} is exponential growth. This means the system is unstable. As such, the stability of the system is fully dependent on the property of the matrix $\mathbf{A}$.

$$x(t) = e^{At}x(0) + \int_0^t e^{A(t-\tau)}Bu(\tau)d\tau \tag{5.3}$$

The eigenvalue of the $\mathbf{A}$ determines the stability characteristic of a system and it has to satisfy as (5.4) [194] [193],

$$\mathbf{A}\boldsymbol{\phi} = \boldsymbol{\lambda}\boldsymbol{\phi} \tag{5.4}$$

To find eigenvalues $\boldsymbol{\lambda}$, the equation (5.4) is written as

$$(\mathbf{A} - \boldsymbol{\lambda}\mathbf{I})\boldsymbol{\phi} = \mathbf{0} \tag{5.5}$$

Therefore, for the non-trivial solution, the equation (5.5) can be rewritten as

$$\mathbf{det}(\mathbf{A} - \boldsymbol{\lambda}\mathbf{I}) = \mathbf{0} \tag{5.6}$$

The eigenvalues $\boldsymbol{\lambda}$ can be real or complex. Complex eigenvalues are always conjugate pairs. The eigenvalue corresponds to the time dependent characteristic of a mode that is given by $e^{\lambda t}$. Therefore, the real part of eigenvalue corresponds to the non-oscillatory mode, whereas the imaginary part of the eigenvalue is responsible for the frequency of oscillation. An eigenvalue can be described as a general complex form

$$\lambda = \sigma \pm j\omega \tag{5.6}$$

The frequency of oscillation is defined as

$$f = \frac{\omega}{2\pi} \tag{5.7}$$

The damping ratio is given by

$$\zeta = \frac{-\sigma}{\sqrt{\sigma^2 + \omega^2}} \tag{5.8}$$

The damping ratio ζ determines the rate of decay of the amplitude of the oscillation [194].

3 Description of Case Study Network

The case study network is firstly introduced, in order to represent small signal state space model of the network. This case study network is simplified based on the real LV distribution network operated by ENWL as described in Chapter one (see Figure 1-4). It is impractical to model the completed LV distribution network with PV generators and energy storage systems. This is due to increased system order associated with the computational and time constraints [192].

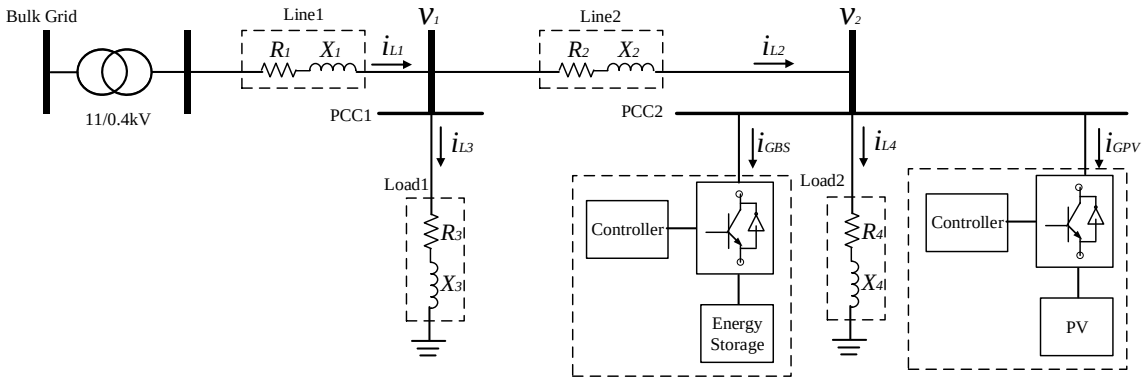

Figure 5-1: Single line diagram of the case study LV distribution network under consideration

Figure 5-1 illustrates the single line diagram of the simplified case study LV distribution network under consideration. Line impedances and static loads are assumed and represented by series-connected RL branches. The network includes the detailed control system models of one storage system and one PV generator that are connected with PCC2. The simplified system parameters are given by Chapter 5, section 5 and listed in Table 5-1 as the steady state operating points for eigenvalue analysis.

4 Formulation of state space model

Formulation of the state space model is an important step for power system small signal stability analysis [192]. The wrong results may be obtained by using too simple a model. However, extremely detailed models are complex to understand, and it may contain unnecessary information for the analysis [192]. The dynamic modelling of a power system can be formed based on object oriented approach [192] [195]. This approach is easy to understand, and it clearly represents relationships between the block of the case study network, generators and controls [192] [195]. Figure 5-2 illustrates the process of small signal analysis based on object oriented method [192]. Firstly, each subsystem model is constructed. These subsystems in this thesis include controllers from the energy storage, controllers from the PV generator, and the model of the LV distribution network that contains line impedances and loads. Once the state space model of each subsystem based on their local dq reference frame is constructed, these subsystems are then shifted to a global model based on global DQ rotating reference frame. The dq transformation is introduced by [196], it aims to reduce the balanced AC three phase circuits quantities to two DC quantities. This enables both active/reactive components of AC output power to be mutually independently controlled. The global DQ rotating reference frame uses the transformation method as illustrated in Figure 5-3 and defined in the equation (5.9) and (5.10) [197][198]. In Figure 5-3, the D-Q axis represents as the global reference frame with its rotating angular frequency of ω_e. The d1-q1 and d2-q2 axis denotes the local reference frame as the PV generator and the energy storage with their rotating angular frequency of ω_{PV} and ω_{BS}.

In equation (5.9) and (5.10), δ_n is defined as the angle between the D axis of the global reference frame and d axis of the n-th subsystem reference frame, such as δ_{PV} and δ_{BS} [197]. The linearized form of (5.9) at an operating point is given by equation (5.11) [197] [198],

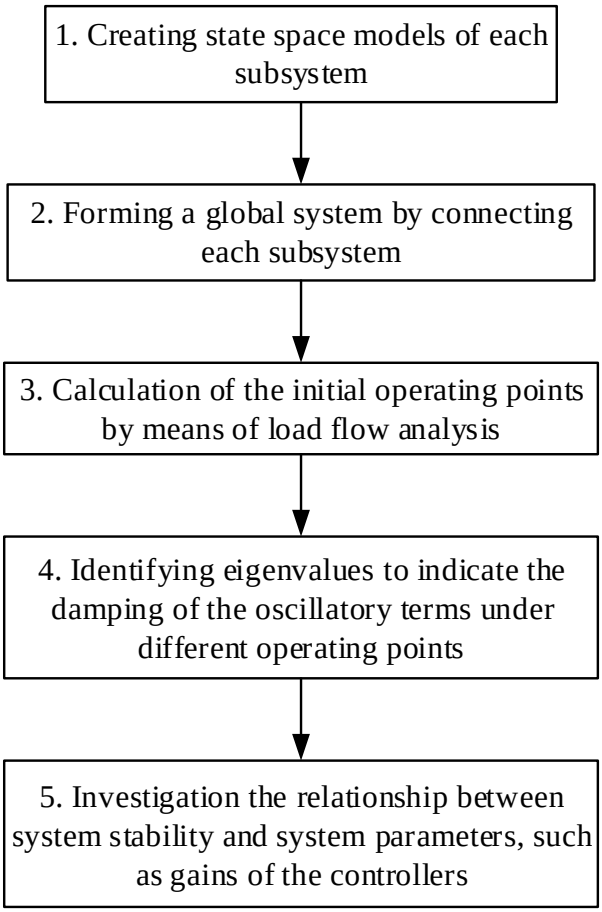

Figure 5-2: The process of small signal analysis based on object oriented approach [192]

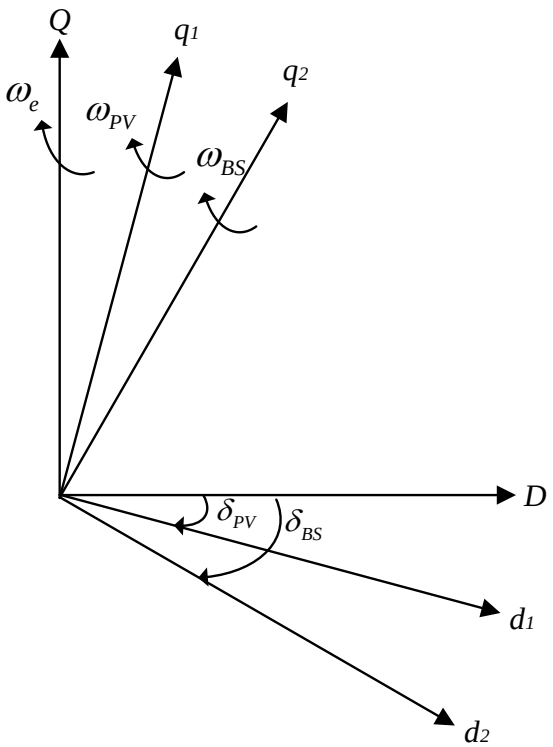

Figure 5-3: Global and local rotating reference frames of the case study network

$$[f_{DQ}] = [T_i][f_{dq}] \tag{5.9}$$

$$T_i = \begin{bmatrix} \cos\delta_n & \sin\delta_n \\ -\sin\delta_n & \cos\delta_n \end{bmatrix} \tag{5.10}$$

$$\begin{bmatrix} \Delta f_q^{\,g} \\ \Delta f_d^{\,g} \end{bmatrix} = \begin{bmatrix} \cos\delta_n^o & \sin\delta_n^o \\ -\sin\delta_n^o & \cos\delta_n^o \end{bmatrix} \begin{bmatrix} \Delta f_q^{\,n} \\ \Delta f_d^{\,n} \end{bmatrix} + \begin{bmatrix} f_d^{\,go} \\ -f_q^{\,go} \end{bmatrix} [\Delta\delta_n] \tag{5.11}$$

where “o” represents for steady state operating points. The term $[\Delta f_q^g \quad \Delta f_d^g]^T$ in (5.11) represents the linearized voltage or current components in global reference rotating frame. The term $[\Delta f_q^n \quad \Delta f_d^n]^T$ is the linearized form of voltage or current components in their local rotating reference frame, and the term $[\Delta f_d^{go} \quad -\Delta f_q^{go}]^T$ is the steady state operating point values of voltage or current components in their local rotating reference frame.

As depicted in Figure 5-2, once the state space model of the case study system is constructed, eigenvalues can be identified according to system steady state initial operating conditions which are evaluated by means of load flow analysis. The eigenvalues are used to indicate the damping of the oscillatory terms under different operating conditions. Finally, a further investigation can be carried out based on sensitivity analysis by tracking eigenvalue loci under certain operating conditions. This aims to investigate the relationship between system stability and system control parameters, such as gains from energy storage controllers.

Figure 5-4 illustrates the block representation of system model that contains control systems from a storage system and the PV generator. The complete system includes three subsystems that are namely; 1) energy storage and its voltage regulation controllers, 2) PV generator and its power controller, 3) LV distribution network containing loads and line impedances. To perform eigenvalue analysis, the nonlinear system ODEs is firstly linearized. These linear quantities are represented by the prefix Δ. Then, the state space representation of these linearized ODEs is transformed to the global DQ reference frame. All three subsystems are finally combined according to their outputs and inputs as depicted in Figure 5-4 [157]. In this thesis, both the PV generator and the energy storage are modelled in the averaged representation. This means that switching devices, such as IGBT, in voltage source converters

are represented by equivalent controlled voltage source. The average model can adequately represent dynamics of the network without considering harmonics generated by converter [199]. For example, the energy storage voltage feedback controllers' dynamics are preserved. Simulations have illustrated that in such situation, high-order harmonics are not presented [199]. Modelling of the energy storage and the PV generator used in this chapter are tested and experimentally validated by several research articles [65], [92], [200] and [201]. As indicated by both [65] and [201], the simpler PV generator model has been suggested for small signal stability analysis. Thus, the PV generator presented in this chapter is considered as a power generator with its active power controller without consideration of dynamic performances of the PV array. In the meantime, energy storage modelling is presented as shown in [92]. However, the control strategy of the energy storage modelling in [92] have been modified for meeting the voltage support requirements.

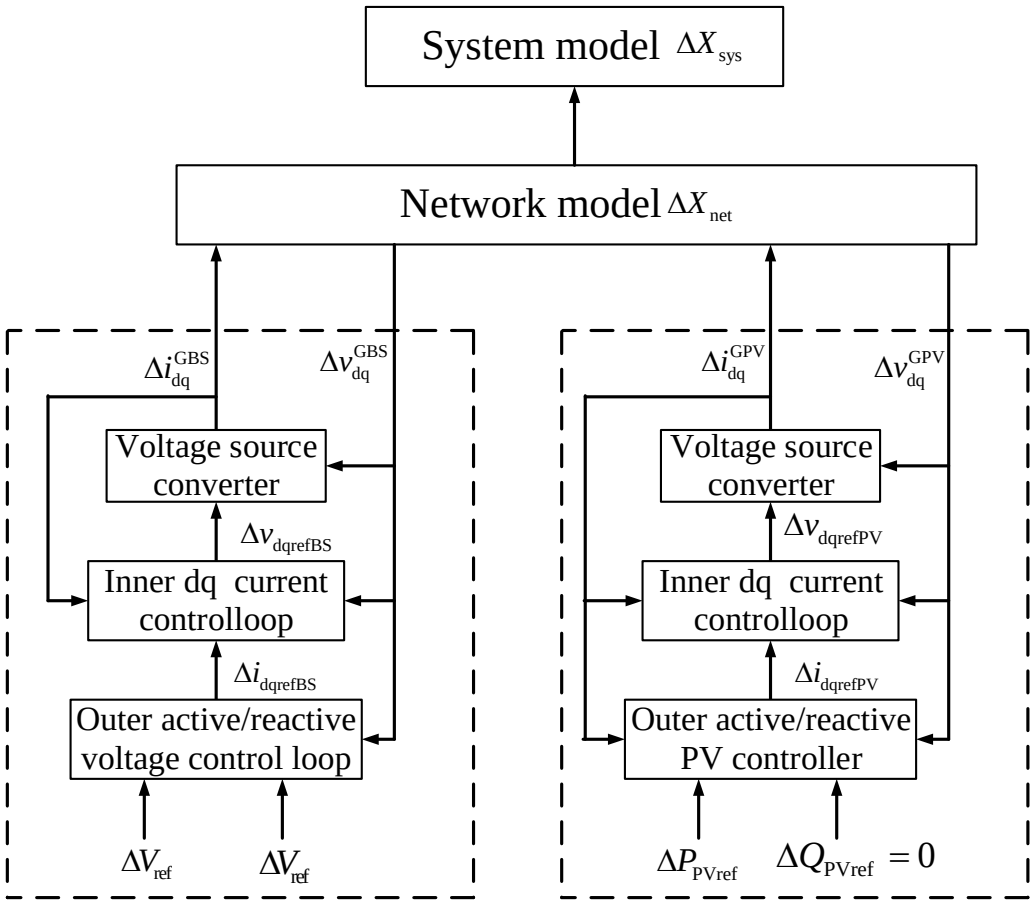

Figure 5-4: Block diagram of small signal model of the case study network

4.1 Small signal model of the energy storage converter model and its control systems

4.1.1 Converter model

The energy storage composed of converter and control systems to connect with the utility grid. Its dynamic model of the AC side power circuit of the storage can be described as equation (5.12) and can be seen as Figure 5-5.

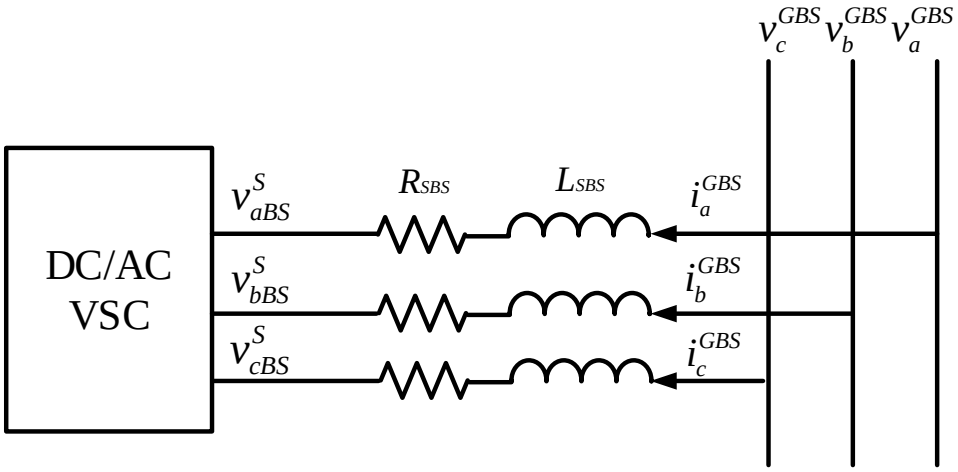

Figure 5-5: Three phase equivalent circuit of VSC AC side

$$v_{abcBS}^S = -R_{SBS} i_{abc}^{GBS} - L_{SBS} \frac{d}{dt} i_{abc}^{GBS} + v_{abc}^{GBS} \tag{5.12}$$

Transforming equation (5.12) to d-q reference frame and rotating at its local frequency ω_{SBS} are shown in equations (5.13) and (5.14).

$$\frac{d}{dt} i_q^{GBS} = -\frac{R_{SBS}}{L_{SBS}} i_q^{GBS} - \omega_{SBS} i_q^{GBS} + \frac{1}{L_{SBS}} (v_q^{GBS} - v_{qBS}^S) \tag{5.13}$$

$$\frac{d}{dt} i_d^{GBS} = -\frac{R_{SBS}}{L_{SBS}} i_d^{GBS} + \omega_{SBS} i_q^{GBS} + \frac{1}{L_{SBS}} (v_d^{GBS} - v_{dBS}^S) \tag{5.14}$$

Where i_{dq}^{GBS}, v_{dqBS}^S, v_{dq}^{GBS}, are the dq (ω_{SBS}) axis components of the converter current, voltages, and bus voltages respectively. According to (5.13) and (5.14), the current components i_{dq}^{GBS} are coupled by the $\pm\omega_{SBS} i_{dq}^{GBS}$ terms. These coupling terms can be removed by introducing new variables $v_{dqBS}^{'}$ as defined by

$$v_{qBS}^{'} = -\omega_{SBS} L_{SBS} i_q^{GBS} + (v_q^{GBS} - v_{qBS}^S) \tag{5.15}$$

$$v_{dBS}^{'} = \omega_{SBS} L_{SBS} i_d^{GBS} + (v_d^{GBS} - v_{dBS}^S) \tag{5.16}$$

Accordingly, equation (5.13) and (5.14) are revised as

$$\frac{d}{dt} i_q^{GBS} = -\frac{R_{SBS}}{L_{SBS}} i_q^{GBS} + \frac{1}{L_{SBS}} v_{qBS}^{'} \tag{5.17}$$

$$\frac{d}{dt} i_d^{GBS} = -\frac{R_{SBS}}{L_{SBS}} i_d^{GBS} + \frac{1}{L_{SBS}} v_{dBS}^{'} \tag{5.18}$$

Equations (5.17) and (5.18) describe decoupled $\pm i_{dq}^{GBS}$ currents. The matrix representation of equations (5.17) and (5.18) are

$$\dot{x}_{GBS} = A_{GBS} x_{GBS} + E_{GBS} v_{BS}^{'} \tag{5.19}$$

$$\begin{bmatrix} \dot{i}_q^{GBS} \\ i_d^{GBS} \end{bmatrix} = \begin{bmatrix} -\frac{R_{SBS}\omega_b}{X_{SBS}} & 0 \\ 0 & -\frac{R_{SBS}\omega_b}{X_{SBS}} \end{bmatrix} \begin{bmatrix} i_q^{GBS} \\ i_d^{GBS} \end{bmatrix} + \begin{bmatrix} \frac{\omega_b}{X_{SBS}} & 0 \\ 0 & \frac{\omega_b}{X_{SBS}} \end{bmatrix} \begin{bmatrix} v_{qBS}^{'} \\ v_{dBS}^{'} \end{bmatrix} \tag{5.20}$$

Since the dynamic equations (5.17) and (5.18) are modelled based on their own load dq rotating axis reference, the final form of equations (5.17) and (5.18) need to be obtained by transferring the term to global DQ rotating reference frame through equation (5.11) [197]. Therefore, the term x_{GBS} at the global DQ reference is given by (5.21)

$$\begin{bmatrix} \Delta i_{qGBS}^{g} \\ \Delta i_{dGBS}^{g} \end{bmatrix} = \begin{bmatrix} \cos\delta_{BS}^{o} & \sin\delta_{BS}^{o} \\ -\sin\delta_{BS}^{o} & \cos\delta_{BS}^{o} \end{bmatrix} \begin{bmatrix} \Delta i_q^{GBS} \\ \Delta i_d^{GBS} \end{bmatrix} + \begin{bmatrix} i_d^{oGBS} \\ -i_q^{oGBS} \end{bmatrix} \begin{bmatrix} \Delta\delta_{BS} \end{bmatrix} \tag{5.21}$$

Linearizing equation (5.20) and substituting the term x_{GBS} from equation (5.21), thus

$$\Delta \dot{x}_{GBS}^{g} = T_{BS} A_{GBS} T_{BS}^{-1} \Delta x_{GBS}^{g} + T_{BS} E_{GBS} \Delta v_{BS}^{'} + T_{BS} A_{GBS} i_{\delta BS}^{o} \Delta\delta_{BS} - T_{BS} i_{\delta BS}^{o} \Delta \dot{\delta}_{BS} \tag{5.22}$$

The ‘o’ describes the system equilibrium point. The term $\Delta\delta_{BS}$ is the angle from the energy storage local reference rotating frame, and it is obtained as

$$v_q^{GBS} = v^{GBS} \sin\delta_{BS} \tag{5.23}$$

$$v_d^{GBS} = v^{GBS} \cos\delta_{BS} \tag{5.24}$$

$$\delta_{BS} = \tan^{-1}\left(\frac{v_q^{GBS}}{v_d^{GBS}}\right) \tag{5.25}$$

The linearized form of (5.25) is written as

$$\Delta\delta_{BS} = m_{qBS} \Delta v_q^{GBS} + m_{dBS} \Delta v_d^{GBS} \tag{5.26}$$

Terms m_{dqBS} is represented as

$$m_{qBS} = \frac{v_d^{oGBS}}{(v_d^{oGBS})^2 + (v_q^{oGBS})^2} \qquad m_{dBS} = \frac{-v_q^{oGBS}}{(v_d^{oGBS})^2 + (v_q^{oGBS})^2}$$

In addition, the term $\Delta\dot{\delta}_{BS}$ from equation (5.22) is the deviation in the rotational frequency of the storage local rotating reference frame that is described as term $\Delta\omega_{SBS}$. Accordingly, the equation (5.22) can be transformed as (5.27)

$$\Delta \dot{x}^{g}_{GBS} = T_{BS} A_{GBS} T^{-1}_{BS} \Delta x^{g}_{GBS} + T_{BS} E_{GBS} \Delta v^{BS'} + T_{BS} A_{GBS} i^{o}_{\delta BS} M_{qdBS} \Delta v^{GBS} - T_{BS} i^{o}_{\delta BS} \Delta \omega_{SBS} \quad (5.27)$$

It is revised as compact form

$$\Delta \dot{x}^{g}_{GBS} = A^{g}_{GBS} \Delta x^{g}_{GBS} + B^{v'}_{GBS} \Delta v^{BS'} + B^{v}_{GBS} \Delta v^{GBS} + B^{\omega}_{GBS} \Delta \omega_{SBS} \quad (5.28)$$

$$A^{g}_{GBS} = T_{BS} A_{GBS} T^{-1}_{BS},\ B^{v'}_{GBS} = T_{BS} E_{GBS},\ B^{v}_{GBS} = T_{BS} A_{GBS} i^{o}_{\delta BS} M_{qdBS},\ B^{\omega}_{GBS} = -T_{BS} i^{o}_{\delta BS}$$

4.1.2 Control system state space representation

Phase locked loop

The phase locked loop is used to recognise the frequency of the bus voltage waveform from synchronising of the converter. The mathematical form of phase locked loop for energy storage is described as (5.29) and its linearized state space model is derived as (5.30) [92][197],

$$\omega_{SBS} = K_{pllBS}(K_{p\omega BS} + \frac{K_{i\omega BS}}{s})(\delta_{refBS} - \delta_{BS}) \quad (5.29)$$

$$\Delta \dot{\omega}_{SBS} = -K_{pllBS} K_{p\omega BS} \Delta \omega_{SBS} - K_{pllBS} K_{i\omega BS} m_{qBS} \Delta v^{GBS}_{q} - K_{pllBS} K_{i\omega BS} m_{dBS} \Delta v^{GBS}_{d} \quad (5.30)$$

The term K_{pllBS} is the amplitude of the input signal, and $K_{p\omega BS}$ $K_{i\omega BS}$ are both the PI controller parameters for the phase locked loop.

Voltage regulation controller for dq axis representation

The voltage regulation controller set the d axis current references $\Delta i_{dBS}\,(ref)$ for the inner d current control loop as seen in Figure 5-4. The rms value of the storage bus voltage, Δv^{GBS}_{rms}, is the input to the voltage regulation control loop. This is acquired by measuring the storage bus voltage dq components, $\Delta v^{GBS}_{d'}$ and $\Delta v^{GBS}_{q'}$. These two quantities are filtered by a low pass filter to reduce the high frequency distortion components. The error of the reference voltage ΔV_{refBS} and Δv^{GBS}_{rms} is fed to a PI controller to generate the desired current reference $\Delta i_{dBS}\,(ref)$.

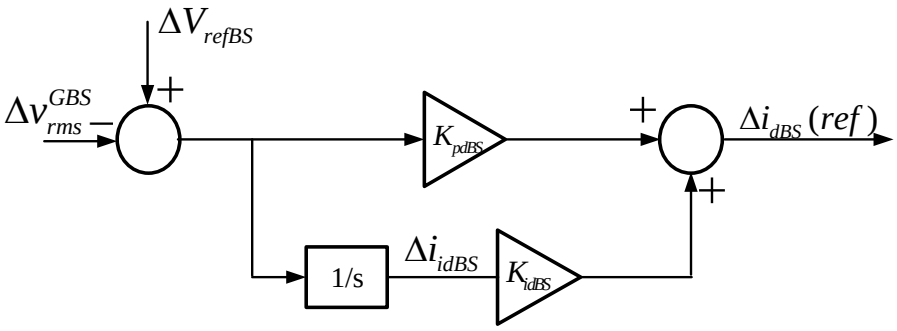

Figure 5-6: Voltage regulation control loop for d axis

The mathematical representation of the v_{rms}^{GBS} based on its local dq rotating axis components is expressed as (5.31),

$$(v_{rms}^{GBS})^2 = (v_{d'}^{GBS})^2 + (v_{q'}^{GBS})^2 \tag{5.31}$$

The linearized form of equation (5.31) is shown in (5.32)

$$\Delta v_{rms}^{GBS} = \frac{v_d^{oGBS}}{v_{rms}^{oGBS}} \Delta v_{d'}^{GBS} + \frac{v_q^{oGBS}}{v_{rms}^{oGBS}} \Delta v_{q'}^{GBS} \tag{5.32}$$

The filter value of $\Delta v_{d'}^{GBS}$ and $\Delta v_{q'}^{GBS}$ from equation (5.32) is derived from

$$\Delta \dot{v}_{d'}^{GBS} = \frac{1}{T_v} \Delta v_d^{GBS} - \frac{1}{T_v} \Delta v_{d'}^{GBS} \tag{5.33}$$

$$\Delta \dot{v}_{q'}^{GBS} = \frac{1}{T_v} \Delta v_q^{GBS} - \frac{1}{T_v} \Delta v_{q'}^{GBS} \tag{5.34}$$

where T_v is the defined time constant.

According to Figure 5-6, the dynamic model of voltage regulation control loop for d axis is represented as (5.35) and (5.36)

$$\dot{i}_{idBS} = V_{refBS} - v_{rms}^{GBS} \tag{5.35}$$

$$i_{dBS}(ref) = K_{idBS} i_{idBS} + K_{pdBS}(V_{refBS} - v_{rms}^{GBS}) \tag{5.36}$$

where both K_{pdBS} and K_{idBS} are the proportional and integral gain for the PI controller. The linearized form of (5.35) is obtained by substituting the (5.32) into (5.35), therefore,

$$\Delta \dot{i}_{idBS} = \Delta V_{refBS} - \frac{v_d^{oGBS}}{v_{rms}^{oGBS}} \Delta v_{d'}^{GBS} + \frac{v_q^{oGBS}}{v_{rms}^{oGBS}} \Delta v_{q'}^{GBS} \tag{5.37}$$

In addition, the linearized form of (5.36) is expressed as (5.38)

$$\Delta i_{dBS}(ref) = K_{idBS}\Delta i_{idBS} + K_{pdBS}\Delta V_{refBS} - K_{pdBS}\frac{v_d^{oGBS}}{v_{rms}^{oGBS}}\Delta v_{d'}^{GBS} - K_{pdBS}\frac{v_q^{oGBS}}{v_{rms}^{oGBS}}\Delta v_{q'}^{GBS} \quad (5.38)$$

The inner current controller generates the reference voltage $\Delta v'_{dBS}$ that is the input for the physical part of converter control model as indicated in Figure 5-7. The mathematical modelling presentation is formed as (5.39) and (5.40)

$$\dot{v}_{idBS} = i_{dBS}(ref) - i_{d'}^{GBS} \quad (5.39)$$

$$v'_{dBS} = K_{iidBS}v_{idBS} + K_{pidPV}(i_{dBS}(ref) - i_{d'}^{GBS}) \quad (5.40)$$

Where K_{iidBS} and K_{pidBS} are the integral and proportional gain for inner current control loop in d axis, the linearized form of (5.39), and (5.40) are presented as (5.41) and (5.42)

$$\Delta\dot{v}_{idBS} = K_{idBS}\Delta i_{idBS} + K_{pdBS}\Delta V_{refBS} - K_{pdBS}\frac{v_d^{oGBS}}{v_{rms}^{oGBS}}\Delta v_{d'}^{GBS} - K_{pdBS}\frac{v_q^{oGBS}}{v_{rms}^{oGBS}}\Delta v_{q'}^{GBS} - \Delta i_{d'}^{GBS} \quad (5.41)$$

$$\Delta v'_{dBS} = K_{iidBS}\Delta v_{idBS} + K_{pidBS}(\Delta i_{dBS}(ref) - \Delta i_{d'}^{GBS}) \quad (5.42)$$

The term $i_{d'}^{GBS}$ is the filtered current and it is presented as (5.42)

$$\Delta\dot{i}_{d'}^{GBS} = \frac{1}{T_i}\Delta i_d^{GBS} - \frac{1}{T_i}\Delta i_{d'}^{GBS} \quad (5.43)$$

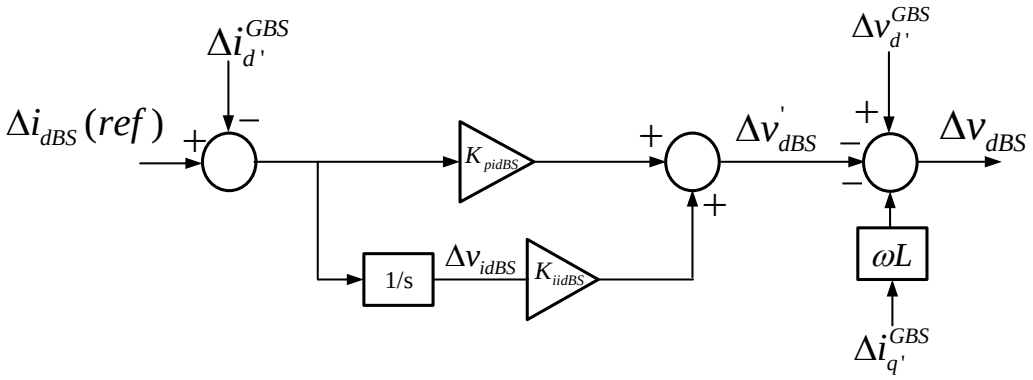

Figure 5-7: d axis Inner current control loop

In this thesis, the reactive power is also considered for voltage regulation. Similarly, the voltage regulation controller set the q axis current reference as Δi_{dBS} *(ref)* for the inner q current control loop. The linearized original differential equations for voltage regulation controller for q axis are represented as (5.44) and (5.45)

$$\Delta \dot{i}_{iqBS} = \Delta V_{refBS} - \frac{v_d^{oGBS}}{v_{rms}^{oGBS}} \Delta v_{d'}^{GBS} + \frac{v_q^{oGBS}}{v_{rms}^{oGBS}} \Delta v_{q'}^{GBS} \quad (5.44)$$

$$\Delta \dot{v}_{iqBS} = K_{iqBS} \Delta i_{iqBS} + K_{pqBS} \Delta V_{refBS} - K_{pqBS} \frac{v_d^{oGBS}}{v_{rms}^{oGBS}} \Delta v_{d'}^{GBS} - K_{pqBS} \frac{v_q^{oGBS}}{v_{rms}^{oGBS}} \Delta v_{q'}^{GBS} - \Delta i_{q'}^{GBS} \quad (5.45)$$

where both K_{pqBS} and K_{iqBS} are the proportional and integral gain for q axis voltage regulation controller. The equation for output voltage before converter is

$$v_{qBS}^{'} = K_{iiqBS} v_{iqBS} + K_{piqPV} (i_{qBS}(ref) - i_{q'}^{GBS}) \quad (5.46)$$

Where K_{iiqBS} and K_{piqBS} are the integral and proportional gain for q axis inner current control loop, and the term,

$$\Delta \dot{i}_{q'}^{GBS} = \frac{1}{T_i} \Delta i_q^{GBS} - \frac{1}{T_i} \Delta i_{q'}^{GBS} \quad (5.47)$$

The output reference current from voltage regulation controller for q axis is linearized and described as equation (5.48),

$$\Delta i_{qBS}(ref) = K_{iqBS} \Delta i_{iqBS} + K_{pqBS} \Delta V_{refBS} - K_{pqBS} \frac{v_d^{oGBS}}{v_{rms}^{oGBS}} \Delta v_{d'}^{GBS} - K_{pdBS} \frac{v_q^{oGBS}}{v_{rms}^{oGBS}} \Delta v_{q'}^{GBS} \quad (5.48)$$

In addition, the equation (5.46) is linearized as (5.49)

$$\Delta v_{qBS}^{'} = K_{iiqBS} \Delta v_{iqBS} + K_{piqBS} (\Delta i_{qBS}(ref) - \Delta i_{q'}^{GBS}) \quad (5.49)$$

Linearized ODEs (5.33), (5.34), (5.37), (5.41), (5.44) and (5.45) are the basis for building the state space model voltage regulation control loop for dq axis.

In addition, the filtered voltage from converter is obtained by equations (5.50) and (5.51),

$$\Delta \dot{v}_{qBS'}^{s} = \frac{1}{T_v} \Delta v_{qBS}^{s} - \frac{1}{T_v} \Delta v_{qBS'}^{s} \quad (5.50)$$

$$\Delta \dot{v}_{dBS'}^{s} = \frac{1}{T_v} \Delta v_{dBS}^{s} - \frac{1}{T_v} \Delta v_{dBS'}^{s} \quad (5.51)$$

State space model of the energy storage control system

According to discussion above, a set of state variables representing the linearized model of the control system of the energy storage is defined as follow

$\Delta v_{d'}^{GBS}$ and $\Delta v_{q'}^{GBS}$ are the filtered values of PCC2 bus voltages

$\Delta v_{dBS'}^{s}$ and $\Delta v_{qBS'}^{s}$ are the filtered values of storage converter output voltages

$\Delta i_{d'}^{GBS}$ and $\Delta i_{q'}^{GBS}$	are the filtered values of storage converter current
Δv_{idBS} and Δv_{iqBS}	are the states of PI controller for storage inner current control loop
Δi_{idBS} and Δi_{iqBS}	are the states of PI controller for voltage control loop
$\Delta\omega_{SBS}$	is the frequency of the d and q reference frame for storage local bus

The linearized state space model of storage control is expressed as

$$\Delta \dot{x}_{cBS} = A_{cBS}\Delta x_{cBS} + C_{GBS}\Delta x_{GBS} + C_{GBS}^{v}\Delta v^{GBS} + C^{vBS}\Delta v^{sBS} + B_{GBS}^{u}\Delta u_{GBS} \tag{5.52}$$

Where,

$$\Delta x_{cBS} = [\ \Delta v_{q'}^{GBS}\quad \Delta v_{d'}^{GBS}\quad \Delta v_{qBS'}^{s}\quad \ldots\ldots\ldots\quad \Delta v_{dBS'}^{s}\quad \Delta i_{iqBS}\quad \Delta i_{idBS}\quad \Delta i_{q'}^{GBS}\quad \Delta i_{d'}^{GBS}\quad \Delta v_{iqBS}\quad \Delta v_{idBS}\quad \Delta\omega_{SBS}\ ]^{T}$$

$$\Delta x_{GBS} = \begin{bmatrix} i_{q}^{GBS} & i_{d}^{GBS} \end{bmatrix}^{T}$$

$$\Delta v^{GBS} = \begin{bmatrix} \Delta v_{q}^{GBS} & \Delta v_{d}^{GBS} \end{bmatrix}^{T}$$

$$\Delta v^{sBS} = \begin{bmatrix} \Delta v_{q}^{sBS} & \Delta v_{d}^{sBS} \end{bmatrix}^{T}$$

$$\Delta u_{GBS} = \begin{bmatrix} \Delta V_{refBS} & \Delta V_{refBS} \end{bmatrix}^{T}$$

Expanded form of coefficients A_{cBS}, C_{GBS}, C_{GBS}^{v}, C^{vBS} and B_{GBS}^{u} from (5.52) are shown in Appendix A.1. Considering linearized equations (5.38), (5.42), (5.48), and (5.49), the voltage vector before the converter output can be described as (5.53)

$$\Delta v^{BS'} = E_{cBS}^{v}\Delta x_{cBS} + E_{uBS}^{v}\Delta u_{GBS} \tag{5.53}$$

Where

$$\Delta v^{BS'} = \begin{bmatrix} \Delta v_{qBS}^{'} \\ \Delta v_{dBS}^{'} \end{bmatrix}$$

$$\Delta x_{cBS} = [\ \Delta v_{q'}^{GBS}\quad \Delta v_{d'}^{GBS}\quad \Delta v_{qBS'}^{s}\quad \ldots\ldots\quad \Delta v_{dBS'}^{s}\quad \Delta i_{iqBS}\quad \Delta i_{idBS}\quad \Delta i_{q'}^{GBS}\quad \Delta i_{d'}^{GBS}\quad \Delta v_{iqBS}\quad \Delta v_{idBS}\quad \Delta\omega_{SBS}\ ]^{T}$$

$$\Delta u_{GBS} = \begin{bmatrix} \Delta V_{refBS} & \Delta V_{refBS} \end{bmatrix}$$

The expanded form of coefficients of (5.53) is shown in Appendix A.1. The dq vector of the converter output voltages are expressed as

$$\Delta v^{sBS} = \Delta v^{GBS'} - \Delta v^{BS'} + E_{cBS}^{s}\Delta i_{GBS}^{'} \tag{5.54}$$

Where

$$\Delta v^{sPV} = \begin{bmatrix} \Delta v_{qBS}^{s} & \Delta v_{dBS}^{s} \end{bmatrix}^{T}$$

$$\Delta v^{GBS'} = \begin{bmatrix} \Delta v_{q'}^{GBS} & \Delta v_{d'}^{GBS} \end{bmatrix}^T$$

$$\Delta v^{BS'} = \begin{bmatrix} \Delta v_{qBS}^{'} \\ \Delta v_{dBS}^{'} \end{bmatrix}$$

$$E_{cBS}^{s} = \begin{bmatrix} 0 & -\dfrac{\omega_e X_{sBS}}{\omega_b} \\ \dfrac{\omega_e X_{sBS}}{\omega_b} & 0 \end{bmatrix}$$

$$\Delta i_{GBS}^{'} = \begin{bmatrix} \Delta i_{q'}^{GBS} \\ \Delta i_{d'}^{GBS} \end{bmatrix} = E_{cBS}^{i} \Delta x_{cBS} = \begin{bmatrix} 0 & 0 & 0 & 0 & 0 & 0 & 1 & 0 & 0 & 0 & 0 \\ 0 & 0 & 0 & 0 & 0 & 0 & 0 & 1 & 0 & 0 & 0 \end{bmatrix} \Delta x_{cBS}$$

$$\Delta \omega_{sBS} = E_{cBS}^{\omega} \Delta x_{cBS} = \begin{bmatrix} 0 & 0 & 0 & 0 & 0 & 0 & 0 & 0 & 0 & 0 & 1 \end{bmatrix} \Delta x_{cBS}$$

The state space representation of the energy storage control system is implemented based on its local dq reference frame. In order to be consistent with the state equations of the rest of the system, the voltage vector Δv^{GBS} and state vector of the converter Δx_{GBS} have to transfer to the global reference frame. Therefore,

$$\Delta x_{GBS} = T_{BS}^{-1} \Delta x_{GBS}^{g} + i_{\delta}^{oGBS} \Delta \delta_{BS} \tag{5.55}$$

$$\Delta v^{GBS} = T_{BS}^{-1} \Delta v_{qd}^{GBS} + v_{\delta}^{oGBS} \Delta \delta_{BS} \tag{5.56}$$

Where the term from (5.55) and (5.56) are expressed as below,

$$\Delta v^{GBS} = \begin{bmatrix} \Delta v_q^{GBS} & \Delta v_d^{GBS} \end{bmatrix}^T \quad \Delta x_{GBS} = \begin{bmatrix} i_q^{GBS} & i_d^{GBS} \end{bmatrix}^T \quad i_{\delta}^{oGBS} = \begin{bmatrix} i_d^{oGBS} & -i_q^{oGBS} \end{bmatrix}^T$$

$$v_{\delta}^{oGBS} = \begin{bmatrix} v_d^{oGBS} & -v_q^{oGBS} \end{bmatrix}^T \quad \Delta \delta_{BS} = m_{qBS} \Delta v_q^{GBS} + m_{dBS} \Delta v_d^{GBS}$$

According to equations (5.55) and (5.56), the state space representation of storage control system is transformed to (5.57),

$$\dot{\Delta x}_{cBS} = A_{cBS} \Delta x_{cBS} + C_{GBS}^{x} \Delta x_{GBS}^{g} + C_{GBS}^{g} \Delta v_{qd}^{GBS} + C^{vBS} \Delta v^{sBS} + B_{GBS}^{u} \Delta u_{GBS} \tag{5.57}$$

Where: $C_{GBS}^{x} = C_{GBS} T_{BS}^{-1}$, $C_{GBS}^{g} = C_{GBS}^{v} T_{BS}^{-1} + C_{GBS} i_{\delta}^{oGBS} M_{qdBS} + C_{GBS}^{v} v_{\delta}^{oGBS} M_{qdBS}$

$$\Delta v^{sBS} = E_{GBS}^{v} \Delta v^{GBS} - \Delta v^{BS'} + E_{cBS}^{s} \Delta i_{GBS}^{'} \tag{5.58}$$

Where: $E_{GBS}^{v} = T_{BS}^{-1} + v_{\delta}^{oGBS} M_{qdBS}$

4.2 State space model of the PV generator

Constructing of state space model of the PV generator is similar to the storage as previous discussed. As such, the converter model of PV generator is expressed as below

$$\dot{x}_{GPV} = A_{GPV} x_{GPV} + E_{GPV} v_{PV}^{'} \tag{5.59}$$

$$\Delta \dot{x}^{g}_{GPV} = A^{g}_{GPV}\Delta x^{g}_{GPV} + B^{v'}_{GPV}\Delta v^{PV'} + B^{v}_{GPV}\Delta v^{GPV} + B^{\omega}_{GPV}\Delta\omega_{SPV} \tag{5.60}$$

Where

$$A^{g}_{GPV} = T_{PV}A_{GPV}T^{-1}_{PV},\ B^{v'}_{GPV} = T_{PV}E_{GPV},\ B^{v}_{GPV} = T_{PV}A_{GPV}i^{o}_{\delta PV}M_{qdPV},\ B^{\omega}_{GPV} = -T_{PV}i^{o}_{\delta PV} \tag{5.61}$$

Expanded form of coefficients from (5.59) and (5.60) is presented in Appendix A.1

The control system of PV generator is expressed as

$$\Delta \dot{x}_{cPV} = A_{cPV}\Delta x_{cPV} + C_{GPV}\Delta x_{GPV} + C^{v}_{GPV}\Delta v^{GPV} + C^{vPV}\Delta v^{sPV} + B^{u}_{GPV}\Delta u_{GPV} \tag{5.62}$$

Where

$$\Delta x_{cPV} = [\ \Delta v^{GPV}_{q'}\quad \Delta v^{GPV}_{d'}\quad \Delta v^{s}_{qPV'}\quad \ldots\ldots\ldots\ldots \\ \Delta v^{s}_{dPV'}\quad \Delta i_{iqPV}\quad \Delta i_{idPV}\quad \Delta i^{GPV}_{q'}\quad \Delta i^{GPV}_{d'}\quad \Delta v_{iqPV}\quad \Delta v_{idPV}\quad \Delta\omega_{SPV}\ ]^{T}$$

$$\Delta x_{GPV} = \begin{bmatrix} i^{GPV}_{q} & i^{GPV}_{d} \end{bmatrix}^{T}$$

$$\Delta v^{GPV} = \begin{bmatrix} \Delta v^{GPV}_{q} & \Delta v^{GPV}_{d} \end{bmatrix}^{T}$$

$$\Delta v^{sPV} = \begin{bmatrix} \Delta v^{sPV}_{q} & \Delta v^{sPV}_{d} \end{bmatrix}^{T}$$

$$\Delta u_{GPV} = \begin{bmatrix} \Delta P_{PV} & \Delta Q_{PV} \end{bmatrix}^{T}$$

The d axis of the PV generator is considered as an active power controller, and the reactive power input from PV generator is assumed as $\Delta Q_{PV} = 0$. The expanded form of coefficients from state space equation (5.62) is expressed in Appendix A.1. Similarly, the voltage vector before the PV converter output can be described as

$$\Delta v^{PV'} = E^{v}_{cPV}\Delta x_{cPV} + E^{v}_{uPV}\Delta u_{GPV} \tag{5.63}$$

Where

$$\Delta v^{PV'} = \begin{bmatrix} \Delta v^{'}_{qPV} \\ \Delta v^{'}_{dPV} \end{bmatrix}$$

$$\Delta x_{cPV} = [\ \Delta v^{GPV}_{q'}\quad \Delta v^{GPV}_{d'}\quad \Delta v^{s}_{qPV'}\quad \ldots\ldots\ldots \\ \Delta v^{s}_{dPV'}\quad \Delta i_{iqPV}\quad \Delta i_{idPV}\quad \Delta i^{GPV}_{q'}\quad \Delta i^{GPV}_{d'}\quad \Delta v_{iqPV}\quad \Delta v_{idPV}\quad \Delta\omega_{SPV}\ ]^{T}$$

$$\Delta u_{GPV} = \begin{bmatrix} \Delta P_{ref} & \Delta Q_{ref} \end{bmatrix}^{T}$$

The expanded form of coefficients of (5.63) is shown in Appendix A.1, and the dq vector of the converter output voltages are expressed as

$$\Delta v^{sPV} = \Delta v^{GPV'} - \Delta v^{PV'} + E^{s}_{cPV}\Delta i^{'}_{GPV} \tag{5.64}$$

The expanded form of (5.64) is

$$\Delta v^{sPV} = \begin{bmatrix} \Delta v^{s}_{qPV} & \Delta v^{s}_{dPV} \end{bmatrix}^{T}$$

$$\Delta v^{GPV'} = \begin{bmatrix} \Delta v^{GPV}_{q'} & \Delta v^{GPV}_{d'} \end{bmatrix}^{T}$$

$$\Delta v^{PV'} = \begin{bmatrix} \Delta v'_{qPV} \\ \Delta v'_{dPV} \end{bmatrix}$$

$$E^{s}_{cPV} = \begin{bmatrix} 0 & -\dfrac{\omega_e X_{sPV}}{\omega_b} \\ \dfrac{\omega_e X_{sPV}}{\omega_b} & 0 \end{bmatrix}$$

$$\Delta i'_{GPV} = \begin{bmatrix} \Delta i^{GPV}_{q'} \\ \Delta i^{GPV}_{d'} \end{bmatrix} = E^{i}_{cPV}\Delta x_{cPV} = \begin{bmatrix} 0 & 0 & 0 & 0 & 0 & 0 & 1 & 0 & 0 & 0 & 0 \\ 0 & 0 & 0 & 0 & 0 & 0 & 0 & 1 & 0 & 0 & 0 \end{bmatrix} \Delta x_{cPV}$$

$$\Delta \omega_{sPV} = E^{\omega}_{cPV}\Delta x_{cPV} = \begin{bmatrix} 0 & 0 & 0 & 0 & 0 & 0 & 0 & 0 & 0 & 0 & 1 \end{bmatrix} \Delta x_{cPV}$$

Again, equations (5.62) and (5.64) at global reference frame is described as

$$\Delta \dot{x}_{cPV} = A_{cPV}\Delta x_{cPV} + C^{x}_{GPV}\Delta x^{g}_{GPV} + C^{g}_{GPV}\Delta v^{GPV}_{qd} + C^{vPV}\Delta v^{sPV} + B^{u}_{GPV}\Delta u_{GBS} \tag{5.65}$$

Where: $C^{x}_{GPV} = C_{GPV}T^{-1}_{PV}$, $C^{g}_{GPV} = C^{v}_{GPV}T^{-1}_{PV} + C_{GPV}i^{oGPV}_{\delta}M_{qdPV} + C^{v}_{GPV}v^{oGPV}_{\delta}M_{qdPV}$

$$\Delta v^{sPV} = E^{v}_{GPV}\Delta v^{GPV} - \Delta v^{PV'} + E^{s}_{cPV}\Delta i'_{GPV} \tag{5.66}$$

Where: $E^{v}_{GPV} = T^{-1}_{PV} + v^{oGPV}_{\delta}M_{qdPV}$

4.3 Small Signal Dynamic Model of Case Study Network

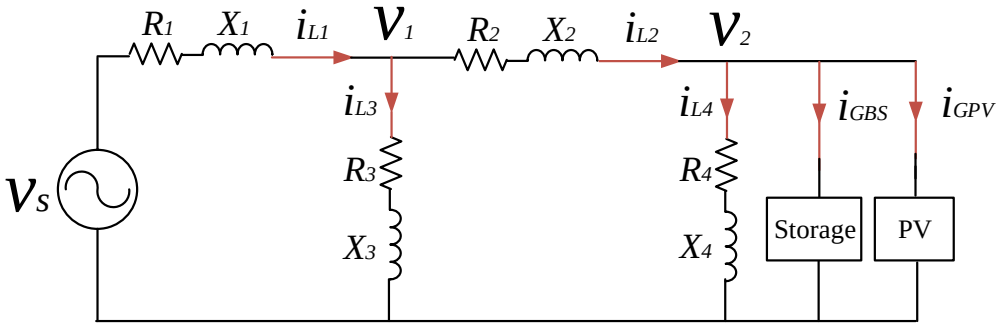

Figure 5-8: Equivalent case study network

The case study network is represented as a dynamic system. Therefore, it is modelled by differential equations rather than algebraic equations [157]. According to Figure 5-8, the linearized network differential equations without the PV and storage can be described as

$$\Delta \dot{x}_{N} = A_{N}\Delta x_{N} + B_{N}\Delta u \tag{5.67}$$

Where

$$\Delta x_N = \begin{bmatrix} \Delta i_q^{L1} & \Delta i_d^{L1} & \Delta i_q^{L2} & \Delta i_d^{L2} & \Delta i_q^{L3} & \Delta i_d^{L3} & \Delta i_q^{L4} & \Delta i_d^{L4} \end{bmatrix}^T$$

$$\Delta u = \begin{bmatrix} \Delta v_{sq} & \Delta v_{sq} & \Delta v_{1q} & \Delta v_{1d} & \Delta v_{q2}^{G2} & \Delta v_{d2}^{G2} & 0 & 0 \end{bmatrix}^T$$

Expanded form of coefficients of A_N and B_N are introduced in Appendix A.1. The bus voltage v_2 is represented based on KCL and KVL

$$i_{L4} = i_{L2} - i_{GBS} - i_{GPV} \tag{5.68}$$

$$v^{G2} = R_4(i_{L2} - i_{GBS} - i_{GPV}) + L_4 \frac{d}{dt}(i_{L2} - i_{GBS} - i_{GPV}) \tag{5.69}$$

Where both currents i_{GBS} and i_{GPV} are from the storage system and the PV generator. It is noted that the storage bus voltage Δv^{GBS} is equal to the PV bus voltage Δv^{GPV} and equal to the bus voltage Δv^{G2}. To be consistent with the control and power converter equations discussed above, the bus2 voltage is replaced with $\Delta v^{G2} = \begin{bmatrix} \Delta v_{q2}^{G2} & \Delta v_{d2}^{G2} \end{bmatrix}^T$. Therefore, equation (5.67) is rewritten as equation (5.70).

$$\Delta \dot{x}_N = A_N \Delta x_N + B_N^1 \Delta u_N + B_N^{v2} \Delta v^{G2} \tag{5.70}$$

where expanded form of coefficients from (5.70) are shown in Appendix A.1.

The linearized form of equation (5.68) after transforming to dq reference frame is shown in (5.71) and (5.72)

$$\begin{aligned} \Delta v_q^{G2} &= R_4 \Delta i_q^{L2} + L_4 \Delta \dot{i}_q^{L2} + L_4 \omega_e \Delta i_d^{L2} - R_4 \Delta i_q^{GBS} \\ &- L_4 \Delta \dot{i}_q^{GBS} - L_4 \omega_e \Delta i_d^{GBS} - R_4 \Delta i_q^{GPV} - L_4 \Delta \dot{i}_q^{GPV} - L_4 \omega_e \Delta i_d^{GPV} \end{aligned} \tag{5.71}$$

$$\begin{aligned} \Delta v_d^{G2} &= R_4 \Delta i_d^{L2} + L_4 \Delta \dot{i}_d^{L2} - L_4 \omega_e \Delta i_q^{L2} - R_4 \Delta i_d^{GBS} \\ &- L_4 \Delta \dot{i}_d^{GBS} + L_4 \omega_e \Delta i_q^{GBS} - R_4 \Delta i_d^{GPV} - L_4 \Delta \dot{i}_d^{GPV} + L_4 \omega_e \Delta i_q^{GPV} \end{aligned} \tag{5.72}$$

Observing equation (5.71) and (5.72) both terms $\begin{bmatrix} \Delta i_q^{L2} & \Delta i_d^{L2} \end{bmatrix}^T$ and $\begin{bmatrix} \Delta \dot{i}_q^{L2} & \Delta \dot{i}_d^{L2} \end{bmatrix}^T$ are contained in equation (5.69) and both terms $\begin{bmatrix} \Delta i_q^{GBS} & \Delta i_d^{GBS} \end{bmatrix}^T$ and $\begin{bmatrix} \Delta \dot{i}_q^{GBS} & \Delta \dot{i}_d^{GBS} \end{bmatrix}^T$ are included in equation (5.20). In addition, both vectors

$\begin{bmatrix} \Delta i_q^{GPV} & \Delta i_d^{GPV} \end{bmatrix}^T$ and $\begin{bmatrix} \Delta \dot{i}_q^{GPV} & \Delta \dot{i}_d^{GPV} \end{bmatrix}^T$ are in equation (5.59). Therefore, equation (5.71) and (5.72) can be revised as

$$\Delta v^{G2} = E_{21}^N \Delta x_N + E_{22}^N \Delta \dot{x}_N + D_{21}^{NBS} \Delta x_{GBS} + D_{22}^{NBS} \Delta \dot{x}_{GBS} + D_{21}^{NPV} \Delta x_{GPV} + D_{22}^{NPV} \Delta \dot{x}_{GPV} \quad (5.73)$$

where the expanded form of above equation (5.73) is shown in Appendix A.1.

4.4 Steady space model of the overall system

Once the case study network with its impedances and loads, the energy storage, and the PV generator are modelled, the completed state space of the overall system can be constructed. The state space representation of the system and the corresponding input/output vectors are summarised as follow

Energy storage

$$\Delta \dot{x}_{GBS}^g = A_{GBS}^g \Delta x_{GBS}^g + B_{GBS}^{v'} \Delta v^{BS'} + B_{GBS}^v \Delta v^{GBS} + B_{GBS}^{\omega} \Delta \omega_{SBS} \quad (5.28)$$

Where: $A_{GBS}^g = T_{BS} A_{GBS} T_{BS}^{-1}$, $B_{GBS}^{v'} = T_{BS} E_{GBS}$, $B_{GBS}^v = T_{BS} A_{GBS} i_{\delta BS}^o M_{qdBS}$, $B_{GBS}^{\omega} = -T_{BS} i_{\delta BS}^o$

$$\Delta \dot{x}_{cBS} = A_{cBS} \Delta x_{cBS} + C_{GBS}^x \Delta x_{GBS}^g + C_{GBS}^g \Delta v_{qd}^{GBS} + C^{vBS} \Delta v^{sBS} + B_{GBS}^u \Delta u_{GBS} \quad (5.57)$$

Where: $C_{GBS}^x = C_{GBS} T_{BS}^{-1}$, $C_{GBS}^g = C_{GBS}^v T_{BS}^{-1} + C_{GBS} i_{\delta}^{oGBS} M_{qdBS} + C_{GBS}^v v_{\delta}^{oGBS} M_{qdBS}$

Vectors of the energy storage output voltage

$$\Delta v^{BS'} = E_{cBS}^v \Delta x_{cBS} + E_{uBS}^v \Delta u_{GBS} \quad (5.53)$$

$$\Delta v^{sBS} = E_{GBS}^v \Delta v^{GBS} - \Delta v^{BS'} + E_{cBS}^s \Delta i_{GBS}^{'} \quad (5.58)$$

Where: $E_{GBS}^v = T_{BS}^{-1} + v_{\delta}^{oGBS} M_{qdBS}$

Supplementary vectors of energy storage

$$\Delta i_{GBS}^{'} = E_{cBS}^i \Delta x_{cBS} \quad \Delta \omega_{sBS} = E_{cBS}^{\omega} \Delta x_{cBS}$$

PV generator

$$\Delta \dot{x}_{GPV}^g = A_{GPV}^g \Delta x_{GPV}^g + B_{GPV}^{v'} \Delta v^{PV'} + B_{GPV}^v \Delta v^{GPV} + B_{GPV}^{\omega} \Delta \omega_{SPV} \quad (5.60)$$

$$A_{GPV}^g = T_{PV} A_{GPV} T_{PV}^{-1}, \; B_{GPV}^{v'} = T_{PV} E_{GPV}, \; B_{GPV}^v = T_{PV} A_{GPV} i_{\delta PV}^o M_{qdPV}, \; B_{GPV}^{\omega} = -T_{PV} i_{\delta PV}^o \quad (5.61)$$

$$\Delta \dot{x}_{cPV} = A_{cPV} \Delta x_{cPV} + C_{GPV}^x \Delta x_{GPV}^g + C_{GPV}^g \Delta v_{qd}^{GPV} + C^{vPV} \Delta v^{sPV} + B_{GPV}^u \Delta u_{GPV} \quad (5.65)$$

Where: $C_{GPV}^x = C_{GPV} T_{PV}^{-1}$, $C_{GPV}^g = C_{GPV}^v T_{PV}^{-1} + C_{GPV} i_{\delta}^{oGPV} M_{qdPV} + C_{GPV}^v v_{\delta}^{oGPV} M_{qdPV}$

Vectors of PV generator output voltage

$$\Delta v^{PV'} = E_{cPV}^v \Delta x_{cPV} + E_{uPV}^v \Delta u_{GPV} \quad (5.63)$$

$$\Delta v^{sPV} = E_{GPV}^v \Delta v^{GPV} - \Delta v^{PV'} + E_{cPV}^s \Delta i_{GPV}^{'} \quad (5.66)$$

Where $E_{GPV}^{v} = T_{PV}^{-1} + v_{\delta}^{oGPV} M_{qdPV}$

Supplementary vectors of PV generator

$$\Delta i_{GPV}^{'} = E_{cPV}^{i} \Delta x_{cPV} \,,\ \Delta \omega_{sPV} = E_{cPV}^{\omega} \Delta x_{cPV}$$

Network

$$\Delta \dot{x}_N = A_N \Delta x_N + B_N^1 \Delta u_N + B_N^{v2} \Delta v^{G2} \tag{5.70}$$

$$\Delta v^{G2} = E_{21}^{N} \Delta x_N + E_{22}^{N} \dot{\Delta x}_N + D_{21}^{NBS} \Delta x_{GBS} + D_{22}^{NBS} \dot{\Delta x}_{GBS} + D_{21}^{NPV} \Delta x_{GPV} + D_{22}^{NPV} \dot{\Delta x}_{GPV} \tag{5.73}$$

The total model of the overall system is described based on state space equations (5.74)

$$\begin{bmatrix} \dot{\Delta x}_{GBS}^{g} \\ \Delta x_{cBS} \\ \Delta x_N \\ \Delta x_{GPV}^{g} \\ \Delta x_{cPV} \end{bmatrix} = \mathbf{A_{sys}} \begin{bmatrix} \Delta x_{GBS}^{g} \\ \Delta x_{cBS} \\ \Delta x_N \\ \Delta x_{GPV}^{g} \\ \Delta x_{cPV} \end{bmatrix} + \mathbf{B_{sys}} \begin{bmatrix} \Delta u_{GBS} \\ \Delta u_N \\ \Delta u_{GPV} \end{bmatrix} \tag{5.74}$$

Where the $\mathbf{A}_{\text{sys}}$ is a 34×34 order matrix and is given by equation (5.75). It is important for system small signal stability analysis. The eigenvalues of system state matrix $\mathbf{A}_{\text{sys}}$ are the system transfer function's poles. These poles are used to determine the system is asymptotically stable or marginally stable.

$$\mathbf{A}_{\text{sys}} = \left(\begin{bmatrix} 1 & 0 & 0 & 0 & 0 \\ 0 & 1 & 0 & 0 & 0 \\ 0 & 0 & 1 & 0 & 0 \\ 0 & 0 & 0 & 1 & 0 \\ 0 & 0 & 0 & 0 & 1 \end{bmatrix} \right.$$

$$\left. \begin{bmatrix} -B_{GBS}^{v} D_{22}^{NBS} & 0 & -B_{GBS}^{v} E_{22}^{N} & -B_{GBS}^{v} D_{22}^{NPV} & 0 \\ -(C_{GBS}^{g} D_{22}^{NBS} + C^{vBS} E_{GBS}^{v} D_{22}^{NBS}) & 0 & -(C_{GBS}^{g} E_{22}^{N} + C^{vBS} E_{GBS}^{v} E_{22}^{N}) & -(C_{GBS}^{g} D_{22}^{NPV} + C^{vBS} E_{GBS}^{v} D_{22}^{NPV}) & 0 \\ -B_{N}^{v2} D_{22}^{NBS} & 0 & -B_{N}^{v2} E_{22}^{N} & -B_{N}^{v2} D_{22}^{NPV} & 0 \\ -B_{GPV}^{v} D_{22}^{NBS} & 0 & -B_{GPV}^{v} E_{22}^{N} & -B_{GPV}^{v} D_{22}^{NPV} & 0 \\ -(C_{GPV}^{g} D_{22}^{NBS} + C^{vPV} E_{GPV}^{v} D_{22}^{NBS}) & 0 & -(C_{GPV}^{g} E_{22}^{N} + C^{vPV} E_{GPV}^{v} E_{22}^{N}) & -(C_{GPV}^{g} D_{22}^{NPV} + C^{vPV} E_{GPV}^{v} D_{22}^{NPV}) & 0 \end{bmatrix} \right)^{-1} \tag{5.73}$$

$$\begin{bmatrix} (B_{GBS}^{v} D_{21}^{NBS} + A_{GBS}^{g}) & (B_{GBS}^{v'} E_{cBS}^{v} + B_{GBS}^{\omega} E_{cBS}^{\omega}) & B_{GBS}^{v} E_{21}^{N} \\ (C_{GBS}^{x} + C_{GBS}^{g} D_{21}^{NBS} + C^{vBS} E_{GBS}^{v} D_{21}^{NBS}) & (A_{cBS} + C^{vBS} E_{cBS}^{s} E_{cBS}^{i} - C^{vBS} E_{cBS}^{v}) & (C_{GBS}^{g} E_{21}^{N} + C^{vBS} E_{GBS}^{v} E_{21}^{N}) \\ B_{N}^{v2} D_{21}^{NBS} & 0 & (A_N + B_{N}^{v2} E_{21}^{N}) \\ B_{GPV}^{v} D_{21}^{NBS} & 0 & B_{GPV}^{v} E_{21}^{N} \\ (C_{GPV}^{g} D_{21}^{NBS} + C^{vPV} E_{GPV}^{v} D_{21}^{NBS}) & 0 & (C_{GPV}^{g} E_{21}^{N} + C^{vPV} E_{GPV}^{v} E_{21}^{N}) \\ B_{GBS}^{v} D_{21}^{NPV} & 0 & \\ (C_{GBS}^{g} D_{21}^{NPV} + C^{vBS} E_{GBS}^{v} D_{21}^{NPV}) & 0 & \\ B_{N}^{v2} D_{21}^{NPV} & 0 & \\ (B_{GPV}^{v} D_{21}^{NPV} + A_{GPV}^{g}) & (B_{GPV}^{v'} E_{cPV}^{v} + B_{GPV}^{\omega} E_{cPV}^{\omega}) & \\ (C_{GPV}^{x} + C_{GPV}^{g} D_{21}^{NPV} + C^{vPV} E_{GPV}^{v} D_{21}^{NPV}) & (A_{cPV} + C^{vPV} E_{cPV}^{s} E_{cPV}^{i} - C^{vPV} E_{cPV}^{v}) & \end{bmatrix}$$

to determine the system is asymptotically stable or marginally stable.

5 Eigenvalue analysis of the overall system

In order to assess the small signal stability dynamic performance of the case study network, the Matlab software is used to construct system state matrix $\mathbf{A}_{sys}$ to obtain the system eigenvalues, and the system operating condition is attained by using the power flow analysis. The system is evaluated based on parameters listed in Table 5-1, and it is assumed to be operating in the nominal

Table 5-1: System operating parameters

Name	Values
System frequency	50Hz
LV network voltage (rms L-L)	0.4kV
Line impedance 1	R_1= 0.164 Ω
	L_1 =0.00014536 H
Line impedance 2	R_2= 0.0443 Ω
	L_1 =0.000057080 H
Load 1	30kW/6kVAr
Load 2	10kW/2.5kVAr
Energy storage filer	R_{BS}= 0.01 Ω
	L_{BS} = 5e-3 H
Voltage controller of the storage	K_{pdBS}= 0.2
	K_{idBS}= 1050
	K_{pqBS}= 0.2
	K_{iqBS}= 1050
Current controller of the storage	K_{pidBS}= 1.86
	K_{iidBS}= 1087.24
	K_{piqBS}= 1.86
	K_{iiqBS}= 1087.24
Power controller of the PV	K_{pdPV} = 0.35
	K_{idPV} = 190
	K_{pqPV} = 0.35
	K_{iqPV} = 190
Current controller of the PV	K_{pidPV} = 1.95
	K_{iidPV} = 807.24
	K_{piqPV} = 1.95
	K_{iiqPV} = 807.24
PLL	K_{pw} = 5.0
	K_{iw} = 0.001

condition. At the designated operating point, the PV generator operates at 200kW. The energy storage is operated by using both dq axis voltage regulation controllers, and the PCC voltage is regulated as the threshold value of 1.085p.u. in the case study network. This value has been selected and tuned by considering secure of regulated PCC voltage that is consistently below the limit of 1.10.

5.1 Eigenvalue analysis

Compete eigenvalues of the studied overall system are illustrated in Table 5-2, and the dominant cluster of eigenvalues based on their real component (system damping) is seen by Figure 5-9. Eigenvalues of the overall system derived from the linearized matrix as seen by equation (5.75). There are total 34 eigenvalues with all of the real parts being negative. The system eigenvalues are highly damped for the designated operating condition and system parameters given. There are 8 pairs of complex conjugate eigenvalues observed, and these eigenvalues represent the system oscillatory modes. There are no synchronous generators or induction generators considered in the system design, which present low electromechanical oscillatory frequency at the range of 0.1 to 2Hz [202]. Therefore, no low oscillatory frequencies are introduced in this study.

The sensitivity analysis of system eigenvalues can be used to investigate the small signal stability margin of the case study network. It contains sensitivity analysis to the control parameters and sensitivity analysis to the system operating points [200]. The sensitivity analysis to the system operating points is important to investigate whether energy storage absorbing active/reactive power reaches the network small signal stability margin. Therefore, it will be presented in Chapter 6. On the other hand, the sensitivity analysis to the control parameters is firstly examined in this Chapter.

As indicated by [200] [159] and [203], controller gains play an important role under the small signal disturbance condition. Therefore, the sensitivity of the system eigenvalues to variations in the proportional gains of the energy storage voltage regulators, $K_{\mathrm{pdBS}}/K_{\mathrm{pqBS}}$, and K_{pdPV}, of the active power controller of the PV generator are firstly examined. Figure 5-10 illustrates the dominant complex eigenvalues, (13, 14) and (20, 21), locus with energy storage voltage controller

Table 5-2: Eigenvalues of the case study system

Eigenvalues	Real (1/sec) 1.0e+03	Imaginary (rad/s) 1.0e+03
1	-9.6248	0
2	-9.6248	0
3	-9.6248	0
4	-9.6248	0
5	-8.9931	0
6	-9.2049	0
7	-9.4647	0
8	-9.4661	0
9	-9.6248	0
10	-9.6248	0
11, 12	-0.3862	± 0.4517i
13, 14	-0.4068	± 0.4329i
15, 16	-1.7043	± 0.3142i
17, 18	-0.1936	± 0.3143i
19	-0.0313	0
20, 21	-0.1605	± 0.0971i
22, 23	-0.2611	± 0.0295i
24	-0.2371	0
25, 26	-0.2063	± 0.3142i
27, 28	-0.2063	± 0.3142i
29	-0.2054	0
30	-0.2054	0
31	-0.2000	0
32	-0.2000	0
33	-9.6248	0
34	-9.6248	0

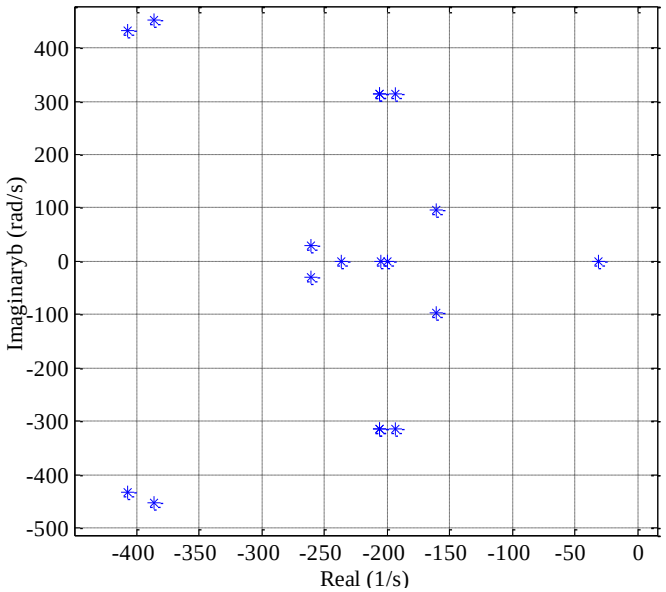

Figure 5-9: Dominant cluster of eigenvalues under designated operating condition

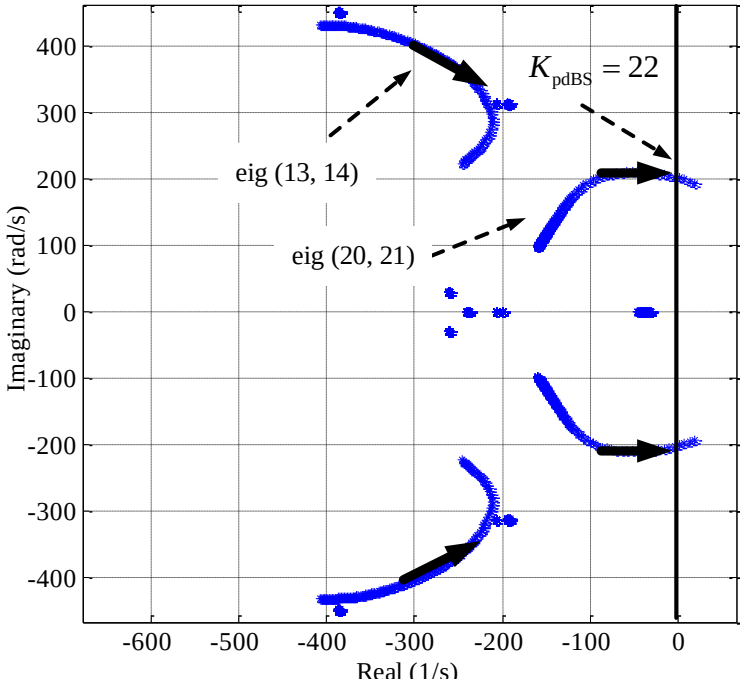

Figure 5-10: Eigenvalue locus with energy storage voltage controller gain KpdBS change

gain, K_{pdBS}, change in the range of 0.2 to 25 with the step 0.2. It can be seen that dominant complex eigenvalues (20, 21) move from left hand plane to the right hand plane when the value of K_{pdBS} reaches 22 at the damping ratio equals to -0.0064 which is derived based on the equation (5.8). This means that the system is unstable. In addition, the complex eigenvalues (13, 14) are moved only within the left hand plane. The similar result is observed for changing controller gain K_{pqBS} of energy storage also in the range of 0.2 to 25 with the step 0.2 (see Figure 5-11). Figure 5-11 indicates that increasing the value of the controller proportional gain K_{pqBS} also has significant effect on system stability. Changing the value of K_{pqBS} has much less sensitive to the complex eigenvalues (20, 21), but it dominates on the eigenvalue (19) that has been moved to left hand plane when the value of K_{pqBS} is beyond 18. As the eigenvalue (19) is not the complex conjugate eigenvalue, the damping ratio is equal -1 when K_{pqBS} is beyond 18. Based on the eigenvalue analysis as seen in Figure 5-10 and the Figure 5-11, the energy storage voltage controller proportional gains K_{pdBS} and K_{pqBS}should be relatively small value. Figure 5-12 illustrates loci of complex eigenvalues (20, 21) corresponding to the variation of PV generator active power controller proportional gain K_{pdPV} in the range of 0.35 to10 with the step 0.2. It can be seen that increasing the value of K_{pdPV}

beyond 8.0 leads to the departure of complex eigenvalues (20, 21) from the left hand plane to the right hand plane. The damping ratio at the value of K_{pdPV} equal to 8.0 becomes -0.0190. As a result, the value of K_{pdPV} should be chosen a relative small value.

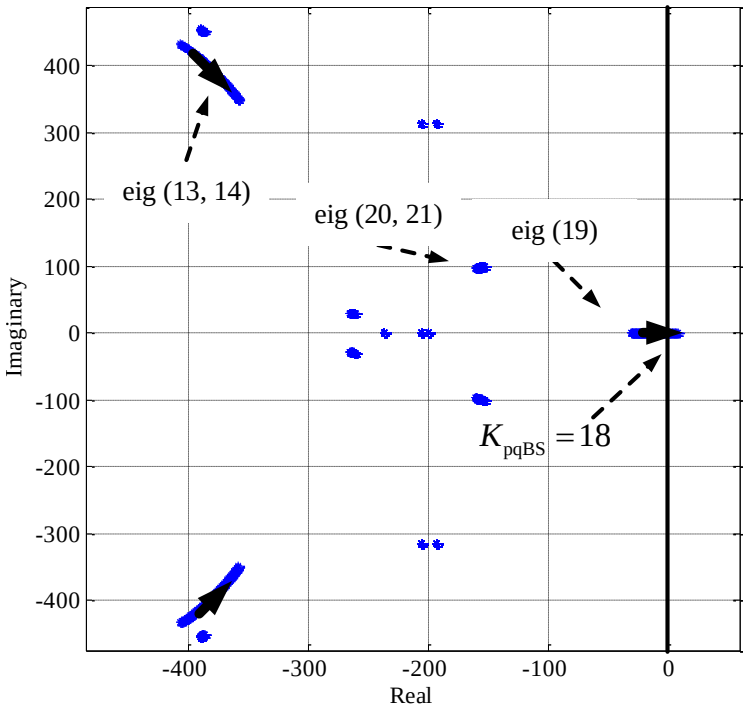

Figure 5-11: Eigenvalue locus with energy storage voltage controller gain KqdBS change

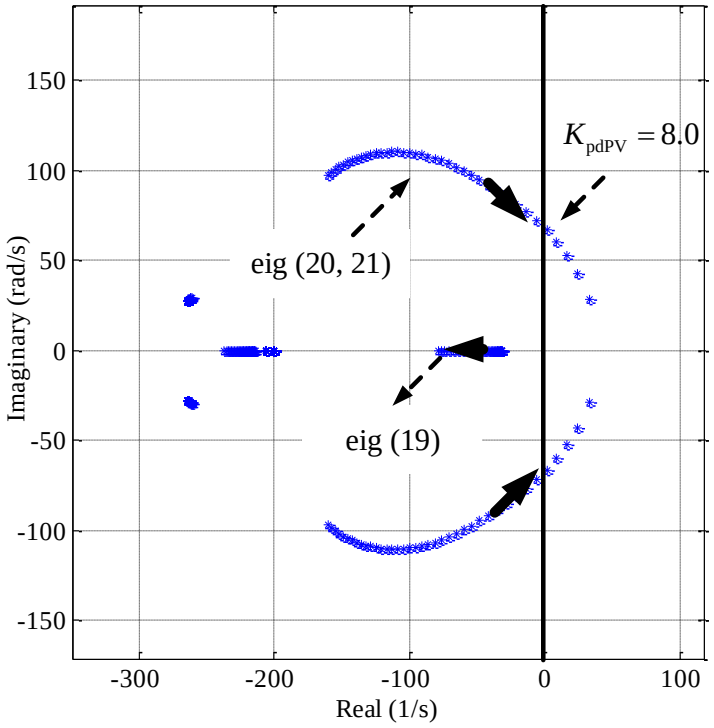

Figure 5-12: Eigenvalue locus with PV generator controller gain KpdPV change

5.2 Simulation studies

Simulation studies based on the linearized model of (5.74) are implemented to evaluate the dynamic response performance of the energy storage voltage regulation controllers corresponding to the suddenly change of PV output power. Such simulation studies can provide information on control characteristics and design criteria, such as rise time, settling time of the system response and overshoot.

Figure 5-13 illustrates simulation results of energy storage voltage regulation controllers' dynamic response to the step change in the PV output power. The energy storage active/reactive powers are controlled in such a way that reactive power voltage controller output is half of active power voltage controller output. This assumption is made because the active power is much effective than reactive power for voltage support in high R/X ratio LV network. The voltage threshold is selected as 1.085 p.u. to avoid any overshoot caused by energy storage voltage regulation controller regarding suddenly change of the PV output. PV power is simulated as the step change with 20kW in one second started from 120kW to 200kW (see Figure 5-13 (a)). The PCC voltage increase due to the increasing of PV output requires that both active/reactive power voltage controllers from the energy storage absorb both active/reactive powers from the grid to maintain the PCC voltage within the legal limit. As illustrated in Figure 5-13 (a) and (b), when the PV output increases sharply at each second, the energy storage absorbing active/reactive power from the grid also increases sharply. The dq axis component of the energy storage current, I_{dBS} and I_{qBS}, firstly change to accommodate variation of the reference signal for the dq axis current. This increases absorbing the active/reactive power of the energy storage from the grid for voltage support as illustrated in Figure 5-13 (d). As depicted in Figure 5-13 (c), the properly tuned voltage regulation controllers have fast response with overshoot less than 1%, and can reach the steady state less than 2 cycles. This meets the design criteria. Accordingly, the PCC voltage controlled by the energy storage has the overshoot less than 0.55% with the sharply change of PV output (see Figure 5-13 (e)).

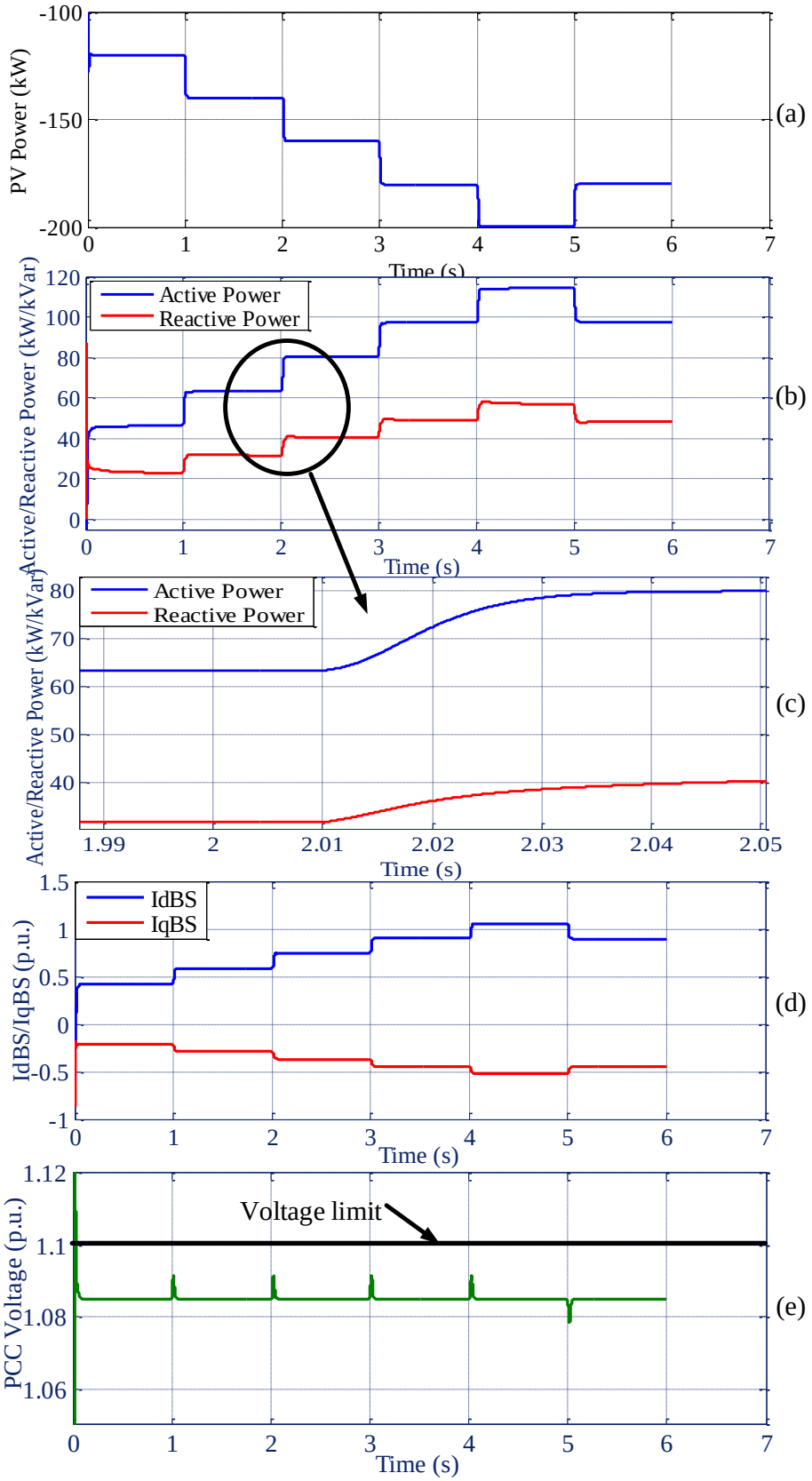

Figure 5-13: Energy storage voltage controller response to step changes in the PV generator (a) Solar PV outputs (b) Energy storage active/reactive power corresponding with changes in PV generator (c) Close look of dynamic response of energy storage at 2 seconds (d) Current IdBS and IqBS (e) PCC voltage after controlled by energy storage

Figure 5-14 shows time domain simulation results of energy storage voltage controllers' response to the change of the real solar irradiation profile. The real high resolution (6 seconds) solar irradiation profile is selected as the time period between 11:00 and 11:10 in summer day 06-Jun according to Figure 1-5 (b). However, this profile is simulated as 0.5 seconds a data change rather than 6 seconds. By doing so, the simulation time is compressed for 47 seconds. Both active/reactive voltage regulation controllers can also be tested whether controllers' performances are satisfied under the real solar irradiation profile. This irradiance profile contains high fluctuated characteristic as seen by Figure 5-14 (a). Such fluctuation is classed as power quality issue and it caused by changes in the PV output by clouds or shading. In addition, the average three phase load data between 11:00 and 11:10 is selected and applied in the work as described in Figure 1-5 (a).

In this case study, the energy storage active/reactive powers are also implemented in such way that reactive power voltage controller output is half of active power voltage controller output. The PV output sharply increasing happens at the time 11 seconds when the solar irradiance is at the end of the cloud passing, the energy storage charging power also increases sharply to mitigate the sudden increase in PCC voltage (see Figure 5-14 (b) and (c)). As illustrated in Figure 5-14 (c), the baseline PCC voltage (red line) at the time 11 seconds suddenly increase to 1.18p.u.. However, the PCC voltage controlled by the energy storage (green line) is maintained at the threshold 1.085 p.u.. Following the PV power sharply decreasing happens at the time 20 seconds and 43 seconds. This requires the energy storage charging power suddenly decrease to preserve the energy usage. The simulation results show that the energy storage voltage regulation controllers with their properly tuned control parameters have good performance for voltage support. This means that the designed voltage regulation controllers can meet the requirement for voltage support under real solar irradiance condition. As seen by Figure 5-14 (c), the PCC voltage controlled by the energy storage is always regulated at its threshold value 1.085 p.u.. Accordingly, the fluctuated PCC voltage has been mitigated.

6 Discussion

A linearized state space model of a LV distribution network is presented in this chapter including the PV generator, the energy storage, network line impedances and static loads. The energy storage, PV generator, and the LV network are modelled in each subsystem and then combined based on global reference rotating frame. The detailed control systems of the energy storage and the PV generator are introduced and the linearized models are developed. The voltage regulation control strategy is introduced to put forward to control the VSC of the energy storage in the averaged representation. However, characteristics of the storage system itself, such as battery dynamics, are not considered in this thesis. As indicated in [92], this assumption is practical to investigate the small signal stability of the energy storage control parameters and its exchanging active/reactive power with the grid. According to [65], the simpler PV generator model has been recommended for small signal stability analysis. Therefore, the PV generator has modelled as a power generator with its active power controller regardless of dynamic characteristic of the PV cell.

There are no synchronous generators and induction motors considering in the system design, which present low electromechanical oscillatory frequency at the range of 0.1 to 2Hz [192] [204]. As such, no low oscillatory frequency modes are observed in this work. However, there is a greater potential for the model presented in this work to comprise any synchronous generators and induction motors for future study.

In addition, the sensitivity analysis of the system eigenvalues to energy storage control parameters is carried out in this chapter. It shows that high proportional gains applied in energy storage voltage regulation controllers can result in system stability. In addition, time domain simulation is implemented based on MATLAB/Simpower environment to test and verify voltage regulation controllers for voltage support. Simulation results under step change of solar output and real solar irradiation conditions reveal that both active/reactive voltage controllers with appropriately tuned parameters have good performances with fast response and less overshoot for voltage support.

However, the sensitivity analysis of the system eigenvalues to system operating

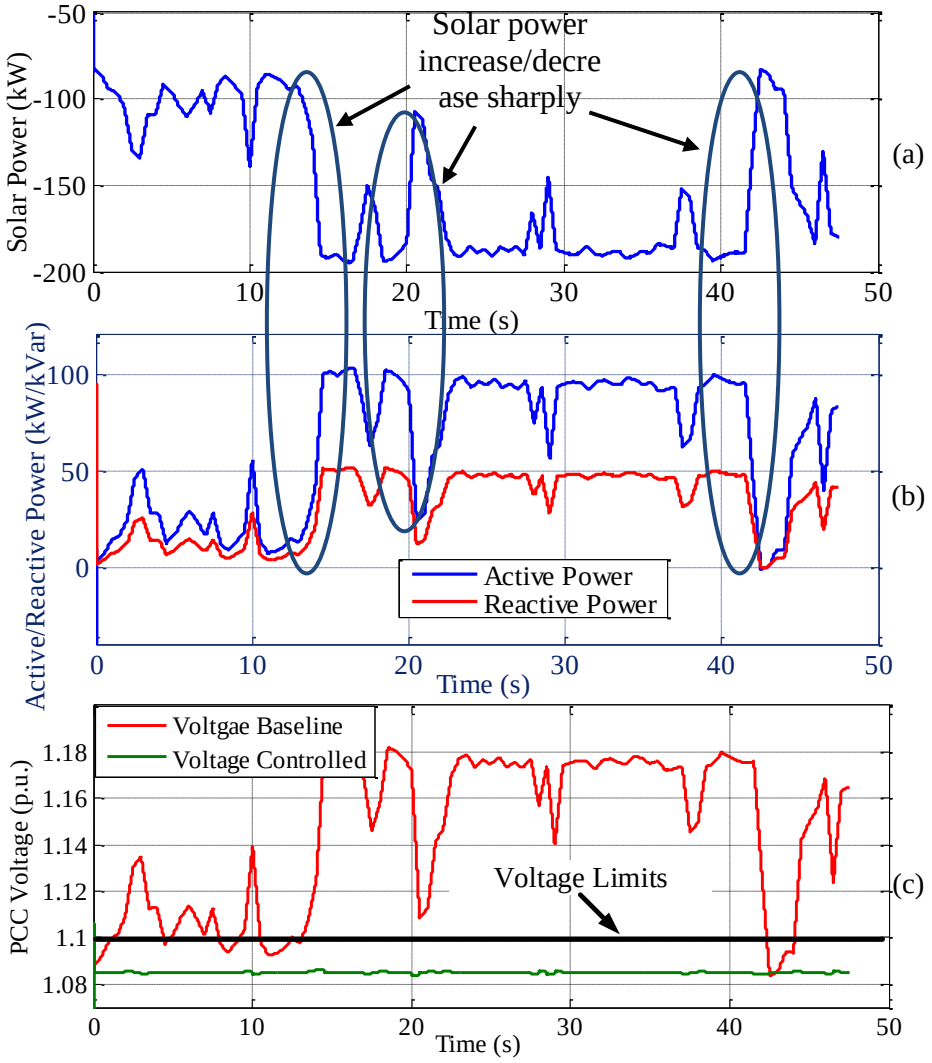

Figure 5-14: Energy storage voltage controller response to the change of the real solar irradiance

points is not implemented in this chapter. This is because such study is imperative to explore whether energy storage its exchanging active/reactive power with the grid can reach the network small signal stability margin. This will be introduced in Chapter 6 to investigate active/reactive power setting of energy storage system under small disturbance.

The energy storage active/reactive powers introduced in this chapter for simulation studies are based on the assumption that reactive power voltage controller output is half of active power voltage controller output. This is not an effective approach to utilise the energy storage active/reactive powers. However, the main focus of this chapter is to represent a systematic state space model based on a set of differential equations for determining the stability margin for control parameters of the energy storage. As a result, a new energy

storage active/reactive power control method for voltage support is developed and is introduced in Chapter 6.

7 Summary and conclusion

In this chapter, a systematic model of the LV distribution network that includes one PV generator and the energy storage are developed. The model developed is valid and can be extended to contain any types of generators and loads. The model is utilised for eigenvalue analysis around a designated operating condition. This can be used to

- Reveal the dynamic performance of energy storage voltage regulation controllers. Based on the eigenvalue sensitivity analysis to energy storage control parameters, the proper control parameters can be selected for voltage regulation controllers without causing small signal stability issues.
- Investigate the sensitivity analysis of the system eigenvalues to system operating points. This can be used to examine energy storage active/reactive power exchanging with the power grid under small disturbance, and identify reliable operating points of energy storage for voltage support. This will be presented in Chapter 6.

Simulation studies are implemented under PV step change output and real solar irradiance conditions to validate the results from the eigenvalue analysis. It shows that active/reactive voltage controllers with appropriately tuned parameters have good performances with fast response and less overshoot for voltage support.

Chapter 6: Active and reactive power control strategy of the energy storage for voltage support in LV distribution network in respect to small signal stability

1.1 Introduction

A storage device, whether installed at the secondary substation or distributed along the feeders, can be used for providing voltage support with large quantities of PV generators connected in an LV distribution network [133], [96], [178] and [205]. Authors in [133] propose a decentralised storage strategy to support voltage control in a LV distribution network. The proposed method is capable of solving voltage excursions through considering voltage violation events during high output from the PV generator [133]. In [178], a detailed control strategy for a storage device integrated with the PV generator is proposed. The proposed method is based on the battery storage charging/discharging rate and can efficiently provide voltage support and reduce voltage fluctuation during peak PV generation in an LV distribution network. A hybrid system, including several generators and an energy storage system is presented for dynamic response analysis under time domain simulations in [124]. It shows that the energy storage is seen as a way for voltage support if solar irradiance or wind speed suddenly increase or decrease [124].

However, this research work solely considers active power for voltage regulation. As indicated in [89] and [206], reactive power is available from the converter allowing the active power rating to be reduced. Reactive power can provide the effort in regulating the voltage, although the reactive power is generally considered to be not sufficient without active power for voltage support in the LV distribution network where the R/X ratio is large. However, using the functionality of reactive power for voltage support, the battery cost can be reduced as the reactive power does not use stored battery energy [205]. The authors in [89] investigate a voltage support strategy for energy storage in the distribution network. The proposed strategy allows the energy storage to import or export both active/reactive power (with reactive power priority) for supporting voltage control. The active and reactive power charged from the energy storage

system is determined based upon the ratio of voltage sensitivities of active and reactive power export [89]. This can minimize the storage device size. A similar control approach is found in [205]. The authors in [205] present a coordinated control strategy for multiple energy storage systems based on voltage sensitivity analysis and battery aging model in the LV distribution network (the primary author of the paper being the author of this thesis). The decentralised controller used in [205] is designed to control its charging/discharging function with reactive power priority to preserve the energy usage of the battery.

In this chapter, an investigation of active and reactive power control from the energy storage for voltage support in the LV distribution network is presented. Firstly, the initial investigation of active/reactive power setting of the energy storage for voltage improvement is carried out. In addition, a sensitivity analysis of small signal stability to the system operating points is implemented to investigate whether the energy storage absorbing active/reactive power reaches the network small signal stability margin. Lastly, the active and reactive power operation control strategy of the energy storage for voltage support is proposed. Two case studies based on the step changed and real solar irradiances are performed to validate and justify the proposed control strategy.

This chapter will demonstrate that proportionally using active and reactive power of the energy storage unit for voltage support can efficiently reduce active power requirement for the energy storage device according to proposed active and reactive power control strategy. This method is able to maximise the usage of the reactive power from the energy storage converter, and minimise the required active power for voltage. This is also design to avert the stability issues which could arise from using active and reactive power from the energy storage. So in this sense, the system stability is to be examined based on system eigenvalue sensitivity analysis.

2 Theory of active and reactive power operation of the energy storage

Although energy storage with active power functionality can efficiently eliminate voltage excursions in an LV distribution network, reactive power functionality can also be included to allow voltage deviation to be tackled. As a result, battery size can be reduced for purpose of the voltage support. Figure 6-1 illustrates

rated active power reduction of the energy storage corresponding to the increased reactive power capability. As shown in Figure 6-1, by reducing the rated active power 10% for a given energy storage converter size, the reactive power capability can be significantly increased.

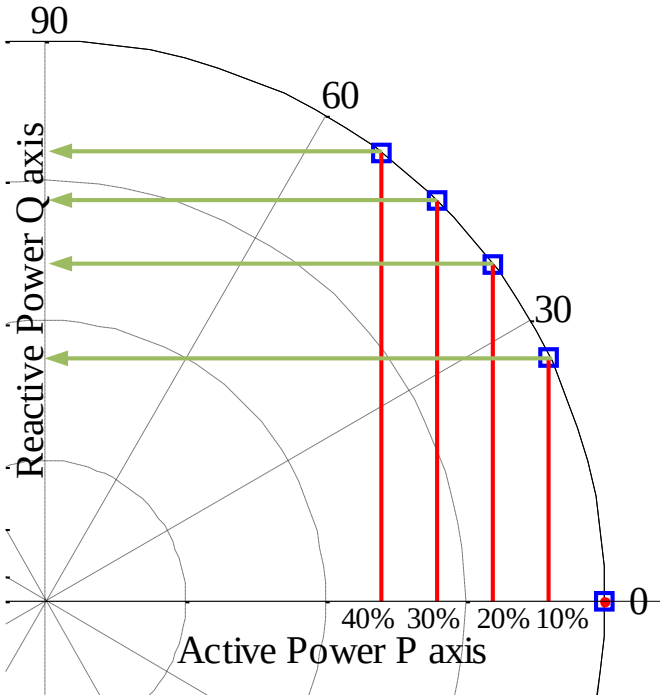

Figure 6-1: Rated active power reduction corresponding to the capability of reactive power increasing

The percentage of increased reactive power capability at rated active power percentage reduction can be determined by using equation (6.1),

$$\beta = \sqrt{2\alpha-\alpha^2} \tag{6.1}$$

Where $\beta=Q_{inc}/P_{rated}$ is the ratio of the percentage of the reactive power capability increase with respect to the rated active power, P_{rated}^{BS}, of the energy storage apparent power. In addition, $\alpha=1-(P_{new}/P_{rated})$ is the ratio of the percentage of the rated active power, P_{rated}^{BS}, reduction. Figure 6-2 shows a plot of equation (6.1). A reduction of 10% of in the rated active power, P_{rated}^{BS}, can increase the reactive power capability from zero to 43.59% corresponding to the rated active power P_{rated}^{BS}. However, the plot also illustrates that the relationship between percentages of the rated active power reduction, α, and the percentage of the reactive power capability increasing, β, initially tends to be steep if percentage reduction of rated active power, α, is less or equal than 40% (β is increased to

80% when α equal to 40%). This implies that by decreasing the rated active power, $P_{\text{rated}}^{\text{BS}}$, less or equal than 40% can increase amounts of the reactive power capability up to 80%.

However, if the percentage reduction of rated active power, α, is greater than 40%, the increase in reactive power is lower per unit decrease in active power. This indicated that by reducing the rated active power, $P_{\text{rated}}^{\text{BS}}$, more than 40%, the reactive power capability, β, does not increase greatly. This can be concluded that since the active power is much more effective than the reactive power for the voltage improvement in the LV distribution network, the increased reactive power capability, β, for voltage support at a given energy storage converter size is better less or equal than 80% which is the 40% reduction of the rated active power $P_{\text{rated}}^{\text{BS}}$.

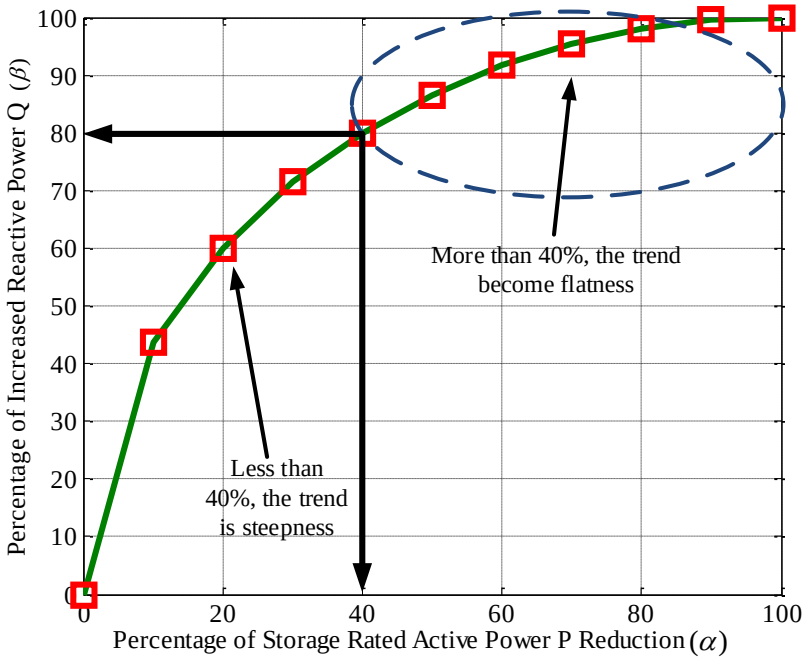

Figure 6-2: Percentage of increased reactive power related to percentage of rated active power reduction

3 Method to implement active/reactive power control of the energy storage for voltage support in the LV distribution network in respect to small signal stability

Figure 6-3 illustrates three procedures that are carried out to investigate active and reactive power control of energy storage for voltage support. The main objective of these procedures is to effectively utilise the active and reactive

power from the energy storage for voltage regulation in the LV distribution network. These procedures provide visibility for the storage operator to understand the dynamic performance of units power exchange with the LV distribution network. These procedures are explained as following.

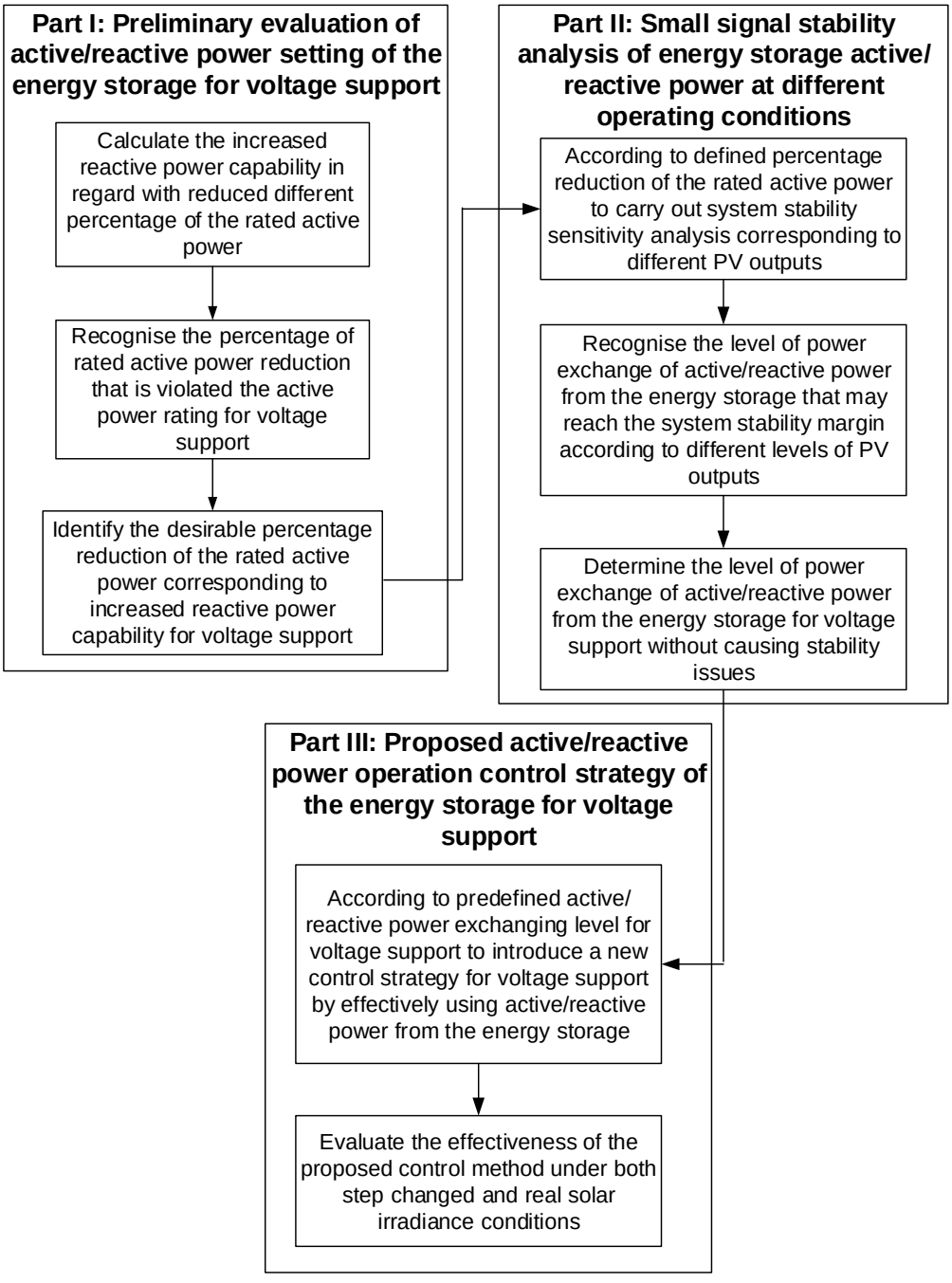

Figure 6-3: Flow chart illustrating procedures used in this thesis investigating the active/reactive power control of energy storage for voltage support in the LV distribution network

As illustrated in Figure 6-3, the Part I is an initial investigation into the active and reactive power setting of energy storage for voltage support based on equation (6.1) and Figure 6-2 to analyse and define the level of energy storage rated

active power percentage reduction, α, with its increased reactive power capability, β, for regulating the PCC voltage in the LV distribution network. This procedure contains three steps.

- The first is to determine the possible ratio for increased reactive power capability, β, corresponding to the rated active power percentage reduction, α. This step is to calculate the increased reactive power capability in regard with reduced different percentage of the rated active power capability at a predefined storage unit rating.
- The second is to examine the level of rated active power reduction with the increased reactive power capability whether it is sufficient for voltage support. For example, although the reactive power capability can be increased if the rated active power capability is reduced, this may not be desirable for voltage regulation in the LV distribution network as a result of high R/X ratio. In such case, the higher required active power, P_{req}^{BS}, is needed, and this may violate the reduced rated active power rating, P_{rated}^{BS}, of the energy storage.
- The third is to predict a desirable level of the rated active power percentage reduction, α, for voltage support. This provides visibility of different reduction levels of rated active power with increased reactive power capability for solving the voltage excursion.

Part II presents small signal stability analysis of energy storage active and reactive power at different operating conditions.

According to a recognised desirable level (defined by part I) of active power reduction, α, with its increased reactive power capability, β, a system sensitivity analysis is carried out based on eigenvalue analysis at different system operating points. This can be used to identify the level of active and reactive power exchange of the energy storage with the LV distribution network for voltage support without causing the instability issue.

Part III proposes a control strategy for energy storage for voltage support. According to eigenvalue sensitivity analysis to different system operating conditions from part II, the level of the rated active power reduction, α, can be defined without reaching a stability margin. As such, a novel active/reactive

power operation control method of the energy storage for voltage regulation is proposed based on predetermined level of active power reduction, α. The proposed method contains two stages to perform the active and reactive power control of energy storage for voltage support.

The first stage uses the reactive power from the storage units for voltage support. If the reactive power capability is not sufficient to solve the voltage excursion, the active power functionality from the second stage will be applied while the reactive power continues at its maximum rated power $Q_{\text{rated}}^{\text{BS}}$. In addition, step changes in solar irradiance (see Figure 6-8) are used to evaluate the effectiveness of the proposed control strategy, such as dynamic response of the controllers to dramatically changed PV output. Finally, a real solar irradiance profile is used to investigate the effectiveness of the proposed controller under real word conditions.

The following subsections are based on the case study to present for the proposed method as discussed above.

3.1 Preliminary evaluation of active and reactive power setting of the energy storage for voltage support in the case study network

A preliminary investigation is conducted to evaluate the increased reactive power capability for voltage support corresponding to the percentage of the storage rated active power reduction in the case study network (see Figure 5-1).

The evaluation is performed based upon active and reactive power charging of the energy storage with different amounts of PV in an LV distribution network. The PV output rating is incrementally increased from 150kW to 300kW with a 50kW step. The rated active power of the energy storage is considered as 100kW, 150kW, 200kW, 250kW depending on the amount of PV. Figure 6-4 illustrates the storage rated active power after reduction, α, corresponding to the increased reactive power capability, β, for voltage support at various PV generator outputs.

As seen by Figure 6-4 (a-d), rated active power, $P_{\text{rated}}^{\text{BS}}$, at both 10% and 20% reduction are much higher than the required active power, $P_{\text{req}}^{\text{BS}}$. This means that the required active power, $P_{\text{req}}^{\text{BS}}$, with increased reactive power capability, $Q_{\text{insd}}^{\text{BS}}$, of

the storage at 10% and 20% reduction are enough to solve voltage excursions at different PV outputs. However, it would not be desirable to use such proportion of active and reactive power from the energy storage for voltage support. This is because there is a big difference between the rated active power, $P_{\text{rated}}^{\text{BS}}$, and required active power, $P_{\text{req}}^{\text{BS}}$, at 10% or 20% reduction (see Figure 6-4(a-d)). The rated active power, $P_{\text{rated}}^{\text{BS}}$, at 30% reduction incorporated with the increased reactive power for voltage regulation would be appropriated in comparison with 10% or 20% reduction. As stated in Figure 6-4, the 30% reduction of the rated active power, $P_{\text{rated}}^{\text{BS}}$, at different PV outputs is slightly higher than the required active power, $P_{\text{req}}^{\text{BS}}$, and the increased reactive power, $Q_{\text{insd}}^{\text{BS}}$, is nearly at the same level of the rated active power, $P_{\text{rated}}^{\text{BS}}$, at different PV outputs.

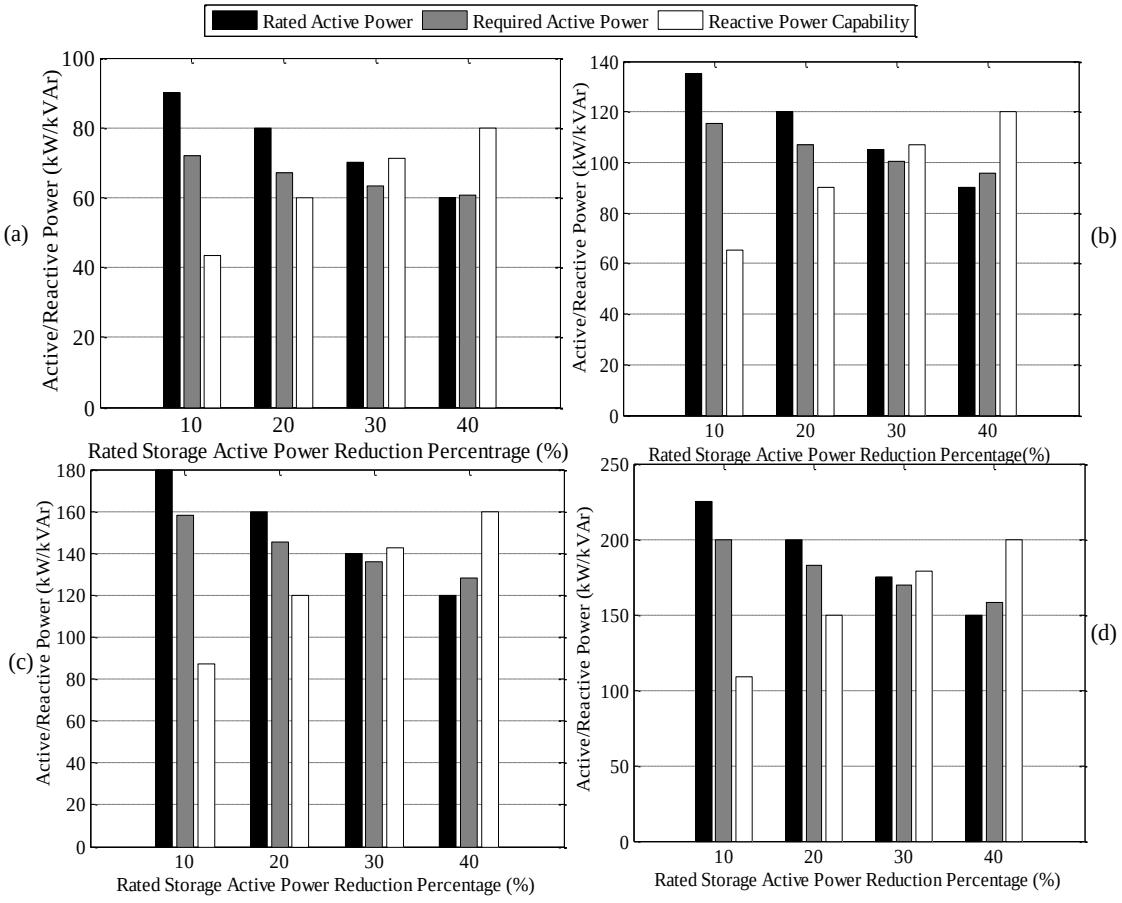

Figure 6-4: Storage rated active power reduction corresponding to the increased reactive power capability for voltage support (a) active/reactive charging from the storage at PV output 150kW (b) active/reactive charging from the storage at PV output 200kW (c) active/reactive charging from the storage at PV output 250kW (d) active/reactive charging from the storage at PV output 300kW

However, if the reduction of the rated active power, $P_{\text{rated}}^{\text{BS}}$, reaches at 40%, the required active power, $P_{\text{req}}^{\text{BS}}$, violates the storage rated active power rating, $P_{\text{rated}}^{\text{BS}}$, after reduction 40% as illustrated in both Figure 6-4 and Figure 6-5. As such, the voltage problem is not able to be solved although the increased reactive power, $Q_{\text{insd}}^{\text{BS}}$, is much higher than the required active power, $P_{\text{req}}^{\text{BS}}$.

Figure 6-5 summarises active power redundancy with different reduction percentage of the rated active power from the energy storage corresponding to different PV outputs. As indicated in Figure 6-5 both 10% and 20% reduction at different levels of the PV outputs allows the energy storage to have more active power redundancy. This is not the best proportion to utilise the active/reactive power from the energy storage. However, 30% reduction is a good choice to apply the active and reactive power of the energy storage for voltage support. This can effectively reduce the active power requirement for voltage regulation so that the storage device capacity, such as the battery, can be minimised. Therefore, 30% reduction of the rated active power,$P_{\text{rated}}^{\text{BS}}$, is selected in this work for proportional using the active/reactive power of the energy storage for voltage regulation.

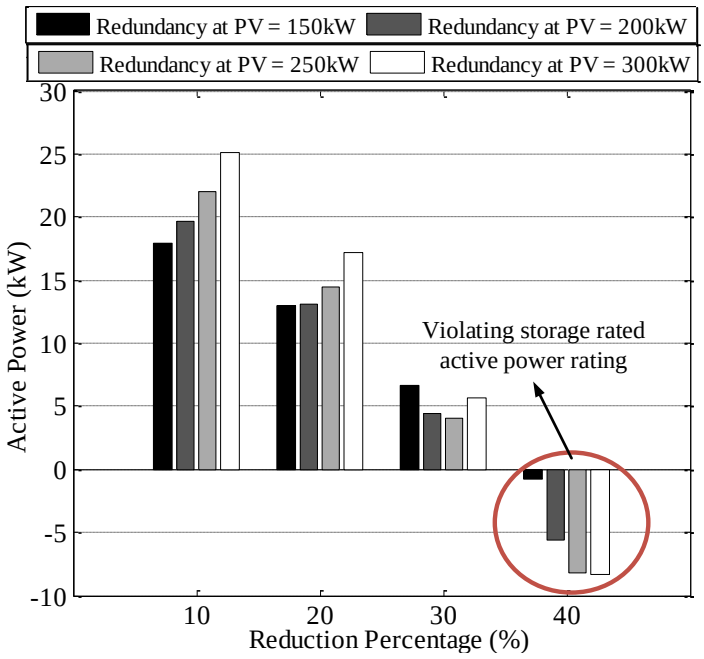

Figure 6-5: Active power redundancy with different reduction percentage of the rated active power of the storage corresponding to different PV output

3.2 Small signal stability analysis of energy storage active/reactive power at different operating conditions

A sensitivity analysis of the system eigenvalues to system operating points is implemented to explore whether exchanging active and reactive power of energy storage with the studied LV distribution network can cause system instability. A 30% reduction of the storage rated active power, $P_{\text{rated}}^{\text{BS}}$, corresponds to 71.41% increased reactive power, $Q_{\text{insd}}^{\text{BS}}$. This ratio is selected in this work for voltage support with system operating points are performed as listed in Table 6-1 considering different level of PV outputs. The active power control only is implemented from the storage device for voltage support in comparison with the scenario of 30% reduction of the storage rated active power. In addition, the consumption of the first load is considered as 20kW/5kVAr, and the consumption of the second load is assumed as 10kW/2kVAr for all scenarios. This is performed using network shown in Figure 5-1.

Table 6-1: System operating points corresponding to sensitivity analysis of the system eigenvalues

PV Output (kW)	Energy Storage Rated Power (kW)	Energy Storage (30% Reduction)			Energy Storage(Active Power Only)
		Rated Active Power after reduction (kW)	Active Power Required (kW)	Reactive Power Increased (kVAr)	Active Power (kW)
150	**100**	70	63.34	71.41	83.57
200	**150**	105	100.59	107.12	133.57
250	**200**	140	135.97	142.82	183.57
300	**250**	175	169.36	178.53	233.57

Figure 6-6 illustrates the locus of eigenvalues oscillatory mode variation considering exchanging active/reactive power for voltage support at different PV outputs. The red crosses represent the case for 30% reduction of the rated active power with increased reactive power capability, whereas the blue crosses represent using only active power control only for voltage support. There are no badly damped oscillatory modes if the active and reactive power of the energy storage is exchanged with the grid for voltage regulation. In addition, increased charging active and reactive power of the energy storage does not have a

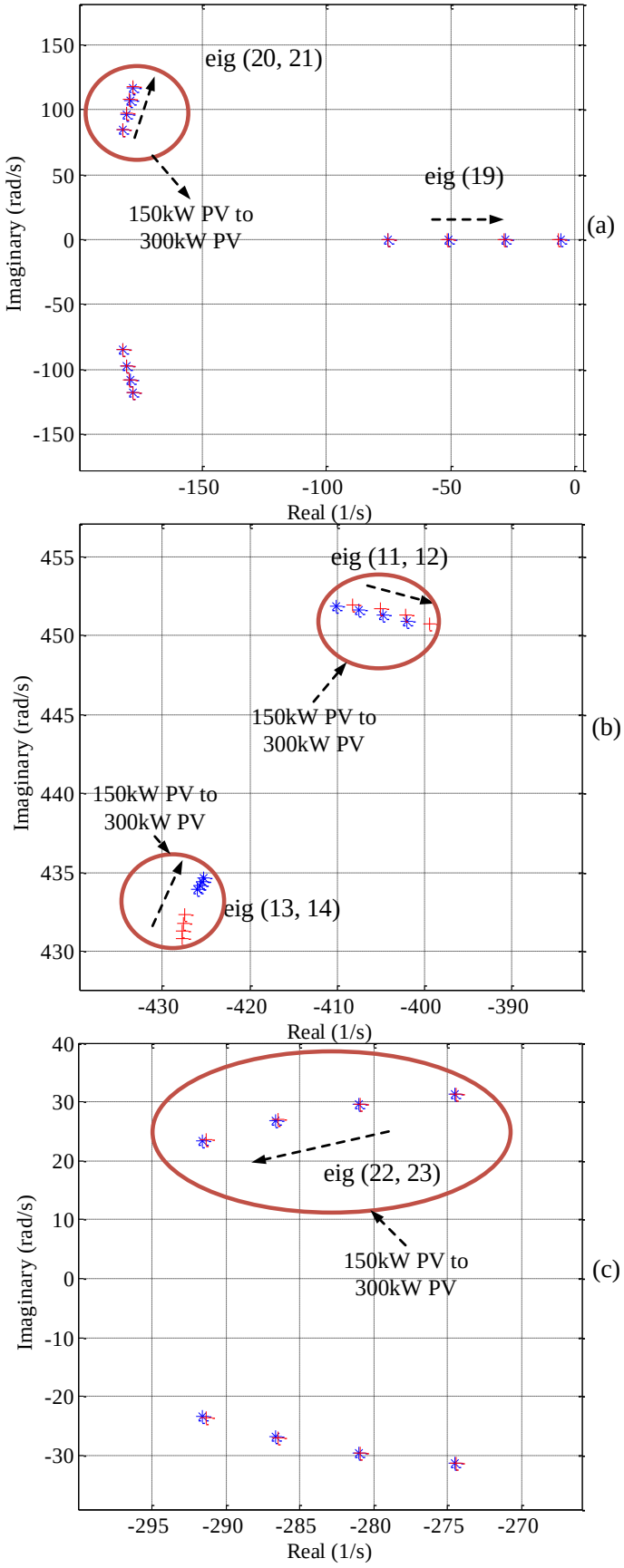

Figure 6-6: Locus of eigenvalues variation with exchanging power of the energy storage for voltage support at different PV outputs (red cross represented for 30% reduction of the rated active power, incorporated with the increased reactive power, blue cross represented for using active power only

significant impact on system oscillatory modes changing. The reasons for this are now explained.

According to Figure 6-6, increasing the level of active and reactive power of the energy storage for voltage support can result in eigenvalues migrating to left hand plane. As can be seen from Figure 6-6(a), eigenvalues (20, 21) and (19), move to the right hand plane when importing the active and reactive power from 63.34kW/71.41kVAr to 169.36kW/178.53kVAr corresponding to increased PV output from 150kW to 300kW. In addition, conjugate pairs of eigenvalues (13, 14) and (17, 18) also move from left hand plane to right hand plane (see Figure 6-6(b)). This result in the damping decrease of the mode and system stability deterioration. Although these conjugate pairs of eigenvalues move towards to right hand plane, these never cross it. It can therefore be concluded that increasing the level of the active/reactive power exchanging with the grid for voltage support in this case study does not cause the stability issue. On the other hand, Figure 6-6(c) depicts that eigenvalues (22, 23) moves to left hand plane with the increasing charging the active and reactive power from the energy storage for regulating voltage. This means the system stability is improved and mode damping is enhanced.

It is worth mentioning that effects of both active power control only and the scenario of 30% reduction of the storage rated active power on eigenvalues movement are similar. Furthermore, as it can be seen from the eigenvalue analysis, applying the active and reactive power from the energy storage for voltage support is not by itself the major important factor influencing the small signal stability of the LV distribution network, but the control parameters from the voltage regulation controller are important as discussed in Chapter 5.

3.3 Proposed active/reactive power operation control strategy of the energy storage for voltage support

The proposed active and reactive power operation control strategy of the energy storage for voltage support considering 30% reduction of the rated active power, $P_{\text{rated}}^{\text{BS}}$, is illustrated in Figure 6-7. It contains two stages to perform the active and reactive power control from the energy storage for voltage support in the proposed strategy.

If the measured PCC voltage, $v_{\text{mead}}^{\text{PCC}}$, is greater than the voltage threshold, $v_{\text{thred}}^{\text{PCC}}$, this will command the reactive power controller for reactive power compensation first (see stage one from Figure 6-7) as this does not use stored energy from the energy storage. However, if the required reactive power, $Q_{\text{req}}^{\text{BS}}$, reaches its maximum rated power limit $Q_{\text{rated}}^{\text{BS}}$, and it is inadequate to regulate the PCC voltage at the threshold, $v_{\text{thred}}^{\text{PCC}}$. The controller will switch from stage one to stage two so that the active power is applied for the voltage compensation. Note that the maximum rated reactive power, $Q_{\text{reted}}^{\text{BS}}$, is equal to the increased reactive power capability, $Q_{\text{insd}}^{\text{BS}}$, at the rated active power reduction (30% as determined in previous section). It is worth remembering that although the required active power, $P_{\text{req}}^{\text{BS}}$, is implemented; the reactive power continues applying it's the rated maximum value to preserve the energy storage SoC.

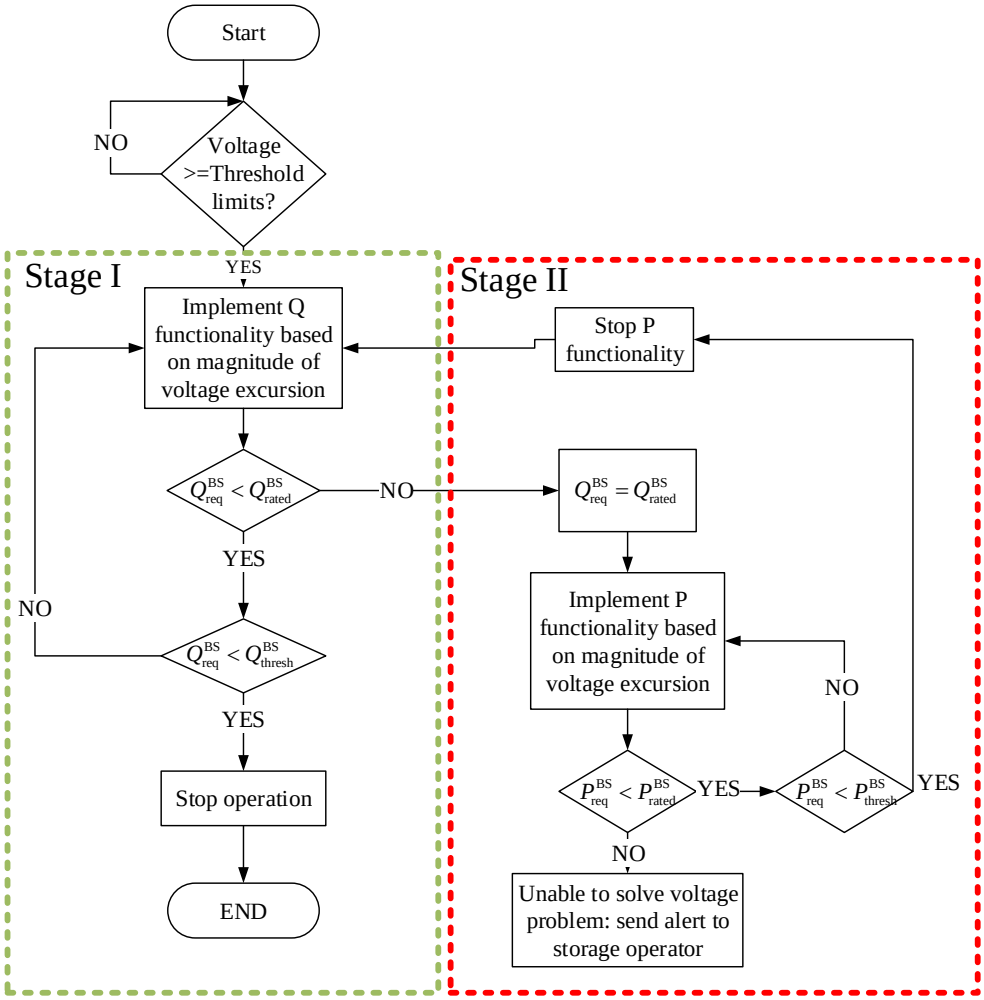

Figure 6-7: Flowchart of the energy storage active/reactive power control strategy for voltage regulation

In addition, active and reactive power threshold values, $P_{\text{thred}}^{\text{BS}}$ and $Q_{\text{thred}}^{\text{BS}}$, are set up in the proposed controller, in order to stop the operation of the controller if the PV output sharply reduces at the beginning of the cloud passing period. This can prevent the energy storage voltage regulation controllers charging the active/reactive power if the measured PCC voltage, $v_{\text{mead}}^{\text{PCC}}$, is below the defined threshold value, $v_{\text{thred}}^{\text{PCC}}$, or prevent the operation of the active power from the storage device if the reactive power compensation, $Q_{\text{req}}^{\text{BS}}$, is sufficient for voltage support. Therefore, if $P_{\text{req}}^{\text{BS}}$ is less than $P_{\text{thred}}^{\text{BS}}$, the active power controller will stop its operation and this action also forces controller from stage II back to stage I starting the reactive power compensation by using $Q_{\text{req}}^{\text{BS}}$. However, when the PV output decreasing happens during a sudden fluctuation in PV output (e.g. due to passing cloud), the voltage controller identifies that, $Q_{\text{req}}^{\text{BS}}$, is less than $Q_{\text{thred}}^{\text{BS}}$, and will commend a signal to stop the operation of the voltage regulation controllers.

Table 6.1 shows threshold values selected for the active and reactive power voltage regulation controllers in the test network. These values are selected and tuned based on experimentation. Firstly, the voltage threshold value, $v_{\text{thred}}^{\text{PCC}}$, is selected to avoid any overshoot caused by energy storage voltage regulation controller in regard with suddenly changing PV output. Secondly, both active power and reactive power threshold values, $P_{\text{thred}}^{\text{BS}}$ and $Q_{\text{thred}}^{\text{BS}}$, are selected as 2 kW/kVAr, this is because such values are relatively small for voltage compensation and the regulated PCC voltage are not to be violated if stop using the energy storage for voltage regulation.

Table 6.1: Threshold values selected in this work

Parameters	Value
Voltage Threshold $v_{\text{mead}}^{\text{PCC}}$	1.085 p.u.
Reactive Power Threshold for Stopping Reactive Power Controller $P_{\text{thred}}^{\text{BS}}$	2 kVAr
Active Power Threshold for Stopping Active Power Controller $Q_{\text{thred}}^{\text{BS}}$	2 kW

4 Description of case study and simulation results

To evaluate the effectiveness of the proposed active and reactive power control strategy for voltage support, two case studies are performed based on an

emulated step changing solar irradiance and measured real solar irradiance. The case study LV distribution network is described in Chapter 5 and illustrated in Figure 5-2. This network is simplified from the real radial residential distribution network as shown in Figure 4-5.

To present the worst scenario of voltage excursion, it is assumed that the step changed PV profile is applied for the first case study as illustrated in Figure 6-8, and the load profile is a constant power load of 30kW/5kVAr. The step changed PV profile is sufficient for initial investigation of the effectiveness of the control strategy, including transition from reactive power control (step I) to active power control (step II) as shown in Figure 6-7, and the dynamic response of the proposed controller.

To implement the proposed control strategy under a real situation, measured real solar irradiance between time periods 11:00 and 11:30 from 06 June 2011 is selected (see Figure 1-5 (b)) and applied in the second case study. The profile is simulated with a 0.5 seconds time step instead of 6 seconds a date change from the original data profile. This compresses the simulation time as 152 seconds and reduces of the computer memory overhead. This also has the benefit of making the solar generation more variable to further test of the controller. It is assumed that there are 106 domestic loads of which 80 have PV generators. The real solar profile selected has a highly fluctuating output (see Figure 6-9) which is used here to understand the effectiveness of the proposed controller for mitigating voltage fluctuation and voltage support under real extreme conditions. As shown in Figure 6-9, the peak solar irradiance with a fluctuating generation characteristic happens between the time period 60s and

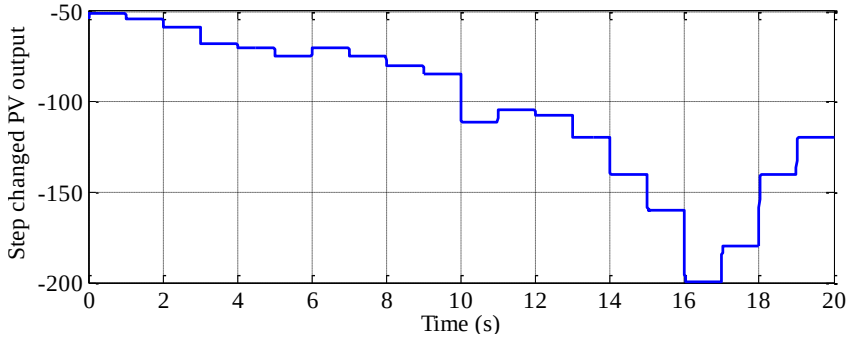

Figure 6-8: Step changed PV profile applied for first case study [note that the time axis has been compressed to the time represented in the simulation]

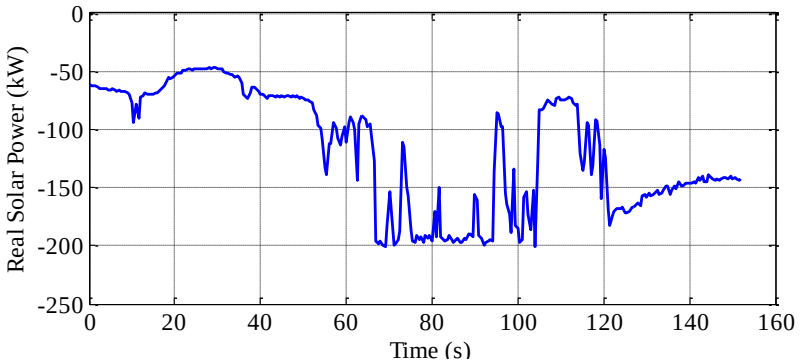

Figure 6-9: Real solar irradiance PV profile applied for second case study [note that the time axis has been compressed to the time represented in the simulation

110s of the simulation. Overvoltage and voltage fluctuation are likely to occur during this time period. In addition, the average load profile is selected from the period 11:00-11:30 as shown in Figure 1-5 (a). The load profile is simulated as 10s a data change instead of 2 minutes a date change from the original load profile.

Furthermore, a design decision is taken to make the energy storage rated active power, $P_{\text{rated}}^{\text{BS}}$, 150kW for using active power only for voltage support. As previously discussed, if the reactive power is applied for voltage support, the converter apparent power rating with a 30% reduction of rated active power is a good choice for voltage support in the case study LV distribution network. The increased reactive power capability is 71.41% of the rated active power at 150kW for 30% reduction. Therefore, the $Q_{\text{req}}^{\text{BS}}$ is equal to 107.12 kVAr and $P_{\text{rated}}^{\text{BS}}$ is equal to 105kW.

4.1 Case study 1: Step changed solar irradiation

Under step changed solar irradiance, the power exchange of proposed control strategy and active power control only for voltage support is illustrated in Figure 6-10. The time sequence of power exchange with the proposed control method and active power control only is summarised as follows.

1. During time interval T1, there is no measured PCC voltage, $v_{\text{mead}}^{\text{PCC}}$, which violates the predefined voltage threshold, $v_{\text{thred}}^{\text{PCC}}$, (1.085p.u.). Therefore, no command is needed to operate the controller for voltage support.

2. During time interval T2, the controller detects the measured PCC voltage, $v_{\text{mead}}^{\text{PCC}}$, is over the voltage threshold, $v_{\text{thred}}^{\text{PCC}}$.
    - The proposed active and reactive power controller firstly operates reactive power control mode from stage I to bring the PCC voltage at threshold. As indicated in Figure 6-10 (c), the reactive power is gradually increased to 63kVAr because of increased PV output. In comparison, applying active power control only consumes much less required active power than the required reactive power (see Figure 6-10 (b-c). This shows that active power is much sufficient

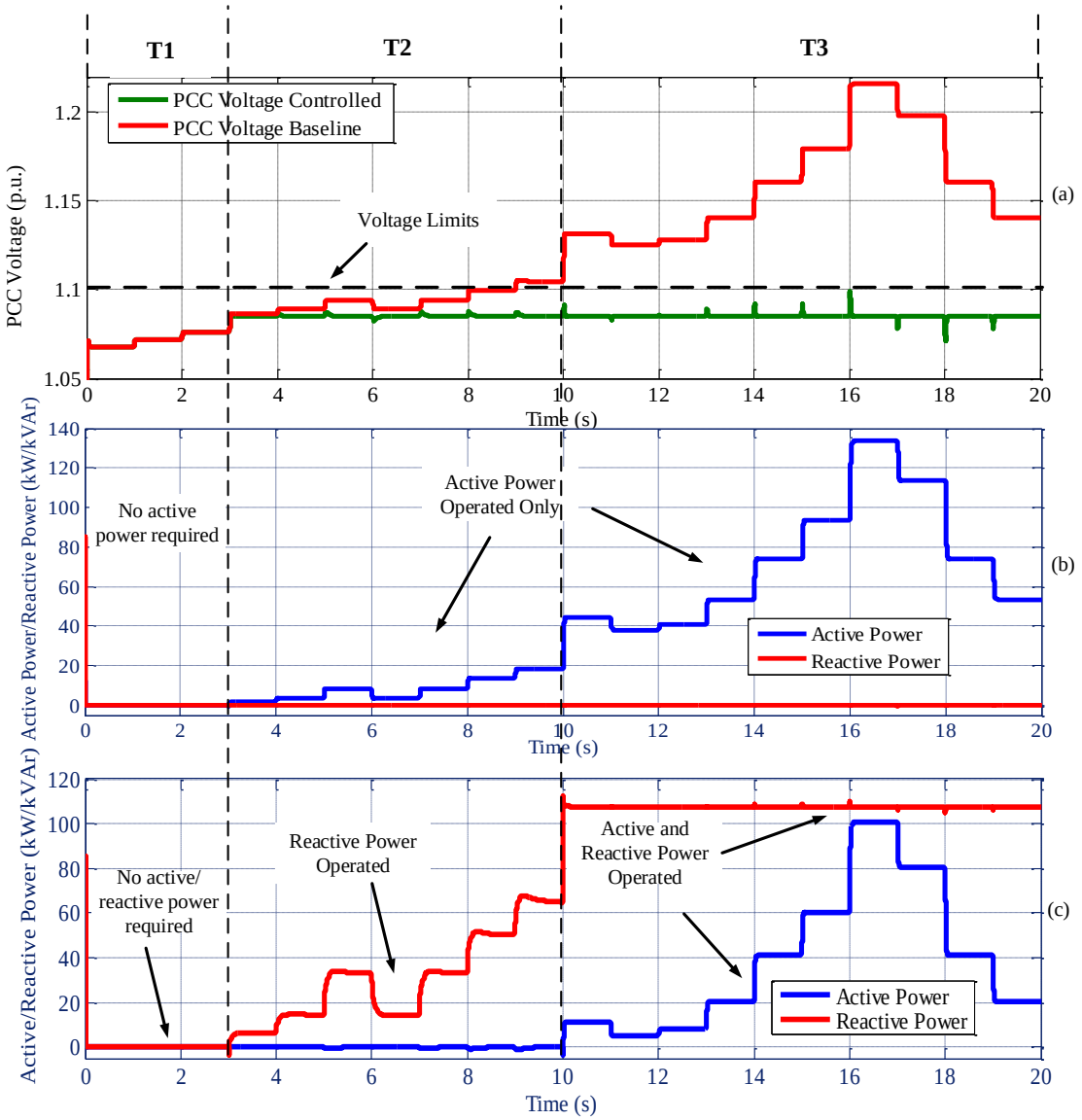

Figure 6-10: Simulation results of proposed voltage regulation controller for voltage support under step changed solar irradiance (a) Voltage controlled by voltage regulation controller compared with baseline voltage (b) Voltage regulation by using active power solely imported to the energy storage (c) Proposed active/reactive power control strategy for voltage regulation

than the reactive power for voltage support in LV distribution network. In addition, the impact of the reactive power mode from the proposed control strategy and active power control only on the PCC voltage is the same (see Figure 6-10 (a))

3. During time interval T3, since the PV output sharply increases to 110kW, the capability of required reactive power, $Q_{\text{req}}^{\text{BS}}$, is insufficient for voltage support.
    - The proposed controller switches the control mode from reactive power control at stage I to active power control at stage II, while the reactive power continues operating at its rated maximum value $Q_{\text{rated}}^{\text{BS}}$as illustrated in Figure 6-10 (c).
    - According to Figure 6-10 (b) and (c), the active power control only is consumed more required active power (up to nearly 140kW) for voltage support compared with the proposed control method (up to 100kW). This implies that the capability of active power from the storage can be reduced with the same converter size for voltage regulation in proposed strategy.

4.2 Case study 2: Real solar irradiations

The effect of the control strategy for voltage support under a real solar irradiance profile is evaluated in case study 2. Simulation of the proposed control method compared with active power control only for voltage support for this case study is illustrated in Figure 6-11. The energy storage power exchange is summarised as follows.

1. During time interval T1, the PCC voltage, $v_{\text{mead}}^{\text{PCC}}$, is below the predefined threshold value, $v_{\text{thred}}^{\text{PCC}}$. As a result, there is no command to start operation of the storage device.
2. During time interval T2, the PCC voltage, $v_{\text{mead}}^{\text{PCC}}$, is slightly violated the predefined threshold.
    - The proposed controller operates its reactive power functionality from stage I to allow the minor voltage excursion to be solved without using the limited energy store.

- A small proportion of required active power, $P_{\text{req}}^{\text{BS}}$, is imported to tackle the voltage excursion by for the active power only control (see Figure 6-11 (c)). This affects the usage of the limited energy store as seen by Figure 6-12. The SoC for the active power control only is increased to 20.2%. In addition, the proposed controller detects, $Q_{\text{req}}^{\text{BS}}$, is less than $Q_{\text{thred}}^{\text{BS}}$, at 13s, and the energy storage therefore stops operation as indicated in Figure 6-11 (e).

3. During time interval T3, there is no PCC voltage, $v_{\text{mead}}^{\text{PCC}}$, violation. Therefore, no command signals are sent to operate the energy storage for voltage support.
4. During time interval T4, there is voltage fluctuation due to fluctuation PV characteristic as seen by Figure 6-11 (a). The fluctuating voltage sharply increases and decreases happen at 63s and 95s respectively.
    - The proposed active and reactive power controller detects that the PCC voltage, $v_{\text{mead}}^{\text{PCC}}$, is beyond the voltage threshold at 49s. Therefore, the reactive power control mode is operated first to import the required, $Q_{\text{req}}^{\text{BS}}$, to maintain the PCC voltage at the threshold value (1.085p.u.). However, the required reactive power, $Q_{\text{req}}^{\text{BS}}$, is greater than the rated reactive power, $Q_{\text{rated}}^{\text{BS}}$, at time 51s. This means that the reactive power functionality is not sufficient for voltage support. The controller therefore makes a transition from stage I to stage II to apply the active power control functionality for regulating the PCC voltage, while the reactive power continues at its maximum rated power, $Q_{\text{rated}}^{\text{BS}}$. The proper tuned control parameters for the active/reactive power controller have fast response with overshoot less 0.55%. As such, the voltage fluctuation and voltage rise are reduced and the PCC voltage, $v_{\text{mead}}^{\text{PCC}}$, is maintained at 1.085p.u. as illustrated in Figure 6-11 (b).
    - The impact of the proposed controller and active power control only on the PCC voltage is similar (see red line and green line from Figure 6-11 (b)). Please note that there is a sharply decrease

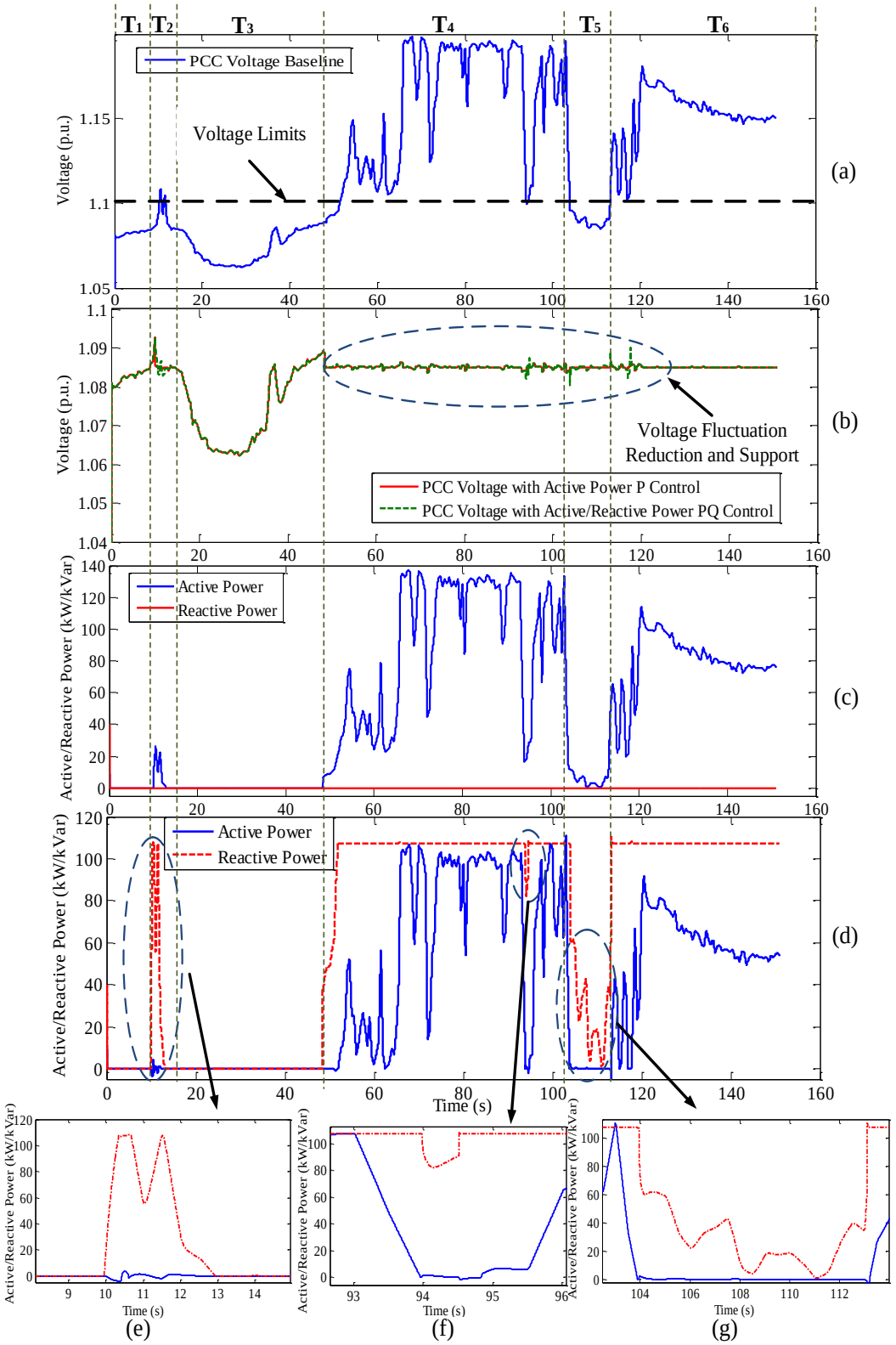

Figure 6-11: Simulation results of proposed voltage regulation controller for voltage support under real solar irradiance (a) Baseline voltage (b) PCC voltage profiles with active power control only and with proposed active/reactive power control strategy (c) Voltage regulation by using active power solely (d) Proposed active/reactive power control strategy for voltage regulation (e) Close look of reactive power performance at time period T2 (f) Close look of reactive power performance at time period T4 (g) Close look of reactive power performance at time period T5

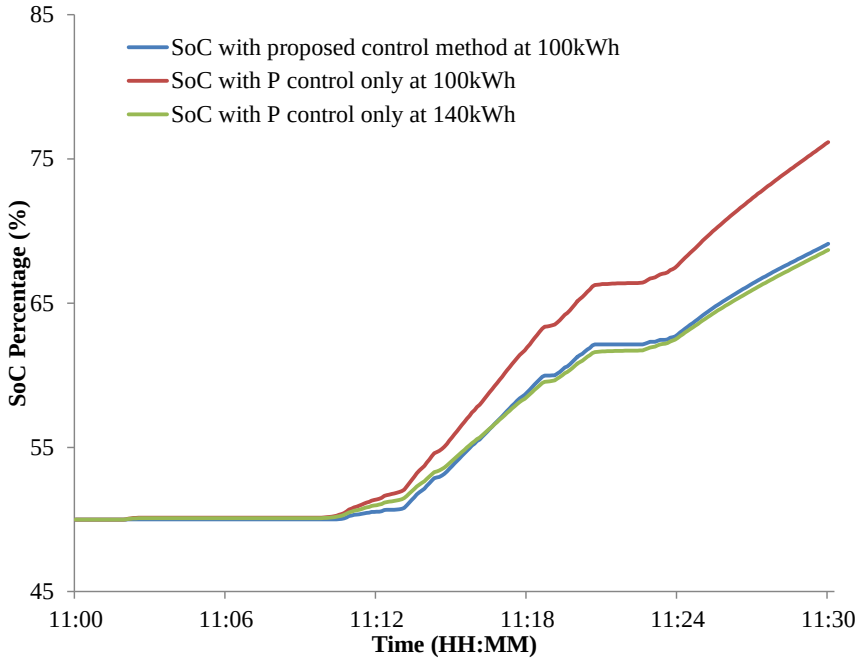

Figure 6-12: Comparison with SoC under active power control only and proposed active/reactive power control

and increase of the PV output at time 94s and 95. This requests the controller to suddenly make a transition from stage II to stage I to use reactive power functionality (see Figure 6-11 (f)).

The controller detects the required active power, $P_{\text{req}}^{\text{BS}}$, is less than the active power threshold, $P_{\text{thred}}^{\text{BS}}$, at time 104s from T5. Accordingly, the active power controller stops operation and the reactive power controller starts operation for voltage support as seen by Figure 6-11 (g). However, the controller identifies that the reactive power functionality is insufficient to maintain the PCC voltage at the threshold value at time 113s. As a result, the active power is commanded from the controller as shown in time interval T6.

4.3 Energy storage state of charge

Figure 6-12 illustrates state of charge (SoC) under both the active power control only and proposed control strategy. It can be seen that the proposed control method reduces energy usage compared to the active power control only. This control can therefore be concluded to reduce the cost of the energy store. Due to the high charging rate, the size of the energy storage device would be designed to be bigger based on the active power control only. As illustrated in Figure 6-12, active power control requires 140kWh capacity to have similar

performance as the proposed control method with capacity 100kWh. This is a 40kWh capacity saving (28.57% saving) for the energy storage used in this case study. It can be concluded that by reduction 30% of rated active power $P_{\text{rated}}^{\text{BS}}$, the low charging rate can be applied for the use of the energy storage with the proposed control strategy. The energy storage device size is reduced significantly, while the size of the energy storage converter is maintained the same. As a result, this can reduce operating and replacement costs for the energy storage owner, but provide the same performance for voltage support.

5 Discussion of Results

An investigation of how to implement active and reactive power of energy storage for voltage support in regard with small signal stability analysis is presented. It is found that sharing the converter apparent power rating with a 30% reduction of rated active power $P_{\text{rated}}^{\text{BS}}$ and corresponding increased reactive power capability $Q_{\text{rated}}^{\text{BS}}$for is a good choice for voltage support in the case study LV distribution network. A sensitivity analysis of system stability shows that using active and reactive power of energy storage for voltage support is not a major factor affecting system stability. The model of induction motors is not considered and is included to the system model. This might be useful to consider with large amounts of inductive loads in LV networks (fridges, heat pumps etc.) or commercial/industrial networks with rotating machines. Therefore, low electromechanical oscillatory frequency is not presented in the eigenvalue analysis. However, the system model has great potential to comprise any induction motors for future study.

An active and reactive power control method of the energy storage unit for voltage support is proposed. This is shown to effectively reduce the usage of the active power from the energy storage, which can reduce operating and replacement costs for the energy storage owner whilst still providing the same performance benefit. In addition, this method greatly improves the performance of decentralised controller presented in Chapter 4 by minimising the active power requirement for voltage support and smoothing the variation voltage caused by fluctuated PV generator. This method has a great potential to be adapted to the coordination control method presented in Chapter 4.

6 Summary and Conclusion

This chapter presents a method to implement active and reactive power of storage units for voltage support. An evaluation of active and reactive power setting of energy storage for voltage support is presented. Therefore, a 30% ratio of rated active power reduction is selected. A small signal stability analysis based on 30% of rated active power reduction is carried out. It is stated that using active and reactive power of the energy storage for voltage support is not the main factor to cause system stability issues. Finally, a method based on the ratio selected is proposed to control active and reactive power of energy storage for voltage support with reactive power priority. This method can efficiently reduce the requirement of active power for voltage support. The energy storage device size is reduced, while the size of the energy storage converter is maintained the same. As such, the cost of the energy storage can be reduced.

Chapter 7: Discussion, Conclusions and Further Research

1 Discussion

This dissertation has considered how to operate energy storage for voltage support in a future LV distribution network with large amounts of low carbon technologies, such as PV. This has been carried out by evaluating different control methodologies for the energy storage for voltage support in both steady state and dynamic analysis. The primary aim of these control methodologies is to provide a detailed assessment of regulating voltage with single or multiple energy storage installed in the LV distribution network. A model of a real LV distribution network provided by Electricity North West Limited is used in this work to evaluate different proposed control methodologies. By applying to real networks, it is aimed to be of more practical and theoretical benefit to DNOs.

The discussion that follows describes this work contribution to high and low level control, modelling and analysis, and the tools needed for this study of energy storage for voltage support. The combination of these enables conclusions to be formed.

1.1 Control

There are two control levels, namely high level control and low level control, considered in this work.

- High level control refers to coordinated and non-coordinated control strategies of storage units for addressing the voltage problem.
- Low level control is associated with the detailed design of energy storage controllers. This is composed of external voltage regulation controllers, inner current decoupling controllers, and voltage feedforward controllers.

These two control levels are both important factors for the performance of addressing overvoltage and energy storage itself aging degradation condition. These two control levels are now discussed.

1.1.1 High level energy storage control

High level control for the single or multiple energy storage units has presented in Chapter 2 and 3. This comprised using energy storage in a smart grid

laboratory to provide voltage support, presenting coordinated control of the single storage unit with the OLTC of the transformer for voltage support, and developing a novel coordinated control of multiple energy storage units in the LV distribution network. These works have published in conference and IEEE transaction on smart grid.

1.1.2 Single energy storage control

Single energy storage control can be either one energy storage unit using its local measurement to control its charging and discharging function or the storage unit is operated cooperatively with other technologies, such as OLTC.

Using the energy storage from the smart grid laboratory for voltage support is examined and presented in Chapter 3. This case study is based on real time power hardware in the loop system to investigate the characteristics of the energy storage for regulating voltage. The use of high resolution generation and demand data in real time allowed a detailed study of the condition of the network and the storage unit. This has been used for evaluating the feasibility of interventions in real networks provided by DNOs. The use of energy storage from the smart grid laboratory can bring the magnitude of the voltage within statutory limits, and enables fluctuated voltage to be smoothed (The voltage stand deviation is mitigated by 84%). In addition, the voltage unbalanced factor has been reduced to legally acceptable levels (less than 1.3%).

There are several practical limitations need to be considered with this study. Real time power hardware in the loop simulation studies can provide high level of detail. However, stable operation and accurate results are an important concern and challenge when performing the power hardware in the loop simulation [207]. These are dependent on the simulation step size and interfacing algorithm [207]. Therefore, future work could consider developing stabilisation methods, such as hardware inductance addition and feedback current filtering for stabilising the unstable interface [207][208]. Doing this is complex because these methods are less developed and these may be suitable for certain smart grid laboratory operating conditions. However, this may be meaningful as the accurate power hardware in the loop systems can provide a thorough recognition of the performance of energy storage in real time. This

also provides the capability for scholars and energy storage manufacturers to simulate large systems where components cannot be suitably modelled to be included as hardware.

The power available from the smart grid laboratory is limited. This is because the size of the inverter and power amplifier. As such, the storage model built from the RTDS simulation platform may also needed. This may alleviate the effects from the power hardware in the loop simulation.

The DNO in the northeast England had specified a preference to locate energy storage unit at the substation. Therefore, a collaborative work was performed to develop a coordinated control of the energy storage with OLTC of the secondary transformer for voltage support and reverse power flow reduction for the future distribution network where large LCT loads and high connection of PV generators are included. This method can help the DNO to effectively relieve transformer overload and mitigate voltage excursions (see Figure 3-14 to Figure 3-18). In the future, multiple energy storage could be installed with network as the cost of storage may be reduced. Therefore, the method for multiple storage devices implementation cooperatively with the OLTC or other technologies, such as DSR are needed to be included the future. This is evidenced by the energy storage trials summarised in Table 2-2.

1.1.3 Multiple energy storage control

Building on the premise that multiple energy storage units might be located within a network, a control strategy for coordination of multiple energy storage for voltage support in an LV distribution network is investigated and presented in Chapter 4. This method is novel in that the control methodology is based on the voltage sensitivity factor and a battery aging model to coordinate the use of multiple energy storage for voltage support. The proposed controller gives parameters that influence which storage devices are selected to provide strict maintenance of voltage limits. Therefore, battery aging analysis is included to modify the system's selection behaviour in response to battery degradation while consistently maintaining voltage limits. In this work, the coordinated and non-coordinated control methods are implemented to evaluate their effectiveness for preventing overvoltage. This shows that the coordinated

control requires smaller power rating (25kW) and energy rating (50kWh) for the energy storage at the network location with the most severe voltage deviations.

This control method provides DNOs with understanding of how to control multiple storage units for voltage regulation in their LV distribution networks if several storage devices are installed in the future.

This control method also allows voltage support to continue if one of the storage units fails. This is due to the fact that other storage units can be automatically called to solve the voltage excursion at the location of the failed unit.

In addition, the location of storage units has significant effects on the ability of units to support each other. If the DNO can install energy storage units closer to the position of worst voltage constraint, the greater the ability to support. However, since the space constraints or the need to provide support to different parts of the LV distribution network, it is seen that the DNO locating storage units closer may not always be feasible.

As further PV systems are added to the network, the voltage deviation location and severity may vary. The system may have greater potential to adapt to the changes in location of extra PV generators by using such control methodology.

The undervoltage problem is not presented in this work for coordinated control of multiple energy storage units, since the LV secondary transformer fixed tap position was set to prevent undervoltage. However, the method can be adapted to achieve solving undervoltage excursions if the peak demand, such as installation of EV or HP, is increased in the future. This can be achieved by mirroring the overvoltage control with thresholds for undervoltage and by discharging rather than charging the energy storage units.

Control of multiple energy storage is detailed in [205] and also in Chapter 4, in which three phase DNO owned storage is studied in LV networks. The method is equally applicable for single phase energy storage in residential homes- however the regulations surrounding the DNO relationship with consumers might make this difficult in the UK.

1.2 Low level control

Low level control in this work has considered designing detailed controllers which are used for charging and discharging of energy storage for voltage support. Simulations have been completed in the time domain.

1.2.1 Voltage sensitivity factor

Voltage sensitivity factor is employed for designing active and reactive power voltage regulation controllers as shown in Figure 4-2 and described in Chapter 4. The voltage sensitivity factor based voltage regulation controllers are governed by voltage threshold values. These threshold values are determined based on DNOs' over and under-voltage tolerance and the ramp rate of changes in solar irradiance. The work presented in Chapter 4 uses conservative parameters for voltage upper, middle and lower thresholds. However, these values could be tuned to reduce the energy storage import and export of both active and reactive power. As the threshold values are narrowed there is a trade-off between the power and energy requirement and the risk of overvoltage. Using such voltage sensitivity factors for voltage regulation controllers is positive for steady state analysis based real time simulation. However, it may be negative for the network during small/large disturbance as the network operating condition changes [162]. Under such conditions, the Jacobian matrix has to be recalculated so that the new voltage sensitivity factor can be obtained. On the other hand, online recalculation of the voltage sensitivity factor matrix is problematic in distribution networks, where the level of on-line information available is much less than that at the transmission level [162].

To obtain a better performance of energy storage charging/discharging functions for voltage support and minimise the usage of energy storage power and energy requirement, a PI controller has been investigated for voltage regulation controllers.

1.2.2 PI regulator

A PI controller is a process of feedback control [209], and it is able to make better adjustments for voltage support according to appropriately turned control parameters. However, the parameters of the PI controller should be properly

designed and turned with fast response time and without causing system instability based on system transfer function. Therefore, the linearized mathematical state space model is introduced in Chapter 5 to select the proper control parameters for voltage regulation controllers without causing stability issues according to eigenvalue analysis.

1.3 Modelling and Analysis

The steady state model and dynamic model are used and applied for different purposes in this thesis.

The steady state model is used to evaluate the performance of proposed high level controller without considering the system dynamics introduced by energy storage controller or PV generators.

A dynamic model of the system is constructed based on ordinary differential equations to determine the range of energy storage voltage regulation control parameters without causing a system stability issue, and to evaluate whether implementation of energy storage unit for voltage support can reach the system stability margin.

1.4 Steady state modelling and analysis

At the beginning of this research project, steady state modelling was constructed to assess and verify the performance of the high level controllers. This is because high level controllers are required to perform simulations of a network under many hours of real world operation. As stated in Chapter 3 and 4, energy storage and PV based on classical DQ decoupling control are needed to construct inner current decoupling controllers although voltage regulator based on PI regulator are not introduced at this stage. In addition, a phase locked loop is required to recognise the locked frequency of the energy storage and PV generator to that of the utility system to ensure precise synchronisation. Such a model is operated without considering outer loop controller dynamics, and it is suitable for long time simulation. This type of model is used in Chapter 3 and Chapter 4 to evaluate the dynamic performance of the proposed high level controllers over one day of real word application. This work is performed in a real time digital simulator and built in RSCAD. In addition, collaborative and comparative work was performed using a MATLAB/OpenDSS model to

investigate the benefits of the aging model over a ten year period as shown in Chapter 4. These steady state models are not able to provide any information for system dynamic stability analysis. Therefore, the dynamic model of the system has to be constructed.

1.5 Dynamic modelling and analysis

Because of a significant presence of PV generators and energy storage in the near future, the LV distribution network cannot be considered as passive. The large increase in connection of PV generation or energy storage has a large influence on power system dynamics. Therefore, system stability issues in the future may be an important concern of DNOs. A systematic linearized state space model of a LV distribution network that includes the PV generator, energy storage unit, network line impedances and static load is introduced and constructed in Chapter 5. This model is used to perform eigenvalue sensitivity analysis to define the range of energy storage voltage regulation controllers' parameters, and to explore whether an energy storage system exchanging active and reactive power with the grid for voltage support can reach the system stability margin which is presented as Chapter 6. There are no synchronous generators and induction motors considered in the system design, which present low electromechanical oscillatory frequency at the range of 0.1 to 2Hz [202][159] and [204]. As such, no low oscillatory frequency modes are observed in this work. However, it is possible for the model presented in this work to comprise any synchronous generators and induction motors for future study.

In addition, characteristics of the storage system itself, such as battery modelling and its dynamics, are not considered in this part of the thesis. This is because this work mainly focuses on the impact of the stability margin of energy storage power exchange with the grid, and energy storage control parameters. In the future, the state space model produced by this work can be supplemented with dynamic modelling of the battery itself for comparing different energy storage designs on the system stability margin.

An investigation of how to implement active and reactive power from the energy storage in regard with small signal stability is presented in Chapter 6. It illustrated that sharing the converter apparent power rating with a 30%

reduction of rated active power and corresponding increased reactive power capability for is a good choice for voltage support in the case study LV distribution network

The eigenvalue sensitivity analysis concluded that applying active and reactive power from energy storage for voltage support is not a major important factor influencing the small signal stability of the LV distribution network. Further, a novel active and reactive power control strategy for voltage support is proposed. This control method can reduce the energy storage active power requirement by using an increased proportion of reactive power for voltage support. Thus, the energy storage capacity can be reduced to 28.57%. In addition, this method has significantly improved the performance of decentralised control strategy presented in Chapter 4 by minimising the usage of energy storage power and energy requirement, and smoothing the voltage fluctuation caused by the sudden change of PV generation.

There are additional factors, such as power loss and harmonic injection, which may affect the proposed operation control strategy for voltage support. In addition, the detailed mathematical model of induction motors can be included in future work investigating the system stability margin. This is because such induction motors are a source presenting low electromechanical oscillatory frequency [204]. The eigenvalues may be sensitive to motor dynamics which may have an effect on defining the use of active and reactive power from the energy storage. For example, absorbing active and reactive power from the energy storage would result in dominant eigenvalue migrating to right hand plane when motors are introduced in the study: potentially resulting in the system instability. In which case, more system damping would need to be included within the energy storage controller design.

In addition, multiple energy storage devices and PV generators can be included in forming the state space model in the future. This requires modelling reduction techniques to reduce the system complexity as stated in [198]. This is due to the fact that the system order with one storage unit and one PV generator in the LV distribution network presented in Chapter 5 has reached to 34 orders. It would be complex to derive the state space model that contains several storage units and PV generators.

1.6 Tools

1.6.1 RTDS

RTDS is a real time digital simulator and can provide capability for continuous real time simulation [164]. This enables users to be productive by completing many power system studies efficiently [210]. The RTDS contains many types of processor cards, communication modules and signal channels [210]. An Ethernet is applied to provide the link between the hardware and RSCAD which is an interface for RTDS simulator hardware [207]. RTDS allows implementation of the close loop testing of the physical equipment, such as energy storage. In addition, the processor card of RTDS in a smart grid laboratory which contains 90 nodes for single phase and allows network solution to be solved in one rack [169]. Another processor is required for solving power system components, such as transformers, generators, voltage source converters when performing a power system simulation. The RTDS used in the smart grid laboratory includes two racks with six PB5 processor cards. This means that it is not possible to simulate anything other than simple LV network. Therefore, a simplified LV distribution network model was used for case studies in Chapter 3 and Chapter 4.

To realise the proposed coordination controller in a real word application, power hardware in the loop simulation can be used in conjunction with the modelled network. To do so, the proposed controller can be constructed in RSCAD and several energy storage units can be installed in smart grid laboratory. As discussed in section 1.1.1 Chapter 7, stabilisation algorithms have to be developed to obtain accurate results and stable operation when performing the power hardware in the loop simulation.

1.6.2 MATLAB/Simpower

MATLAB/Simpower provides a capability for simulating power system, and modelling power system components for both steady state and dynamic analysis [211]. The state space equation (see equation 5.73) derived in Chapter 5 was constructed in MATLAB, and Simpower to provide operating points for eigenvalue analysis using load flow. Simpower with the MATLAB control toolbox is able to provide capability for power system controller design under frequency

and time domain analysis. This has been done by designing parameters for energy storage voltage regulation controllers. The RTDS is not able to provide such capability. Although there are no nodes limitation in Simpower simulation environment, large detailed power system modelling which contains power system components and control system is difficult to implement in Simpower. This is because of the computer memory overhead, and long simulation times. Future work can consider of how to integrate MATLAB/Simpower and RTDS. This can provide feasible solution to simulate the power system by using both advantages from RTDS and MATLAB/Simpower, as RTDS performs as real time simulation, whereas MATLAB/Simpower can provide capability for controller design. This can be beneficial to both high level and low level controller design.

1.7 Summary of discussion

The discussion has concentrated on control levels, and modelling and analysis for the use of energy storage for voltage support. It presented coordinated control strategies for single or multiple energy storage units for voltage support in the LV distribution network. High level control strategies can be formulated that adapt to changes in PV locations and load growth. This is important for DNOs understand how to control and deploy energy storage in their network. Low level control strategies are introduced and compared. Voltage sensitivity factor is useful for steady state analysis, but it is not desirable for application during small disturbances as the network operating condition changes. Therefore, a proportional integral regulator can be employed to make better real time adjustment for voltage support. On the other hand, the PI controller should be properly designed and turned with fast response time and without causing system instability.

A discussion surrounding modelling and analysis was then completed. This considers whether steady state model is suitable for evaluation the performance of high level controllers without considering the system dynamics. However, dynamic model is formulated to determine the range of energy storage voltage regulation control parameters, and to evaluate whether power exchange of the energy storage with the grid can reach the system stability margin.

A discussion between the RTDS and MATLAB/Simpower are finally accomplished. This discussed advantages and disadvantages of RTDS and MATLAB/Simpower for power system simulation and modelling. The future work can be included regarding how to integrate MATLAB/Simpower and RTDS by considering their capabilities to power system simulation.

2 Conclusion

This dissertation investigated control strategies for single or multiple energy storage units for voltage support in the LV distribution network.

Two functional strategies for use of the single energy storage unit in smart grid laboratory for voltage support are introduced. The first strategy examines the performance of lab based energy storage for voltage support. It stated that using active power from single phase energy storage can effectively bring the voltage within regulatory limits, and enable voltage unbalance to be reduced within statutory limits. The second strategy is proposed for coordinating the energy storage unit with an OLTC for voltage excursion management and to reduce reverse power flow. This method is an alternative to upgrading network infrastructure. These works have published in conference as [212] and [213].

A method for controlling multiple energy storage units for voltage support in the LV distribution network is proposed. By considering voltage sensitivity factor and a battery aging model, an operational matrix is formed to select the preference order of energy storage units to provide strict maintenance of voltage limits. It has shown that voltage problems can be solved by sharing power and energy between storage units, while voltage excursions cannot be regulated within the statutory limit by using the non-coordinated control strategy. The rated power and energy of the storage unit can be reduced by using the proposed method. The scheme uses storage units more evenly and therefore reduces the costs of battery replacement to the storage operator in terms of both number of batteries and maintenance visits. This is a novel finding available in published work by the author [205].

A systematic linearized state space model is then introduced and constructed. This model is used to perform eigenvalue sensitivity analysis to define the range of energy storage voltage regulation controllers' parameters, and to investigate

whether energy storage exchanging active and reactive power with the grid for voltage support can reach the system stability margin. This considers practical application for the use of energy storage, and it demonstrates that control parameters of PI regulator are necessary to maintain dynamic performance of energy storage.

In addition, a study for utilising active and reactive power of the energy storage for voltage support is presented. It indicated that sharing the converter apparent power rating with a 30% reduction of rated active power and corresponding increased reactive power capability for is a good choice for voltage support in the case study LV distribution network. Performing eigenvalue sensitivity analysis found that applying active and reactive power from energy storage for voltage support is not a major factor influencing the small signal stability of the LV distribution network. Using the proposed active and reactive power control strategy for voltage support can significantly reduce the energy storage active power requirement to 100kW. Therefore the energy usage can be reduced. Such considerations are important to make practical application of the LV energy storage more cost effective for practical installation by DNOs.

3 Further research

A number of further research directions can be obtained by the contribution of this thesis. This section presents the further research that can be carried out. This could contribute benefits for future coordinated and non-coordinated control of energy storage for voltage support projects.

- Voltage unbalance has been reduced by single phase energy storage unit from smart grid laboratory as discussed in Chapter 3. Voltage unbalance compensation can also be achieved by operating three phase energy storage unit based on its synchronous (dq) reference frame control method for its converter. This can be done by methods described as [214][215] that can be included in future work. In [214], a negative sequence voltage compensator based on synchronous reference frame rotating in the opposite direction against the positive sequence is proposed to regulate the negative sequence load current. As such, the voltage unbalance from unbalanced load can be reduced [214]. As

indicated by [215], DGs are controlled as a negative sequence conductance and operated in the synchronous reference frame to compensate voltage unbalance in the micro-grid [215]. In addition, the negative sequence conductance is generated based on the negative sequence reactive power, and it is used to produce the reference current for voltage unbalance compensation [215].

- Multiple energy storage units could be installed with network as the cost of storage may be reduced in the future. Therefore, the proposed coordinated method for multiple storage devices implementation cooperatively with the OLTC or other technologies, such as DSR are needed to be included the future.
- There are no synchronous generators and induction motors are included in the system design. Therefore, no low oscillatory frequency modes are observed in this work. However, such generators can present low electromechanical oscillatory frequency at the range of 0.1 to 2Hz [159][202] and [204]. As such, the further research can consider comprising synchronous generators and induction motors for the model presented in this work.
- This work mainly focuses on the impact of the stability margin of energy storage power exchange with the grid, and energy storage control parameters, the characteristics of the battery storage system itself (such as battery modelling and its dynamics), are not introduced in this part of the thesis. The state space model produced by this work can be supplemented with dynamic modelling of the battery itself for further investigation of energy storage to power system stability. For example, in [216], a model was produced which included the battery dynamic characteristic and converter equivalent circuit is presented to examine the effect of its dynamic behaviour on the power system dynamic stability. The eigenvalue analysis is performed and shows the battery storage with a designed first order lead-lag controller can significantly improve the system damping [216]. This can be as an auxiliary service to power system.
- Although real time power hardware in the loop simulation studies are capable of offering high level of detail, stable operation and accurate

results are an important concern and are reliant on the simulation step size and interfacing algorithm [207]. The future work could consider developing stabilisation methods, such as hardware inductance addition and feedback current filtering for stabilising the unstable interface [207][208]. However, this may be complex as these methods are less developed and these may be suitable for certain smart grid laboratory operating conditions. This is important for achieving the accurate power hardware in the loop systems that can provide a thorough recognition of the performance of energy storage in real time.

- The application of power line communication (PLC) for energy storage control can be included in the future research work. The advantage of PLC is that it can implement communication tasks over the existing electrical infrastructure without a need for the wireless communication provided by telecommunication companies [217]. Such technology has been applied for communicating between the energy management system (EMS) and several battery management systems (BMS) through the DC power lines to optimise the battery lifetime and meet the requirement of the power grid [218]. In addition, the data (cell voltages and battery temperature) is exchanged between the EMS and the BMS through the PLC solution can take the advantage of the existing controller area network (CAN) protocol [218].

Appendix

A.1 Expanded form of matrices in Chapter 5

$$A_{cBS}=\begin{bmatrix}
-\frac{1}{T_v} & 0 & 0 & 0 & 0 & 0 & 0 & 0 & 0 & 0 & 0 \\
0 & -\frac{1}{T_v} & 0 & 0 & 0 & 0 & 0 & 0 & 0 & 0 & 0 \\
0 & 0 & -\frac{1}{T_v} & 0 & 0 & 0 & 0 & 0 & 0 & 0 & 0 \\
0 & 0 & 0 & -\frac{1}{T_v} & 0 & 0 & 0 & 0 & 0 & 0 & 0 \\
\frac{v_q^{oGBS}}{v_{rms}^{oGBS}} & -\frac{v_d^{oGBS}}{v_{rms}^{oGBS}} & 0 & 0 & 0 & 0 & 0 & 0 & 0 & 0 & 0 \\
\frac{v_q^{oGBS}}{v_{rms}^{oGBS}} & -\frac{v_d^{oGBS}}{v_{rms}^{oGBS}} & 0 & 0 & 0 & 0 & 0 & 0 & 0 & 0 & 0 \\
0 & 0 & 0 & 0 & 0 & 0 & -\frac{1}{T_i} & 0 & 0 & 0 & 0 \\
0 & 0 & 0 & 0 & 0 & 0 & 0 & -\frac{1}{T_i} & 0 & 0 & 0 \\
-K_{pqBS}\frac{v_q^{oGBS}}{v_{rms}^{oGBS}} & -K_{pqBS}\frac{v_d^{oGBS}}{v_{rms}^{oGBS}} & 0 & 0 & K_{iqBS} & 0 & -1 & 0 & 0 & 0 & 0 \\
-K_{pdBS}\frac{v_q^{oGBS}}{v_{rms}^{oGBS}} & -K_{pdBS}\frac{v_d^{oGBS}}{v_{rms}^{oGBS}} & 0 & 0 & 0 & K_{idBS} & 0 & -1 & 0 & 0 & 0 \\
0 & 0 & 0 & 0 & 0 & 0 & 0 & 0 & 0 & 0 & -K_{pllBS}K_{p\omega BS}
\end{bmatrix}$$

$$C_{GBS}=\begin{bmatrix}
0 & 0 & 0 & 0 & 0 & 0 & \frac{1}{T_i} & 0 & 0 & 0 & 0 \\
0 & 0 & 0 & 0 & 0 & 0 & 0 & \frac{1}{T_i} & 0 & 0 & 0
\end{bmatrix}^T$$

$$C_{GBS}^{v}=\begin{bmatrix}
\frac{1}{T_v} & 0 & 0 & 0 & 0 & 0 & 0 & 0 & 0 & 0 & -K_{pllBS}K_{i\omega BS}m_{qBS} \\
0 & \frac{1}{T_v} & 0 & 0 & 0 & 0 & 0 & 0 & 0 & 0 & -K_{pllBS}K_{i\omega BS}m_{dBS}
\end{bmatrix}^T$$

$$C^{vBS}=\begin{bmatrix}
0 & 0 & \frac{1}{T_v} & 0 & 0 & 0 & 0 & 0 & 0 & 0 & 0 \\
0 & 0 & 0 & \frac{1}{T_v} & 0 & 0 & 0 & 0 & 0 & 0 & 0
\end{bmatrix}^T$$

$$B_{GBS}^{v}=\begin{bmatrix}
0 & 0 & 0 & 0 & 1 & 0 & 0 & 0 & K_{pqBS} & 0 & 0 \\
0 & 0 & 0 & 0 & 0 & 1 & 0 & 0 & 0 & K_{pdBS} & 0
\end{bmatrix}^T$$

$$E_{cBS}^{v}=\begin{bmatrix}
-K_{piqBS}K_{pdBS}\frac{v_q^{oGBS}}{v_{rms}^{oGBS}} & -K_{piqBS}K_{pqBS}\frac{v_d^{oGBS}}{v_{rms}^{oGBS}} & 0 & 0 & K_{piqBS}K_{iqBS} & 0 & -K_{piqBS} & 0 & K_{iiqBS} & 0 & 0 \\
-K_{pidBS}K_{pdBS}\frac{v_q^{oGBS}}{v_{rms}^{oGBS}} & -K_{pidBS}K_{pdBS}\frac{v_d^{oGBS}}{v_{rms}^{oGBS}} & 0 & 0 & 0 & K_{pidBS}K_{idBS} & 0 & -K_{pidBS} & 0 & K_{iidBS} & 0
\end{bmatrix}$$

$$E_{uBS}^{v}=\begin{bmatrix} K_{piqBS}K_{pqBS} & 0 \\ 0 & K_{pidBS}K_{pdBS} \end{bmatrix}$$

$$A_{cPV}=\begin{bmatrix}
-\frac{1}{T_v} & 0 & 0 & 0 & 0 & 0 & 0 & 0 & 0 & 0 & 0 \\
0 & -\frac{1}{T_v} & 0 & 0 & 0 & 0 & 0 & 0 & 0 & 0 & 0 \\
0 & 0 & -\frac{1}{T_v} & 0 & 0 & 0 & 0 & 0 & 0 & 0 & 0 \\
0 & 0 & 0 & -\frac{1}{T_v} & 0 & 0 & 0 & 0 & 0 & 0 & 0 \\
-i_{d'}^{oGPV} & i_{q'}^{oGPV} & 0 & 0 & 0 & 0 & v_{d'}^{oGPV} & -v_{q'}^{oGPV} & 0 & 0 & 0 \\
-i_{q'}^{oGPV} & -i_{d'}^{oGPV} & 0 & 0 & 0 & 0 & -v_{q'}^{oGPV} & -v_{d'}^{oGPV} & 0 & 0 & 0 \\
0 & 0 & 0 & 0 & 0 & 0 & -\frac{1}{T_i} & 0 & 0 & 0 & 0 \\
0 & 0 & 0 & 0 & 0 & 0 & 0 & -\frac{1}{T_i} & 0 & 0 & 0 \\
-K_{pqPV}i_{d'}^{oGPV} & K_{pqPV}i_{q'}^{oGPV} & 0 & 0 & K_{iqPV} & 0 & K_{pqPV}v_{d'}^{oGPV}-1 & -K_{pqPV}v_{q'}^{oGPV} & 0 & 0 & 0 \\
-K_{pdPV}i_{q'}^{oGPV} & -K_{pdPV}i_{d'}^{oGPV} & 0 & 0 & 0 & K_{idPV} & -K_{pdPV}v_{q'}^{oGPV} & -K_{pdPV}v_{d'}^{oGPV}-1 & 0 & 0 & 0 \\
0 & 0 & 0 & 0 & 0 & 0 & 0 & 0 & 0 & 0 & -K_{pllPV}K_{p\omega PV}
\end{bmatrix}$$

$$C_{GPV}=\begin{bmatrix} 0 & 0 & 0 & 0 & 0 & 0 & \frac{1}{T_i} & 0 & 0 & 0 & 0 \\ 0 & 0 & 0 & 0 & 0 & 0 & 0 & \frac{1}{T_i} & 0 & 0 & 0 \end{bmatrix}^T$$

$$C_{GPV}^{v}=\begin{bmatrix} \frac{1}{T_v} & 0 & 0 & 0 & 0 & 0 & 0 & 0 & 0 & 0 & -K_{pllPV}K_{i\omega PV}m_{qPV} \\ 0 & \frac{1}{T_v} & 0 & 0 & 0 & 0 & 0 & 0 & 0 & 0 & -K_{pllPV}K_{i\omega PV}m_{dPV} \end{bmatrix}^T$$

$$C^{vPV}=\begin{bmatrix} 0 & 0 & \frac{1}{T_v} & 0 & 0 & 0 & 0 & 0 & 0 & 0 & 0 \\ 0 & 0 & 0 & \frac{1}{T_v} & 0 & 0 & 0 & 0 & 0 & 0 & 0 \end{bmatrix}^T$$

$$B_{GPV}^{v}=\begin{bmatrix} 0 & 0 & 0 & 0 & 1 & 0 & 0 & 0 & -K_{pqPV} & 0 & 0 \\ 0 & 0 & 0 & 0 & 0 & 1 & 0 & 0 & 0 & K_{pdPV} & 0 \end{bmatrix}^T$$

$$E_{21}^{N}=\begin{bmatrix} R_4 & \frac{X_4\omega_e}{\omega_b} \\ -\frac{X_4\omega_e}{\omega_b} & R_4 \end{bmatrix}\begin{bmatrix} 0 & 0 & 1 & 0 & 0 & 0 & 0 & 0 \\ 0 & 0 & 0 & 1 & 0 & 0 & 0 & 0 \end{bmatrix}$$

$$E_{22}^{N}=\begin{bmatrix} \frac{X_4}{\omega_b} & 0 \\ 0 & \frac{X_4}{\omega_b} \end{bmatrix}\begin{bmatrix} 0 & 0 & 1 & 0 & 0 & 0 & 0 & 0 \\ 0 & 0 & 0 & 1 & 0 & 0 & 0 & 0 \end{bmatrix}$$

$$D_{21}^{NBS} = \begin{bmatrix} -R_4 & -\dfrac{X_4\omega_e}{\omega_b} \\ \dfrac{X_4\omega_e}{\omega_b} & -R_4 \end{bmatrix}$$

$$\Delta x_{GBS} = \begin{bmatrix} \Delta i_q^{GBS} \\ \Delta i_d^{GBS} \end{bmatrix}$$

$$D_{22}^{NBS} = \begin{bmatrix} -\dfrac{X_4}{\omega_b} & 0 \\ 0 & -\dfrac{X_4}{\omega_b} \end{bmatrix}$$

$$\dot{\Delta x}_{GBS} = \begin{bmatrix} \dot{\Delta i}_q^{GBS} \\ \dot{\Delta i}_d^{GBS} \end{bmatrix}$$

$$D_{21}^{NPV} = \begin{bmatrix} -R_4 & -\dfrac{X_4\omega_e}{\omega_b} \\ \dfrac{X_4\omega_e}{\omega_b} & -R_4 \end{bmatrix}$$

$$\Delta x_{GPV} = \begin{bmatrix} \Delta i_q^{GPV} \\ \Delta i_d^{GPV} \end{bmatrix}$$

$$D_{22}^{NPV} = \begin{bmatrix} -\dfrac{X_4}{\omega_b} & 0 \\ 0 & -\dfrac{X_4}{\omega_b} \end{bmatrix}$$

$$\dot{\Delta x}_{GPV} = \begin{bmatrix} \dot{\Delta i}_q^{GPV} \\ \dot{\Delta i}_d^{GPV} \end{bmatrix}$$

A.2 dq transformation

The dq transformation is introduced by [168], and it can transfer three phase stationary coordinate system to the dq rotating coordinate system. Therefore, it applies in this thesis to enable both active and reactive components of AC output power to be independently controlled. The transformation matrix is obtained as [168],

$$T = \frac{2}{3}\begin{bmatrix} \cos\theta & \cos(\theta-\frac{2}{3}\pi) & \cos(\theta+\frac{2}{3}\pi) \\ -\sin\theta & -\sin(\theta-\frac{2}{3}\pi) & -\sin(\theta+\frac{2}{3}\pi) \\ \frac{1}{2} & \frac{1}{2} & \frac{1}{2} \end{bmatrix} \quad \text{(A.1)}$$

Where $\theta = \omega t + \delta$ is the angle at the time t between the rotating and coordinate system. δ is the initial phase shift of the signal. Accordingly, the inverse transformation from the dq is defined as [168],

$$T_{\text{inv}} = \begin{bmatrix} \cos\theta & -\sin\theta & 1 \\ \cos(\theta-\frac{2}{3}\pi) & -\sin(\theta-\frac{2}{3}\pi) & 1 \\ \cos(\theta+\frac{2}{3}\pi) & -\sin(\theta+\frac{2}{3}\pi) & 1 \end{bmatrix} \quad \text{(A.2)}$$

The instantaneous active and reactive power at dq space are defined as

$$P = V_d I_d + V_q I_q \quad \text{(A.3)}$$

$$Q = V_q I_d - V_d I_q \quad \text{(A.4)}$$

In addition, the voltage magnitude and voltage angle can be obtained by

$$V_{\text{rms}} = \sqrt{V_d^2 + V_q^2} \quad \text{(A.5)}$$

$$\delta = \tan^{-1}(\frac{v_q}{v_d}) \quad \text{(A.6)}$$

References

[1] National Grid, “Electricity Ten Year Statement 2014,” 2015.

[2] National Grid, “What we do: Electricity,” 2014. [Online]. Available: http://www2.nationalgrid.com/About-us/What-we-do/Electricity/. [Accessed: 12-Mar-2015].

[3] Scottish and Southern Energy, “What we do: Electricity transmission.” [Online]. Available: http://sse.com/whatwedo/networks/electricitytransmission/. [Accessed: 12-Mar-2015].

[4] Scottish Power, “Our Transmission Network - SP Energy Networks.” [Online]. Available: http://www.spenergynetworks.co.uk/pages/our_transmission_network.asp. [Accessed: 12-Mar-2015].

[5] Ofgem, “The GB electricity transmission network | Ofgem,” 2014. [Online]. Available: https://www.ofgem.gov.uk/electricity/transmission-networks/gb-electricity-transmission-network. [Accessed: 12-Mar-2015].

[6] National Grid, “What we do in the Electrcity Industry.” [Online]. Available: http://www2.nationalgrid.com/uk/our-company/electricity/. [Accessed: 12-Mar-2015].

[7] National Grid, “Distribution Network Operator Companies | National Grid,” 2014. [Online]. Available: http://www2.nationalgrid.com/uk/Our-company/electricity/Distribution-Network-Operator-Companies/. [Accessed: 16-Mar-2015].

[8] Ofgem, “The GB electricity distribution network | Ofgem,” 2014. [Online]. Available: https://www.ofgem.gov.uk/electricity/distribution-networks/gb-electricity-distribution-network. [Accessed: 16-Mar-2015].

[9] Ofgem, “Who we are | Ofgem,” 2014. [Online]. Available: https://www.ofgem.gov.uk/about-us/who-we-are. [Accessed: 16-Mar-2015].

[10] UKWED, “RenewableUK | Technologies,” 2015. [Online]. Available: http://www.renewableuk.com/en/renewable-energy/wind-energy/small-and-medium-scale-wind/technologies.cfm. [Accessed: 18-Mar-2015].

[11] National Statistics, “Energy Trends section 6: renewables - Publications - GOV.UK,” 2015. [Online]. Available: https://www.gov.uk/government/statistics/energy-trends-section-6-renewables. [Accessed: 20-Jan-2016].

[12] RenewableUK, “RenewableUK | UK Wind Energy Database (UKWED),” 2016. [Online]. Available: http://www.renewableuk.com/en/renewable-energy/wind-energy/uk-wind-energy-database/index.cfm/map/1/country/343/project_type/onshore/. [Accessed: 03-Jan-2016].

[13] Department of Climate Change, “UK Renewable Energy Roadmap,” no. July, 2011.

[14] UK government, “CLIMATE CHANGE ACT 2008,” vol. 2008, no. November, pp. 1–81, 2008.

[15] G. Innes, A. Jones, I. Marchant, and S. Trotter, “The future role for energy storage in the UK Main Report The Energy Research Partnership,” no. June, 2011.

[16] UK Government, “Increasing the use of low-carbon technologies - Policy - GOV.UK,” 2012. [Online]. Available: https://www.gov.uk/government/policies/increasing-the-use-of-low-carbon-technologies. [Accessed: 16-Mar-2015].

[17] National Grid, “Electricity Ten Year Statement | National Grid,” 2014. [Online]. Available: http://www2.nationalgrid.com/UK/Industry-information/Future-of-Energy/Electricity-Ten-Year-Statement/. [Accessed: 16-Mar-2015].

[18] National Grid, “National Grid’s UK Future Energy Scenarios 2013 | National Grid,” 2013. [Online]. Available: http://www2.nationalgrid.com/mediacentral/uk-press-releases/2013/national-grid-s-uk-future-energy-scenarios-2013/. [Accessed: 16-Mar-2015].

[19] UK Government, “Electricity System : Assessment of Future Challenges - Summary The GB Electricity System,” no. August 2012.

[20] UK Government, “AN UPDATED FULL REPORT TO THE ELECTRICITY NETWORKS,” no. February, 2012.

[21] ENA, “Distributed Generation Connection Guide,” no. November, 2011.

[22] Department of Climate Change, “2050 Pathways Analysis,” no. July, 2010.

[23] Ofgem, “Distributed generation | Ofgem,” 2012. [Online]. Available: https://www.ofgem.gov.uk/electricity/distribution-networks/connections-and-competition/distributed-generation. [Accessed: 16-Mar-2015].

[24] U.S.Department of Energy, “Using Distributed Energy Resources Energy Resources : A How-To How do I know if DER systems are the right,” 2013.

[25] National Grid, “National Grid - Introduction to Distributed Generation,” 2014. [Online]. Available: https://www.nationalgridus.com/masselectric/business/energyeff/4_introduction.asp. [Accessed: 17-Mar-2015].

[26] “Distributed Generation Capacity Expected To Double By 2023 | CleanTechnica,” 2014. [Online]. Available: http://cleantechnica.com/2014/12/09/distributed-generation-capacity-expected-double-2023/. [Accessed: 18-Mar-2015].

[27] Department of Climate Change, “Feed-in Tariff statistics - GOV.UK,” 2014. [Online]. Available: https://www.gov.uk/government/collections/feed-in-tariff-statistics. [Accessed: 17-Mar-2015].

[28] World Future Council, “Feed-In Tariffs – Boosting Energy for our Future A guide to one of the world ’ s best environmental policies,” 2010.

[29] T. Couture and Y. Gagnon, “An analysis of feed-in tariff remuneration models: Implications for renewable energy investment,” *Energy Policy*, vol. 38, no. 2, pp. 955–965, Feb. 2010.

[30] Ofgem, “Feed-in Tariff (FIT) scheme | Ofgem,” 2014. [Online]. Available: https://www.ofgem.gov.uk/environmental-programmes/feed-tariff-fit-scheme. [Accessed: 17-Mar-2015].

[31] Energy Saving Trust, “Feed-in Tariff scheme | Energy Saving Trust.” [Online]. Available: http://www.energysavingtrust.org.uk/domestic/content/feed-tariff-scheme. [Accessed: 17-Mar-2015].

[32] Solarbuzz, “UK ranked in sixth place for small-scale solar in 2013 | Solar Power Portal,” 2013. [Online]. Available: http://www.solarpowerportal.co.uk/guest_blog/uk_ranked_in_sixth_place_for_small_scale_solar_in_2013_23566. [Accessed: 17-Mar-2015].

[33] Department of Climate Change, “Solar photovoltaics deployment - Publications - GOV.UK,” 2015. [Online]. Available: https://www.gov.uk/government/statistics/solar-photovoltaics-deployment. [Accessed: 18-Mar-2015].

[34] Solar power portal, “UK solar PV industry reaches 5GW installed capacity | Solar Power Portal,” 2014. [Online]. Available: http://www.solarpowerportal.co.uk/guest_blog/uk_solar_pv_industry_reaches_5gw_installed_capacity_3467. [Accessed: 18-Mar-2015].

[35] UKWED, “RenewableUK | UK Wind Energy Database (UKWED),” 2015. [Online]. Available: http://www.renewableuk.com/en/renewable-energy/wind-energy/uk-wind-energy-database/index.cfm. [Accessed: 18-Mar-2015].

[36] UKWED, “Small and Medium Wind UK Market Report,” no. March, 2015.

[37] Energy saving trust, “Feed-in Tariff scheme | Energy Saving Trust,” 2015. [Online]. Available: http://www.energysavingtrust.org.uk/domestic/cy/content/feed-tariff-scheme. [Accessed: 18-Mar-2015].

[38] U.S. Department of Energy, “The potential benefits of distributed generation and rate-related issues that may impede their expansion.” 2007 [Online]. Available: https://www.ferc.gov/legal/fed-sta/exp-study.pdf. [Accessed: 22-Apr-2015].

[39] N. Y. Amponsah, M. Troldborg, B. Kington, I. Aalders, and R. L. Hough, “Greenhouse gas emissions from renewable energy sources: A review of lifecycle considerations,” *Renew. Sustain. Energy Rev.*, vol. 39, pp. 461–475, Nov. 2014.

[40] “IEEE 1547-2003.” [Online]. Available: http://www.techstreet.com/products/1094603. [Accessed: 23-Apr-2015].

[41] A. Ellis, R. Nelson, E. Von Engeln, J. MacDowell, L. Casey, E. Seymour, and W. Peter, “Reactive power performance requirements for wind and solar plants,” in *2012 IEEE Power and Energy Society General Meeting*, 2012, pp. 1–8.

[42] P. A. Daly and J. Morrison, “Understanding the potential benefits of distributed generation on power delivery systems,” in *2001 Rural Electric Power Conference. Papers Presented at the 45th Annual Conference (Cat. No.01CH37214)*, 2001, pp. A2/1–A213.

[43] N. D. Hatziargyriou and A. P. Sakis Meliopoulos, “Distributed energy sources: technical challenges,” in *2002 IEEE Power Engineering Society Winter Meeting. Conference Proceedings (Cat. No.02CH37309)*, 2002, vol. 2, pp. 1017–1022.

[44] J. A. P. Lopes, “Integration of dispersed generation on distribution networks-impact studies,” in *2002 IEEE Power Engineering Society Winter Meeting. Conference Proceedings (Cat. No.02CH37309)*, 2002, vol. 1, pp. 323–328.

[45] M. M. Fuchs, *Power Quality in Power Systems and Electrical Machines*. Elsevier, 2008.

[46] R. Passey, T. Spooner, I. MacGill, M. Watt, and K. Syngellakis, “The potential impacts of grid-connected distributed generation and how to address them: A review of technical and non-technical factors,” *Energy Policy*, vol. 39, no. 10, pp. 6280–6290, Oct. 2011.

[47] HSE, “Electricity Safety, Quality and Continuity Regulations (ESQCR) - HSE.” [Online]. Available: http://www.hse.gov.uk/esqcr/. [Accessed: 23-Apr-2015].

[48] Y.-J. Kim, S.-J. Ahn, P.-I. Hwang, G.-C. Pyo, and S.-I. Moon, “Coordinated Control of a DG and Voltage Control Devices Using a Dynamic Programming Algorithm,” *IEEE Trans. Power Syst.*, vol. 28, no. 1, pp. 42–51, Feb. 2013.

[49] A. Canova, L. Giaccone, F. Spertino, and M. Tartaglia, “Electrical Impact of Photovoltaic Plant in Distributed Network,” *IEEE Trans. Ind. Appl.*, vol. 45, no. 1, pp. 341–347, 2009.

[50] A. Crossland, “Application of stochastic and evolutionary methods to plan for the installation of energy storage in voltage constrained LV networks,” vol. 0, 2014.

[51] P. M. Costa and M. A. Matos, “Avoided losses on LV networks as a result of microgeneration,” *Electr. Power Syst. Res.*, vol. 79, no. 4, pp. 629–634, Apr. 2009.

[52] M. A. Kashem, A. D. T. Le, M. Negnevitsky, and G. Ledwich, “Distributed generation for minimization of power losses in distribution systems,” in *2006 IEEE Power Engineering Society General Meeting*, 2006, p. 8 pp.

[53] A. R. Oliva and J. C. Balda, “A PV dispersed generator: a power quality analysis within the IEEE 519,” *IEEE Trans. Power Deliv.*, vol. 18, no. 2, pp. 525–530, Apr. 2003.

[54] E. Muljadi, C. P. Butterfield, H. Romanowitz, and R. Yinger, “Self-Excitation and Harmonics in Wind Power Generation,” *J. Sol. Energy Eng.*, vol. 127, no. 4, p. 581, Nov. 2005.

[55] T.-L. Lee, P.-T. Cheng, H. Akagi, and H. Fujita, “A Dynamic Tuning Method for

Distributed Active Filter Systems," *IEEE Trans. Ind. Appl.*, vol. 44, no. 2, pp. 612–623, 2008.

[56] T.-L. Lee and P.-T. Cheng, "Design of a New Cooperative Harmonic Filtering Strategy for Distributed Generation Interface Converters in an Islanding Network," *IEEE Trans. Power Electron.*, vol. 22, no. 5, pp. 1919–1927, Sep. 2007.

[57] L. Wang, D. Liang, A. Crossland, N. Wade, and D. Jones, "Using a smart grid laboratory to investigate battery energy storage to mitigate the effects of PV in distribution networks," in *22nd International Conference and Exhibition on Electricity Distribution (CIRED 2013)*, 2013, pp. 0504–0504.

[58] M. M. Fuchs, *Power Quality in Power Systems and Electrical Machines*. Elsevier, 2008.

[59] X. Meng, S. Zhao, X. Song, and W. Sheng, "Maximum penetration level of distributed generation in consideration of voltage fluctuations based on multi-resolution model," *IET Gener. Transm. Distrib.*, vol. 9, no. 3, pp. 241–248, 2015.

[60] A. Woyte, V. V. Thong, R. Belmans, and J. Nijs, "Voltage Fluctuations on Distribution Level Introduced by Photovoltaic Systems," *IEEE Trans. Energy Convers.*, vol. 21, no. 1, pp. 202–209, Mar. 2006.

[61] C. Luo, H. Banakar, B. Shen, and B.-T. Ooi, "Strategies to Smooth Wind Power Fluctuations of Wind Turbine Generator," *IEEE Trans. Energy Convers.*, vol. 22, no. 2, pp. 341–349, Jun. 2007.

[62] R. Majumder and E. Engineering, "MODELING , STABILITY ANALYSIS AND CONTROL OF MICROGRID .," no. February, 2010.

[63] Energy Networks Association, "Engineering Recommendation P29: Planning Limits for Voltage Unbalance in the United Kingdom." 1990.

[64] P. V. Santos Valois, "Voltage unbalance in low voltage distribution networks," in *16th International Conference and Exhibition on Electricity Distribution (CIRED 2001)*, 2001, vol. 2001, pp. v2–41–v2–41.

[65] S. Dahal, N. Mithulananthan, and T. K. Saha, "Assessment and Enhancement of Small Signal Stability of a Renewable-Energy-Based Electricity Distribution System," *IEEE Trans. Sustain. Energy*, vol. 3, no. 3, pp. 407–415, Jul. 2012.

[66] M. Reza, D. Sudarmadi, F. Viawan, W. Kling, and L. Der Sluis, "Dynamic Stability of Power Systems with Power Electronic Interfaced DG," in *2006 IEEE PES Power Systems Conference and Exposition*, 2006, pp. 1423–1428.

[67] GridTECH, "FACTS (Flexible Alternating Current Transmission System)." [Online]. Available: http://www.gridtech.eu/project-scope/technologies/12-technologies/21-facts-flexible-alternating-current-transmission-system. [Accessed: 24-Apr-2015].

[68] C.-S. Chen, C.-H. Lin, W.-L. Hsieh, C.-T. Hsu, and T.-T. Ku, "Enhancement of PV Penetration With DSTATCOM in Taipower Distribution System," *IEEE Trans. Power*

Syst., vol. 28, no. 2, pp. 1560–1567, May 2013.

[69] I. Wasiak, "Application of DSTATCOM compensators for mitigation of power quality disturbances in low voltage grid with distributed generation," in *2007 9th International Conference on Electrical Power Quality and Utilisation*, 2007, pp. 1–6.

[70] M. J. Newman, D. G. Holmes, J. G. Nielsen, and F. Blaabjerg, "A Dynamic Voltage Restorer (DVR) With Selective Harmonic Compensation at Medium Voltage Level," *IEEE Trans. Ind. Appl.*, vol. 41, no. 6, pp. 1744–1753, Nov. 2005.

[71] F. A. L. Jowder, "Design and analysis of dynamic voltage restorer for deep voltage sag and harmonic compensation," *IET Gener. Transm. Distrib.*, vol. 3, no. 6, pp. 547–560, Jun. 2009.

[72] J. Shi, A. Kalam, A. Noshadi, and P. Shi, "Genetic algorithm optimised fuzzy control of DSTATCOM for improving power quality," in *2014 Australasian Universities Power Engineering Conference (AUPEC)*, 2014, pp. 1–6.

[73] H. Ren, X. Yu, and D. Watts, "Impacts of optimal allocation of DFACTS on the penetration capacity of distributed generation," in *2010 International Conference on Power System Technology*, 2010, pp. 1–5.

[74] P. Wolfs and A. M. T. Oo, "Improvements to LV distribution system PV penetration limits using a dSTATCOM with reduced DC bus capacitance," in *2013 IEEE Power & Energy Society General Meeting*, 2013, pp. 1–5.

[75] K. M. Rogers and T. J. Overbye, "Power flow control with Distributed Flexible AC Transmission System (D-FACTS) devices," in *41st North American Power Symposium*, 2009, pp. 1–6.

[76] R. S. Bajpai and R. Gupta, "Voltage and power flow control of grid connected wind generation system using DSTATCOM," in *2008 IEEE Power and Energy Society General Meeting - Conversion and Delivery of Electrical Energy in the 21st Century*, 2008, pp. 1–6.

[77] X. Fu, H. Chen, and X. Jin, "Transient stability of a distribution network with DFACTS devices and FSWT," in *2013 IEEE PES Asia-Pacific Power and Energy Engineering Conference (APPEEC)*, 2013, pp. 1–6.

[78] K. Clement-Nyns, E. Haesen, and J. Driesen, "The impact of vehicle-to-grid on the distribution grid," *Electr. Power Syst. Res.*, vol. 81, no. 1, pp. 185–192, Jan. 2011.

[79] R. Tonkoski and L. A. C. Lopes, "Impact of active power curtailment on overvoltage prevention and energy production of PV inverters connected to low voltage residential feeders," *Renew. Energy*, vol. 36, no. 12, pp. 3566–3574, Dec. 2011.

[80] A. G. Madureira and J. A. Peças Lopes, "Coordinated voltage support in distribution networks with distributed generation and microgrids," *IET Renew. Power Gener.*, vol. 3, no. 4, p. 439, 2009.

[81] R. Tonkoski, L. A. C. Lopes, and T. H. M. El-Fouly, "Coordinated Active Power

Curtailment of Grid Connected PV Inverters for Overvoltage Prevention," *IEEE Trans. Sustain. Energy*, vol. 2, no. 2, pp. 139–147, Apr. 2011.

[82] S. Ghosh, S. Rahman, and M. Pipattanasomporn, "Local distribution voltage control by reactive power injection from PV inverters enhanced with active power curtailment," in *2014 IEEE PES General Meeting | Conference & Exposition*, 2014, pp. 1–5.

[83] A. Pina, C. Silva, and P. Ferrão, "The impact of demand side management strategies in the penetration of renewable electricity," *Energy*, vol. 41, no. 1, pp. 128–137, May 2012.

[84] P. Palensky and D. Dietrich, "Demand Side Management: Demand Response, Intelligent Energy Systems, and Smart Loads," *IEEE Trans. Ind. Informatics*, vol. 7, no. 3, pp. 381–388, Aug. 2011.

[85] I. T. Papaioannou, A. Purvins, and E. Tzimas, "Demand shifting analysis at high penetration of distributed generation in low voltage grids," *Int. J. Electr. Power Energy Syst.*, vol. 44, no. 1, pp. 540–546, Jan. 2013.

[86] G. Strbac, "Demand side management: Benefits and challenges," *Energy Policy*, vol. 36, no. 12, pp. 4419–4426, Dec. 2008.

[87] N. Balta-Ozkan, R. Davidson, M. Bicket, and L. Whitmarsh, "The development of smart homes market in the UK," *Energy*, vol. 60, pp. 361–372, Oct. 2013.

[88] N. S. Wade, P. C. Taylor, P. D. Lang, and P. R. Jones, "Evaluating the benefits of an electrical energy storage system in a future smart grid," *Energy Policy*, vol. 38, no. 11, pp. 7180–7188, Nov. 2010.

[89] M. A. Kashem and G. Ledwich, "Energy requirement for distributed energy resources with battery energy storage for voltage support in three-phase distribution lines," *Electr. Power Syst. Res.*, vol. 77, no. 1, pp. 10–23, Jan. 2007.

[90] P. Wang, D. H. Liang, J. Yi, P. F. Lyons, P. J. Davison, and P. C. Taylor, "Integrating Electrical Energy Storage Into Coordinated Voltage Control Schemes for Distribution Networks," *IEEE Trans. Smart Grid*, vol. 5, no. 2, pp. 1018–1032, Mar. 2014.

[91] I. Wasiak, R. Pawelek, and R. Mienski, "Energy storage application in low-voltage microgrids for energy management and power quality improvement," *IET Gener. Transm. Distrib.*, vol. 8, no. 3, pp. 463–472, Mar. 2014.

[92] X. Tang, W. Deng, and Z. Qi, "Investigation of the Dynamic Stability of Microgrid," *IEEE Trans. Power Syst.*, vol. 29, no. 2, pp. 698–706, Mar. 2014.

[93] R. Majumder, "Some Aspects of Stability in Microgrids," *IEEE Trans. Power Syst.*, vol. 28, no. 3, pp. 3243–3252, Aug. 2013.

[94] N. Wade, P. Taylor, P. Lang, and J. Svensson, "Energy storage for power flow management and voltage control on an 11kV UK distribution network." in *CIRED Workshop: Integration of Renewables into the Distribution Grid*, 2009, pp. 1–4.

[95] A. O. F. Regulations, “ELECTRICITY The Electricity Safety , Quality and Continuity Regulations 2002,” no. 2665, 2003.

[96] C. A. Hill, M. C. Such, D. Chen, J. Gonzalez, S. Member, and W. M. Grady, “Battery Energy Storage for Enabling Integration of Distributed Solar Power Generation,” vol. 3, no. 2, pp. 850–857, 2012.

[97] Power Technology, “Energy storage in the UK: is the government doing enough? - Power Technology.” [Online]. Available: http://www.power-technology.com/features/featureenergy-storage-in-the-uk-is-the-government-doing-enough-4207896/. [Accessed: 30-Apr-2015].

[98] The Guardian, “George Osborne: make UK a world leader in energy storage | Environment | The Guardian.” [Online]. Available: http://www.theguardian.com/environment/2012/nov/09/george-osborne-uk-energy-storage. [Accessed: 30-Apr-2015].

[99] Business Green, “The UK needs to develop an energy storage market in 2015 - 29 Dec 2014 - Opinion from BusinessGreen.” [Online]. Available: http://www.businessgreen.com/bg/opinion/2386792/the-uk-needs-to-develop-an-energy-storage-market-in-2015. [Accessed: 30-Apr-2015].

[100] T. H. E. E. Storage, “DEVELOPMENT OF ELECTRICITY STORAGE IN THE NATIONAL INTEREST.” 2009.

[101] G. Strbac, M. Aunedi, D. Pudjianto, P. Djapic, and F. Teng, “Strategic Assessment of the Role and Value of Energy Storage Systems in the UK Low Carbon Energy Future Report for,” no. June, 2012.

[102] Ofgem, “Low Carbon Networks Fund | Ofgem,” 2014. [Online]. Available: https://www.ofgem.gov.uk/electricity/distribution-networks/network-innovation/low-carbon-networks-fund. [Accessed: 30-Apr-2015].

[103] ELEXON, “Electricity storage in the GB market,” 2015.

[104] D. Moneta, L. Bisone, G. Mauri, and R. Meda, “New interactions between LV customers and the network: further possibilities for home automation functions,” in *Proceedings 2007 IEEE International Conference on Robotics and Automation*, 2007, pp. 2886–2891.

[105] O. M. Toledo, D. Oliveira Filho, and A. S. A. C. Diniz, “Distributed photovoltaic generation and energy storage systems: A review,” *Renew. Sustain. Energy Rev.*, vol. 14, no. 1, pp. 506–511, Jan. 2010.

[106] M. Beaudin, H. Zareipour, A. Schellenberglabe, and W. Rosehart, “Energy storage for mitigating the variability of renewable electricity sources: An updated review,” *Energy Sustain. Dev.*, vol. 14, no. 4, pp. 302–314, Dec. 2010.

[107] H. Chen, T. N. Cong, W. Yang, C. Tan, Y. Li, and Y. Ding, “Progress in electrical energy storage system: A critical review,” *Prog. Nat. Sci.*, vol. 19, no. 3, pp. 291–312, Mar. 2009.

[108] The Energy Research, “Energy innovation milestones to 2050 Energy innovation milestones to 2050 Foreword,” no. March, 2010.

[109] J. S. and R. C. Sergio Faias, *Renewable Energy*. InTech, 2009.

[110] H. Ibrahim, A. Ilinca, and J. Perron, “Energy storage systems—Characteristics and comparisons,” *Renew. Sustain. Energy Rev.*, vol. 12, no. 5, pp. 1221–1250, Jun. 2008.

[111] D. J. Swider, “Compressed air energy storage in an electricity system with significant wind power generation,” *IEEE Trans. Energy Convers.*, vol. 22, no. 1, pp. 95–102, 2007.

[112] H. Daneshi and A. K. Srivastava, “Security-constrained unit commitment with wind generation and compressed air energy storage,” *IET Gener. Transm. Distrib.*, vol. 6, no. 2, pp. 167–175, 2012.

[113] V. A. Boicea, “Energy storage technologies: The past and the present,” *Proc. IEEE*, vol. 102, no. 11, pp. 1777–1794, 2014.

[114] Samir Succar and Robert H. Williams, “Compressed Air Energy Storage : Theory , Resources , And Applications For Wind Power Acknowledgments,” no. April, 2008.

[115] J. Kondoh, I. Ishii, H. Yamaguchi, a. Murata, K. Otani, K. Sakuta, N. Higuchi, S. Sekine, and M. Kamimoto, “Electrical energy storage systems for energy networks,” *Energy Convers. Manag.*, vol. 41, no. 17, pp. 1863–1874, Nov. 2000.

[116] D. D. Banham-Hall, G. A. Taylor, C. A. Smith, and M. R. Irving, “Flow batteries for enhancing wind power integration,” *IEEE Trans. Power Syst.*, vol. 27, no. 3, pp. 1690–1697, 2012.

[117] D. D. Banham-Hall, G. a. Taylor, C. a. Smith, and M. R. Irving, “Frequency control using Vanadium redox flow batteries on wind farms,” *2011 IEEE Power Energy Soc. Gen. Meet.*, pp. 1–8, 2011.

[118] Y. Suzuki, A. Koyanagi, M. Kobayashi, and R. Shimada, “Novel applications of the flywheel energy storage system,” *Energy*, vol. 30, no. 11–12, pp. 2128–2143, Aug. 2005.

[119] S. M. Schoenung and W. Hassenzahl, “Energy storage systems cost update,” *Sandia Natl. Lab. Albuquerque*, no. April, p. 30, 2013.

[120] N. S. Pearre and L. G. Swan, “Technoeconomic feasibility of grid storage: Mapping electrical services and energy storage technologies,” *Appl. Energy*, vol. 137, pp. 501–510, 2015.

[121] J. Leadbetter and L. G. Swan, “Selection of battery technology to support grid-integrated renewable electricity,” *J. Power Sources*, vol. 216, pp. 376–386, 2012.

[122] A. Joseph and M. Shahidehpour, “Battery Storage Systems in Electric Power Systems Ami Joseph and Mohammad Shahidehpour,” pp. 1–8, 2006.

[123] N. C. Nair and N. Garimella, “Battery energy storage systems: Assessment for small-scale renewable energy integration,” *Energy Build.*, vol. 42, no. 11, pp. 2124–2130, Nov. 2010.

[124] D.-J. Lee and L. Wang, “Small-Signal Stability Analysis of an Autonomous Hybrid Renewable Energy Power Generation/Energy Storage System Part I: Time-Domain Simulations,” *IEEE Trans. Energy Convers.*, vol. 23, no. 1, pp. 311–320, Mar. 2008.

[125] Zhong Chen, Ming Ding, Jianhui Su, Zinian Chen, Yaqiao Luo, and Guoqiang Zheng, “Control scheme for power condition system of large capacity battery energy storage under unbalanced grid,” in *IEEE PES Innovative Smart Grid Technologies*, 2012, pp. 1–6.

[126] X. Li, D. Hui, and X. Lai, “Battery Energy Storage Station (BESS)-Based Smoothing Control of Photovoltaic (PV) and Wind Power Generation Fluctuations,” *IEEE Trans. Sustain. Energy*, vol. 4, no. 2, pp. 464–473, Apr. 2013.

[127] M. K. Hossain and M. H. Ali, “Small scale energy storage for power fluctuation minimization with spatially diverged PV plants,” in *2013 Proceedings of IEEE Southeastcon*, 2013, pp. 1–6.

[128] U. K. P. Networks, “Demonstrating the benefits of short-term discharge energy storage on an 11kV distribution network,” no. June, 2014.

[129] Scottish and Southern Energy, “LCNF Tier 1 Closedown Report Low Voltage Connected Energy Storage Document Owner (s),” pp. 1–80, 2014.

[130] J. Baker, J. Cross, I. Lloyd, and N. Powergrid, “Lessons Learned Report Electrical Energy Storage,” no. December, 2014.

[131] P. F. Lyons, N. S. Wade, T. Jiang, P. C. Taylor, F. Hashiesh, M. Michel, and D. Miller, “Design and analysis of electrical energy storage demonstration projects on UK distribution networks,” *Appl. Energy*, vol. 137, pp. 677–691, Jan. 2015.

[132] Western Power Distribution, “SoLa Bristol - Western Power Innovation.” [Online]. Available: http://www.westernpowerinnovation.co.uk/Projects/SoLa-Bristol.aspx#FAQLink41;javascript:void(0); [Accessed: 04-May-2015].

[133] F. Marra, G. Yang, C. Træholt, J. Østergaard, S. Member, and E. Larsen, “A Decentralized Storage Strategy for Residential Feeders With Photovoltaics,” vol. 5, no. 2, pp. 974–981, 2014.

[134] A. A. Akhil, G. Huff, A. B. Currier, B. C. Kaun, D. M. Rastler, S. B. Chen, A. L. Cotter, D. T. Bradshaw, and W. D. Gauntlett, “DOE / EPRI 2013 Electricity Storage Handbook in Collaboration with NRECA,” no. July, 2013.

[135] M. N. Kabir, Y. Mishra, G. Ledwich, S. Member, Z. Y. Dong, and K. P. Wong, “Coordinated Control of Grid-Connected Photovoltaic Reactive Power and Battery Energy Storage Systems to Improve the Voltage Pro fi le of a Residential Distribution Feeder,” vol. 10, no. 2, pp. 967–977, 2014.

[136] M. J. E. Alam, S. Member, K. M. Muttaqi, S. Member, and D. Sutanto, “A Novel Approach for Ramp-Rate Control of Solar PV Using Energy Storage to Mitigate Output Fluctuations Caused by Cloud Passing,” vol. 29, no. 2, pp. 507–518, 2014.

[137] G. Wang, S. Member, M. Ciobotaru, V. G. Agelidis, and S. Member, “Power Smoothing of Large Solar PV Plant Using,” vol. 5, no. 3, pp. 834–842, 2014.

[138] K. H. Chua, Y. S. Lim, P. Taylor, S. Member, and S. Morris, “Energy Storage System for Mitigating Voltage Unbalance on Low-Voltage Networks With Photovoltaic Systems,” vol. 27, no. 4, pp. 1783–1790, 2012.

[139] K. T. Tan, S. Member, P. L. So, S. Member, Y. C. Chu, and M. Z. Q. Chen, “Coordinated Control and Energy Management of Distributed Generation Inverters in a Microgrid,” vol. 28, no. 2, pp. 704–713, 2013.

[140] M. Arnold and G. Andersson, “Model Predictive Control of Energy Storage including Uncertain Forecasts,” *Power Syst. Comput. Conf.*, 2011.

[141] S. J. Qin and T. a. Badgwell, “A survey of industrial model predictive control technology,” *Control Eng. Pract.*, vol. 11, no. 7, pp. 733–764, 2003.

[142] L. Dai, Y. Xia, M. Fu, and M. S. Mahmoud, “Discrete-Time Model Predictive Control,” *Adv. Discret. Time Syst.*, 2012.

[143] J. Yi, P. Wang, P. C. Taylor, P. J. Davison, P. F. Lyons, D. Liang, S. Brown, and D. Roberts, “Distribution Network Voltage Control Using Energy Storage and Demand Side Response,” pp. 1–8, 2012.

[144] S. Lamichhane, H. Nazaripouya, and S. Mehraeen, “Micro Grid Stability Improvements by Employing Storage,” in *2013 IEEE Green Technologies Conference (GreenTech)*, 2013, pp. 250–258.

[145] O. Anuta, A. Crossland, D. Jones, and N. Wade, “Regulatory and financial hurdles for the installation of energy storage in UK distribution networks,” in *CIRED 2012 Workshop: Integration of Renewables into the Distribution Grid*, 2012, pp. 219–219.

[146] G. Mokhtari, G. Nourbakhsh, and A. Ghosh, “Smart Coordination of Energy Storage Units (ESUs) for Voltage and Loading Management in Distribution Networks,” *IEEE Trans. Power Syst.*, vol. 28, no. 4, pp. 4812–4820, Nov. 2013.

[147] L. Wang, D. H. Liang, A. F. Crossland, P. C. Taylor, D. Jones, and N. S. Wade, “Coordination of Multiple Energy Storage Units in a Low-Voltage Distribution Network,” *IEEE Trans. Smart Grid*, pp. 1–1, 2015.

[148] J. M. Guerrero, J. Matas, L. G. De Vicuña, M. Castilla, and J. Miret, “Decentralized Control for Parallel Operation of Distributed Generation Inverters Using Resistive Output Impedance,” vol. 54, no. 2, pp. 994–1004, 2007.

[149] Yun Wei Li and Ching-Nan Kao, “An Accurate Power Control Strategy for Power-Electronics-Interfaced Distributed Generation Units Operating in a Low-Voltage Multibus Microgrid,” *IEEE Trans. Power Electron.*, vol. 24, no. 12, pp. 2977–2988,

Dec. 2009.

[150] N. Pogaku, M. Prodanovic, and T. C. Green, “Modeling, Analysis and Testing of Autonomous Operation of an Inverter-Based Microgrid,” *IEEE Trans. Power Electron.*, vol. 22, no. 2, pp. 613–625, Mar. 2007.

[151] J. A. P. Lopes, C. L. Moreira, and A. G. Madureira, “Defining Control Strategies for MicroGrids Islanded Operation,” *IEEE Trans. Power Syst.*, vol. 21, no. 2, pp. 916–924, May 2006.

[152] J. C. Vasquez, D. Kooning, M. Josep, T. L. Vandoorn, J. M. Guerrero, and J. D. M. De Kooning, “Decentralized and centralized control of islanded microgrids including reserve management,” 2013.

[153] A. Bracale, R. Angelino, M. Mangoni, and D. Proto, “Centralized control of dispersed generators providing ancillary services in distribution networks Part II: Numerical applications,” Jan. 2009.

[154] X. Liu, S. Member, A. Aichhorn, L. Liu, and S. Member, “Coordinated Control of Distributed Energy Storage System With Tap Changer Transformers for Voltage Rise Mitigation Under High Photovoltaic Penetration,” *IEEE Trans. Smart Grid* vol. 3, no. 2, pp. 897–906, 2012.

[155] H. Zhao, Q. Wu, C. Wang, L. Cheng, and C. N. Rasmussen, “Coordinated Control of Battery Energy Storage System and Dispatchable Distributed Generation Units in Microgrid.”

[156] Jong-Yul Kim, Jin-Hong Jeon, Seul-Ki Kim, Changhee Cho, June Ho Park, Hak-Man Kim, and Kee-Young Nam, “Cooperative Control Strategy of Energy Storage System and Microsources for Stabilizing the Microgrid during Islanded Operation,” *IEEE Trans. Power Electron.*, vol. 25, no. 12, pp. 3037–3048, Dec. 2010.

[157] F. Katiraei and M. R. Iravani, “Power Management Strategies for a Microgrid With Multiple Distributed Generation Units,” *IEEE Trans. Power Syst.*, vol. 21, no. 4, pp. 1821–1831, Nov. 2006.

[158] E. Liegmann and R. Majumder, “An Efficient Method of Multiple Storage Control in Microgrids,” *IEEE Trans. Power Syst.*, vol. PP, no. 99, pp. 1–8, 2015.

[159] F. Katiraei, M. R. Iravani, and P. W. Lehn, “Small-signal dynamic model of a micro-grid including conventional and electronically interfaced distributed resources,” *IET Gener. Transm. Distrib.*, vol. 1, no. 3, p. 369, May 2007.

[160] M. S. Mahmoud and F. M. AL-Sunni, *Control and Optimization of Distributed Generation Systems*. Springer, 2015.

[161] Xisheng Tang and Zhiping Qi, “Energy storage control in renewable energy based microgrid,” in *2012 IEEE Power and Energy Society General Meeting*, 2012, pp. 1–6.

[162] Q. Zhou and J. W. Bialek, “Generation curtailment to manage voltage constraints in distribution networks,” *IET Gener. Transm. Distrib.*, vol. 1, no. 3, p. 492, 2007.

[163] Spitzenberger & Spies, “PAS series of 4-Quadrant Amplifiers,” pp. 1–10, 2013.

[164] RTDS, “COMPANY PROFILE | RTDS Technologies Inc.” [Online]. Available: https://www.rtds.com/about/company-profile/. [Accessed: 02-Oct-2015].

[165] P. Forsyth, T. Maguire, and R. Kuffel, “Real Time Digital Simulation for Control and Protection System Testing,” *2004 IEEE 35th Annu. Power Electron. Spec. Conf. (IEEE Cat. No.04CH37551)*, vol. 1, pp. 329–335, 2004.

[166] H. Li, M. Steurer, K. L. Shi, S. Woodruff, and D. Zhang, “Development of a Unified Design, Test, and Research Platform for Wind Energy Systems Based on Hardware-in-the-Loop Real-Time Simulation,” *IEEE Trans. Ind. Electron.*, vol. 53, no. 4, pp. 1144–1151, 2006.

[167] H. W. Dommel, “Digital computer solution of electromagnetic transients in single and multiphase,” *Networks IEEE*, vol. 88, no. 4, pp. 388–399, 1969.

[168] RTDS, “RTDS ® Simulator Hardware,” pp. 2–3.

[169] RTDS, “PB5 CARD | RTDS Technologies Inc.” [Online]. Available: https://www.rtds.com/the-simulator/our-hardware/pb5-card/. [Accessed: 02-Oct-2015].

[170] T. R. Simulator, “RTDS ® Simulator Software — RSCAD The RTDS Simulator has an advanced and easy to use graphical user interface - RSCAD .,” pp. 2–3.

[171] RTDS, “RTDS-Technologies,” 2015.

[172] M. Brenna, E. De Berardinis, L. Delli Carpini, F. Foiadelli, P. Paulon, P. Petroni, G. Sapienza, G. Scrosati, and D. Zaninelli, “Automatic Distributed Voltage Control Algorithm in Smart Grids Applications,” *IEEE Trans. Smart Grid*, vol. 4, no. 2, pp. 877–885, Jun. 2013.

[173] M. A. Kashem and G. Ledwich, “Multiple Distributed Generators for Distribution Feeder Voltage Support,” *IEEE Trans. Energy Convers.*, vol. 20, no. 3, pp. 676–684, Sep. 2005.

[174] K. H. Chua, J. Wong, Y. S. Lim, P. Taylor, E. Morris, and S. Morris, “Mitigation of Voltage Unbalance in Low Voltage Distribution Network with High Level of Photovoltaic System,” *Energy Procedia*, vol. 12, pp. 495–501, 2011.

[175] Electricity North West, “Electrolink no.6,” 2014.

[176] D. T. Rizy and J. D. Kueck, “Tap Changer for Distributed Power,” in *19th International Conference on Electricity Distribution*, 2007, no. 0736, pp. 21–24.

[177] Ofgem, “DECC and Ofgem Smart Grid Forum | Ofgem.” [Online]. Available: https://www.ofgem.gov.uk/electricity/distribution-networks/forums-seminars-and-working-groups/decc-and-ofgem-smart-grid-forum. [Accessed: 17-May-2015].

[178] M. J. E. Alam, S. Member, K. M. Muttaqi, S. Member, and D. Sutanto, “Mitigation of Rooftop Solar PV Impacts and Evening Peak Support by Managing Available

Capacity of Distributed Energy Storage Systems," vol. 28, no. 4, pp. 3874–3884, 2013.

[179] H. Bindner, T. Cronin, P. Lundsager, J. F. Manwell, U. Abdulwahid, and I. Baring-gould, *Lifetime Modelling of Lead Acid Batteries*, vol. 1515, no. April. 2005.

[180] "Schoenung, S. M. (2011). Energy Storage Systems Cost Update. Albuquerque, NM. - Bing." .

[181] R. Dufo-López, J. M. Lujano-Rojas, and J. L. Bernal-Agustín, "Comparison of different lead–acid battery lifetime prediction models for use in simulation of stand-alone photovoltaic systems," *Appl. Energy*, vol. 115, pp. 242–253, Feb. 2014.

[182] M. J. E. Alam, K. M. Muttaqi, and D. Sutanto, "Distributed energy storage for mitigation of voltage-rise impact caused by rooftop solar PV," in *2012 IEEE Power and Energy Society General Meeting*, 2012, pp. 1–8.

[183] Deka Solar, "Photovoltaic Batteries," 2012. .

[184] A. F. Crossland, D. Jones, and N. S. Wade, "Planning the location and rating of distributed energy storage in LV networks using a genetic algorithm with simulated annealing," *Int. J. Electr. Power Energy Syst.*, vol. 59, pp. 103–110, Jul. 2014.

[185] F. Z. Peng and J.-S. Lai, "Dynamic performance and control of a static VAr generator using cascade multilevel inverters," *IEEE Trans. Ind. Appl.*, vol. 33, no. 3, pp. 748–755, 1997.

[186] A. Timbus, M. Liserre, R. Teodorescu, P. Rodriguez, and F. Blaabjerg, "Evaluation of Current Controllers for Distributed Power Generation Systems," *IEEE Trans. Power Electron.*, vol. 24, no. 3, pp. 654–664, Mar. 2009.

[187] "solar irradiance redc.nrel.gov/ solar/calculators/PVWATTS/version1/ - Bing." .

[188] "RMDS Guidance."

[189] Ofgem, "Electricity Distribution Price Control Review Initial Consultation Document | Ofgem," 2008. .

[190] Prabha Kundur, *Power System Stability and Control*. New York, US: McGraw-Hill Education, 1994.

[191] P. Kundur, J. Paserba, V. Ajjarapu, G. Andersson, A. Bose, C. Canizares, N. Hatziargyriou, D. Hill, A. Stankovic, C. Taylor, T. Van Cutsem, and V. Vittal, "Definition and Classification of Power System Stability IEEE/CIGRE Joint Task Force on Stability Terms and Definitions," *IEEE Trans. Power Syst.*, vol. 19, no. 3, pp. 1387–1401, Aug. 2004.

[192] A. Ishchenko, *Dynamics and Stability of Distribution Networks with Dispersed Generation*. 2008.

[193] Song Guo, "Adaptive Parameter Estimation of Power System Dynamic Models Using Modal Information," 2014.

[194] P. Kundur, N. J. Balu, and M. G. Lauby, *Power system stability and control*. McGraw-Hill, 1994.

[195] E. Allen, N. LaWhite, Y. Yoon, J. Chapman, and M. Ilic, "Interactive object-oriented simulation of interconnected power systems using SIMULINK," *IEEE Trans. Educ.*, vol. 44, no. 1, pp. 87–94, 2001.

[196] R. H. Park, "Two-reaction theory of synchronous machines generalized method of analysis-part I," *Trans. Am. Inst. Electr. Eng.*, vol. 48, no. 3, pp. 716–727, Jul. 1929.

[197] Faridaddin Katiraei, *Dynamic Analysis and Control of Distributed Energy Resources in a Micro-Grid*. 2005.

[198] J. Uudrill, "Dynamic Stability Calculations for an Arbitrary Number of Interconnected Synchronous Machines," *IEEE Trans. Power Appar. Syst.*, vol. PAS-87, no. 3, pp. 835–844, Mar. 1968.

[199] MATLAB, "Average Model - MATLAB & Simulink Example - MathWorks United Kingdom." [Online]. Available: http://uk.mathworks.com/help/physmod/sps/examples/wind-farm-dfig-average-model.html. [Accessed: 20-Aug-2015].

[200] F. Katiraei and M. R. Iravani, "Power Management Strategies for a Microgrid With Multiple Distributed Generation Units," *IEEE Trans. Power Syst.*, vol. 21, no. 4, pp. 1821–1831, Nov. 2006.

[201] R. Shah, N. Mithulananthan, A. Sode-Yome, and K. Y. Lee, "Impact of large-scale PV penetration on power system oscillatory stability," in *IEEE PES General Meeting*, 2010, pp. 1–7.

[202] S. Dahal, N. Mithulananthan, and T. K. Saha, "Assessment and Enhancement of Small Signal Stability of a Renewable-Energy-Based Electricity Distribution System," *IEEE Trans. Sustain. Energy*, vol. 3, no. 3, pp. 407–415, Jul. 2012.

[203] B.-S. Chen and Y.-Y. Hsu, "A Minimal Harmonic Controller for a STATCOM," *IEEE Trans. Ind. Electron.*, vol. 55, no. 2, pp. 655–664, 2008.

[204] F. Mei and B. Pal, "Modal Analysis of Grid-Connected Doubly Fed Induction Generators," *IEEE Trans. Energy Convers.*, vol. 22, no. 3, pp. 728–736, Sep. 2007.

[205] L. Wang, D. H. Liang, A. F. Crossland, P. C. Taylor, D. Jones, and N. S. Wade, "Coordination of Multiple Energy Storage Units in a Low-Voltage Distribution Network," *IEEE Trans. Smart Grid*, vol. PP, no. 99, pp. 1–1, 2015.

[206] Y. Liu, J. Bebic, B. Kroposki, J. de Bedout, and W. Ren, "Distribution System Voltage Performance Analysis for High-Penetration PV," in *2008 IEEE Energy 2030 Conference*, 2008, pp. 1–8.

[207] M. Dargahi, A. Ghosh, G. Ledwich, and F. Zare, "Studies in power hardware in the loop (PHIL) simulation using real-time digital simulator (RTDS)," in *2012 IEEE International Conference on Power Electronics, Drives and Energy Systems (PEDES)*,

2012, pp. 1–6.

[208] W. Ren, M. Steurer, and T. L. Baldwin, “Improve the Stability and the Accuracy of Power Hardware-in-the-Loop Simulation by Selecting Appropriate Interface Algorithms,” in *2007 IEEE/IAS Industrial & Commercial Power Systems Technical Conference*, 2007, pp. 1–7.

[209] “Control Tutorials for MATLAB and Simulink - Introduction: PID Controller Design.” [Online]. Available: http://ctms.engin.umich.edu/CTMS/index.php?example=Introduction&section=ControlPID. [Accessed: 02-Oct-2015].

[210] C. A. Apostolopoulos and G. N. Korres, “Real-time implementation of digital relay models using MATLAB/SIMULINK and RTDS,” *Eur. Trans. Electr. Power*, vol. 20, no. 3, pp. 290–305, Apr. 2010.

[211] MATLAB, “Electrical Power Systems Simulation - SimPowerSystems - Simulink - MathWorks United Kingdom.” [Online]. Available: http://uk.mathworks.com/products/simpower/. [Accessed: 02-Oct-2015].

[212] L. Wang, A. Crossland, D. Liang, N. Wade, and D. Jones, “Using a smart grid laboratory to investigate battery energy storage to mitigate the effects of PV in distribution networks,” in *22nd International Conference and Exhibition on Electricity Distribution (CIRED 2013)*, 2013, pp. 0504–0504.

[213] D. Liang, P. Taylor, L. Wang, D. Miller, and V. Thornley, “Coordinated voltage and power flow control in distribution network,” in *22nd International Conference and Exhibition on Electricity Distribution (CIRED 2013)*, 2013, pp. 0711–0711.

[214] P. Hsu and M. Behnke, “A three-phase synchronous frame controller for unbalanced load,” *29th Annu. IEEE Power Electron. Spec. Conf. 1998. PESC 98 Rec.*, pp. 1369–1374, 1998.

[215] P. T. Cheng, C. A. Chen, T. L. Lee, and S. Y. Kuo, “A cooperative imbalance compensation method for distributed-generation interface converters,” *IEEE Trans. Ind. Appl.*, vol. 45, no. 2, pp. 805–815, 2009.

[216] C. F. Lu, C. C. Liu, and C. J. Wu, “Dynamic modelling of battery energy storage system and application to power system stability,” *IEE Proceedings-Generation, Transm. Distrib.*, vol. 142, no. 4, pp. 429–435, 1995.

[217] L. T. Berger, A. Schwager, and J. J. Escudero-garzás, “Power Line Communications for Smart Grid Applications,” vol. 2013, 2013.

[218] J. Jousse, N. Ginot, C. Batard, and E. Lemaire, “Power Line Communication Management of Battery Energy Storage in a Small-Scale Autonomous Photovoltaic System,” pp. 1–9, 2016.